Design and Multistep Synthesis of Ligands for the GPR18 and GPR183: Related Orphan G Protein-Coupled Receptors with Immunoregulatory Functions

Dissertation
zur
Erlangung des Doktorgrades (Dr. rer. nat.)
der
Mathematisch-Naturwissenschaftlichen Fakultät
der
Rheinischen Friedrich-Wilhelms-Universität Bonn

vorgelegt von
Filomena Perri
aus
Cosenza

Bonn, 2024

Angefertigt mit Genehmigung der Mathematisch-Naturwissenschaftlichen
Fakultät der Rheinischen Friedrich-Wilhelms-Universität Bonn

Gutachterin/Betreuerin: Prof. Dr. Christa E. Müller
Gutachter: Prof. Dr. Finn Hansen

Tag der Promotion: 14.02.2025
Erscheinungsjahr: 2025

Table of Contents

ABBREVIATIONS

25HC	25-Hydroxycholesterol
27HC	27-Hydroxycholesterol
5-HT6R	5-Hydroxytryptamine 6 Receptor
7α,25-OHC	7α,25-Dihydroxycholesterol
7α,27-OHC	7α,27-Dihydroxycholesterol
8-CT	8-Chlorotheophylline
Abn-CBD	Abnormal Cannabidiol
AC	Adenylate Cyclase
ACN	Acetonitrile
ACPA	*N*-(Cyclopropyl)-Eicosatetraenamide
AEA	Anandamide
BIPY	2,2'-Bipyridine
BODIPY	Boron-Dipyrromethene
BRET	Bioluminescence Resonance Energy Transfer
cAMP	Cyclic Adenosine Monophosphate
CBD	Cannabidiol
CNR	Cannabinoid receptor
CREB	cAMP Response Element-Binding Protein
Cryo-EM	Cryo-Electron microscopy
CTX	Cholera Toxin
CYP27A1	Cytochrome P450 Family 27 Subfamily A Member 1
CYP7B1	Cytochrome P450 Family 7 Subfamily B Member 1
DAG	Diacylglycerol
DC	Dendritic Cell
DCE	Dichloroethane
DCM	Dichloromethane
DIPEA	Diisopropylethylamine
DMAP	4-Dimethylaminopyridine
DMF	Dimethylformamide
DMF-DEA	DMF-Diethylacetal

DMTU	N,N'-Dimethylthiourea
EBI2	Epstein-Barr Virus-Induced Receptor 2
ECL	Extracellular Loop
ERK	Extracellular Signal-Regulated Kinase
FSK	Forskolin
GPCR	G Protein-Coupled Receptor
GRK	G Protein-Coupled Receptor Kinase
HDX	Hydrogen-Deuterium Exchange
HGMD	Human Gene Mutation Database
ICL	Intracellular Loop
IL	Intracellular Lumen
IP3	Inositol 1,4,5-Trisphosphate
JNK3	Jun N-Terminal Kinases 3
LC-MS	Liquid Chromatography-Mass Spectrometry
LR	Lawesson's Reagent
MAPK	Mitogen-Activated Protein Kinase
MAS	Mas1 Oncogene Receptor
NAGly	*N*-Arachidonoylglycine
NBD	4-Nitro-7-Aminobenzofurazan
NC-IUPHAR	Nomenclature Committee Of The Union Of Basic And Clinical Pharmacology
NCS	*N*-Chlorosuccinimmide
NFAT	Nuclear Factor of Activated T-Cells
NF-B	Nuclear Factor-κb
NMP	*N*-Methy-2-Lpyrrolidinone
NMR	Nuclear Magnetic Resonance
ORF	Open Reading Frame
PEG	Polyethylene Glycol
PERK	Phosphorylated Extracellular Signal-Regulated Kinase
PI3K	Phosphoinositide 3-Kinase
PKA	Protein Kinase A
PKC	Protein Kinase C

PLC	Phospholipase C
PMBC	Peripheral Blood Mononuclear Cell
PMN	Polymorphonuclear Leukocyte
PTX	Pertussis Toxin
RVD2	Resolvind2
SRF	Serum Response Factor
STZ	Serum-Treated Zymosan
T3P	Propylphosphonic Anhydride
TAMRA	Tetramethylrhodamine
TEA	Triethylamine
TEOF	Triethylorthoformate
THF	Tetrahydrofuran
TLC	Thin Layer Chromatography
TM	Transmembrane
TRPV1	Transient Receptor Potential Vanilloid 1
TSCL	Tosylchloride
TSOH	*p*-Toluensulfonic Acid
β_2AR	β_2 Adrenergic Receptor
Δ^9-THC	Tetrahydrocannabinol

1. INTRODUCTION

1.1 G protein-coupled receptors

G protein-coupled receptors (GPCRs) are the largest group of mammalian receptors comprising over 800 subtypes. Despite the great diversity, the identifying features of GPCRs include a seven transmembrane topology, coupling to heterotrimeric G proteins, and phosphorylation by G protein-coupled receptor kinases (GRKs) followed by recruitment of β-arrestins. GPCRs play crucial roles in nearly every aspect of human pathophysiological processes and are therefore always in the spotlight for drug discovery studies with 30-40% of all marketed drugs targeting this receptor family.{Formatting Citation} As graphically shown in Figure 1, approximately half of all GPCRs in the human genome are olfactory receptors, widely expressed throughout the body and playing important functions beyond the detection of odorants.[3,4]

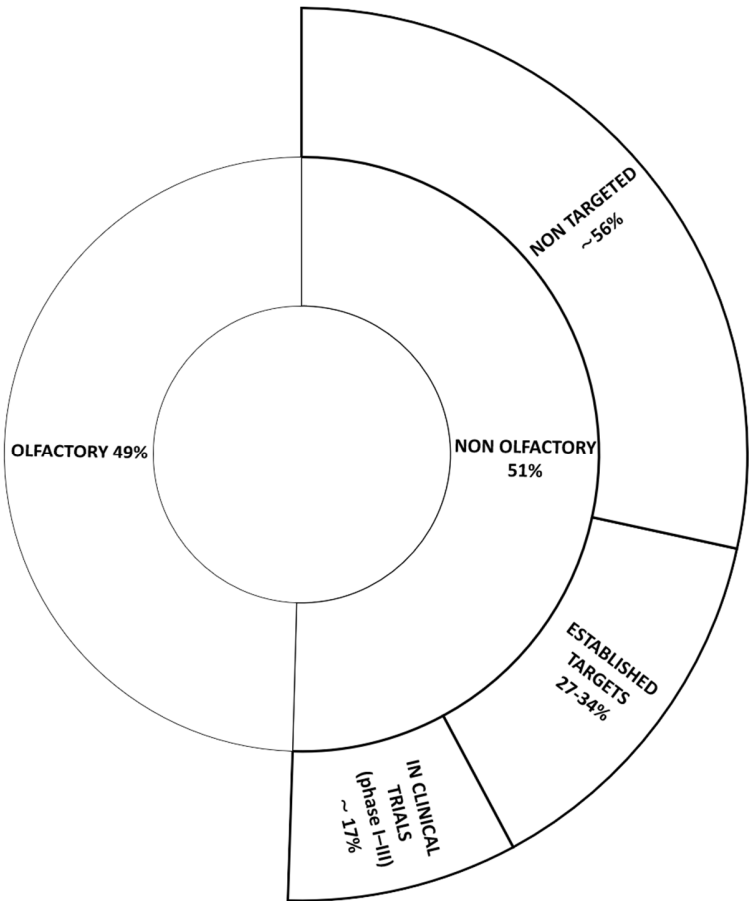

Figure 1. GPCRs as drug targets. Data summarized from literature.[1-2,5-8]

Among the around 400 non-olfactory GPCRs, 27-34% represent established targets for drugs approved in the United States or the European Union (mostly aminergic and opioid receptors).[5] A recent analysis reveals that 66 potentially novel GPCRs are addressed by agents in clinical trials (phases I-III), including many peptide receptors, as well as chemokine receptors, neuropeptide Y receptors, and the receptor family GPR18, GPR55 and GPR119.[6] The remaining non-sensory receptors have yet to be pharmaceutically exploited with great therapeutic potential, especially in genetic and immune system disorders. Trends indicate a rise in biological drugs (e.g.,

monoclonal antibodies), allosteric modulators, biased agonists, and multivalent ligands.[5–8] To date, orphan GPCRs (without known physiologic agonists) are ~100 and — with few exceptions — they are not currently targeted.[1] Therefore, we can expect that the number of GPCR drug targets, the number of GPCR-targeted drugs, and perhaps the types of drugs will likely increase, thus further expanding the GPCR repertoire.

To support these endeavors, recent advances in the structural biology of GPCRs have significantly expanded our understanding of these crucial receptors. The application of X-ray crystallography has led to an increase in the number of high-resolution three-dimensional GPCR structures. The advent of cryo-electron microscopy (cryo-EM) in 2017 further revolutionized the field, allowing for detailed structural studies of GPCRs in various states and complexes. These insights into ligand recognition and receptor activation have opened new avenues for structure-based drug design. Additionally, novel technologies such as nuclear magnetic resonance (NMR), hydrogen-deuterium exchange (HDX), and advanced bioassays have been instrumental in identifying biased and allosteric modulators, thereby uncovering new binding sites and mechanisms of action.[5,8,9] The development of computational methods to predict three-dimensional protein structures from the protein sequence (e.g. homology modeling) is also worth mentioning. The use of Artificial Intelligence, particularly DeepMind's AlphaFold, has played a transformative role in predicting protein structures with high accuracy, thus accelerating the discovery and development of new drugs.[10] Advances in genetic and molecular biology have also allowed for the manipulation of GPCR expression and function in vivo, providing a powerful tool for studying the role of GPCRs in health and disease.[11]

Together, these developments enhance both basic and translational research in GPCR drug discovery.

1.1.1 Classification

Given the vastness of the GPCR family, several classification methods have been used to sort them out. Initially, in 1994 they were classified into six classes (A-F) based on functional similarity and sequence homology.[12] A subsequent analysis of the human repertoire using a phylogenetic analysis established 5 families according to their common evolutionary origin: glutamate, rhodopsin, adhesion, frizzled/taste2, and secretin (referred to as GRAFS).[13] The most studied and largest family is the Rhodopsin family (previously called either the rhodopsin-like receptors or class A in

the aforementioned A-F classification system), whose lead receptor was first identified in the late nineteenth century.[14] Common features of this class include the NSxxNPxxY motif in transmembrane 7 (TM7) and the DRY motif or D(E)-R-Y(F) in TM3, which is presumedly important to keep the receptors in the inactive state.[15] Furthermore, for such receptors, it is known that the TM domain offers a binding pocket for small ligands, whilst large ligands (e.g. peptides) are more likely to bind to the external loops and/or the amino terminus of their receptors.[16] This family has been further divided into sub-classes named α-, β-, γ- and δ-branch. The latter includes 4 main receptor clusters: MAS-related (MAS1 oncogene and related receptors MRGs and MRGXs), glycoprotein (glycoprotein hormone receptors and the leucine-rich-repeat–containing receptors), olfactory receptors (solid cluster of around 460 receptors) and purine (formyl peptide receptors, nucleotide receptors, and orphan GPCRs). As shown in Figure 2, two structurally related and highly "druggable" orphan GPCRs, GPR18 and GPR183, belong to this branch.[13,17]

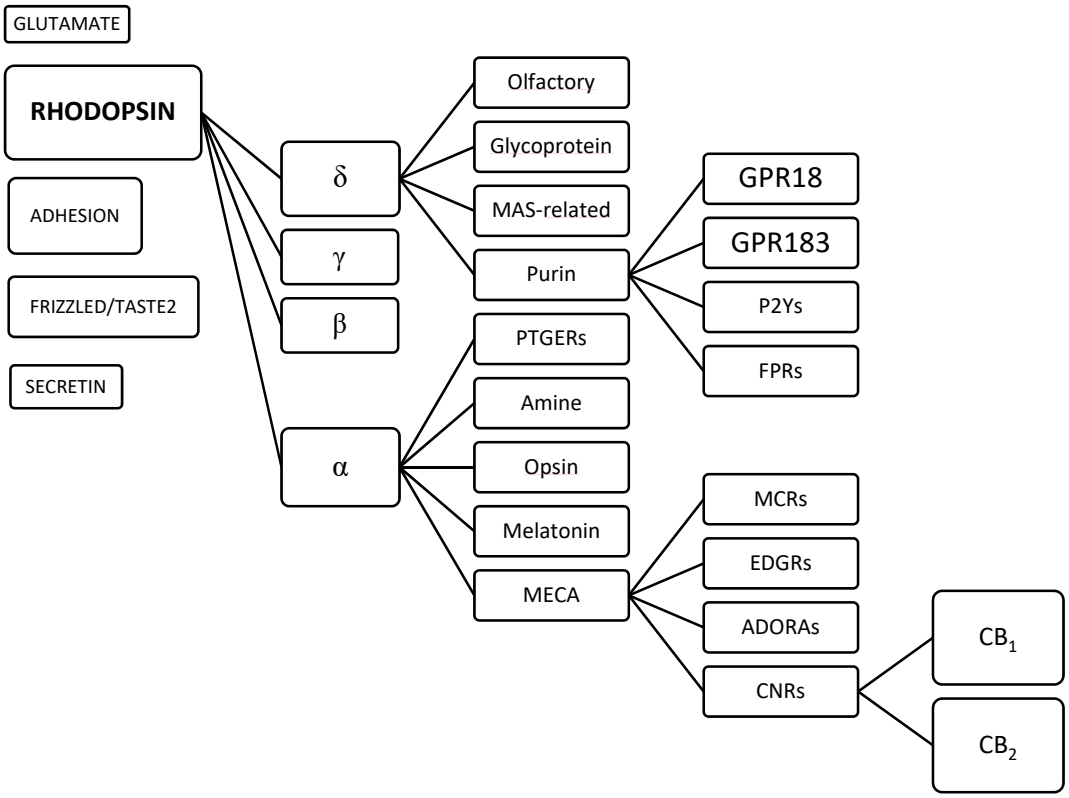

Figure 2. Abridged representation of the GRAFS classification of GPCRs. MAS-related: MAS1 oncogene receptor (MAS) and the MAS-related receptors; PTGERs: prostaglandin receptors; Melanocortin/EDG/Cannabinoid/Adenosine (MECA) receptors: melanocortin receptors (MCRs), endothelial differentiation G-protein coupled receptors (EDGRs), cannabinoid receptors (CNRs), and adenosine receptors (ADORAs); P2Ys: nucleotide receptors; FPRs: Formyl Peptide Receptors. CB_1: Cannabinoid receptor type 1, CB_2, Cannabinoid receptor type 2; GPR18: G protein-coupled receptor 18; GPR183: G protein-coupled receptor 183.

1.1.2 Activation and canonical signaling

GPCRs can transduce a heterogeneous and wide plethora of stimuli ranging from small molecules, peptides, hormones, neurotransmitters, ions, lipids, and natural odorants to even photons.[18]

The process of GPCR activation begins with the binding of one of these ligands to the orthosteric binding site, which is typically located on the extracellular receptor surface, including the extracellular N-terminus, different extracellular loops, and/or the exofacial segments of various TM domains. This binding induces a conformational change in the receptor that propagates through the receptor's transmembrane helices to the intracellular side, designated for the interaction with the G protein. The largest change to stabilize the active conformation is the movement of TM6, which rotates outward from the receptor's central axis. This movement, together with some rearrangements of TM5 and TM7 as well, creates a space for the G protein or β-arrestin protein to bind.[19]

These heterotrimeric G proteins, constituted by the subunits α, β, and γ, act as molecular switches, cycling between an inactive guanosine diphosphate (GDP)-bound state and an active guanosine triphosphate (GTP)-bound state. The conformational change of the receptor results in the release of GDP from the α subunit, and eventually, the binding of GTP and the dissociation from the βγ protein subunit. As illustrated in Figure 3, the signal transduction pathways strongly depend on the type of Gα-subunits present in the heterotrimeric protein — major ones are $G\alpha_s$ and $G\alpha_{i/o}$ protein, stimulating or inhibiting the activity of adenylate cyclase (AC) respectively, $G\alpha_{q/11}$ activating phospholipase C (PLC) and $G\alpha_{12/13}$, involved in the regulation of cell shape and motility, activating the Rho family of small GTPases.[20]

There are 5 different types of β-subunits and 12 different types of γ-subunits. Members of each family have structural similarities and functional properties. It has been shown that the βγ complex can also interact with a big array of downstream effectors including ion channels, adenylate cyclases, kinases, etc. The number of molecules reported to interact with this complex is increasing daily, but there is still a need to fully explain the basic mechanisms underlying molecular recognition and regulation of effectors by Gβγ.[21] The majority of GPCRs activate more than one G protein subtype. Therefore, the activation of GPCRs is a result of several signal transduction cascades via Gα- sometimes Gβγ- subunits. Hence, the GPCR interaction does neither occur in a specific nor a completely promiscuous manner.[22]

The signaling pathway is terminated via serine-threonine phosphorylation of the receptors, which is facilitated by members of the GRK family and second messenger-activated protein kinases, such as protein kinase A (PKA) and protein kinase C (PKC). This is then followed by the binding of arrestins, which inhibits further activation of G proteins through steric hindrance. Subsequently, the ligand-bound receptor can be internalized through the arrestin-mediated engagement of clathrin-coated pits. Once internalized, GPCRs are sorted in endosomal membranes and either recycled back to the cell surface or targeted to lysosomes for degradation.[23]

There is growing interest in understanding the structural and mechanistic aspects of GPCR–β-arrestin interaction, since it has been shown that other than terminating G protein coupling, and mediating receptor endocytosis they can initiate separate downstream signaling pathways leading to different functional outcomes.[24]

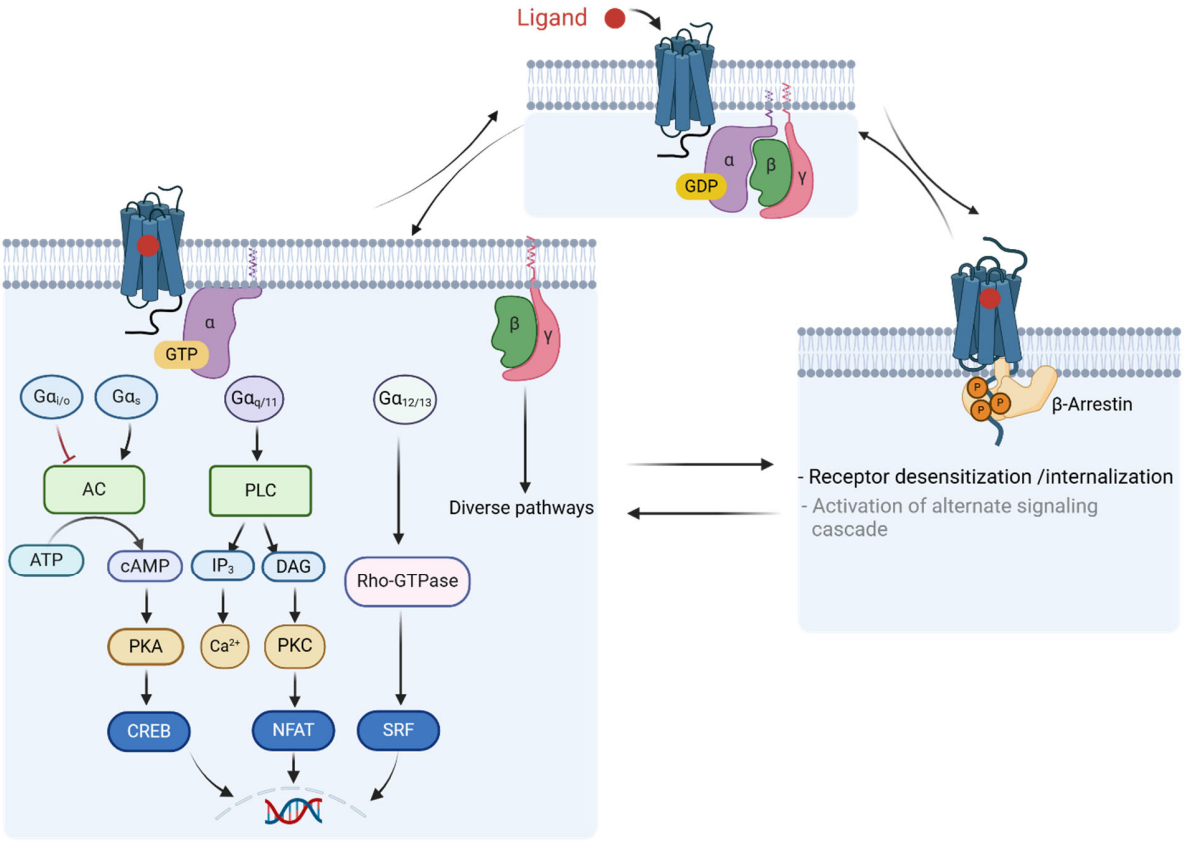

Figure 3. GPCR activation cycle. AC: adenylate cyclase; PLC: phospholipase C; cAMP: cyclic AMP; IP_3: inositol 1,4,5-trisphosphate; DAG: diacylglycerol; PKC: protein kinase C; CREB: cAMP response element-binding protein; NFAT: Nuclear factor of activated T-cells; SRF: Serum Response Factor.

1.1.3 G protein-independent pathways and biased signaling

Increasing evidence shows that GPCRs may have other signaling cascades in addition to and in the absence of heterotrimeric G proteins. The various intracellular proteins that GPCRs interact with, such as β-arrestins, tyrosine kinases, and PDZ-domain-containing proteins, may play a role in mediating G protein-independent signaling.[25] Many receptors have been reported to directly interact (mostly through the C-terminal tail of the receptor) with different members of the Src tyrosine kinase family, responsible for triggering the Extracellular Signal-Regulated Kinase (ERK) pathway and ultimately involved in cell proliferation, survival, differentiation, adhesion, migration, and cell cycle control.[26] Examples include the β2 adrenergic receptor (β2AR), the purinergic receptor $P2Y_2$ and the 5-hydroxytryptamine 6 receptor (5-HT6R).[27] Independent pathways are also involved in the modulation of Na^+ currents in the cell like shown for the β2AR and muscarinic receptors.[28]

Nevertheless, as previously mentioned, the most studied G protein-independent interaction is the one with arrestins. This family of small cytosolic proteins comprises 4 different members (termed arrestin 1-4), but due to their ubiquitous expression in the majority of mammalian cells and tissues, the two therapeutically relevant ones are arrestin-2 and arrestin-3 (or β-arrestin-1 and -2, respectively).[29] Other than being important regulators of GPCR signaling by promoting receptor desensitization, internalization, and degradation, β-arrestins might act as downstream signal transducers themselves. The formation of signal- and function-specific protein complexes referred to as encryptomes can have various signaling effects depending on the specific GPCR and signaling proteins involved. They include c-Src family tyrosine kinases, components of the $ERK_{1/2}$ and Jun N-terminal kinases 3 (JNK3) MAP kinase cascades, the serine/threonine kinase AKT, the PP_2 family of phosphatases, nuclear factor-κB (NF-B), and phosphoinositide 3-kinase (PI_3K). The type of interaction is strongly driven by the different involvement of the receptor tail and receptor core since the distinct conformational states differentially correlate with G proteins and β-arrestins.[29–31]

Around two decades ago, the discovery of these G protein-independent signaling cascades led to the realization that GPCRs are far from being simple on/off switches and possess a "pluridimensional efficacy" with different ratios of active state complexes.[32] Furthermore the different signaling pathways can be pharmacologically distinguished, introducing the concept of ligand bias.[33] Biased signaling is the phenomenon in which a 7-transmembrane receptor

preferentially activates one over the several pathways available to it. These insights paved the way for the development of biased therapeutics. For instance, the redundancy in the chemokine system, where several ligands bind to a single receptor and can trigger various intracellular signaling patterns, makes it an ideal target for biased ligands.[34] It is noteworthy, though, that the ability of certain ligands to activate multiple signaling pathways can lead to various side effects.[35] For example, the analgesic effects associated with opioids are suggested to be regulated through the G_i-dependent pathway, while various negative outcomes such as tolerance, addiction, and respiratory depression are regulated through the β-arrestin pathway at the μ-opioid receptor (μ-OR).[36] However, this is still under debate.

In conclusion, to properly evaluate a potential pharmaceutical product in vitro, it is insufficient to test its activity through just one signaling pathway. Additionally, when the target of interest is expressed in multiple tissues, it is essential to confirm that the observed response is consistent across other tissue types or cell lines.

Nevertheless, this also suggests that we are at the cusp of a new era of GPCR drugs, as ligand bias can now be utilized to modulate drug efficacy by targeting a specific signaling cascade.

1.1.4 The deorphanization process

As mentioned above, around 15% of all GPCRs are still orphan, i.e. there is a lack of knowledge concerning their endogenous ligands.[37] Substantial literature has proven that ligands aimed towards these receptors could be useful in treating disorders arising from their abnormal signaling, being responsible for many pathophysiological processes e.g. neurodegenerative diseases,[38] inflammation, and cancer.[39,40] Therefore the "deorphanization" process or the development of surrogate agonists is one of the hottest and most challenging topics in research.[41]

Many strategies could be used in this attempt, the most famous one that has taken over in recent years is the so-called "reverse pharmacology". It entails expressing these orphan GPCRs in eukaryotic cells via DNA transfection and then testing ligands. As a result of this methodology, numerous peptide hormones, such as ghrelin, kisspeptin, metastin, orexin, and hypocretin, have been discovered as endogenous ligands of GPCRs.[41,42] Nevertheless, the effectiveness of this approach is dependent on several factors, including sufficient expression of the orphan receptor, the quality of the ligands employed, and, as the most challenging element, the robustness of the screening assays. The pace of GPCR deorphanization declined sharply in the early 21st century,

indicating a potential gap in the processes. Limited knowledge about orphan GPCRs, including their physiological functions and roles as signal transmitters, makes experimental design challenging due to the lack of assays and positive controls. Most deorphanization approaches rely on monitoring second messenger changes regulated by G proteins, yet GPCRs can transduce various signal pathways, as extensively mentioned before.[41]

In conclusion, publications on orphan receptors, whose physiological agonists and functions are unknown, are usually rare. However, a few orphan receptors, namely GPR143 and GPR15, have more than 100 articles. This uneven distribution of data highlights that the research on numerous GPCRs is still in its early stages, and further investigation is necessary to determine their involvement in (patho)physiology.[6]

1.1.5 Fluorescent ligand design and NanoBRET assays for GPCR pharmacology

In cell biology and pharmacology, the ability to monitor protein-protein or drug-protein interactions with precision and sensitivity is fundamental. Bioluminescence Resonance Energy Transfer (BRET) assays have emerged as a preferred method due to their ease of use and capacity for real-time monitoring in live cells. BRET technology relies on the energy transfer between a bioluminescent donor, such as luciferase oxidizing its substrate, and a fluorescent acceptor, often called biosensors. Various donor-acceptor pairs have been used successfully in BRET assays, including combinations like the *Renilla* luciferase variant Rluc8 and the GFP variant, Venus. Recent advances include NanoLuc, a novel luciferase variant that is smaller and significantly brighter than native luciferase. NanoLuc can be attached to the N terminus or other suitable site of a GPCR, allowing for a detailed study of ligand-receptor interactions in live cells.[43,44]

As shown in Figure 4, the typical NanoBRET assay involves incubating cells with a fluorescently labeled ligand followed by the addition of the optimal NanoLuc substrate, furimazine. This process results in the oxidation of furimazine to furimamide, producing photons that transfer energy to the attached fluorophore if both biosensors are in close proximity. This energy transfer excites the fluorophore, emitting light of a longer wavelength, which can be detected and quantified. By measuring both donor (NanoLuc) and acceptor emissions, researchers can calculate BRET ratios, providing insights into ligand-receptor interactions.

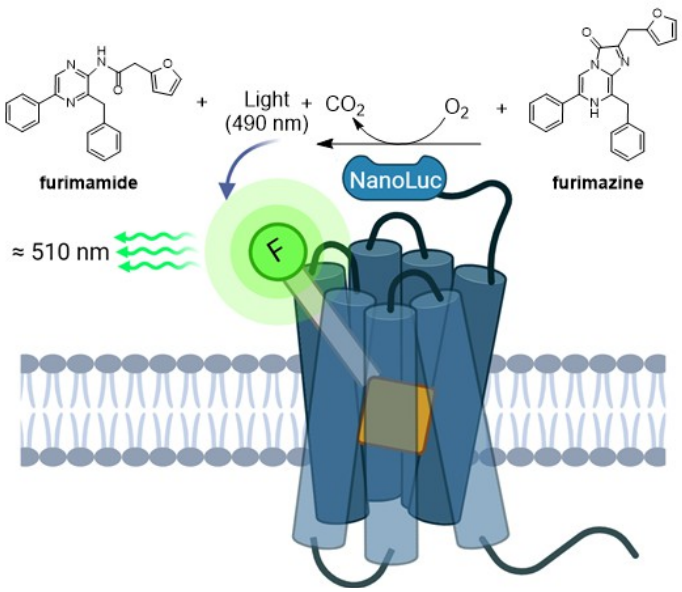

Figure 4. Bioluminescence resonance energy transfer (BRET) mechanism based on the NanoLuc protein. The fluorescent ligand consists of three elements: pharmacophore (mustard), linker (grey), and fluorophore (green). The emission wavelength of the fluorophore is provided as an example.

The efficiency of this process depends on the spectral overlap between NanoLuc's emission and the excitation and emission profiles of the acceptor fluorophores. Spectral overlap is crucial for resonance energy transfer.[43]

Factors such as fluorescence intensity, photostability, and spectral properties must be carefully considered during fluorophore selection. Three common fluorescent dyes used for NanoBRET are tetramethylrhodamine (TAMRA), boron-dipyrromethene (BODIPY), and 4-nitro-7-aminobenzofurazan (NBD). BODIPY fluorophores are highly versatile and widely used for tagging biological agents. They offer high fluorescence and absorption levels, making them ideal for NanoBRET assays. BODIPY dyes typically exhibit excitation spectra in the range of 480-520 nm and emission spectra in the range of 500-550 nm. However, there are many variants of BODIPY dyes that cover a broader range, with some extending into the near-infrared region. Their advantageous properties include good solubility in many solvents (excluding aqueous ones) and stability against changes in polarity and pH.[45,46]

Other than fluorophores, the process of designing fluorescent ligands involves other two crucial elements: a suitable pharmacophore and a linker connecting the two elements.

Firstly, the pharmacophore serves as the core structure responsible for maintaining the desired biological activity. In selecting suitable pharmacophores, it is important to identify compounds with functional groups able to attach additional elements without significantly compromising their activity. For instance, certain compounds may possess side chains or substituents that allow for facile modification.

Secondly, the linker plays a pivotal role in connecting the pharmacophore to the fluorophore moiety. The linker composition and length can vary depending on the specific requirements of the

ligand design. The choice of linker influences the flexibility, spatial orientation, and overall stability of the ligand-receptor complex. Analyzing linker types reveals two main categories: flexible and rigid linkers. Flexible linkers, like alkyl-based and polyethylene glycol (PEG)-based, are prevalent due to their ease of synthesis and ability to enhance solubility, stability, and pharmacokinetics.[47] PEG, in particular, improves solubility and reduces nonspecific interactions, leading to better bioavailability.[48] Rigid linkers, such as triazole-based and cycloalkane-based, offer enhanced stability and specific reactivity. Triazole-based linkers benefit from "click chemistry," easing synthesis, while cycloalkane-based linkers, like piperazines, improve stability and cell permeability.[47]

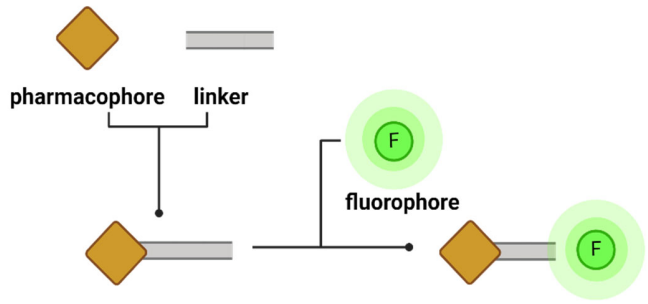

Figure 5. Fluorescent ligand elements.

Figure 5 shows that by strategically combining these three components, we can develop fluorescent ligands with enhanced binding affinity, specificity, and fluorescence properties for various biomedical applications, including drug discovery, molecular imaging, and biomolecular interaction studies. Importantly any combination of pharmacophore + linker and subsequently the entire fluorescent ligand need to be treated like unique pharmacological entities and therefore subject to biological evaluation.

1.2 GPR18

1.2.1 Discovery and expression

The first isolation of the gene fragment encoding the partial sequence of the receptor later designated GPR18 — Human Gene Mutation Database (HGMD)-approved name — occurred unexpectedly during a relaxed stringency PCR experiment aiming to isolate the gastrin-releasing peptide receptor from canine parietal cells and Colo 320DM cells (a human colon cancer cell line).[49] This study showed that the Open Reading Frames (ORF) of the canine and human GPR18 genes are highly conserved: 89% nucleotide identity and 92% amino acid similarity are reported between the two species. The authors localized it to the human chromosome region 13q32 by fluorescence *in situ* hybridization, by its localization to distal mouse chromosome 14.[37] The most

related receptor is GPR183 (also formerly known as Epstein-Barr Virus-induced receptor 2 — EBI2), while, despite GPR18 has been shown to respond to tetrahydrocannabinol (described below), it is phylogenetically very distant from canonical cannabinoid receptors, which belong to the α-branch of the rhodopsin family, as seen in Figure 2.[50]

1.2.2 Putative pathophysiological roles

The original cloning of the receptor showed a rich expression in organs and tissues related to the immune system, e.g. spleen, thymus, peripheral blood leukocytes, small intestine, appendiceal, and lymph node tissues. Together with its expression in human lymphoid cells, this suggests a potential role in the control of immune responses and consequently in inflammation and pain.[51–54]

Within immune cells, GPR18 is most highly expressed in leukocytes, e.g. in peripheral blood polymorphonuclear leukocytes (PMNs) and monocytes, as well as in monocyte-derived macrophages. Interestingly, GPR18 appears to play a crucial role during the resolution phase of inflammation. Although it is associated with anti-inflammatory effects, GPR18 is paradoxically upregulated in M1 macrophages but not in M2 macrophages. Additionally, GPR18 was reported to regulate leukocyte trafficking during acute inflammation.[55,56]

It is also expressed in the rostral ventrolateral medulla, heart, and endothelial cell lines, underlining the potential role in the modulation of cardiovascular functions. Expression in retinal cells, where GPR18-based signaling is allegedly responsible for the regulation of intraocular pressure, and in sperm, with a high expression in the most terminally differentiated cells, the spermatids, implying a function immediately before fertilization has been reported. Moreover, glioblastoma cell lines and melanoma metastases appear to express GRP18, suggesting a potential role in the malignant behavior of melanoma itself as well as in cancer and regulation of cell death.[57–62]

Furthermore, GPR18 may be relevant in metabolic diseases. In fact, it is highly expressed in neurons of the medium-basal hypothalamus, where the expression is regulated by dietary fats, as well as in tissues relevant to metabolic functions like adipose tissue, skeletal muscle, pancreas, spleen, and liver.[63,64] Moreover, the signaling cascades allegedly stimulated by GPR18, e.g. MAPK activity, are involved in obesity-associated inflammation.[65]

Some publications have suggested that CB2R and GPR18 might collaborate in regulating microglial cell migration.[66,67] Afterwards, microglia-expressed CB_2R-GPR18 receptor complexes were reported, which may be targets for neuroprotection.[68,69]

Taking into account all the biological processes in which GPR18 may be involved, it is a very promising drug target for inflammatory diseases and immunotherapeutic approaches, e.g. for the treatment of cancer.[40,52]

1.2.3 Controversial findings on ligands and signaling

Since its first identification, GPR18 has been the object of many controversial findings concerning its ligands and possible G protein-coupling partners.

Cannabinoid-like molecules were the first class of compounds studied as putative ligands. In particular, "abnormal cannabidiol" (abn-CBD), the synthetic regioisomer of cannabidiol (CBD) emerged as a pharmacological tool in the discovery of GPR18, causing mesenteric vasodilation in wild-type mice and in mice lacking CB_1 receptors or both CB_1 and CB_2.[70] Such endothelium-dependent vasodilation is elicited by both abnormal-cannabidiol (abn-CBD) and its synthetic analog O-1602 and antagonized by both cannabidiol and its synthetic analog O-1918.[71,72] Anandamide (AEA), tetrahydrocannabinol (Δ^9-THC) and the lipoamino acid *N*-arachidonoylglycine (NAGly), caused migration of the human endometrial HEC-1B cells with a CB_1 receptor-independent mechanism.[73] The authors carried out MAPK activation assays in stably transfected HEK293-GPR18 cells showing that in order of potency NAGly, O-1602, Abn-CBD, Δ^9-THC, AEA and *N*-(cyclopropyl)-eicosatetraenamide (ACPA) appeared to be full agonists at GPR18; CBD and AM251 appeared to be weak partial agonists.[74] Some modifications in the scaffold like the change from a tricyclic to bicyclic structure, but also the substitution of the alkyl chain from Abd-CBD with residues with the ability to form hydrogen bonds may be the key to understanding why this molecule lacks efficacy towards canonical cannabinoid receptors, but retains high binding affinity to GPR55 and possibly to GPR18. O-1918, another synthetic cannabinoid also was reported to show agonistic activity towards GPR18 in ERK1/2 phosphorylation and Ca^{2+} assays with a lack of activity in β-arrestin recruitment assays.[75] The same compound was suggested to act as an antagonist that blocks or reduces the migration induced by NAGly, Abn-CBD, and O-1602 in BV-2 or HEK293-GPR18 cells.[76]

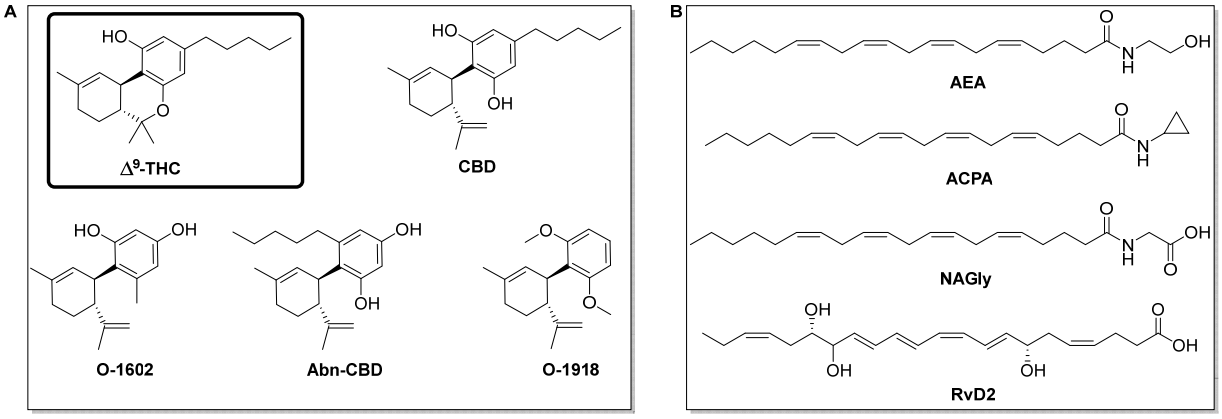

Figure 6. A cannabinoid-like ligands; B lipid-like ligands. The bold square indicates the only confirmed agonist to date, Δ^9-THC.

In 2006 NAGly was pointed out by Kohno *et al*. as the endogenous ligand for GPR18.[51] GPR18 expression was high in HTLV-1-transformed cell lines, lymphoid cell lines, and in lymphocyte subsets (e.g. $CD4^+$). NAGly induced an increase in intracellular Ca^{2+} concentration in GPR18-transfected cells at 10 μM; this was further confirmed by similar results obtained comparing the intracellular Ca^{2+} mobilization in two other kinds of stably GPR18-transfected cells (K562 and CHO cells). NAGly, at sub-nanomolar concentrations, markedly influenced migration of BV-2 microglial and HEK293-GPR18 transfected cells, as well as migration of the human endometrial HEC-1B cell.[73,76] NAGly was claimed to lead to the resolution of inflammation in GPR18-transfected HEK-293 cells.[53] Lately, NAGly has been shown to cause apoptosis in the mouse macrophage-derived cell line, RAW264.7.[77] Knocking down the expression of GPR18 and pre-treatment with pertussis toxin (PTX) resulted in resistance to the effects of NAGly. Additionally, to further confirm GPR18 involvement, the authors examined the effects of NAGly in mouse peritoneal macrophages; a proinflammatory stimulation of such cells resulted in an increase in GPR18 mRNA levels as well as a decrease in viability due to NAGly.

Another lipid-related molecule, Resolvin-D2 (RvD2), was proposed as a GPR18 ligand.[55] It is an eicosapentaenoic acid (EPA)–derived E-series resolvin, suggested to mediate resolution of acute inflammation. In those experiments monitoring changes in impedance upon ligand binding to receptors, both NAGly and RvD2 elicited impedance changes activating CHO cells overexpressing human GPR18 (CHO-*h*GPR18). Surprisingly this action was not blocked by the action of PTX, but by the action of cholera toxin (CTX), a well-known decoupling agent for $G\alpha_s$ proteins, suggesting their involvement in the RvD2-GPR18 actions in CHO-hGPR18 cells. The effects

induced by RvD2 like the enhancement of Mφ phagocytosis of serum-treated zymosan (STZ), live *E. coli,* and apoptotic PMN as well as an increase in cAMP were augmented by *h*GPR18 overexpression and decreased with specific shRNA targeting *h*GPR18 (knockdown). Furthermore, the specific binding of RvD2 to recombinant GPR18 was reported with a Kd ≈ 10 nM.

All the aforementioned findings, could not be independently confirmed by many other research groups, including ours. In fact, in a β-arrestin PathHunter^{TM} assay system, NAGly was inactive at GPR18.[78] In another study, neither NAGly nor other previously reported putative agonists such as AEA and Abn-CBD were able to modulate the currents of N-type (Cav2.2) calcium channels in rat sympathetic neurons heterologously expressing GPR18.[79] In 2016, Finlay et *al.* showed that high concentrations of NAGly or other putative ligands were not able to elicit significant ligand-mediated responses in earlier reported signaling pathways like pERK activation and reduction in Forskolin(FSK)-induced cAMP levels.[61]

A recent patent showed cannabidiol analogs with a pyrazolylbenzene-1,3-diol structure to be used in pharmacological studies associated with GPR18 and/or the transient receptor potential vanilloid 1 (TRPV1). As for GPR18, the described compounds S4, S5, and S9, whose structures are reported in Figure 7, appear to have different pharmacological profiles. In the β-arrestin complementation assay, S5 is an agonist (EC_{50} 9 μM), whereas inverse agonistic activity is reported for S4 (at 10 and 30 μM) and S9 (30 μM). In intracellular calcium measurements, S5 and S9 augmented the concentration of Ca^{2+} in human GPR18-expressing cell lines both at 10 μM, while S4 on its own did not affect the calcium concentration, but was able to block the S5-induced increase in $[Ca^{2+}]_i$.[80,81]

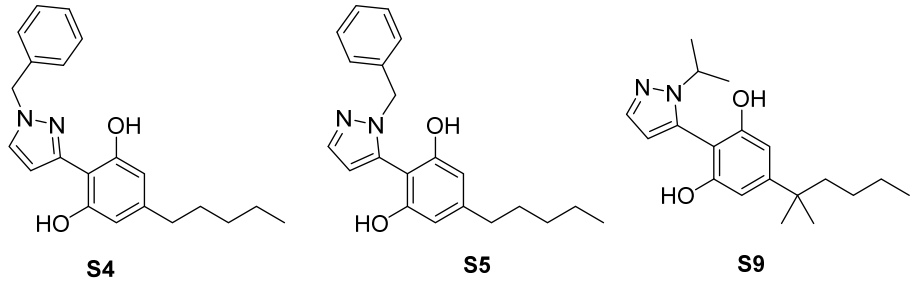

Figure 7. Pyrazolylbenzene-1,3-diols described for the treatment of diseases associated with GPR18 and/or TPRV1.[81]

As for the signal transduction, $G\alpha_{i/o}$ and $G\alpha_{q/11}$ have been proposed as the coupling partners of GPR18 in several studies.[51,75,77] However other research groups found no effect, e.g. on cAMP levels and there was no GPR18-mediated response to NAGly, and at the same time they could not detect coupling through $G\alpha_z$ or $G\alpha_{15}$.[79], Coupling through $G\alpha_s$ has been suggested, as well.[55] Cannabinoid ligands (Δ^9-THC, abn-CBD, O-1918 and O-1602) and NAGly were investigated in MAPK signaling, Ca^{2+} mobilization and β-arrestin signaling. All the tested molecules resulted in a Ca^{2+} increase and MAPK activity, They found both cannabinoid compounds and NAGly to stimulate with the signal being sensitive to both PTX and the $G_{\alpha q}$ inhibitor, [D-Trp^{7,9,10}]-substance P. Surprisingly, only Δ^9-THC and partly also CBD, produced a signal in a β-arrestin assay. The authors concluded that biased signaling of the compounds towards β-arrestin or $G_{\alpha q}$ or $G_{\alpha i}$ took place.[75] Furthermore, some studies in yeast suggested that GPR18 may show constitutive activity.[61]

In 2014 our research group identified the first GPR18-selective antagonist (Figure 8), an indole-containing natural product produced by a marine-derived fungal strain of *Dichotomomyces cejpii*. The most interesting compound in this regard was 27-*O*-methylasporyzin C, showing an IC_{50} value of 13.4 μM measured in a functional assay versus Δ^9-THC 7.5 μM. In the same paper, also compound JBIR-03, a hexacyclic indole derivative, showed antagonistic activity at GPR18 (IC_{50} 9.9 μM), but was similarly potent at CB_1 (K_i 4.40 μM) and CB_2 (K_i 4.76 μM).[82] Later, another natural compound from a marine sponge-derived fungus, namely the diketopiperazine amauromine, showed antagonistic activity on both CB_1 receptors (K_i 0.178 μM) and GPR18 (IC_{50} 3.74 μM).[83]

Subsequently, the screening of a library of imidazothiazinones at the human receptor in a β-arrestin recruitment assay with Δ^9-THC as the agonist resulted in compounds PSB-CB-27 and PSB-CB-5 as the first potent and selective GPR18 antagonists. PSB-CB5, with a *p*-chlorobenzyloxybenzylidene residue attached to an imidazo[2,1-b]thiazine scaffold was the most potent antagonist of that series with IC_{50} 0.279 mM.[84] In a computational-focused paper, PSB-CB-148, another compound of this series, emerged as an even more potent antagonist, but detailed data have not been published yet.[85]

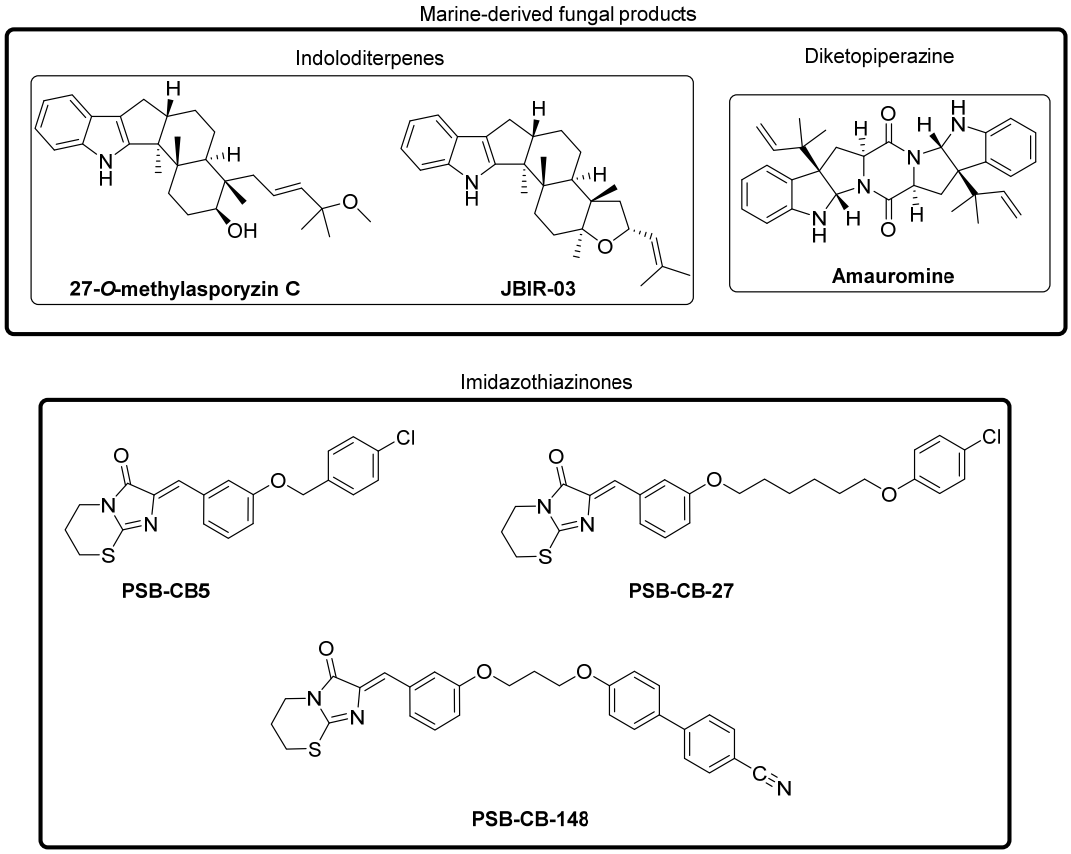

Figure 8. Reported GPR18 antagonists.

Our group also described the first non-lipid-like agonists based on a tricyclic xanthine-derived scaffold: with an EC_{50} of 0.562 µM, PSB-KD107 displayed significantly higher potency and efficacy than THC (β-arrestin recruitment assay) and was found to be selective versus the other cannabinoid-interacting receptors, CB_1, CB_2, and GPR55.[86] This agonist then served as a lead structure for the development of the most potent non-lipid-like GPR18 agonist known to date: PSB-KK-1415 with an EC_{50} of 19.1 nM. In the same recently published series compound PSB-KK-1445 (EC_{50} = 45.4 nM) is the most selective GPR18 agonist determined vs cannabinoid receptors CB_1 and CB_2 and the cannabinoid-like receptor, GPR55.[87,88] Together with the imidazothiazinone antagonists, these compounds have been used as potent pharmacological tools to investigate the role of GPR18 in intestinal inflammation and inflammatory pain, relaxation of pulmonary arteries, and very recently also in mood, pain, and eating disorders.[89–91]

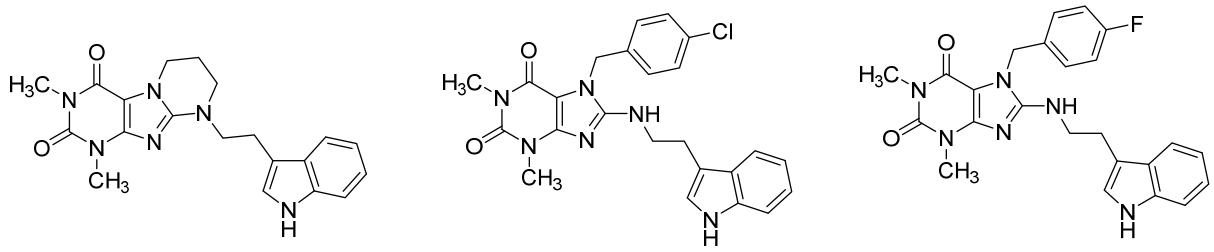

Figure 9. Potent and selective xanthine-based GPR18 agonists.

All the aforementioned information is summarized in Table 1.

To sum up, due to the incomplete and controversial findings on all the aforementioned putative agonists, the only confirmed one is Δ^9-THC and GPR18 is still classified by the Nomenclature Committee of the Union of Basic and Clinical Pharmacology (NC-IUPHAR) as orphan.

Many groups, including ours, did not observe any constitutive activity, and findings on the G protein coupling are quite incoherent.

Because of the increasing evidence indicating that GPCRs may also signal through G protein-independent pathways,[25] together with the incapability to replicate reported results, the concept of GPR18 not being G protein-coupled is taking hold more and more.

Table 1. Summary of the reported, but mostly unconfirmed pharmacological profile of different ligands towards human GPR18. Adapted from Morales et al.[80] AG=agonist; AT= Antagonist; n.e.= no effect.

Cmpd.	Ca^{2+} Mobilization				cAMP	BRET/ cAMP	β-Arrestin recruitment		Cell migration and viability				p44/42 MAPK	ERK 1/2
	GPR18 - K562 and GPR18-CHO	GPR18-L929	GPR18-HEK-CAMYEL	GPR18-HEK293	GPR18-CHO	GPR18-HEK-CAMYEL	GPR18-HEK293-BAEA	GPR18-CHO-K1	BV-2	GPR18-HEK293	HEC-1B	RAW 264.7	GPR18-HEK293	GPR18-HEK293
CANNABINOID-LIKE														
Δ^9-THC				AG[75]				AG[75,92]					Full AG[73]	AG[75]
Abn-CBD			n.e.[79]	AG[75]				n.e.[75]	Potent AG[93]				Full AG[73]	AG[75] n.e.[61]
CBD								Weak AG[75]		AT[93,94]			Partial AG/AT [73]	
O-1602			n.e.[79]	AG[75]		n.e. [61]	n.e.[75]	n.e.[75]	Potent AG[93]				Full AG[73] n.e.[61]	AG[75] n.e.[61]
O-1918				AG[75]				n.e.[75]	AT[93]	AT[93]				AG[75]
LIPID-LIKE														
NAGly	AG[51]	Weak AG[51]	n.e.[79]	AG[75]	inhibition[51]	n.e[61,79]	n.e.[78]	n.e.[75,84]	Potent AG[76]		AG[73]	AG[77]	Potent AG[73]	AG[75] n.e.[61]
RvD2					stimulation [55]			Potent AG[55]						
AEA						n.e[61]	n.e.[78]	n.e.[75]	Potent AG[93]		AG[73]		Full AG[73]	n.e.[61]
2-AG							n.e.[78]		Potent AG[93]					

PYRAZOLYLBENZENE-1,3-DIOLS								
S4	AT[80,81]				Inverse AG[80]			
S5	AG[80]				Partial AG[80]			
S9	AG[80]				Inverse AG[80]			
MARINE-DERIVED FUNGAL PRODUCTS								
27-*O*-methylasporyzin C					AT[82]			
JBIR-03					AT[82]			
Amauromine					AT[83]			
BICYCLIC IMIDAZOLE-4-ONE								
PSB-CB5					Potent AT[84]			
PSB-CB27					Potent AT[84]			
TRICYCLIC XANTHINE								
PSB-KD107					AG[86]			
PSB-KK-1415					Potent AG[88]			

1.3 GPR183

1.3.1 Expression pattern and consequential pathophysiological roles

GPR183, previously known as Epstein-Barr virus-induced gene 2 (EBI2) was identified by Birkenbach et *al*. in 1993 as one of the most upregulated genes in EBV-infected lymphocytes.[95]

The expression pattern of GPR183 varies depending on the cell type and is also tissue-specific. The crucial role of GPR183 activation in the adaptive immune response has been largely demonstrated. GPR183 expression is found in lymphoid tissues, such as spleen, lymph nodes, and Peyer's patches, as well as in peripheral blood leukocytes.[96,97] Different research groups reported a critical role of GPR183 in regulating the migration of B cells during immune activation. Naïve B cells expressed high levels of GPR183, which further increased upon B cell activation. Interestingly, although GPR183 did not seem to directly affect B cell activation and proliferation, B cells deficient in GPR183 led to defective antibody responses *in vivo*. It seems that during the initial phases of B cell responses, GPR183 regulates the movement of activated B cells toward the interfollicular and outer follicular regions. This relocation process is critical for triggering the production of antibodies.[98–100] Furthermore, increased GPR183 expression has been reported in EBV latency III infections, characterized by cell proliferation and conversion of B-cells into lymphoblastoid cell lines.[101] All these findings suggest that, together with some chemokine receptors, GPR183 seems to be a pivotal chemotactic receptor in guiding B cell migration.[102]

The expression of this receptor is substantially defined in other immune cells as well like T cells (highest in Th17 cells and regulatory T cells), dendritic cells, and $CD4^+$ T lymphocytes.[103] Furthermore, it was shown that GPR183 activation reduced bacterial growth during *Mycobacterium tuberculosis* infection in primary human monocytes, through regulation of interferons.[104]

In non-immune tissues, GPR183 expression has been detected in the brain, liver, lung, and adipose tissue. In the Central Nervous System, GPR183 is expressed in astrocytes and has a role in their signaling and migration in response to inflammatory stimuli.[105] In brown adipose tissue, GPR183 expression is induced by the adipogenic transcription factor PPARγ and negatively modulates energy expenditure.[99,106] In the lungs, it is expressed in Pulmonary Conventional Dendritic Cell Type 2, and loss of function or antagonism of the receptor has resulted in beneficial therapeutic

results in both viral and inflammatory respiratory diseases (including SARS-CoV-2 infection).[107–109]

In conclusion, GPR183 acts mainly as a chemotactic receptor in many cell types and since its transcription was strongly observed in areas related to the immune system, it could be a drug target for B cell malignancies and/or for inflammatory/autoimmune diseases like type I diabetes. It could also counteract metabolic diseases like obesity and be beneficial in inflammation-based disorders in the lungs and the brain.

1.3.2 Ligands

In 2011, Hannedouche *et al.* and Liu *et al.* discovered independently that GPR183 responded to some oxysterols, hydroxylated forms of cholesterol. In vitro 7α,25-OHC (7α,25-dihydroxycholesterol) was the most potent ligand followed by 7α,27-OHC (10-fold less potent), while the corresponding mono-hydroxylated molecules 25-HC (25-hydroxycholesterol) and 27-HC (27-hydroxycholesterol) had only a minimal activity. Furthermore, according to in vivo investigations, mice deficient in Ch25h (the gene coding for the enzyme cholesterol 25-hydroxylase — as shown in Figure 10) exhibited impairments in the localization of B and T cells as well as antibody responses comparable to mice lacking GPR183. These findings indicate that 7α,25-OHC might be the exclusive ligand that acts on GPR183 in lymphoid tissues functioning as a chemotactic molecule for B cells,[99,102] although, one study has shown that also 7α,27-OHC operates as a directional signal and unveils a multifaceted function of GPR183 in the positioning of dendritic cells (DCs).[110]

In general, all the aforementioned pathophysiological roles ascribed to GPR183 are mediated by 7α,25-OHC, so that many publications refer to it as the oxysterol-GPR183 axis, specifically relevant for immune regulation, cell positioning, and the orchestration of immune responses. Additionally, although the precise role of GPR183 in EBV infections is not yet fully understood, emerging knowledge suggests that macrophages might produce oxysterols as part of a strategy to fight viral infections.[111]

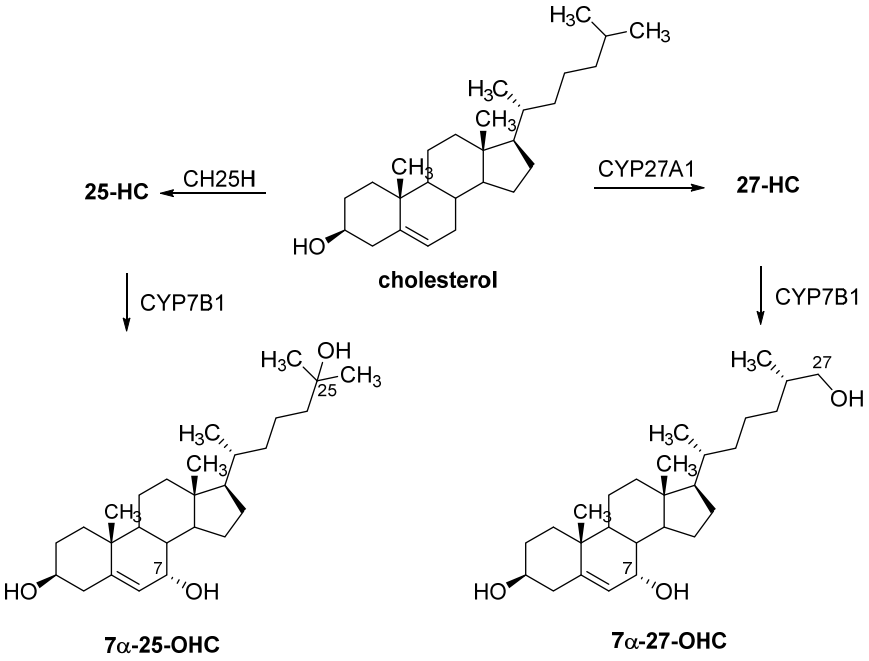

Figure 10. Biosynthesis of the oxysterols 7α,25-OHC (7α,25-dihydroxycholesterol) and 7α,27-OHC (7α,27-dihydroxycholesterol). 25HC: 25-hydroxycholesterol; 27HC: 27-hydroxycholesterol; CH25H: cholesterol 25-hydroxylase; CYP27A1: Cytochrome P450 Family 27 Subfamily A Member 1; CYP7B1: Cytochrome P450 Family 7 Subfamily B Member 1.

As shown in Figure 11, concurrently with the identification and isolation of oxysterols as the endogenous ligands, compound GSK682753A emerged as a potent inverse agonist able to inhibit the apparent constitutive activity. The same authors 2 years later studied the antagonistic properties of this compound, given that the observable constitutive activity of the receptor could have been a result of oxysterol contamination in the medium. It potently suppressed 7α,25-OHC-induced G protein activation, β-arrestin recruitment, B cell chemotaxis, and ERK activation. Their results suggested then that GSK682753A is a competitive antagonist that binds in the same pocket as 7α,25-OHC. Almost simultaneously, another research group identified compound ML401 with a cinnamyl function, as a potent and selective antagonist of GPR183. [112–115]

A later screening campaign helped to identify other small molecule modulators, namely the agonist NIBR51 and the two antagonists NIBR127 and NIBR189. The latter shares the piperazine core and cinnamyl feature with ML401.[116]

Both GSK682753A and NIBR189 were used to build a pharmacophore model for an *in silico* screen of a database of 5 million compounds. As a result, 16 commercially available small molecules were tested for their antagonistic activity towards GPR183 leading to the identification

of SAE-1, SAE-10, and SAE-14 as GPR183 antagonists that inhibit with low nanomolar potency 7α,25-OHC–induced calcium mobilization *in vitro* and reverse nerve injury-induced allodynia in mice.[117,118] Their suitability for in vivo studies was confirmed by the usage of SAE-14 in studies for behavioral hypersensitivity.[119] Recently, SAE-1 was the starting point for the development of novel potent antagonists.[120]

Structures of these potent antagonists and especially the piperazine diamide core of NIBR189 helped more recently in the discovery of new agonists showing low nanomolar potency in Ca^{2+} mobilization assays and BRET assays determining $G\alpha_i$ coupling.[121]

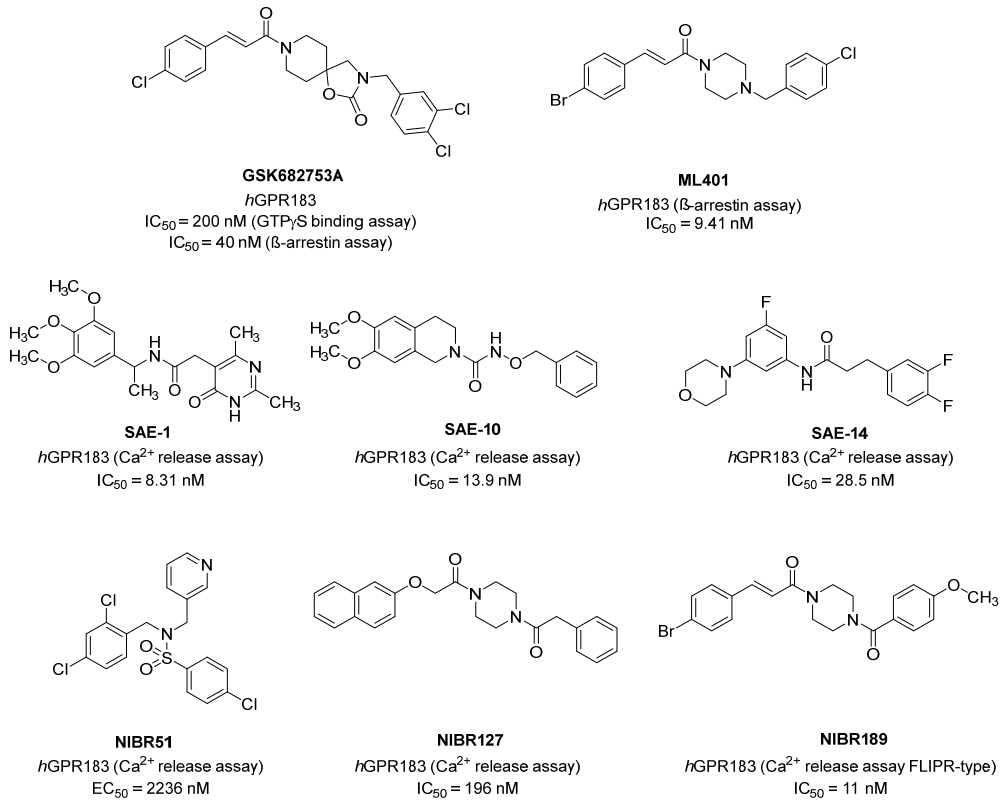

Figure 11. Small molecule modulators of GPR183. See text for references and details.

1.3.3 Signaling and binding mode

All of the abovementioned potent ligands, both agonists and antagonists, were employed as useful pharmacological tools for the discovery of the signaling pathways of GPR183. Other than coupling to $G\alpha_i$, as noted earlier, it is also a strong β-arrestin recruiter.[102,113,114,122]

Using a mutagenic approach and docking simulations with a GPR183 homology model, key residues for the binding of 7α,25-OHC were identified. The same researchers also suggested that Asn114 is a crucial residue influencing the equilibrium between G protein-dependent and G protein-independent pathways, while simultaneously facilitating the interaction with sodium.[114,123]

This binding mode was then recently confirmed by the unveiling of the cryo-EM structures of the active GPR183 in complex with its endogenous agonist 7α,25-OHC, and that of an inactive GPR183 bound to GSK682753A. Indeed 7α,25-OHC binds deeply in a hydrophobic cavity formed by TMIII-VII while a hydrogen bond network is ensured by the residues Tyr116 and Tyr260 engaging the 7-hydroxyl group (which needs to be in the α-position for these bonds to form), Arg87 and Tyr112 binding to the 25-hydroxyl group and Gln162 connecting to the 3β-hydroxyl group. While, similarly to CB_1 and CB_2, the orientation and binding of GPR183 to the heterotrimeric $G\alpha_i$ is possible thanks to the residues Arg144, Asn230, and Pro231. As for the binding of the GSK compound, the cryo-EM studies revealed that it binds less deeply but with a more extensive involvement of TMII. All seven TMs create hydrophobic contacts with the antagonist and the the guanidino group in Arg87 participates in hydrophilic interactions. Finally, the authors also suggested that, due to their low solubility, the endogenous agonists might access the binding site from the lipid bilayer through a gap between TMIV and TMV in the extracellular leaflet rather than from the extracellular lumen, in the same fashion as other δ-subgroup GPCRs.[124]

This last hypothesis led to a deeper investigation of the role of the plasma membrane and especially potential associations between GPR183 and membrane domains, such as lipid rafts or caveolae. This more recent publication sheds light on the complex internalization mechanisms of GPR183, distinguishing between constitutive and ligand-induced internalization. The first one seems to be indeed mainly driven by caveolae and dynamin with the contribution of clathrin-mediated endocytosis (CME) in a β-arrestin- and $G\alpha_i$-independent manner. Ligand-induced internalization was found to have a partial dependence on β-arrestin1/2, as their knockout reduced the efficacy of internalization. The authors were also able to show that the internalization and the main biological function, chemotaxis, are decoupled events in the same fashion as for the chemokine receptor CCR2. In fact, chemotaxis did not happen in the presence of the agonist TUG-2292, which was shown to activate the G protein signaling pathway, but not the β-arrestin pathway. These findings suggest that while β-arrestins may not be pivotal for receptor internalization, they are still crucial

for the chemotaxis, allowing a more rapid method to deactivate signaling hindering the receptor's ability to bind to the G protein.[125]

Once again, the dichotomy between G protein-dependent and -independent signaling pathways plays an important role like for GPR18 and other related receptors.

1.3.4 Comparison between GPR18 and GPR183

As extensively described, GPR18 and GPR183 are two GPCRs that have gained significant attention due to their potential roles in various physiological and pathological processes.

Figure 12. Sequence alignment of human GPR183 and human GPR18, performed using Clustal Omega version 1.2.4 (https://www.ebi.ac.uk/jdispatcher/msa/clustalo).[126] *The input sequences are shown on the left. Amino acids involved in the 7α,25-OHC binding site of GPR183 are highlighted in yellow. The conservation score symbols used are as follows: "*" indicates that the amino acids in that column are identical across all sequences in the alignment; ":" indicates that the amino acids in that column have conserved substitutions—while not identical, they share similar properties (e.g., size or charge) and can perform similar functions; "." for semi-conservative substitutions; "-" represents a gap in the sequence alignment.*

Despite all the classifications and clustering of GPCRs proposed over the years, the close relation between GPR18 and GPR183 seems constant. They are located in the same chromosomal region,

13q32.3, only with a 33 kbp difference, and, similarly to some chemokine receptors, they may have evolved from gene duplication events.[50,122]

Having a ~27% sequence identity and 37% sequence similarity, GPR18 and GPR183 have a good deal of structural analogy (Figure 12).[50]

As summarized in Table 2, an in-silico analysis has highlighted that they share similar physical and chemical properties like the number of amino acids, number of atoms, and theoretical isoelectric point. Interestingly, both receptors are hydrophobic proteins. The secondary structure of these two proteins shows the characteristics of typical GPCRs, mainly consisting of α-helix and random coil.[127]

Table 2. In silico comparison of the protein structure of GPR18 and GPR183. Summarized from Li et al. [127]

Property		GPR18	GPR183
Number of amino acids		331	361
Number of atoms		5465	5861
Theoretical isoelectric point		9.38	9.31
The most hydrophobic amino acid		Ile-35	Ile-250
The most hydrophilic amino acid		Lys-165	Arg-344
Number of hydrophobic amino acids		301.68	275.966
Number of hydrophilic amino acids		120.446	138.401
Phosphorylation site	Serine	21	24
	Threonine	26	22
	Tyrosine	17	14
Secondary structure	α-helix	47.43 %	30.51 %
	Random coil	42.35 %	35.73 %

As for the endogenous ligands, for GPR18 the only disputed agonist up to date is Δ^9-THC, while it has been widely recognized that GPR183 responds to oxysterols. Overall, despite the different ligand binding profiles, both receptors respond to lipophilic molecules.

The signaling cascade elicited by those agonists is also quite different. No confirmed G protein coupling exists for GPR18, while activation of GPR183 initiates $G\alpha_{i/o}$-dependent signaling pathways. It is noteworthy that both receptors show strong recruitment of β-arrestin.

With regards to their distribution, they are highly expressed in organs and tissues related to the immune system, with the highest overlap in lymph nodes, small intestine and spleen, and Peripheral Blood Mononuclear Cells (PMBCs). They also share a moderate expression in lung tissue, but GPR18 was also found in different areas of the brain. On the contrary, GPR183 has a low expression in the brain, whereas it seems to exhibit a more specialized distribution in B cells and dendritic cells. The distinct expression profiles of these receptors indicate their involvement in different immune-related processes.[80,122]

In conclusion, these receptors share a high degree of structural analogy, and together with their similar expression pattern and close chromosomal localization, they might have related biological functions and play a key immunomodulatory role. Whether they are co-regulated is yet to be determined, but understanding the similarities and differences between GPR18 and GPR183 is essential for unraveling their specific roles and developing potential therapeutic strategies.

2. BACKGROUND AND AIM OF THE STUDY

2.4 GPR18 agonists

To develop potent and selective agonists for GPR18, a screening campaign of a xanthine sub-library of the Pharma-Zentrum Bonn compound library was performed using the β-arrestin recruitment assay.[87]

As a result, compound **PSB-KD-107** was discovered as a potent GPR18 agonist with an EC_{50} value of 0.556 μM. It showed high selectivity for GPR18 versus other cannabinoid-responsive receptors, namely GPR55, CB_1, and CB_2 receptors. It consists of a xanthine moiety annealed with a tetrahydropyrimidine and an indolylethyl residue. [6,86]

Optimization of the hit compound was performed considering SAR analysis and variables such as target selectivity, and ease of chemical synthesis.

The tricyclic core has been proven to be not essential and it offers limited possibilities for substitution, leading to a focus on preserving the xanthine-based framework while exploring extensive variations at the *N*1, *N*3, and especially the *N*7 positions (Figure 13).

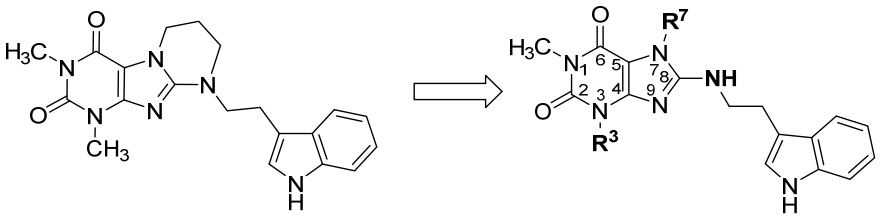

*Figure 13. Optimization of **PSB-KD107.***

Previous SAR analysis revealed that a substituent at *N*1 was indeed necessary — with the unsubstituted derivative showing a 17-fold reduction in activity, but it demonstrated strict tolerance for only a methyl group.[87,88] *N*3 and especially *N*7 offered more room for exploration.

A selection of previously synthesized compounds from Mahardhika et *al.*, useful to later describe the design rationale for the molecules in this work, is reported in Tables 1-3.[88]

Table 3: Compounds bearing a substituent on N7 of the xanthine core

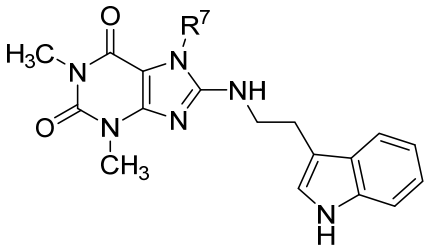

Cmpd.	R^7	Human GPR18 Agonistic activity (% activation)[a] [Efficacy][b]
MZ 1416	CH_3	**0.902** ± 0.148 [132%]
MZ 1412	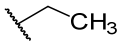	**0.190** ± 0.043 [113%]
MZ 1411	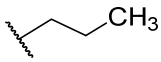	**0.196** ± 0.059 [127%]
MZ 1413	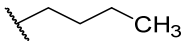	**0.151** ± 0.045 [103%]
MZ1437	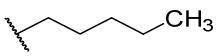	**0.0602** ± 0.0108 [111%]
MZ1438	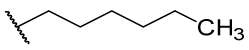	**0.127** ± 0.034 [110%]

MZ1439		**0.0614** ± 0.0136 [69%]
MZ1440	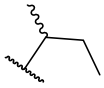	**0.0532** ± 0.040 [45%]
MZ1441	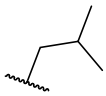	**0.204** ± 0.042 [122%]
MZ1443		**>10** (36%)
MZ 1449	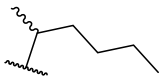	**0.048** ± 0.006 [119%]
MZ 1432	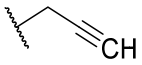	**0.247** ± 0.036 [90%]
TH75	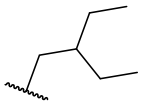	**0.0504** ± 0.0021 [68%]
TH76	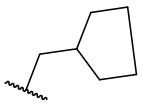	**0.0361** ± 0.0050 [69%]
TH78	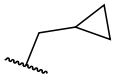	**0.0500** ± 0.043 [88%]
TH79	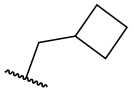	**0.0503** ± 0.0158 [84%]
MZ 1414	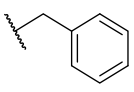	**0.149** ± 0.056 [134%]

MZ 1455	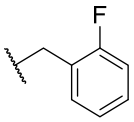	**0.137** ± 0.032 [123%]
MZ 1460	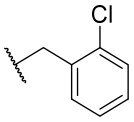	**0.0604** ± 0.0122 [169%]
MZ 1454	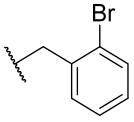	**0.189** ± 0.027 [148%]
MZ 1448	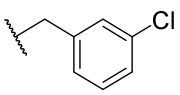	**0.0711** ± 0.0174 [85%]
MZ 1456	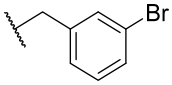	**0.101** ± 0.013 [134%]
MZ 1452	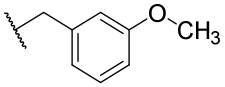	**0.166** ± 0.024 [122%]
MZ 1451	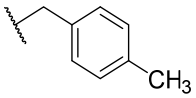	**0.0246** ± 0.051 [117%]
MZ 1463	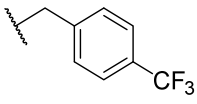	**0.136** ± 0.017 [111%]
MZ 1461	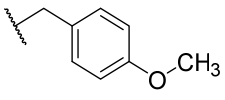	**0.138** ± 0.013 [121%]
MZ 1462	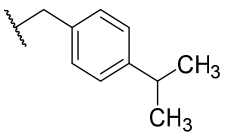	**0.352** ± 0.096 [111%]

NBO G27	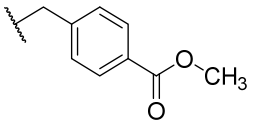	**0.469** ± 0.074 [125%]
NBO G31	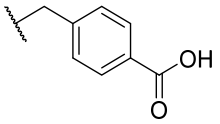	**>10** (8%)
NBO G100	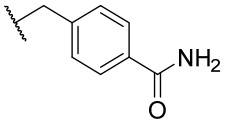	**3.60** ± 0.19 [88%]
NBO G128	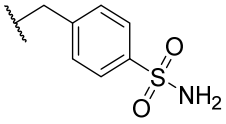	**6.64** ± 2.68 [70%]
NBO G130	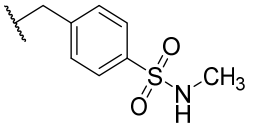	**3.67** ± 1.07 [116%]
MZ 1445	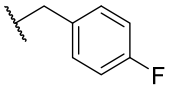	**0.0454** ± 0.081 [84%]
PSB-KK-1415	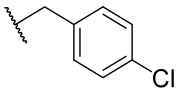	**0.0191** ± 0.0034 [141%]
MZ 1446	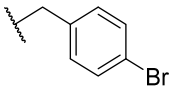	**0.0724** ± 0.547 [65%]
MZ 1457	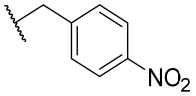	**0.0426** ± 0.0155 [98%]
MZ 1442	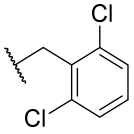	**0.347** ± 0.0136 [45%]

MZ 1444	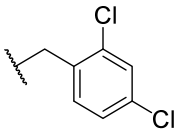	**0.0642** ± 0.0308 [72%]
NBO G7	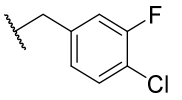	**0.0801** ± 0.0131 [110%]
MZ 1509	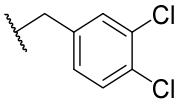	**0.0741** ± 0.023 [82%]
NBO G66	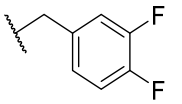	**0.142** ± 0.019 [113%]
NBO G67	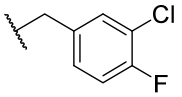	**0.193** ± 0.028 [110%]
MZ 1453	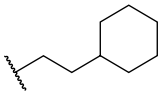	**0.102** ± 0.024 [103%]
MZ 1417	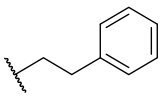	**0.442** ± 0.152 [155%]
MZ 1418	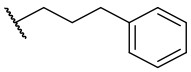	**0.120** ± 0.027 [176%]
MZ 1429	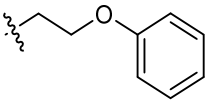	**0.229** ± 0.048 [64%]
MZ 1430	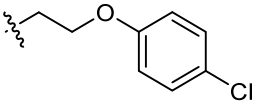	**0.417** ± 0.173 [64%]

NBOG68	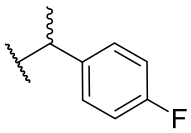	**0.0579** ± 0.004 [82%]
NBOG110	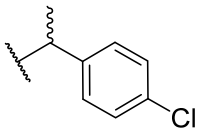	**0.0230** ± 0.0054 [114%]
NBOG135	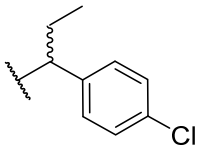	**0.0258** ± 0.0078 [98%]

*[a]Compounds were tested at a concentration of 10 µM. Effects were normalized to the signal induced by 10 µM THC (for human GPR18) or 0.3 µM of **PSB-KK-1415** (for mouse GPR18) .[b]Efficacy relative to the maximal effect of the standard agonist (30 µM THC for human GPR18; 3 µM of **PSB-KK-1415** for mouse GPR18) set at 100%.*

As shown in

Table 3, the substitution of the *N7* position with lipophilic aromatic groups proved to increase the activity, with *p*-substitutions preferred over *meta* and *ortho,* and surprisingly no additional benefit on the activity for di-substitutions on the ring.

Finally, compounds bearing a "branched" substituent on the benzylic carbon (**NBOG68, G110, G135**), showed comparable results to the molecule that showed the highest activity, namely **PSB-KK-1415** (EC_{50} = 0.0191 µM).

Once established that a *p*-chlorobenzyl moiety was the best on *N*7, some modifications on N3 were attempted (Table 4).

Table 4. Compounds bearing a substituent on N3 of the xanthine core.

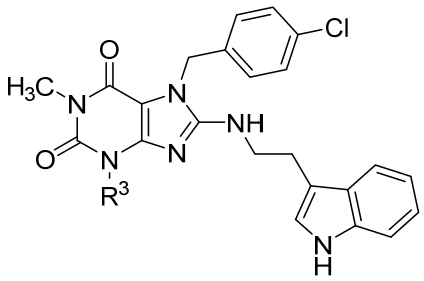

Cmpd.	R^3	Human GPR18 Agonistic activity (% activation)[a] [Efficacy][b]
MZ1445		**0.0191** ± 0.0034 [141%]
NBO G54	H	**0.206** ± 0.023 [100%]
MZ 1508	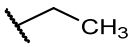	**0.0950** ± 0.0069 [85%]
NBO G46	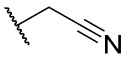	**1.22** ± 0.17 [70%]
NBO G41	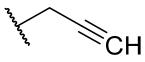	**>10** (18%)
NBO G18	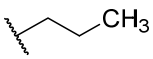	**>10** (45%)
NBO G24	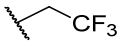	**0.486** ± 0.072 [75%]
NBO G47	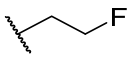	**0.351** ± 0.017

		[78%]
NBO G23	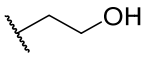	**1.63** ± 0.13 [80%]
NBOG42	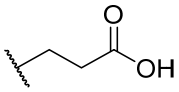	**> 10** (5%)
NBOG139	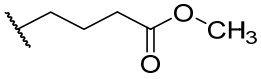	**0.415** ± 0.180 [88%]
NBOG140	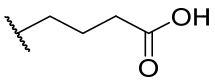	**1.55** ± 0.28 [98%]
NBO G33	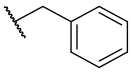	**>10** (4%)

*[a]Compounds were tested at a concentration of 10 µM. Effects were normalized to the signal induced by 10 µM THC (for human GPR18) or 0.3 µM of **PSB-KK-1415** (for mouse GPR18).[b]Efficacy relative to the maximal effect of the standard agonist (30 µM THC for human GPR18; 3 µM of **PSB-KK-1415** for mouse GPR18) set at 100%.*

Modifications on *N*3 revealed also some limited space for exploration and, similarly to position *N*1, only a methyl seems to be best tolerated whereas a naked NH resulted in a ~11-fold decrease in the activity (**NBO G54**).

Subsequently, an investigation on the indolylethylamino portion was performed resulting in the compounds shown in

Table 5.

The indole residue proved to be crucial for GPR18 activation. No improvement was achieved by substitutions on the ring, bioisosteric replacements, or alkylation of the indole NH (**TH20A, TH25A**).

Additionally, a steep loss in activity was the result of alkylating the amino group of the ethylamino linker (**TH20B**).

Table 5. Compounds with modifications in the indolylethylamino partial structure.

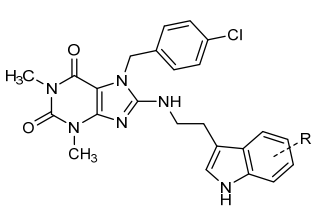

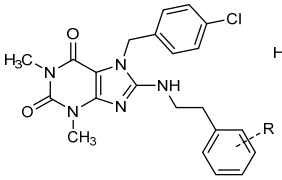

TH2, TH8, TH4

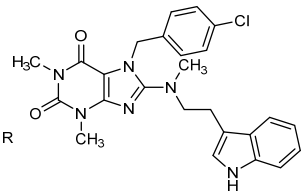

TH20B

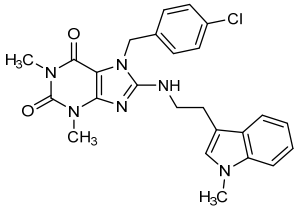

TH20A

Cmpd.	R	Human GPR18 Agonistic activity (% activation)[a] [Efficacy][b]
PSB-KK-1415	-	**0.0191** ± 0.0034 [141%]
TH38	5-OCH_3	**0.299** ± 0.173 [111%]
MZ1464	5-OH	**0.340** ± 0.069 [114%]
TH53	6-OCH_3	**>1** (39%)
NBOG34	6-Cl	**1.37** ± 0.09 [60%]
NBOG48	2-CH_3	**0.557** ± 0.025 [81%]
NBOG49	4,5-F	**0.827** ± 0.057 [53%]
NBOG53	6-F	**0.0711** ± 0.008 [121%]
NBOG76	2-CH_3, 5-OCH_3	**0.644** ± 0.104 [98%]
NBOG102	7-OCH_3	**1.66** ± 0.13 [60%]
TH 2	4-OH	**>10** (3%)

TH 8	3,4-OH	**>10** (4%)
TH 4	3,4-OCH_3	**>10** (4%)
TH20B	-	**>1** (45%)
TH20A	-	**0.0701** ± 0.0221 [70%]

*[a]Compounds were tested at a concentration of 10 µM. Effects were normalized to the signal induced by 10 µM THC (for human GPR18) or 0.3 µM of **PSB-KK-1415** (for mouse GPR18).[b]Efficacy relative to the maximal effect of the standard agonist (30 µM THC for human GPR18; 3 µM of **PSB-KK-1415** for mouse GPR18) set at 100%.*

As summarized in Figure 14, the hit-to-lead process led to the identification of the most potent non-lipid agonist known to date: 8-((2-(1*H*-indol-3-yl)ethyl)amino)-7-(4-chlorobenzyl)-1,3-dimethyl-1*H*-purine-2,6(3*H*,7*H*)-dione (**PSB-KK-1415**) with an EC_{50} value of 0.0191 µM.[88]

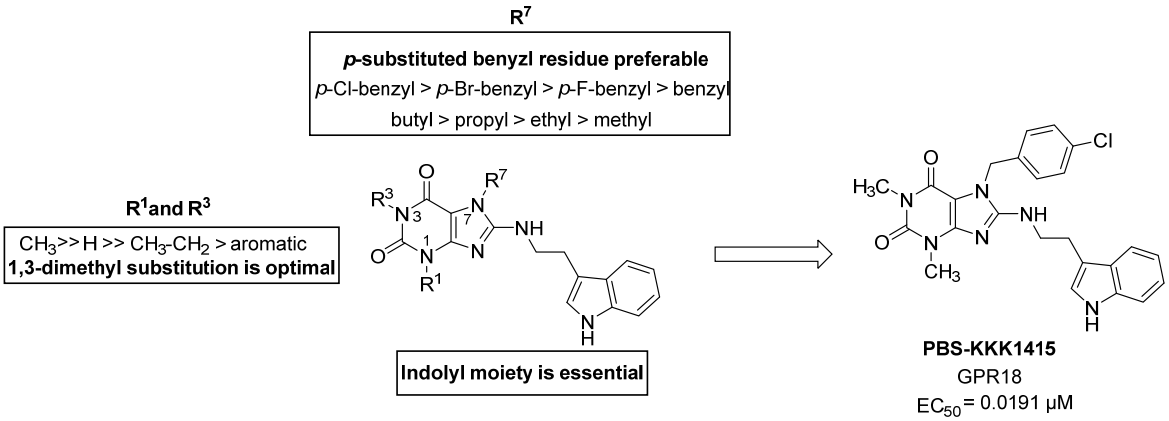

Figure 14. Previous SAR studies on the indolylethylaminoxanthine scaffold.

PSB-KK1415 is the perfect starting point for a more in-depth study.

In this study, compounds will be rationally designed with a major focus on *N*7. The goal is to both increase potency enough to make a radiolabeled ligand and/or to find a suitable linkage position to obtain fluorescent probes to establish a BRET (Bioluminescence Resonance Energy Transfer) assay that could be used to directly measure ligand affinities and residence times.

In fact, at present, the only method used by our group to test GPR18 ligands is the β-arrestin recruitment assay. Developing a second assay determining affinities and activities of ligands is required.

A fluorescent receptor ligand consists of three parts: the pharmacophore, the fluorophore, and the linker region (different in length and composition) connecting these two pieces. Furthermore, every new molecule generated by combinations of these elements must be treated as an individual pharmacological entity.[128]

Compounds bearing suitable functional groups and different linkers will be designed and tested.

As for the fluorophores, optimization of the reaction conditions for the synthesis of different dyes will be performed and they will afterwards be used on the most promising combination of pharmacophore and linker.

Modifications on the xanthine core as well as the indolylethylamino moiety will still be performed but with lower priority.

Finally, rational design will involve attempts at improving physicochemical properties of the target compounds.

2.5 GPR183 antagonists

During our research on GPR18 agonists, some prominent compounds were also tested for their activity towards GPR183, being two very closely related receptors.

Among those compounds, an indolylethylamino benzamide (**FPE-48B,** Figure 15), while not showing any remarkable activity for GPR18, stood out as a promising antagonist for GPR183 with an IC_{50} value in the micromolar range, determined in a β-arrestin recruitment assay.

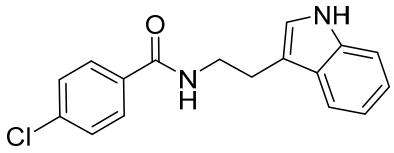

FPE-48B

IC_{50}= 4.06 ± 0.09 μM

*Figure 15. Structure and antagonistic activity of **FPE-48B**.*

This small molecule has some features in common with the most potent GPR183 antagonists known to date (Figure 11), like the amide bond and the *p*-chlorophenyl moiety at the outermost part of the molecule.

The majority of these known compounds also present nitrogen-containing aliphatic ring systems like piperazine or morpholine, as well as a characteristic cinnamyl moiety.

Information on the above-mentioned molecules, and especially the two most active ones (**ML401** and **NIBR189**) will be used for the design and synthesis of new GPR183 ligands.

Three main series will be synthesized: benzoic acid amides, piperazine derivatives, and cinnamic acid amides (Figure 16).

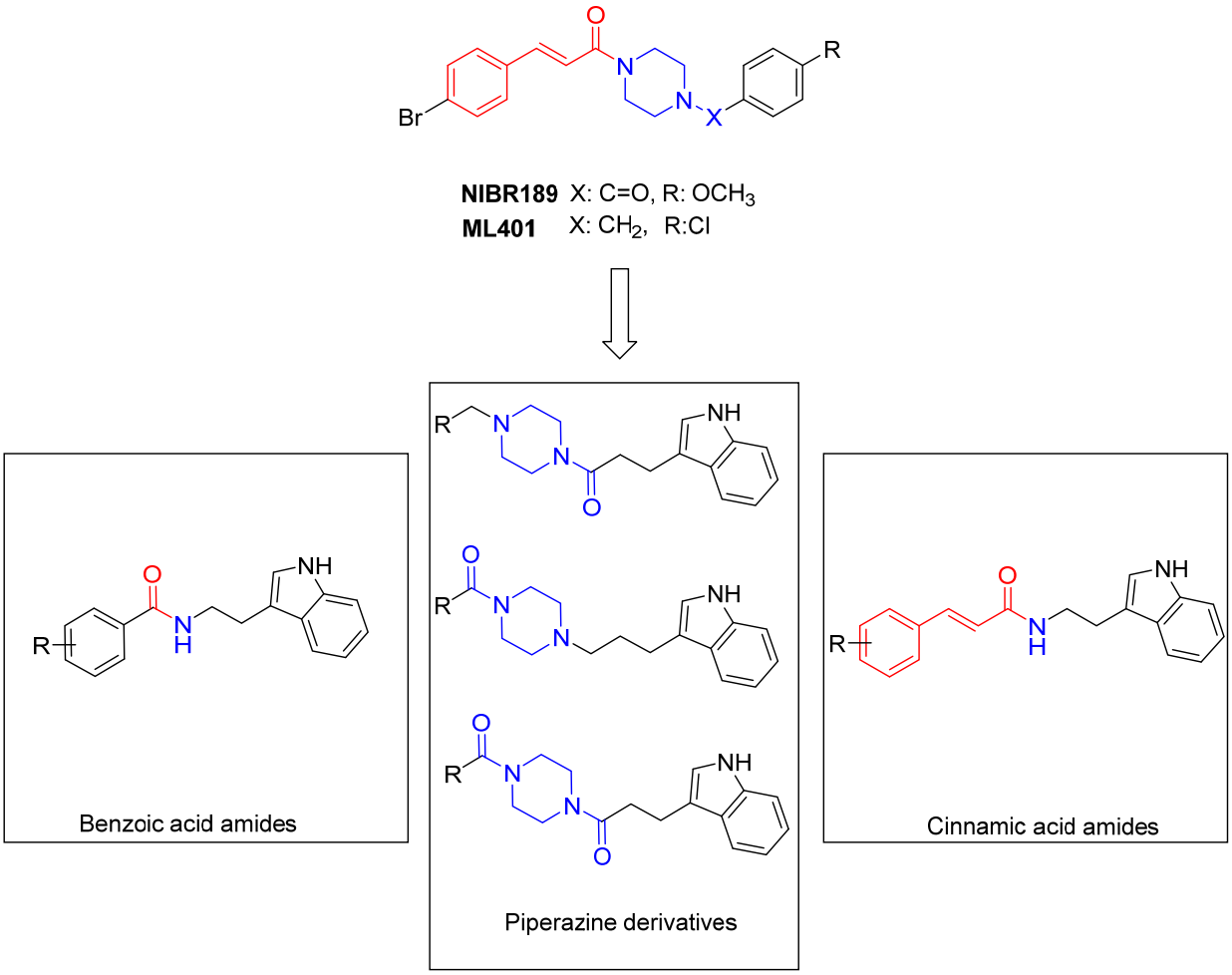

Figure 16. Target molecules for GPR183 antagonists.

3 RESULTS AND DISCUSSION

3.1 Synthesis of ligands for GPR18 based on the 8-(indolylethylamino)xanthine scaffold

3.1.1 Modifications on the *N*7-position of the xanthine core

3.1.1.1 Synthetic approaches

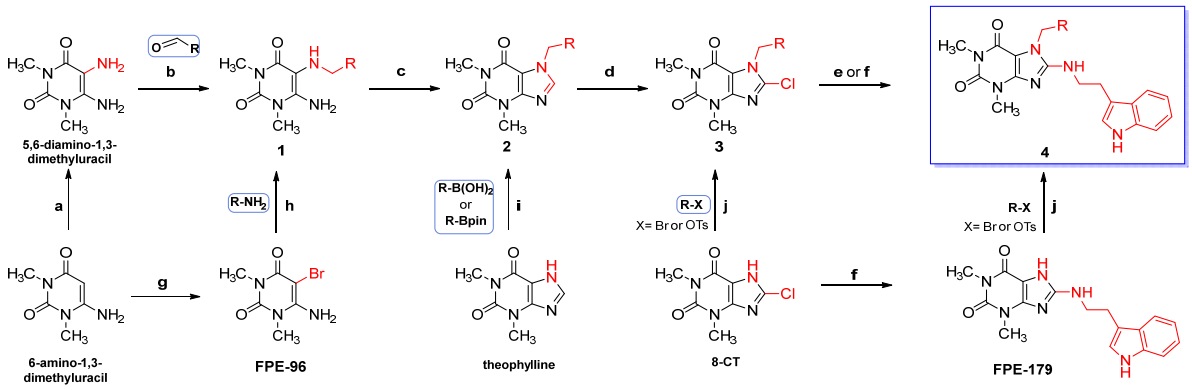

Scheme 1. Strategies for the synthesis of the xanthine ligands. Conditions: ***a:*** *i) $NaNO_2$, AcOH (50% water), 10 min, 65°C; ii) $Na_2S_2O_4$, NH_4OH (12.5 % in water), 10 min, 70°C;* ***b:*** *i) AcOH, H_2O, RT, 15 min; ii) $NaBH_3CN$, AcOH, DCM: MeOH (1:1) RT, 16h;* ***c:*** *TEOF, 145°C, 5h;* ***d:*** *NCS, THF, RT, 16h;* ***e:*** *Tryptamine, DIPEA, NMP, 145°C, 18h;* ***f:*** *tryptamine, DIPEA, NMP, 195°C, 22 min, 150 W;* ***g:*** *NBS, ACN, reflux, 1.5h;* ***h:*** *Et_3N, DMF, 120°C, 24h;* ***i:*** *Na_2CO_3, $Cu(OAc)_2$, Bipy, DCE, 70°C, 5h;* ***j:*** *K_2CO_3, DMF, RT, 2.5 h. DCM: Dichloromethane; TEOF: triethylorthoformate; NCS: N-chlorosuccinimmide; THF: tetrahydrofuran; DIPEA: N,N-Diisopropylethylamine; NMP: N-methyl-2-pyrrolidinone; NBS: N-bromosuccinimmide; ACN: acetonitirile; DMF: dimethylformamide; Bipy: 2,2'-bipyridine; DCE: dichloroethane; 8-CT: 8-chlorotheophylline.*

As shown in Scheme 1 many different synthetic approaches were used to achieve substitution on *N*7 of the xanthine core. The strategy strongly depended on the functional group that the desired substituent (R) was bearing. Many times, different approaches were used simultaneously to obtain the tearget compound, in which case rate of success and/or yields are reported.

The longest strategy, hereinafter strategy I, proceeds all the way from reaction a to f (*Scheme 1*). It starts with the commercially available 6-amino-1,3-dimethyluracil and with a sequence of nitrosation followed by the reduction of the nitroso group in the presence of sodium dithionite, yielding the desired diamino uracil derivative. This building block is then available to react with diverse benzaldehydes to give first the corresponding Schiff base which is reduced to the secondary amine (structure **1**). Ring closure is achieved with triethylorthoformate (structure **2**) and this *N*7-substituted theophylline is then chlorinated at position *C*8 with NCS (strucure **3**).[129] The final step involves coupling with tryptamine to achieve the wanted final compounds (structure **4**).[88]

Strategy II, is somehow comparable to the previously mentioned one, but in this case the 6-amino-1,3-dimethyluracil is brominated in position *C*6 (**FPE-96**) so that the corresponding secondary amine can be obtained by S_NAr with the appropriate primary amine (reaction h).[130] Ring closure, chlorination and tryptamine coupling follow as per usual (reactions c-f).

With strategy III one step can be avoided. The reaction of theophylline with the appropriate boronic acid or its pinacol ester via Chan-Lam-Evans coupling allowed to achieve *N*7-substituted derivatives otherwise unfeasible. It is a cross-coupling reaction catalyzed by a copper complex leading to an aryl amine (reaction i). The reaction is conducted in air allowing oxygen to reoxidize copper in the catalytic cycle. Chlorination and tryptamine coupling follow the same standard procedure as before (reactions d-f).

Strategy IV simply involves the direct usage of 8-chlorotheophylline (8-CT) and an alkylating agent being an alkyl bromide or a tosylated alcohol with the appropriate residue and proceeds according to a standard S_N2 reaction (reaction j). S_NAr with tryptamine follows generating the final compounds in only two steps.

Finally, the reaction conditions of the coupling between 8-chlorotheophylline and tryptamine were optimized by performing it under microwave irradiation. With strategy V, this building block with a naked *N*7 (**FPE-179**) was used to generate final compounds especially when the desired substituent could be damaged by the harsh coupling conditions.

3.1.1.2 Variously substituted benzyl moieties

The *p*-nitro-benzyl derivative (**MZ1457**) was one of the most active compounds with an EC_{50} value of **0.0426** μM. Therefore, bioisosteric substituents were tried as well (Figure 17). Among these, -CO_2Me, -CO_2H, $CONH_2$, -SO_2NH_2 and -SO_2NHCH_3 moieties at the *p*-benzyl residue were all less active.

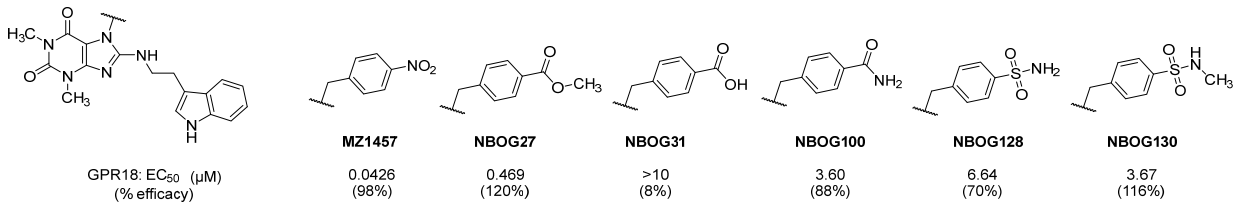

*Figure 17. Biological activity of the p-nitrobenzyl bearing compound **MZ1457** and its bioisosteres.*

These findings further demonstrate that increased lipophilicity is crucial for activity. The methylated carboxylic acid and sulfonamide derivatives (**NBOG27** and **NBOG130**) were significantly more potent, showing a 21-fold (**NBOG31**) and 1.8-fold (**NBOG128**) increase in activity compared to their non-alkylated counterparts. To explore this trend further, a sulfonamide with longer alkyl chain was synthesized. Similarly, since the non-substituted amide was already twice as potent (**NBOG100,** EC_{50} 3.60 μM) as the sulfonamide analog (**NBOG128**, EC_{50} 6.64 μM) an alkylated amide derivative was also synthesized for comparison.

In the case of **FPE-15**, bearing a propyl sulfonamide group, synthesis started from the preparation of the alkylating agent: 4-(bromomethyl)benzenesulfonyl chloride and 1-propylamine were reacted as shown in Scheme 2, yielding **FPE-11**.

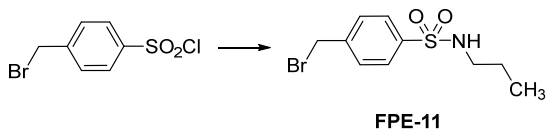

FPE-11

*Scheme 2. Synthesis of **FPE-11.** Conditions: propylamine, DCM, RT, 20h.*

The product of the reaction (**FPE-11)** was used as shown in Scheme 3 to alkylate 8-chlorotheophylline according to strategy IV.

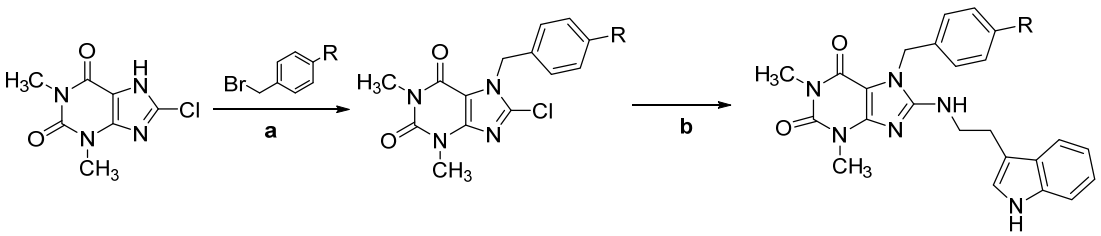

FPE-14, FPE-75, FPE-26

FPE-15, FPE-76

c → **FPE-27**

c → **FPE-29**

d → **FPE-31**

R=
FPE-14, FPE-15: $SO_2NHCH_2CH_2CH_3$
FPE-75, FPE-76: $COCH_3$
FPE-26, FPE-27: CO_2CH_3
FPE-29: CO_2H
FPE-31: $CONHCH_2CH_2CH_3$

*Scheme 3. Synthesis of derivatives **FPE-15, FPE-27, FPE-76, FPE-29, FPE-31.** Conditions: **a)** K_2CO_3, DMF, RT, 2.5 h; **b)** tryptamine, DIPEA, NMP, 145°C, 18h; **c)** LiOH · H_2O, THF, RT, overnight; **d)** propylamine, Et_3N,T3P, DCM, RT, overnight. T3P: Propylphosphonic anhydride.*

As for the corresponding propylamide derivative, after the resynthesis of the *p*-methoxy derivative **FPE-27** via strategy IV, hydrolysis of the ester with LiOH to get the corresponding carboxylic acid and subsequent amide coupling of the latter with propylamine in the presence of the coupling agent T3P led to the wanted product **FPE-31**. Finally, to have a complete overview of the effect of the carbonyl in this position, **FPE-76** was synthesized.

As shown in Figure 18, the biological test results show once again an improvement in the activity when comparing to the free amide (**NBOG100**) and to the corresponding *N*-propylsulfonamide (**FPE-15**).

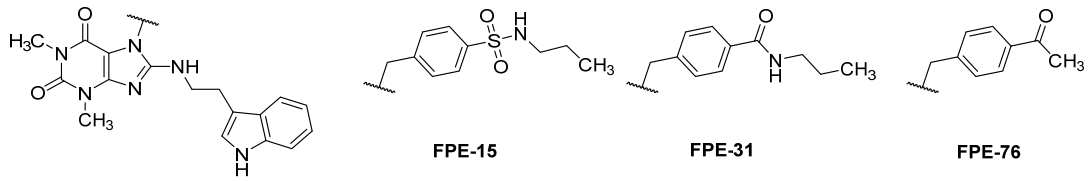

*Figure 18. Biological activity of **FPE-15, FPE-31 and FPE-76.***

As shown in Figure 20, another compound that showed some good activity was **MZ1461** bearing a methoxy group in the *p*-position. Therefore, the same strategy of testing out longer, bulkier chains was planned. As shown in Scheme 4, after the resynthesis of the *p*-methoxy derivative by the noted strategy IV, a demethylation with BBr_3 was performed getting to the desired compound **FPE-13**. As aforementioned, further steps would include alkylation on the hydroxyl moiety. Nevertheless, theoretically, alkylation of **FPE-13** may have not been straightforward on the target hydroxyl group due to the presence of an *–NH* group in the ethylamino chain of tryptamine that may have interfered. Therefore, while synthesizing **FPE-13**, another synthetical strategy was applied: performing the demethylation reaction on **FPE-8**, getting to **FPE-16**. Initially, we were aiming at alkylating the *p*-hydroxy moiety of **FPE-16**. Thus, **FPE-16** was reacted with 1-bromo-2-fluoroethane in the presence of Cs_2CO_3 as a base in DMF.[131] These turned out to be very harsh conditions since many by-products were formed, the most abundant one being **FPE-17B**. Following the reaction over time, it appeared most likely that alkylation on the hydroxyl group may initially occur, followed by debenzylation and subsequent reaction of excess alkylating reagent. The side-product **FPE-17B** was isolated and further reacted with tryptamine to yield **FPE-22**.

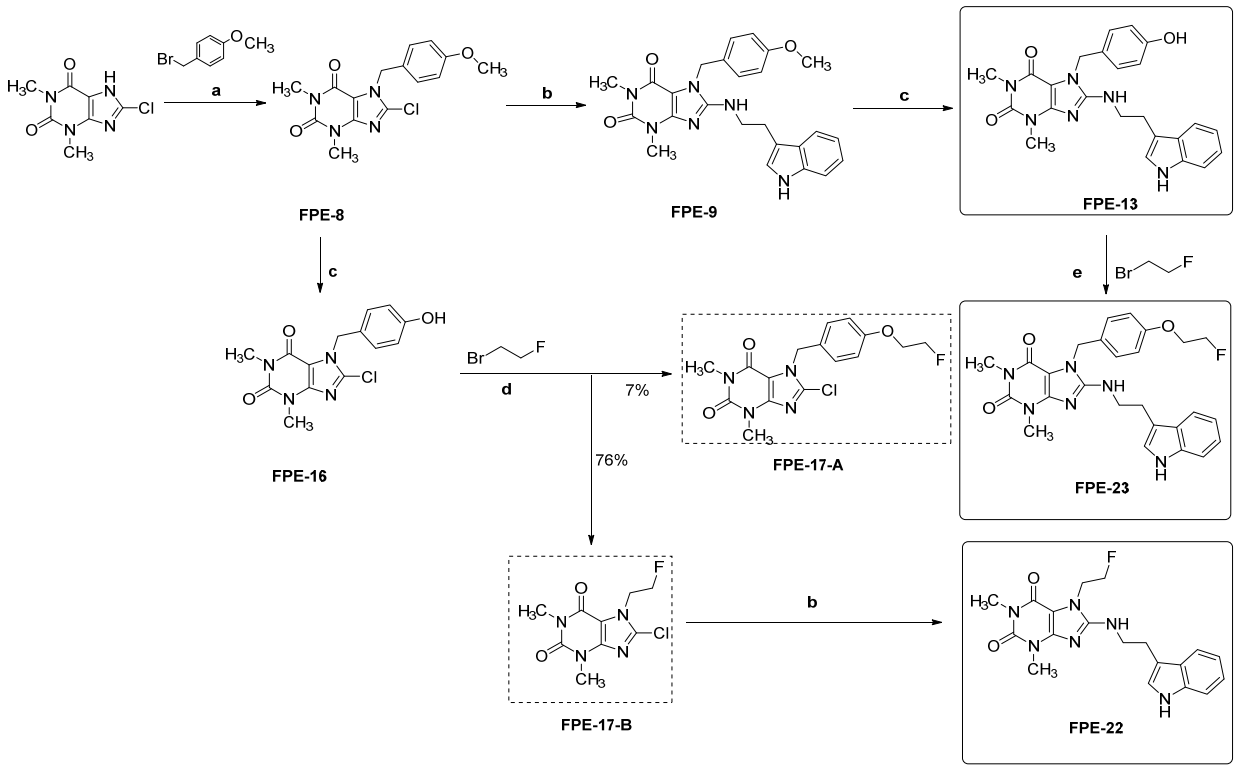

Scheme 4. Synthesis of the p-hydroxy derivative and its alkylation approaches. Conditions: ***a)*** *K_2CO_3, DMF, RT, 2.5 h;* ***b)*** *tryptamine, DIPEA, NMP, 145°C, 18h;* ***c)*** *BBr_3, DMF, 5°C, 3h;* ***d)*** *Cs_2CO_3, 60°C, 2.5h;* ***e)*** *K_2CO_3, DMF, 80°C, overnight.*

As shown in Table 6**,** other attempts to optimize the reaction conditions for the alkylation of **FPE-16** with 1-bromo-2-fluoroethane did not result in any improvement to get the desired product **FPE-17-A.**

Table 6. Reaction conditions for the alkylation of ***FPE-16****.*

Base	**Time (h)**	**Temperature (°C)**	**Comment**
Cs_2CO_3	2.5	60	See text
Cs_2CO_3	2.5	25	No go
K_2CO_3	16	25	No go

No other experiments were made in this direction because, as reported in Scheme 4, the parallel attempt of alkylation of **FPE-13** in the presence of K_2CO_3 at 80°C overnight yielded the initially desired compound **FPE-23**.

The rationale for selecting the 2-fluoroethyl moiety aligns with insights gained from another promising compound series in our group, which showed activity as GPR18 agonists (unpublished results), facilitating the transfer of SAR knowledge.

Given the moderate activity shown by similar alkyl substituents in this position (EC_{50}= 0.190 µM for ethyl — **MZ1411** and EC_{50}= 0.196 µM for propyl — **MZ1412**), **FPE-22** was deemed interesting. However, as shown in Figure 19, it did not result in any improvement compared to the related compounds.

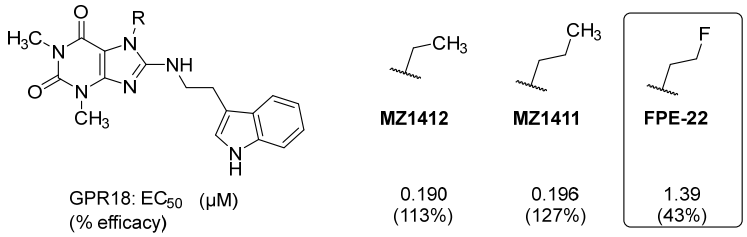

*Figure 19. Biological activity of compounds **MZ1412** and **MZ1411** in relation to **FPE-22.** Framed: newly synthesized compound.*

Much differently and to our own surprise, as shown in Figure 20, **FPE-13** bearing a free hydroxy group resulted in a 3.5-fold increase in potency compared to the corresponding methoxy group of **MZ1461**. Increasing the length of the alkyl chain with a fluoroethoxy residue in **FPE-23** decreased the activity, but was still tolerated. This could be later explored for the eventual attachment of a longer linker.

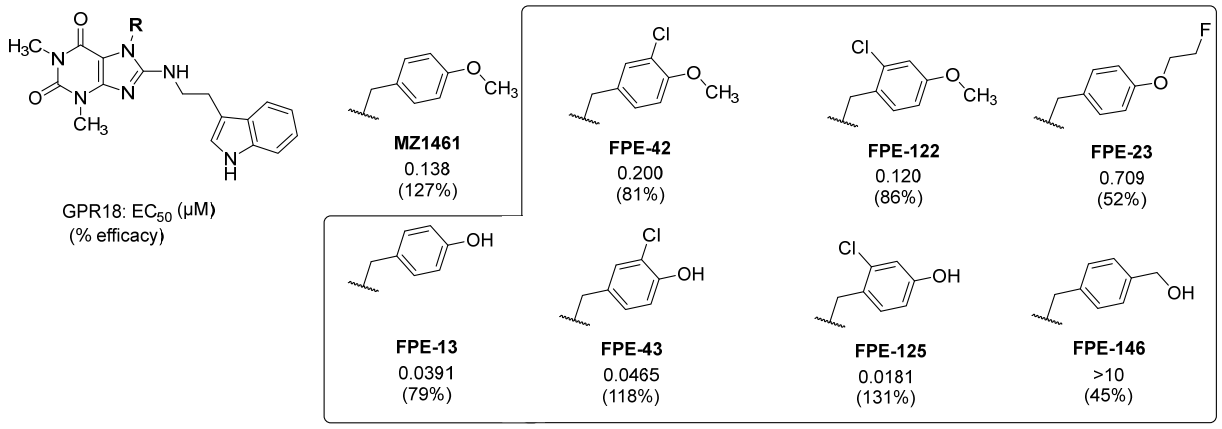

*Figure 20. Biological activity of compounds related to the p-methoxybenzyl derivative **MZ1461**. Framed: newly synthesized compounds.*

Despite the lack of any remarkable improvement in activity shown by di-substitueted derivatives in previous SAR studies (

Figure 21), four more compounds were synthesized, where OH was kept in the *p*-position and an additional substituent was chosen for the *m*- or *o*-positions (Figure 20).

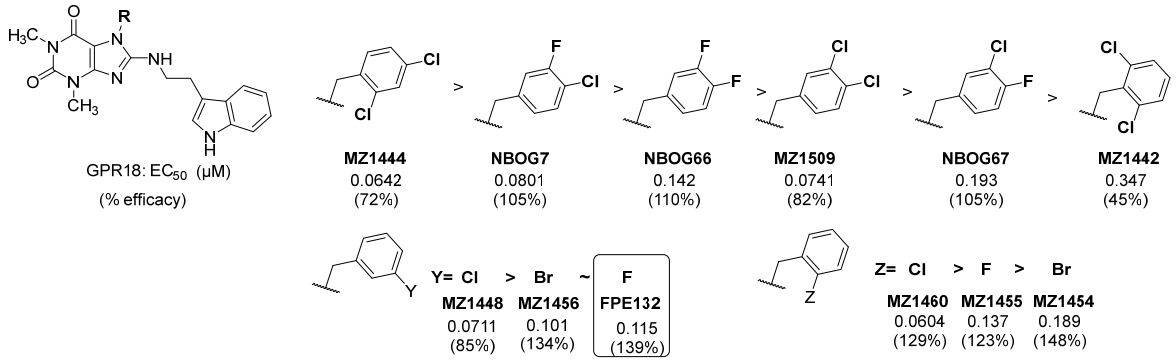

Figure 21. Biological activity of previously synthesized derivatives bearing disubstituted, m-substituted and o-substituted benzyl moieties. Framed: newly synthesized compound.

Halogens were shown to be the best among all the substituents on the benyzl ring. To complete the SAR studies, one additional compound, **FPE-132**, bearing a *m*-fluorobenzyl moiety, was synthesized according to strategy IV (*Scheme 1*) and did not show an improvement in potency as compared to chlorine (

Figure 21). As a conclusion, in addition to the *p*-hydroxy group, chlorine was picked as the other main substituent on the ring because it showed the best activity both in *m*- and *o*-positions (**MZ1448, MZ1460**).

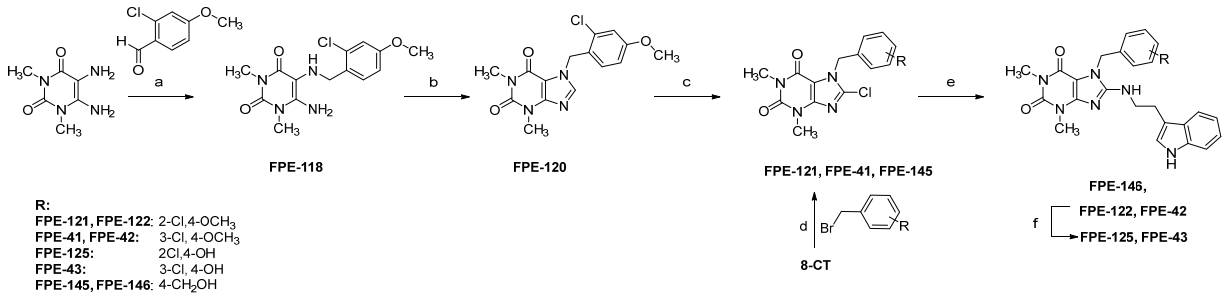

*Scheme 5. Synthesis of compounds **FPE-42, FPE-122, FPE-125** and **FPE-43.** Conditions: **a)** i) AcOH, H_2O, RT, 15 min; ii) $NaBH_3CN$, AcOH, DCM: MeOH (1:1) RT, 16h; **b)** TEOF, 145°C, 5h; **c)** NCS, THF, RT, 16h; **d)** K_2CO_3, DMF, RT, 2.5 h; **e)** tryptamine, DIPEA, NMP, 145°C, 18h; **f)** BBr_3, DMF, 5°C, 3h. 8-CT: 8-chlorotheophylline; AcOH: acetic acid.*

As shown in *Scheme 5*, compound **FPE-122** with 2-Cl,4-OCH_3 substitution was synthesized according to strategy I starting from 6-amino-1,3-dimethyluracil and the required benzaldehyde.

Compound **FPE-42** with 3-Cl,4-OCH_3 was synthesized according to strategy IV from 8-chlorotheophylline and the corresponding benzylbromide. Demethylation with BBr_3 of both methoxy-bearing final compounds (**FPE-122 and FPE-125**), led to the corresponding free hydroxyl derivatives, **FPE-125** and **FPE-43**.

Additionally, as seen in Scheme 4, alkylation of **FPE-13** often resulted in debenzylation. For this reason and to check whether only a phenolic OH results in enhanced potency, compound **FPE-146** with *p*-hydroxymethyl moiety was synthesized as shown in Scheme 5.

As shown in Figure 20, the trend of a free OH being superior to the corresponding methoxy compound is confirmed with a 4.3-fold and 6.6-fold increase in potency, respectively, for **FPE-43** and **FPE-125.**

FPE-146 showed no activity. This implies that the specific structural features and chemical properties of phenol, such as its acidity, hydrogen bonding capability, and lack of steric hindrance, contribute to the observed activity in **FPE-13** compared to **FPE-146 (**Figure 20**)**.

The assumed interactions formed by the hydroxyl moiety in **FPE-13,** are very interesting and therefore, a bioisosteric replacement with an amino group was pursued. The similar steric size, spatial arrangement, and the ability of OH and NH_2 groups to act as either hydrogen bond donors is the reason why they are very successfully used as bioisosteres.[132] As shown in *Scheme 6*, the synthesis proceeded with the usual reactions of alkylation and tryptamine coupling, using the alkylating reagent 4-nitrobenzyl bromide. **FPE-40** then underwent a reduction through hydrogenation over palladium/carbon to obtain the desired compound **FPE-44**. The amino group will also give the possibility for synthesizing future derivatives, including inverted amides and inverted sulfonamides. Given the poor yield obtained when reducing the nitro group on **FPE-40**, in order to obtain the inverted sulfonamide **FPE-72**, a different strategy was used. The nitro group on **FPE-38** was firstly reduced with $SnCl_2$, followed by the formation of the sulfonamide with methanesulfonylchloride and the usual tryptamine coupling.

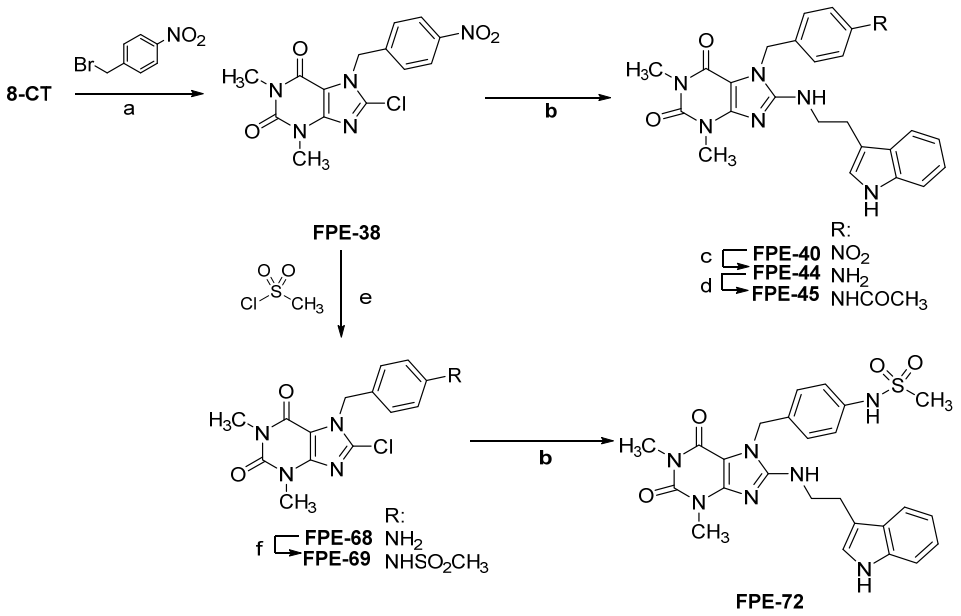

*Scheme 6. Synthesis of compounds **FPE-44, FPE-45, FPE-72**. Conditions: **a)** K_2CO_3, DMF, RT, 2.5 h; **b)** tryptamine, DIPEA, NMP, 145°C, 18h; **c)** Pd/C, H_2, MeOH, RT, 7h; **d)** acetic anhydride, DCM, RT, 1h; e) $SnCl_2$, EtOH, 70°C, 1.5h; f) DCM, RT, 24h.*

As it is depicted in Figure 22, **FPE-44** did not show improvement in the activity compared to **FPE-13**.

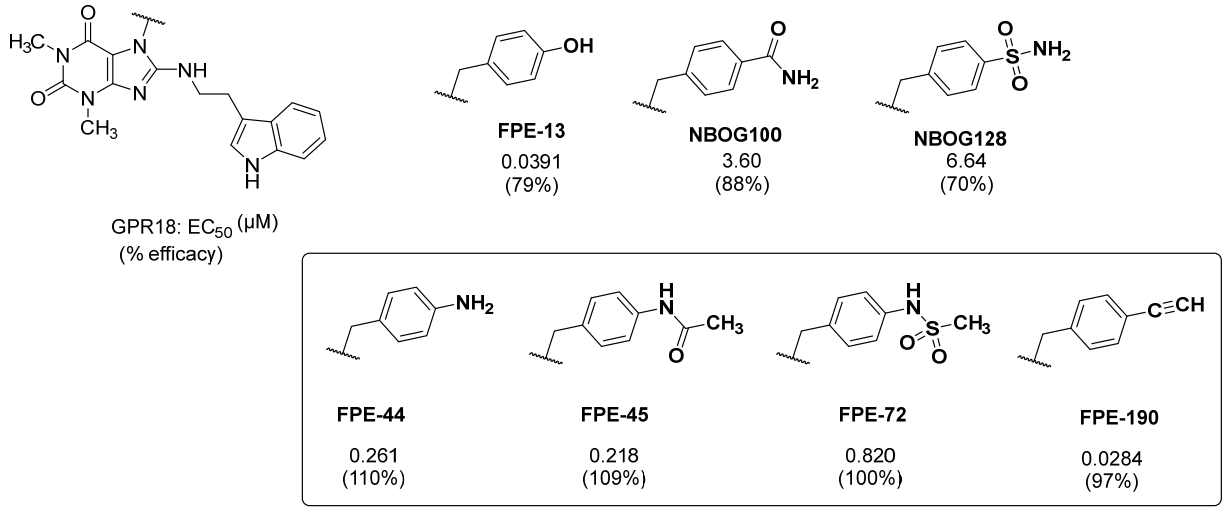

*Figure 22. Biological test results for **FPE-44, FPE-45, FPE-72, FPE-190.** Framed: newly synthesized compounds.*

The substitution of the phenol moiety with a *p*-aminophenyl group can indeed result in a loss of activity in certain cases, despite the potential for the hydroxy and amino groups to act as

bioisosteres. The amino group may not be able to form the same hydrogen bonding network or may do so with different orientation or strength.

FPE-45 and **FPE-72** showed a 16-fold and an 8-fold increase in potency, respectively, compared to the corresponding "regular" amide and sulfonamide **NBOG100** and **NBOG128**.

For high potency, next compound **FPE-190**, featuring an acidic terminal alkyne, was synthesized, as shown in Scheme 7.

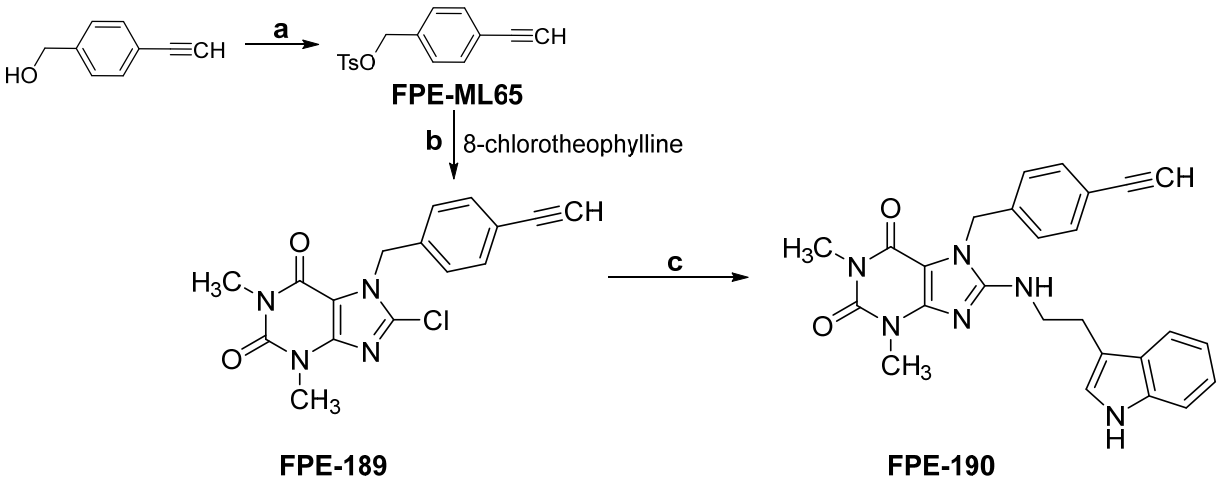

*Scheme 7. Synthesis of **FPE-190**.Conditions: **a)** TsCl, KOH, THF, RT, 12h; **b)** K_2CO_3, DMF, RT, 2.5 h; **c)** tryptamine, DIPEA, NMP, 145°C, 18h.*

This will facilitate subsequent fluorophore attachment via click chemistry. The synthesis proceeded according to strategy IV (*Scheme 1*). **FPE-190** showed a slightly better activity than its hydroxy analog (Figure 22).

3.1.1.3 Bioisosteric replacement of the benzyl moiety

Synthetic efforts involved systematic examination of the effects of substituents on the benzyl moiety, alongside exploration of bioisosteric replacements of the benzyl core, encompassing both aromatic and non-aromatic residues. This approach aimed at maintaining or improving the biological activity, while optimizing the pharmacodynamic properties of the compounds by modulating steric, electronic, and hydrophobic characteristics.

As mentioned for **FPE-22**, another promising series of GPR18 agonists currently under development in our working group (unpublished results), served as source of inspiration for SAR transfer.

Particularly, a comparison between the binding modes of these unpublished series and indolylaminoxanthine derivatives reveals that the aromatic portion (a pyridyl residue) of the former may bind in proximity to ECL2, aligning with the substituent at *N*7 of the latter.

Therefore, the choice of pyridine as the initial heterocyclic bioisostere was driven by its observed binding similarity and the potential to enhance solubility. As shown in *Scheme 8*, **FPE-30, FPE-ML22, FPE-33 and FPE-35** were all synthesized according to strategy IV.

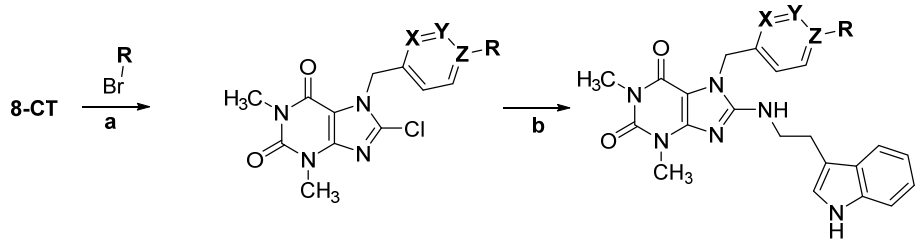

	X	Y	Z	R
FPE-28, FPE-30	CH	CH	N	-
FPE-ML21, FPE-ML22	CH	N	CH	CH
FPE-32, FPE-33	CH	N	CH	Cl
FPE-34, FPE-35	N	CH	CH	Cl

Scheme 8. Synthesis of pyridine-containing derivatives. Conditions: ***a)*** *K_2CO_3, DMF, RT, 2.5 h****; b)*** *Tryptamine, DIPEA, NMP, 145°C, 18h.*

Derivatives featuring unsubstituted pyridine with nitrogen in both *p*- and *m*-positions were synthesized. Subsequently, to maintain the favorable activity observed with the *p*-chlorobenzyl moiety, corresponding *p*-chloropyridine-containing analogs were synthesized.

The biological test results (Figure 23), showed that unsubsituted pyridine (**FPE-30** and **FPE-ML22)** exhibit a substantial drop in activity compared to their benzyl counterpart (**MZ1414;** ca 3-4 fold lower). Lipophilicity in this area appears to be a key element for biological activity, with few exceptions (e.g. phenol, aniline). In fact, once the chlorine is introduced at the *p*-position in **FPE-33** and **FPE-35** there is only a small 4-fold decrease in activity compared to the lead compound **PSB-KK-1415**, regardless of the position of the nitrogen.

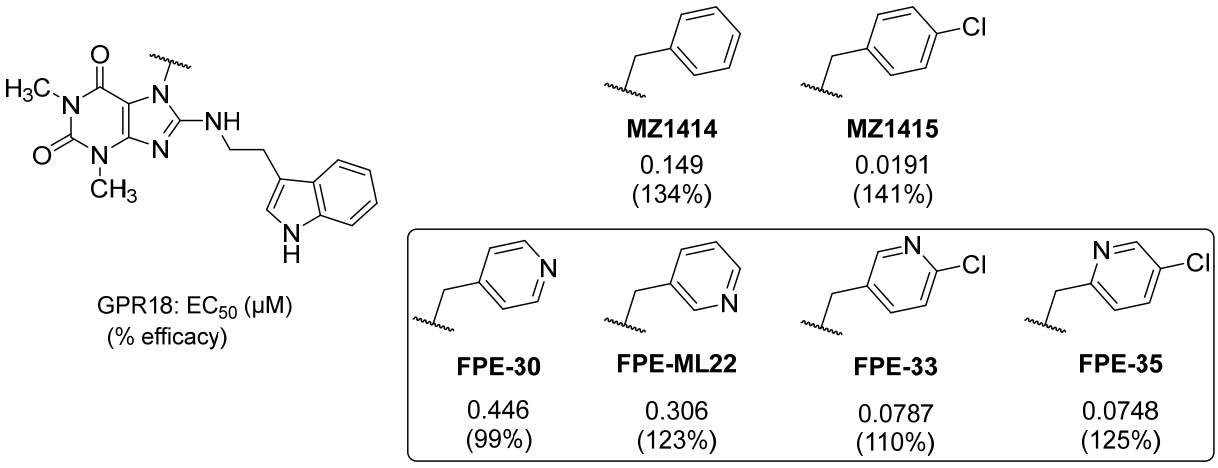

Figure 23. Biological test results of pyridil-substituted analogs. Framed: newly synthesized compounds.

Considering the moderate activity exhibited by both the *p*-methoxybenzyl derivative **(MZ1461)** and the newly synthesized *p*-hydroxybenzyl derivative **FPE-13** (see *Figure 20*), compound **FPE-33** was selected for conversion to the corresponding 2-alkoxy pyridine, as outlined in existing literature.[133] The resulting compound was intended to be subjected to demethylation to yield the final product. However, treatment of **FPE-33** with metallic sodium in methanol, as depicted in Scheme 9, failed to produce the desired product. Due to insufficient quantity of **FPE-33** for additional attempts and the lower priority assigned to this series, no further efforts were made.

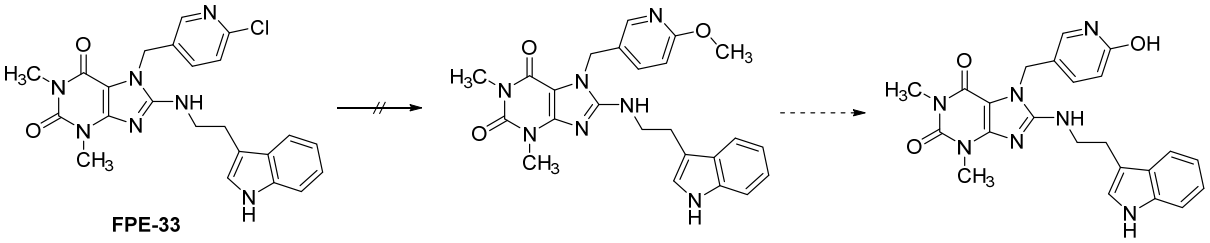

Scheme 9. Attempt to synthesize 2-methoxypyridine derivative and planned demethylation. ***Conditions****:* ***a)*** *metallic Na, MeOH, 0°C to reflux, 3.5h.*

Numerous attempts were made to synthesize a ligand featuring a 4-methyl-1*H*-imidazole. This compound, incorporating an imidazole moiety as the aromatic component is interesting both as a bioisosteric substitution of the phenyl ring and due to the opportunity to functionalize the NH present in the ring.

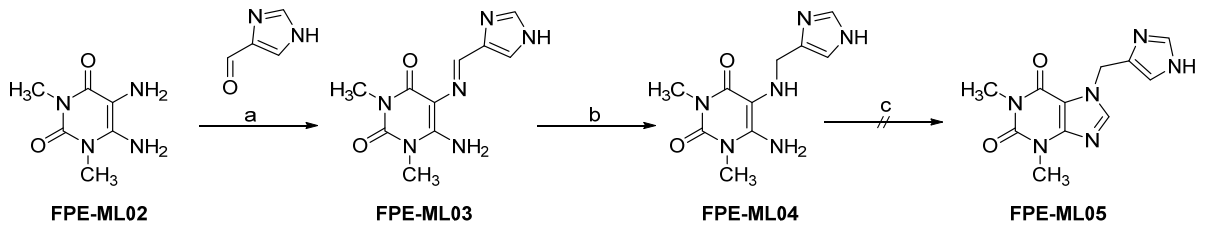

*Scheme 10. The planned synthetic strategy to synthesize **FPE-ML56**. Conditions: **a)** AcOH, 15 min, rt; **b)** $NaBH_3CN$, AcOH, DCM:MeOH (1:1), overnight, rt; **c)** TEOF, 5h, 145°C.*

As shown in Scheme 10, initially, following strategy I, the reduction of the Schiff base (**FPE-ML04**) was pursued. However, post reduction in the presence of $NaBH_3CN$ and acetic acid, the resulting product exhibited poor solubility in organic solvents, necessitating purification by HPLC using a methanol-water system. Unfortunately, this purification method failed to yield adequately pure fractions. Despite the limited quantity obtained, it was utilized in subsequent ring closure reactions. Additionally, ring closure (**FPE-ML05**) according to strategy I proved challenging, despite prolonged stirring under heating. Although TLC-MS monitoring indicated the presence of the desired compounds, the extremely small reaction scale precluded isolation.

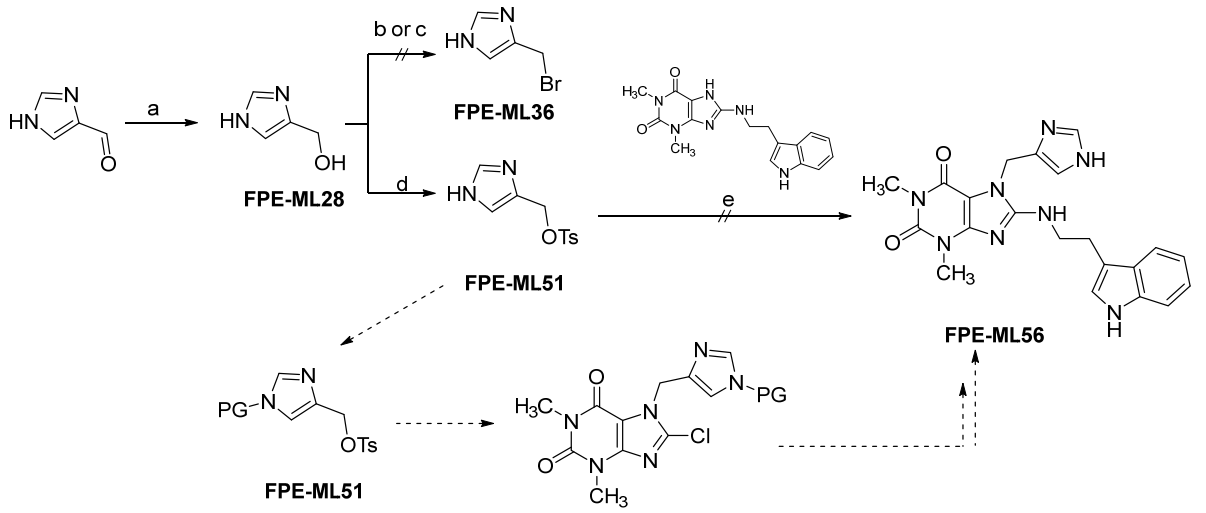

*Scheme 11. Attempted reaction for **FPE-ML56**. Conditions: **a)** $NaBH_4$, MeOH, 0.5h, 0°C; **b)** PBr_3, ACN, 2h, 80°C; **c)** DMTU, NBS, DCM, 1d, rt; **d)** Et_3N, DMAP, TsCl, Ar, overnight, rt; **e)** K_2CO_3, dry DMF, 3d, rt. DMTU: N,N'-dimethylthiourea; DMAP: 4-dimethylaminopyridine; TsCl: toluenesulfonyl chloride.*

Due to difficulties with strategy I, larger-scale attempts were made, coupled with the adoption of a new synthetic approach.

Given the commercial availability of 1*H*-imidazole-4-carbaldehyde, efforts to convert it to the corresponding alcohol for subsequent bromination or tosylation were performed, not without hurdles. As shown in Scheme 11, bromination with phosphorus tribromide (PBr_3) or dimethylene triurea/*N*-bromosuccinimide (DMTU/NBS) proved unsuccessful, whereas tosylation with 4-toluenesulfonyl chloride (TsCl) and 4-dimethylaminopyrrolidine (DMAP) under an inert gas atmosphere afforded the desired compound, **FPE-ML51**, albeit in a modest yield of 5.1%.

Attempts to utilize this tosylated alcohol as an alkylating agent for the building block **FPE-179**, following strategy V (*Scheme 1*), were unsuccessful despite prolonged reaction times. Future endeavors may explore the potential use of **FPE-ML51** as an alkylating agent on 8-chlorotheophylline according to strategy I.

While exploring various options for the replacement of the terminal *p*-substituted phenyl ring, several sp^3-rich ring systems have been considered. This trend is increasingly prominent in medicinal chemistry, as it offers numerous advantages beyond π-π interactions. These include enhanced conformational flexibility, three-dimensionality, and the potential to modify physicochemical properties by reducing lipophilicity, while keeping lipophilic interactions.[134]

Additionally, as already shown in chapter 2, some derivatives presenting an aliphatic, better if branched, chain at *N*7 instead of an aromatic ring, also resulted in good activity (Figure 24).

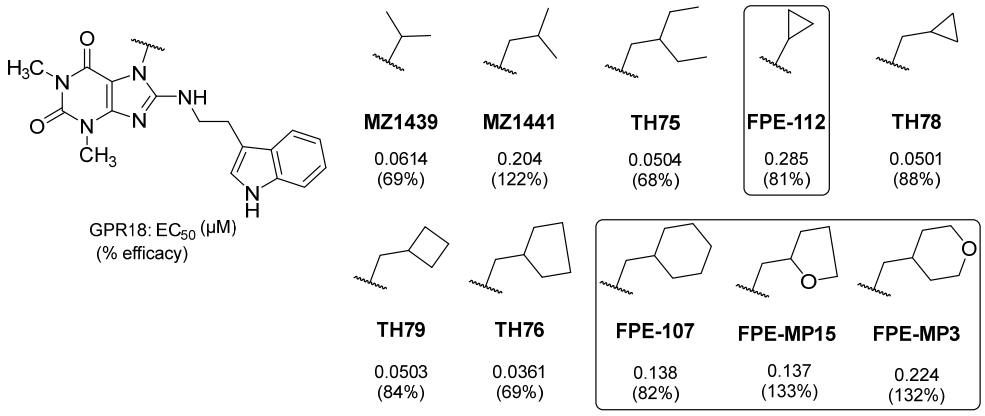

Figure 24. Biological activity of derivatives with acyclic and cyclic sp3-rich substitutions at N7. Framed: newly synthesized compounds.

When rings were positioned to mimic the conformation of aliphatic chains, this often resulted in increased activity. For example, transitioning from the isobutyl group of **MZ1441** to the less flexible methylcyclopropyl moiety of **TH78** led to a 4-fold increase in activity.

To confirm this trend, based on the even better activity shown by **MZ1439**, its isopropyl moiety will be converted into a fixed ring, therefore a compound bearing a cyclopropyl substituent on *N7* was synthesized as shown in Scheme 12. According to strategy II, the previously synthesized **FPE-96 (***Scheme 1*) served as the starting material for the nucleophilic substitution with cyclopropylamine leading to **FPE-97**. Ring closure was peformed with trimethylorthoformate in the presence of *p*-toluenesulfonic acid (Scheme 12). As shown in Table 7, conditions for reaction 1 to synthezise **FPE-97** were modified in order to optimize the yield that unfortunately was always very poor. The reaction proceeded slowly, never reaching completion in terms of starting material consumption, moreover, prolonged reaction times led to the formation of numerous byproducts, likely stemming from the decomposition of cyclopropylamine. Given that **FPE-97** represented only the initial step of a four-step process, the low yield posed a hindrance to the successful preparation of the final product. Therefore, another strategy was put in place: trying to add the cyclopropyl moiety directly on the xanthine scaffold. Using bromocyclopropane as the alkylating agent on both theophylline and 8-chlorotheophylline with different reaction conditions did not result in the desired products unless in extremely low yields. The successful strategy was the *N*-alkylation by a cross-coupling reaction with cyclopropyl boronic acid in the presence of a catalytic amount of cupper(II) acetate according to literature.[135] This approach led to **FPE-99** in good, yet improvable yield, but was not as effective with 8-chlorotheophylline. **FPE-99** underwent chlorination at position 8 to give **FPE-111**, and the general procedure for the coupling with tryptamine resulted in the final product **FPE-112**.

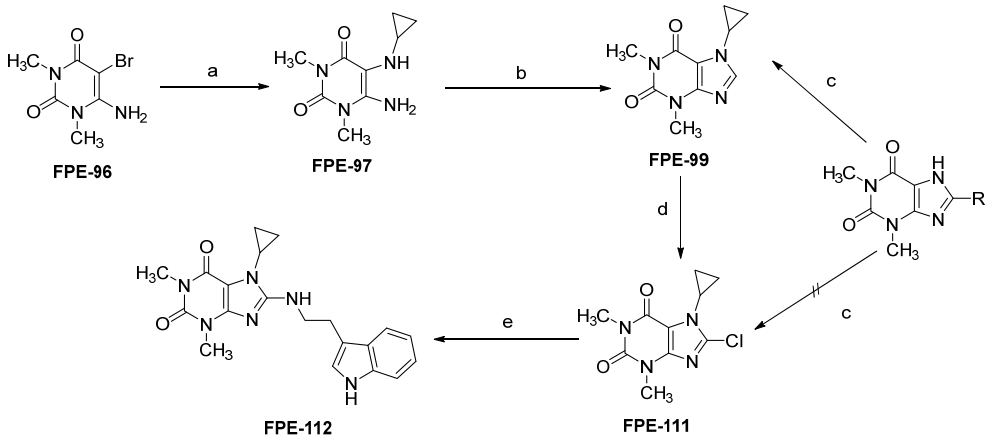

Scheme 12. Synthetic approaches for the preparation of the derivative bearing cyclopropyl moiety on N7. Conditions: a) see Table 2; b) trimethylorthoformate, TsOH, DMF, 100°C, 12h; c) see Table 2; ***d)*** *NCS, THF, RT, 16h; e) tryptamine, DIPEA, NMP, 145°C, 18h. TsOH: p-toluenesulfonic acid.*

Table 7. Summary of the reaction conditions used to achieve cyclopropylation on N7.

Reaction	Attempt	R	Reagent	Conditions	Yield	Comments
a	I	-	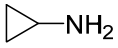	Water, 80°C, 5 h	≈10-12 % (crude)	Reaction does not reach completion, harsh purification
	II	-	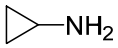	Water, 70°C, 12h	≈ 27 % (crude)	Reaction does not reach completion, instead many by-products are formed, harsh purification
	III	-	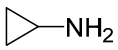	Toluene, $Pd_2(dba)_3$, BINAP, NaOtBu, 80°C, 24h	-	No go
c	I	Cl	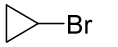	K_2CO_3, DMF, RT → 60°C → 80°C, 2 days	< 1%	Extremely slow formation of the product
	II	H	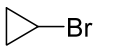	KOH, THF, 18-crown-6, 55°C, 12h	-	No go
		Cl	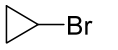	KOH, THF, 18-crown-6, 55°C, 12h	-	No go
	III	H	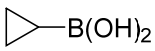	Na_2CO_3, $Cu(OAc)_2$, Bipyridine, dichloroethane, 70°C, 5h	35%	Yield can be improved
		Cl	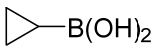	Na_2CO_3, $Cu(OAc)_2$, Bipyridine, dichloroethane, 70°C, 12h	-	Very slow formation of the product and does not reach completion

As for the biological assays, **FPE-112** resulted in a 4-fold loss in potency compared to its acyclic counterpart, **MZ1439** was less active than all the other compounds of the same series, both cyclic and acyclic, that present a methylene or methine bridge directly attached to *N*7. This is likely the result of the rigidity imposed by the very strained cyclopropane ring, limiting its conformational adaptability.

Consequently, the series progressed with the synthesis of derivatives incorporating the aforementioned methylene bridge, followed by cyclobutene, cyclopentane and cyclohexane (compounds **TH79** and **TH76** — obtained from collaborators, and **FPE-107**). Subsequently, oxygen-containing derivatives, namely **FPE-MP15** and **FPE-MP3**, were prepared according to strategy IV, as illustrated in *Scheme 13*.

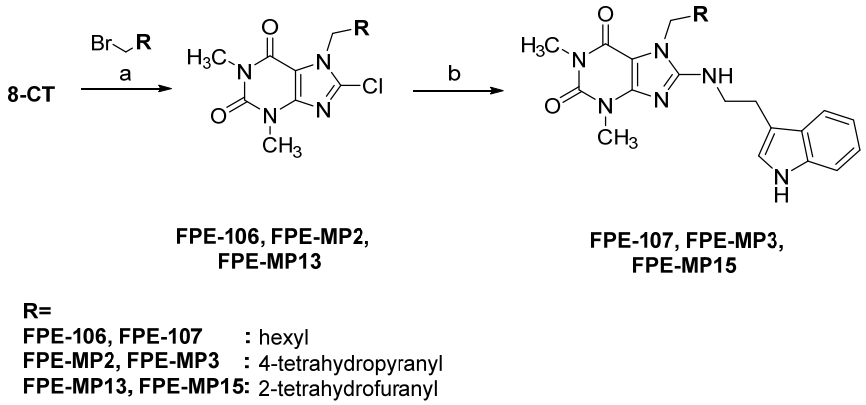

*Scheme 13. Synthesis of derivatives **FPE-107, FPE-MP3, FPE-MP15**. Conditions: **a)** K_2CO_3, DMF, RT, 2.5 h; **b)** tryptamine, DIPEA, NMP, 145°C, 18h.*

The observed differences in biological activity among derivatives likely arise from variations in molecular size, shape, and flexibility. Compounds featuring rings composed of 3 to 5 atoms (compounds **TH78, TH79, TH76**) exhibit good activity, whereas the introduction of a cyclohexane ring resulted in a notable decrease in activity, approximately 3-fold. It may disrupt optimal interaction and geometric compatibility with the receptor binding site, with no option of π-π stacking like for a benzyl ring. Ultimately, the inclusion of oxygen within the ring resulted in a reduction in activity for both tetrahydrofuranyl and tetrahydropyranyl derivatives (**FPE-MP15** and **FPE-MP3**) compared to their respective cycloalkane analogs. This underscores the significance of lipophilicity as a critical property within this region of the binding site.

3.1.1.4 Focus on the benzylic linker (branched and longer chains)

Previous encouraging results allow speculation that growing the branched chain on the atom adjacent to the *N*7 will improve the activity (Figure 25).

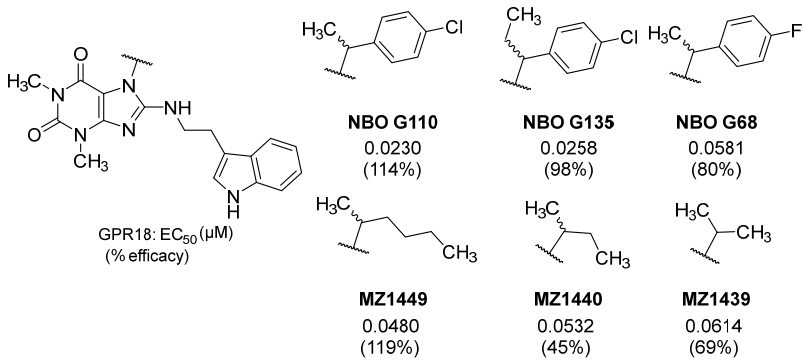

Figure 25. Biological activity of branched compounds.

Alkylating this site with longer chains offers the opportunity to explore spatial interactions and investigate the feasibility of a fluorescent probe. Additionally, transitioning to a carbonyl group, an untested modification, presents a valuable avenue for investigation.

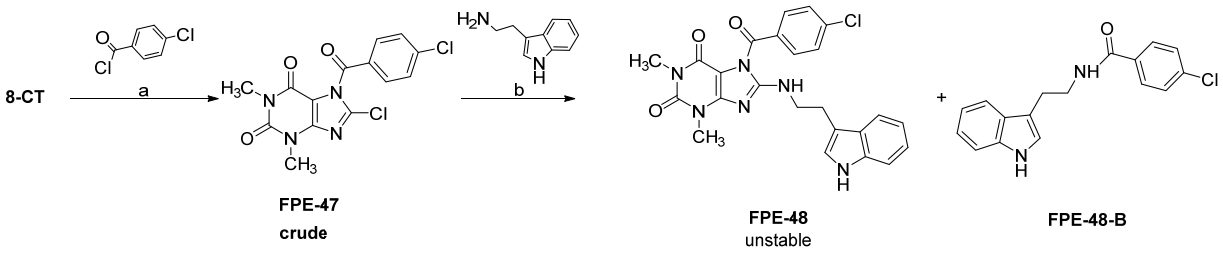

Scheme 14. Direct amidation on N*7. Conditions:* ***a)*** *Et3N, DCM, RT, 2h;* ***b)*** *DIPEA, NMP; 145°C, 18h. 8-CT: 8-Chlorotheophylline.*

As shown in Scheme *14*, amidation on *N*7 with the proper benzoyl chloride led to the intermediate **FPE-47**, used as crude material for the next step.

During the well-established tryptamine coupling procedure, the desired compound, **FPE-48** albeit formed as confirmed by TLC-MS (Advion Expression MS), proved unstable, with concurrent generation of the side product **FPE-48B**. The most plausible mechanism for this appears to be transamidation, given the excess of tryptamine, elevated temperature, prolonged reaction times, and potential contamination by in-situ formed benzoic acid from the preceding reaction step. This aligns with the proposed mechanism documented by *Wu et al.* reporting a comparable example involving tryptamine and benzamide in the presence of catalytic amounts of benzoic acid. [136]

Another strategy, in which amide formation occurs after tryptamine coupling, specifically on compound **FPE-179**, may appear less favorable due to the presence of numerous other free NH groups that could potentially interfere. Initial acetylation might offer a more promising avenue for future trials, albeit of lower priority.

Despite the unsuccessful direct amidation, the resultant side product, **FPE-48B**, exhibited antagonistic activity at the closely related receptor **GPR183**. Further exploration of this compound will be undertaken as described in subsequent chapters.

As for branching the benzylic carbon, due to the unavailability of commercial alkylating agents presenting the desired substituents, the synthesis involved reacting suitable aldehydes with Grignard reagents to produce secondary alcohols bearing the desired moieties. The hydroxyl group would then be transformed into a good leaving group upon tosylation or bromination resulting in a convenient alkylating agent for the *N*7. The first Grignard reaction carried out is presented in Scheme 15.[137] *p*-Methoxybenzaldehyde was reacted with methylmagnesium bromide to give **FPE-80**. However, neither tosylation nor bromination reactions under the described conditions were successful.

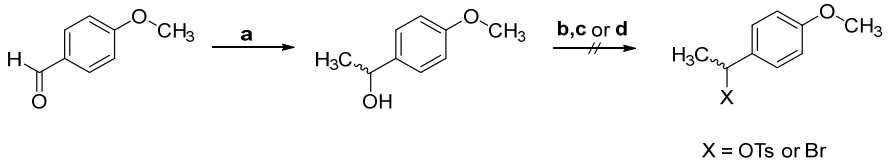

*Scheme 15. Grignard reaction leading to **FPE-80**. Conditions: **a)** CH_3MgBr, dry THF, Ar, 0°C to RT, 4h; **b)** TsCl, toluene, pyridine, RT, 18h; **c)** HBr, toluene, RT, 12h; **d)** PBr_3, ACN, reflux, 3h.*

Scheme 16 shows another very interesting procedure reported in literature, that involves the tosylation of *N*7 of theophylline followed by nucleophilic attack of the hydroxyl group of the desired alcohol in the presence of DBU as a base.[138]

Once **FPE-87** was obtained, it was worth trying a tryptamine coupling with the sulfonamide directly attached to *N*7. Once again, due to the harsh conditions of this reaction, the compound **FPE-88** was unstable and, as already seen for **FPE-48**, the tosyl group ended up being linked to the tryptamine itself. As for the main strategy of reacting the tosylated 8-chlorotheophylline with an alcohol, it did not work out with the conditions reported in literature. Most likely, the chlorine

at *C*8 hindered the success of the reaction. A future approach may include the synthesis of *N*-tosylated theophylline followed by reaction with an alcohol, and chlorination only at a later stage.

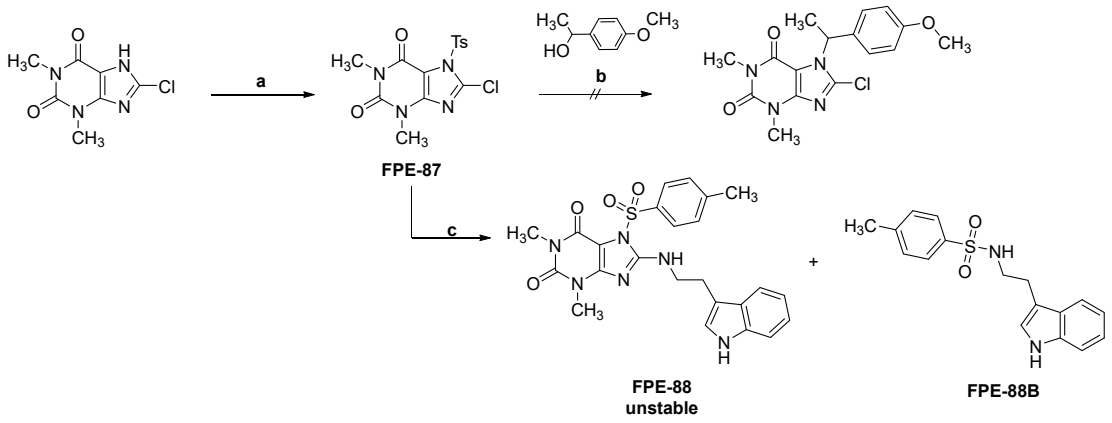

*Scheme 16. Synthesis of N-tosylated 8-chlorotheophylline (**FPE-87**) as a precursor for branched derivatives. Conditions: **a)** TsCl, Et_3N, ACN, reflux, 4h; **b)** DBU, ACN, reflux 12h ; **c)** tryptamine, DIPEA, NMP; 145°C, 18h.*

At the same time, another synthesis following strategy II was pursued. As shown in *Scheme 17*, **FPE-96** was reacted with an α-branched amine to achieve **FPE-123**, the corresponding diamino uracil derivative. Ring closure successfully yielded **FPE-127**, while the following step, initially aiming at achieving chlorination at position 8, resulted mainly (75%) in a chlorination also on the benzyl ring in the *o*-position with regard to the methoxy group, given the *ortho/para* directing nature of the latter. The crude mixture underwent tryptamine coupling but with scarce success and extreme difficulties in the isolation of the desired compound.

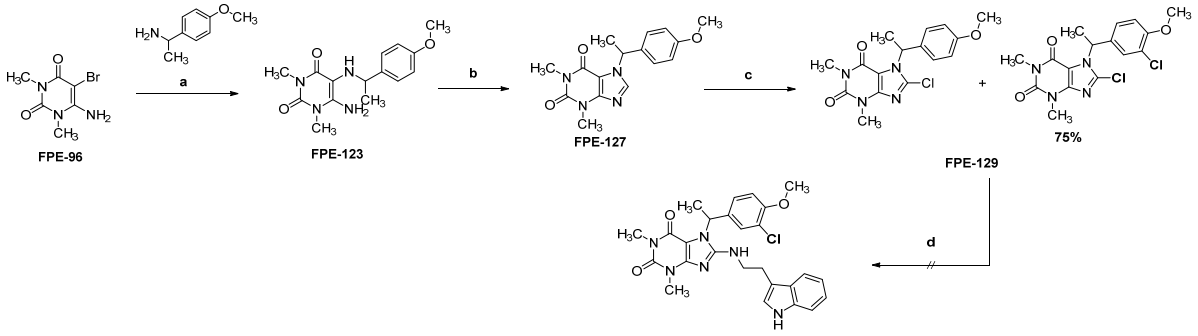

*Scheme 17. Strategy II for the synthesis of branched compounds. Conditions: **a)** Et_3N, DMF, 120°C, 24h; **b)** TEOF, 145°C, 5h; **c)** NCS, THF, RT, 16h; **d)** tryptamine, DIPEA, NMP, 145°C, 18h.*

A promising approach would be the optimization of a multi-component Petasis reaction. A first attempt was made as shown in Scheme 18. Theophylline was reacted with the corresponding boronic acid and aldehyde in a microwave-assisted one-pot reaction as reported in literature.[139–141]

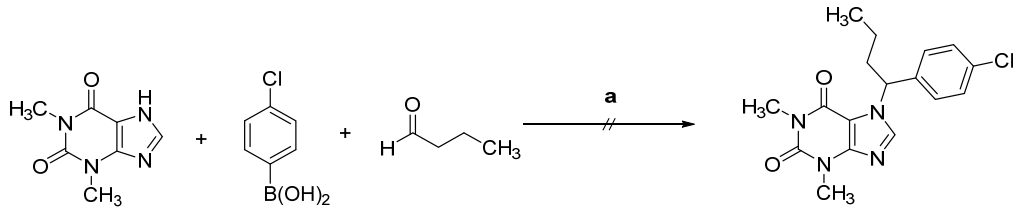

Scheme 18. Attempt at a multi-component Petasis reaction. Conditions: a) ACN, DMF, 15 min, 120°C, 100 W.

This attempt was not successful, but a future strategy could be to try this multi-component approach on the diamino-uracil, as suggested in Scheme 19. This would be very interesting and has never been performed on xanhines before.

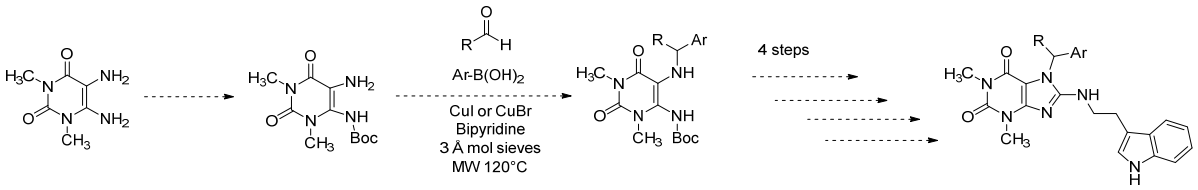

Scheme 19. Suggested approach for the optimization of the Petasis reaction starting from diamino- uracil.[139]

While branched compounds with an alkyl chain were very difficult to obtain, another compound was pursued in the meanwhile. This will allow further exploration of the SARs as well as provide an opportunity for further elongation of the chain with different moieties via amide or ester bonds.

As shown in *Scheme 20*, in our group a xanthine derivative presenting a methoxy ester on the benzylic linker was previously reacted with tryptamine according to the standard, quite harsh, conditions resulting in the formation of the corresponding amide, rather than in the wanted compound.

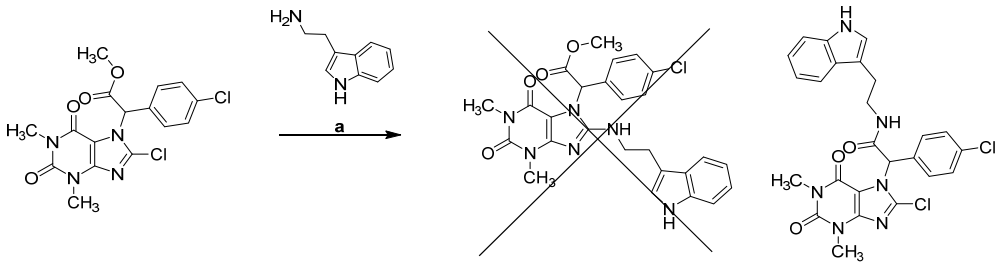

Scheme 20. Past attempt at achieving a compound bearing a methoxy ester on the benzylic linker.

A new strategy was put in place, "protecting" the CO_2H with a *t*Butyl group. *tert*-Butyl esters are more stable and may resist to the harsh conditions used for the tryptamine coupling. Moreover, they react with $SOCl_2$ to give the corresponding acid chloride (more reactive for future elongations) whereas benzyl, methyl, ethyl are essentially unreactive.[142]

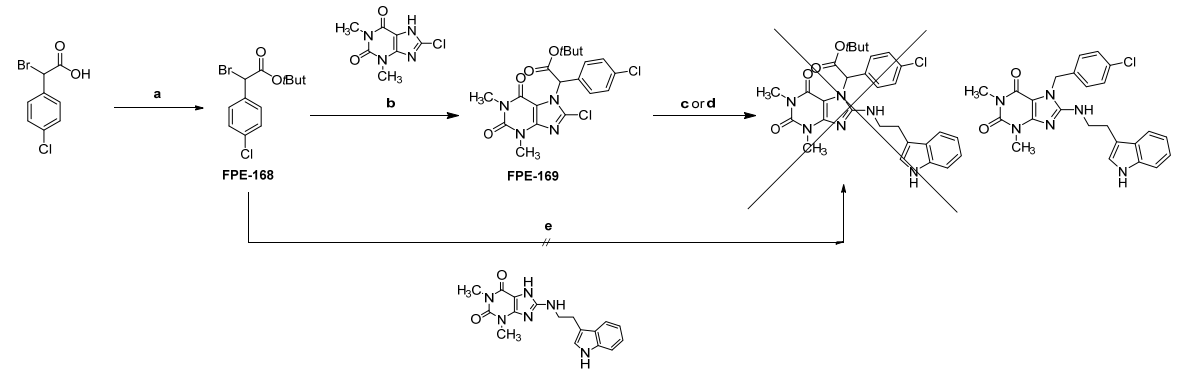

Scheme 21 . Synthetic approaches to achieve a compound bearing a CO_2H group on the benzylic linker. Conditions: ***a)*** *tButyl acetate, $HClO_4$, RT, 12h, Ar;* ***b)*** *K_2CO_3, DMF, 65°C, 2h;* ***c)*** *tryptamine, DIPEA, NMP, 145°C, 12h;* ***d)*** *tryptamine, DIPEA, NMP, 195°C, 100W, 20 min;* ***e)*** *K_2CO_3, DMF, 60°C, 24h.*

Once the alkylating agent **FPE-168** was synthesized and reacted with 8-chlorotheophylline as shown in Scheme 21, unfortunately, the harsh conditions of the tryptamine coupling led not only to the removal of the *t*-butyl group but also to decarboxylation. This occurred very rapidly, as evidenced by the same result obtained even when conditions were altered to microwave irradiation for only 20 minutes. Another attempt using the unmodified building block was made with extended reaction times but yielded no improvement. Better results could possibly be obtained by the use of a catalyst or microwave irradiation to push the reaction further to (even partial) completion.

Taking inspiration from peptide chemistry, one could think of the approach suggested in

Scheme 22, in the same fashion as strategy II starting from **FPE-96**.

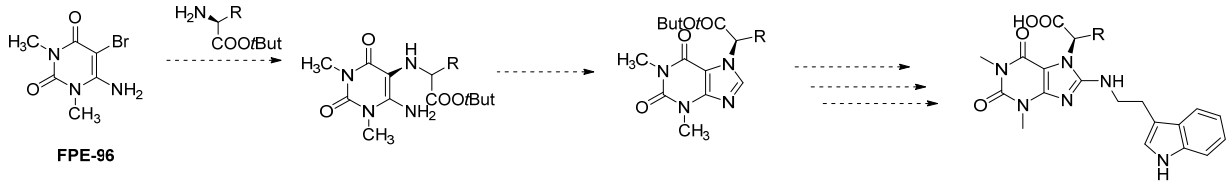

Scheme 22. Suggested strategy to obtain a compound bearing a CO_2H group on the benzylic linker, starting from amino acids.

While branched compounds presented significant interest, their synthesis demanded considerable effort, time, and resources. Despite not achieving the synthesis of the desired compounds, this

endeavor yielded valuable insights into the reactivity of the scaffold and prompted complex chemistry discussions on potential future strategies.

Finally, another approach to better explore the SARs was to find out how the distance between *N*7 and the aromatic ring affects biological activity. Similar derivatives have been synthesized in the past and showed some tolerable results (

Figure 26).

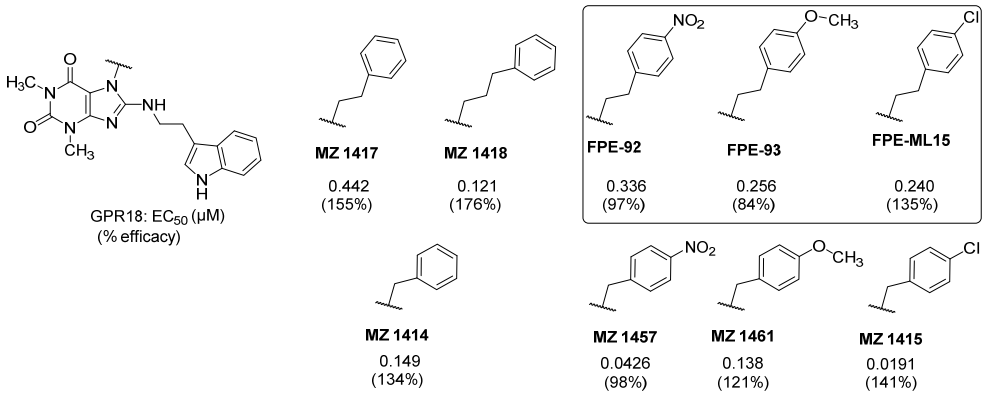

Figure 26. Biological results of compounds with a longer linker between N7 and the aromatic moiety. Framed: newly synthesized compounds.

As seen in Scheme 23, synthesis of **FPE-92** and **FPE-93** was successful. *p*-Nitro and *p*-methoxy moieties were the reagents of choice, because as extensively seen in the previous sections they are very effective and converting them into the corresponding amino and hydroxyl group could pave the road for the attachment of a fluorophore. The synthesis of **FPE-93** followed strategy II from **FPE-96** with 4-methoxyphenethylamine. Due to the small scale both **FPE-124** and **FPE-128** were used as crude materials without further purification. The synthesis of **FPE-92** and **FPE-ML15** was made according to strategy IV from 8-chlorotheophylline and the appropriate alkylating reagents.

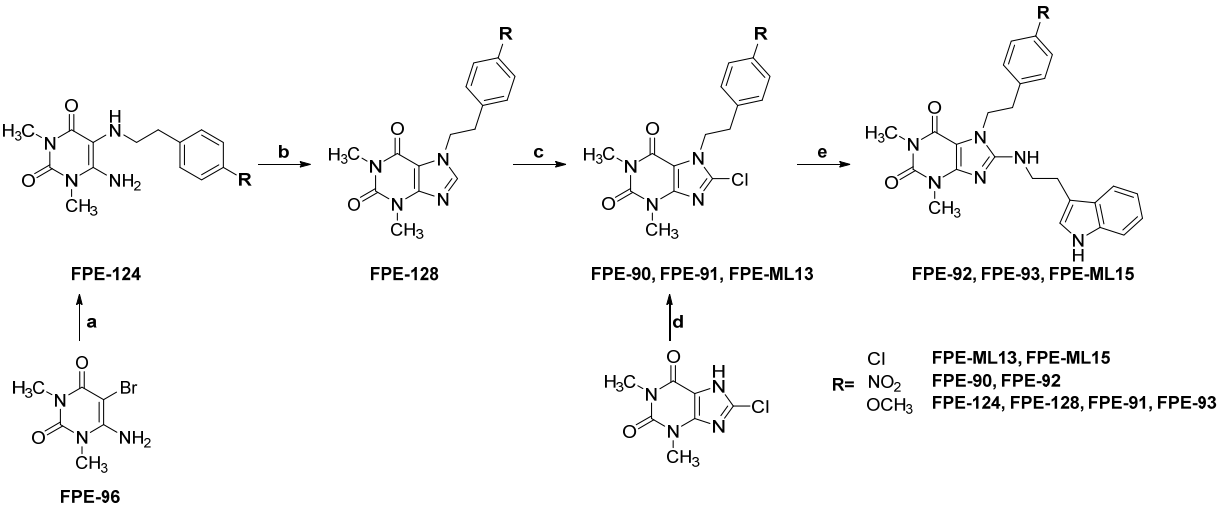

*Scheme 23. Synthesis of compounds **FPE-92** and **FPE-93**. Conditions: **a)** 4-methoxyphenethylamine, Et_3N, DMF, 120°C, 24h; **b)** TEOF, 145°C, 5h; **c)** NCS, THF, RT, 16h; **d)** 1-(2-bromoethyl)-4-nitrobenzene or 1-(2-bromoethyl)-4-chlorobenzene , K_2CO_3, DMF, RT, 2.5 h **e)** tryptamine, DIPEA, NMP, 145°C, 18h.*

As seen in Figure 26, compounds with an odd number of carbons between the aromatic ring and the xanthine scaffold (**MZ1414** and **MZ1418**) showed better biological activity compared to compounds with an even number of carbons (**MZ1417, FPE-92, FPE-93, FPE-ML15**).

Compounds with an odd number of carbons between the aromatic ring and the xanthine scaffold may exhibit better biological activity due to increased conformational flexibility, more favourable spatial orientation and alignment with the target protein's binding site. In contrast, even-numbered linkers might restrict this flexibility, leading to suboptimal interactions and reduced activity.

To further confirm this trend, an attempt at synthesizing the corresponding -(4-methoxyphenyl)propyl derivative was made.

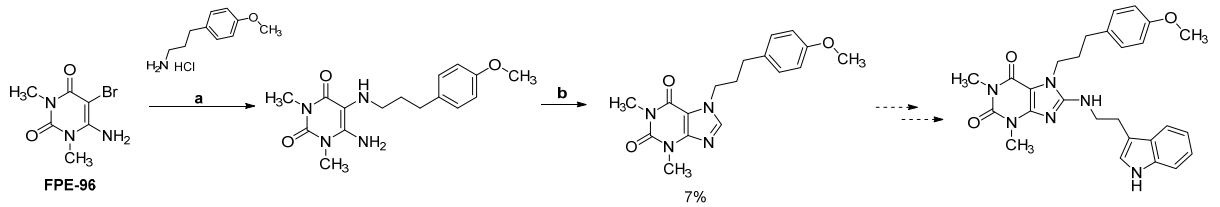

*Scheme 24. Attempt to synthesize a compound bearing a 4-(methoxyphenyl)propyl moiety. Conditions : **a)** Et_3N, DMF, 120°C, 24h; **b)** TEOF, 145°C, 5h.*

The synthesis of this compound using 3-(4-methoxyphenyl)propan-1-amine hydrochloride according to strategy II was not successful (*Scheme 24*). The cyclization step using triethyl

orthoformate resulted in a very low yield (< 7%), producing only a small amount of the desired compound — insufficient for the subsequent two steps. To continue with this approach, optimizing the reaction conditions or scaling up the synthesis may be necessary. In the same fashion, simple alkyl chains attached to *N*7 exhibit a trend similar to previous findings: molecules with an odd number of carbons in the chain show the best biological activity. (Figure 27).

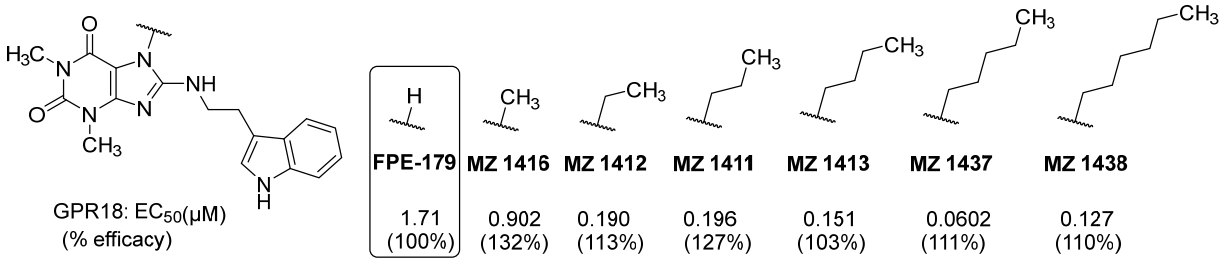

*Figure 27. Biological acitivity of **FPE-179** and previously synthesized compounds with longer alkyl chains. Framed: newly synthesized compound.*

Before additional experiments were performed, **FPE-179**, synthesized according to what reported in *Scheme 1*, was biologically assessed. Compared to even a small methyl group (**MZ1416**), the absence of a substituent, diminishing the ability to optimize interactions within the binding site, causes nearly a 2-fold decrease in potency.

Afterwards, using **FPE-179** as building block and to further explore this trend and the potential for linker-fluorophore attachment, **FPE-ML46** was synthesized (*Scheme 25*).

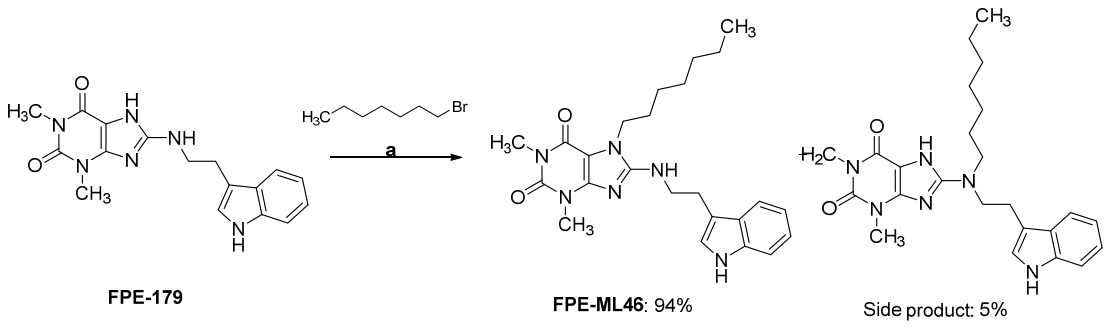

*Scheme 25. Synthesis of **FPE-ML46.** Conditions: **a)** K_2CO_3, DMF, RT, 2.5 h.*

FPE-179 was alkylated with 1-bromoheptane using strategy V, resulting in two products: the desired *N*7-alkylated compound and an unexpected alkylated product where the free NH in the ethylamino linker was modified. Both products were detectable via LC-MS and NMR, with similar retention times of 8.044 s and 8.338 s, respectively. Despite the purification attempts, they

ethylamino linker was modified. Both products were detectable via LC-MS and NMR, with similar retention times of 8.044 s and 8.338 s, respectively. Despite the purification attempts, they overlapped on TLC, and their HPLC retention times were too close for isolation. In the ^{1}H-NMR spectrum, the *N*7-alkylated product showed a free amine signal between 3-ethyl-1*H*-indole and theophylline at 7.45 ppm, while the free NH-alkylated product had a peak at 11.5 ppm. Interestingly, no dialkylated product was observed. This may be due to the very small excess amount of alkyl bromide, which might not have been sufficient to react with both amine sites. Alternatively, steric hindrance could be a factor, where the flexibility of the heptane chain might limit the alkylation of the second amine once the first is modified. Strategy IV starting from 8-chlorotheophylline would be a more suitable option for this specific substitution.

3.1.1.5 Bicyclic systems

The previous paragraph extensively showed that an improvement in the activity is achieved when ramification on the benzylic linker was introduced, especially when the *p*-chloro-substituted aromatic moiety was kept in place. Therefore, exploring the effect of a less flexible bicyclic residue in this position could be interesting (Figure 28).

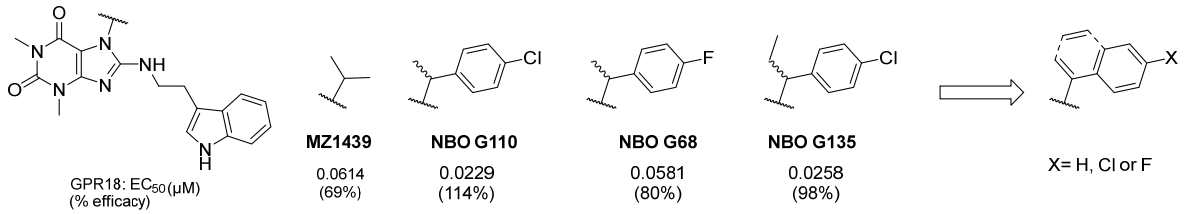

Figure 28. Plan for a bicyclic aromatic moiety on N7.

Since it is important to keep the same space orientation, the first compound was designed to bear a naked 1-naphthalene (*Scheme 26*).

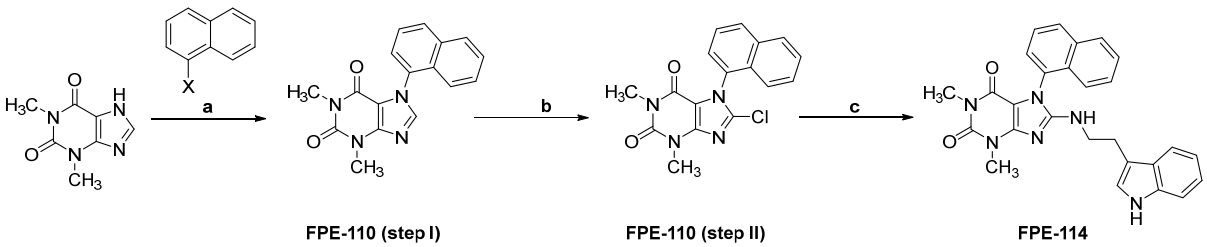

Scheme 26. Synthesis of ***FPE-114*** *bearing a naphthyl moiety on N7. Conditions:* ***a)*** *see Table 8;* ***b)*** *NCS, THF, RT, 16h* ***c)*** *tryptamine, DIPEA, NMP, 145°C, 12h.*

As seen in Table 8, the bulky nature of the alkylating agent did not allow reaction under the standard conditions used for strategy IV, even when reacted for longer times (entry 1). The addition of metallic Cu powder as catalyst was not effective as well (entry 2) at room temperature. Changing the alkylating agent from 1-bromo to 1-iodonaphathalene with adjusted conditions and a stronger base, Cs_2CO_3, cupper iodide as a catalyst and higher temperature did not lead to the desired compound, but only to a series of unidentified subproducts — indicated by TLC-MS monitoring (entry 3). The previously seen strategy for the synthesis of **FPE-112** with a boronic acid was the next and successful attempt (Entry 4).

Table 8. Attempts to synthezise an N7-naphthyl-substituted xanthine derivative.

Entry	X =	Base	Catalyst	Solvent	Conditions	Comments
1	Br	K_2CO_3	-	DMF	RT, 12h	No go
2[143]	Br	K_2CO_3	Cu powder	nitrobenzene	RT 10 h	No go
3[144]	I	Cs_2CO_3	CuI	DMF	145°C, 48h	Unidentified subproducts
4[135]	$B(OH)_2$	Na_2CO_3, 2,2′-Bipyridine	$Cu(OAc)_2$	DCE	70°C, 5h	10%

As seen in Figure 29**, FPE-114** is equipotent to the lead compound **PSB-KK-1415**. This suggests that exploring various bicyclic moieties with different substituents in this position could be worthwhile. However, before proceeding, the potential influence of directly attaching a phenyl ring to *N*7 was explored. In fact, by synthesizing a compound with a phenyl ring instead of the naphthyl present in **FPE-114**, we can determine which ring plays a greater role in the compound's activity.

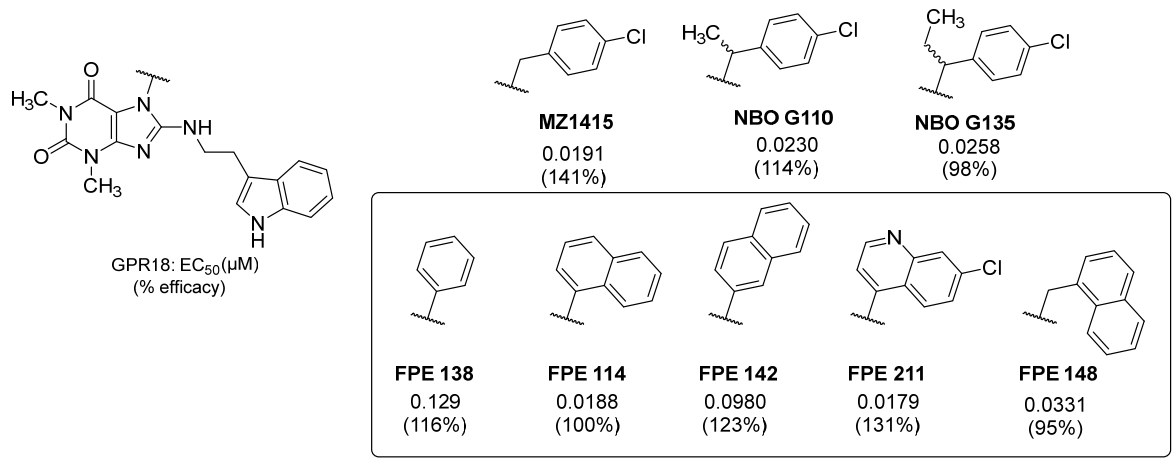

Figure 29. Biological data of bicyclic and related compounds. Framed: newly synthesized compounds.

FPE-138 was therefore synthesized according to strategy III (*Scheme 27*). The biological activity showed almost a 7-fold decrease (*Figure 29*).

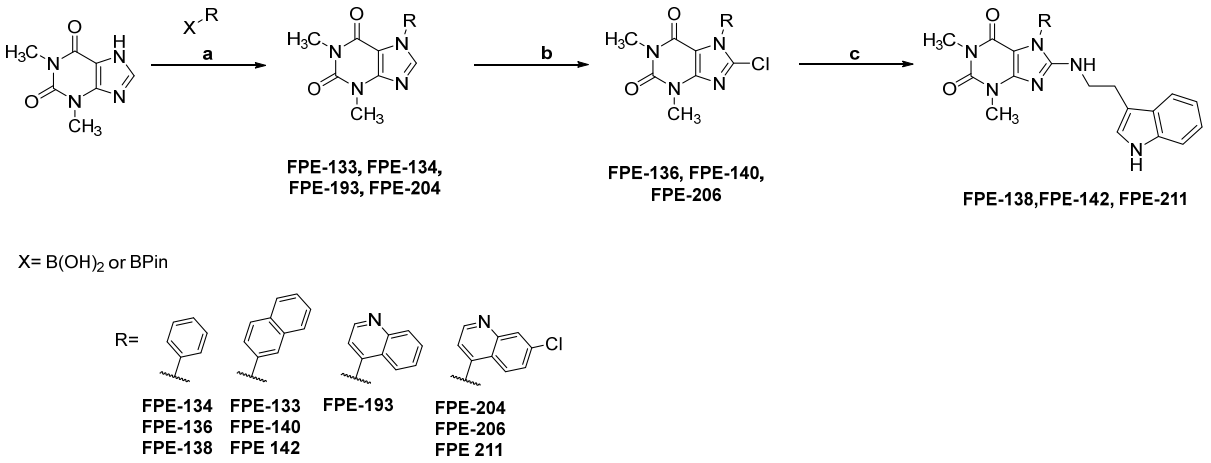

*Scheme 27. Synthesis of compounds **FPE-138, FPE-142, FPE-211.** Conditions: **a)** Na_2CO_3, 2,2´-bipyridine, $Cu(OAc)_2$, DCE, 70°C, 5h; **b)** NCS, THF, RT, 16h; **c)** tryptamine, DIPEA, NMP, 145°C.*

Switching from 1-naphthyl (**FPE-114**) to 2-naphthyl with compound **FPE-142** resulted in ~5-fold decrease in the activity. This shows that compared to the phenyl in **FPE-138** a bulkier, more lipophilic substituent is always preferred in this position, but a certain orientation of the fused ring may be more favourable like for **FPE-114**.

In line with this observation, other bicyclic moieties were explored. A compound featuring a naphthyl group with chlorine at position 6 could potentially mimic the lead structure's orientation

and contribute to its activity. However, acquiring the corresponding boronic acid proved to be challenging due to its limited availability and high cost. As an alternative, commercially available 7-chloro-4-quinolyl boronic acid was employed to synthesize compound **FPE-211**. Activity was again equipotent to that of the lead structure (*Figure 29*) and of **FPE-114**. Although we anticipated enhanced activity from the chlorine substitution, the presence of nitrogen likely restricted this improvement.

To validate this hypothesis, an attempt was made to synthesize a compound bearing only a 4-quinolyl moiety. Although the first Chan-Lam coupling step successfully yielded compound **FPE-193** (*Scheme 27*), the subsequent chlorination step at a small scale yielded insufficient quantities of the desired product, which could only be obtained in limited amounts. Future efforts may involve optimizing reaction conditions and scaling up of the synthesis to obtain the target compound.

Finally, compound **FPE-148** with a naphthyl moiety connected via a CH_2 linker was synthesized using strategy IV (Scheme 1). Its EC_{50} value in the nanomolar range (*Figure 29*) shows once again that aromatic residues and lipophilicity are beneficial.

To determine potential changes in biological activity according to the size of rings introduced as substituents, the synthesis of **FPE-163** and **FPE-ML12** were attempted. In both cases, the reaction happened quite slowly and with the formation of many side products.

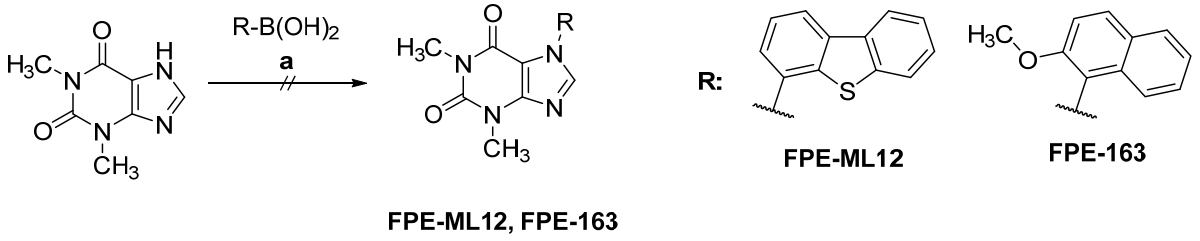

*Scheme 28. Attempt at the synthesis of **FPE-ML12** and **FPE-163**.*

This difference compared to the previously synthesized derivatives in our group (especially referring to the reaction with 1-naphthaleneboronic acid) could be explained by the larger steric hindrance as well as by the presence of an electron-donating atom in *o*-position to the boronic acid that may create a hydrogen bond (Figure 30).

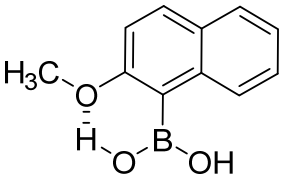

Figure 30. H-bond formation between methoxy group and the boronic acid leading to lower reactivity and inefficient reaction.

This could lead to a lower capability of the boronic acid itself to act as a leaving group. These reactions yielded extremely low amounts of desired product, and low purity. Therefore, the corresponding final compounds could not be synthesized in the end.

The abovementioned findings will help in the design and synthesis of future compounds with other lipophilic bicyclic cores. They establish that direct substitutions of *N*7 with aromatic systems are effective only with the use of boronic acids/esters via Chan-Lam-Evans coupling reactions with some exceptions for which a different strategy should be put in place.

3.1.1.6 Design of a fluorescent ligand

In designing fluorescent ligands, as discussed in paragraph 1.1.5, we focus on three main parts. First, the pharmacophore, which maintains the ligand's biological activity while allowing for further modifications. Second, the linker, connecting the pharmacophore to the fluorophore, varying in composition and length. Lastly, the fluorophore itself, adding fluorescence for detection.[1] As for the suitable pharmacophore, good opportunities are offered by the compounds shown in Figure 31. In fact, they present functional groups interesting for further substitution.

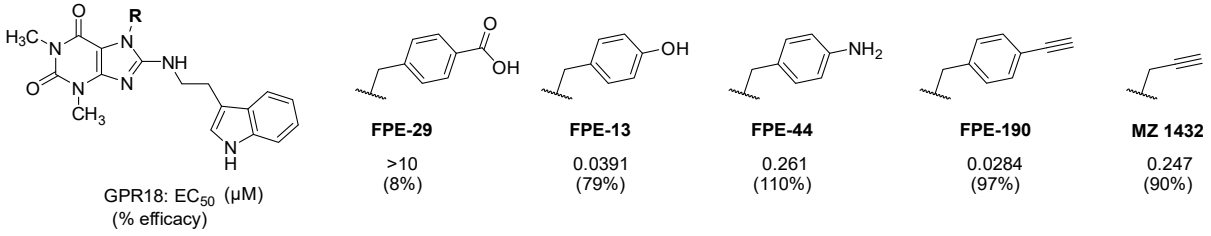

Figure 31. Molecules presenting functional groups suitable for further substitutions.

As for the linkers, polyethylene glycol (PEG) chains are commonly used as linkers in medicinal chemistry due to their biocompatibility and ability to improve solubility and pharmacokinetic properties of compounds. Tetraethylene glycol (TEG) was chosen as the foundation for the linker moieties, since the four units offer an optimal intermediate linker length. For a versatile approach, the linker should be designed and synthesized as a bifunctional molecule, incorporating a conjugatable group, such as an azide or ethynyl group for click chemistry, or an amino group for amide formation, along with a reactive group for attachment to the pharmacophore. The tosyl group

was chosen for its high reactivity and its ability to render the linker detectable via TLC and LC-MS.

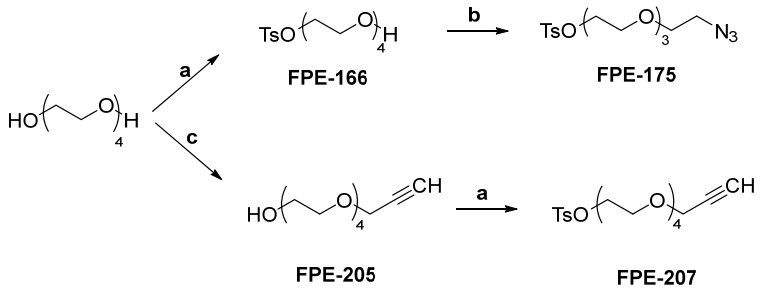

*Scheme 29. Synthesis of bifunctionalized linkers **FPE-175, FPE-207**. Conditions: **a)** TsCl, TEA, CH_2Cl_2, 0°C to RT, 3 h; **b)** NaN_3, DMF, RT, 16 h. **c)** (i) NaH, DMF, 0°C, 15 min; (ii) propargyl bromide, RT, 6 h. TEA: triethylamine.*

As for the fluorophores, in NanoBRET assays, efficient energy transfer depends on the overlap between the donor emission and acceptor excitation wavelengths. NanoLuc, with an emission peak at around 460 nm, pairs well with simple BODIPY fluorophores, which have excitation peaks between 490-520 nm and emission peaks in the 510-550 nm range, making them well-suited for clear signal detection in these assays.[1]

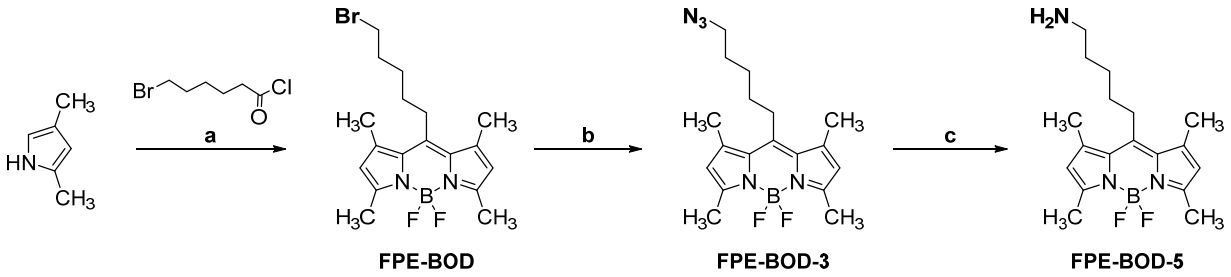

*Scheme 30. Synthesis of functionalized BODIPY fluorophores. Conditions: **a.1)** DCM, 0°C to RT, 4h; **a.2)** Et_3N, 0°C, 0.5 h; **a.3)** $BF_3{\cdot}OEt_2$, 0°C to RT,1h; **b)** NaN_3, dry DMF, 50°C, 2.5h; **c)** PPh_3, THF, RT, 12h.*

Following a well-established one-pot procedure in our group (*Scheme 30*), **FPE-BOD** was synthesized initially by reacting 2,4-dimethyl-1*H*-pyrrole with 6-bromohexanoyl chloride in a three-step process. Subsequent treatment with sodium azide and heating produced **FPE-BOD-3**. The latter underwent Staudinger reaction to convert the azide to amine and obtain **FPE-BOD-5**. This method differs from the conventional approach described by Heisig et *al.*, which utilizes methanolic ammonia under microwave irradiation to obtain the NH_2 BODIPY.[145]

3.1.1.7 Design of a fluorescent ligand — flexible linkers

With the abovementioned linkers in hand, the first strategy was to use the very good activity shown by **FPE-13**. As previously said, longer alkyl chains on the hydroxyl group of this derivative are worth being tested, to assess the possibility of future connection to fluorescent probes. Therefore, a TEG-containing linker presenting a tosyl group on one side and azide on the other was attached to **FPE-13** via S_N2 as shown in Scheme 31.

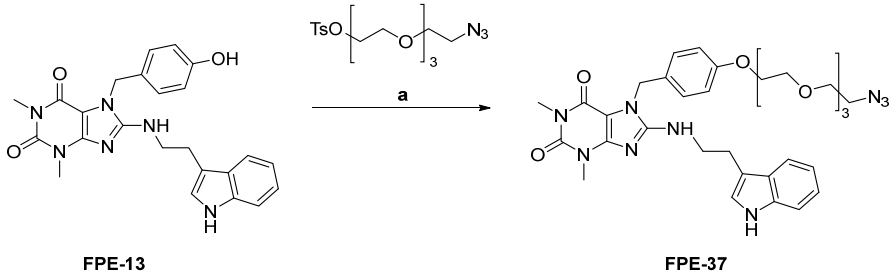

*Scheme 31. Synthesis of **FPE-37**. Conditions: **a)** K_2CO_3, DMF, 80°C, 12h.*

It is important that any combination of pharmacophore + linker as well as pharmacophore + linker + fluorophore is treated as its own pharmacological entity with different properties and biological activity. As such, before proceeding with a fluorophore attachment via click chemistry on the azide side, **FPE-37** was tested (Figure 32). With an EC_{50} value of 0.681 μM, **FPE-37** is not entirely to be discarded, but still does not represent an optimal linker candidate. This may be due to the fact that, according to the biological results to date and the molecular modeling predictions, the area where this portion of the molecule positions itself is a very lipophilic one.

To further confirm this, compound **FPE-191** was synthesized as shown in Scheme 32.

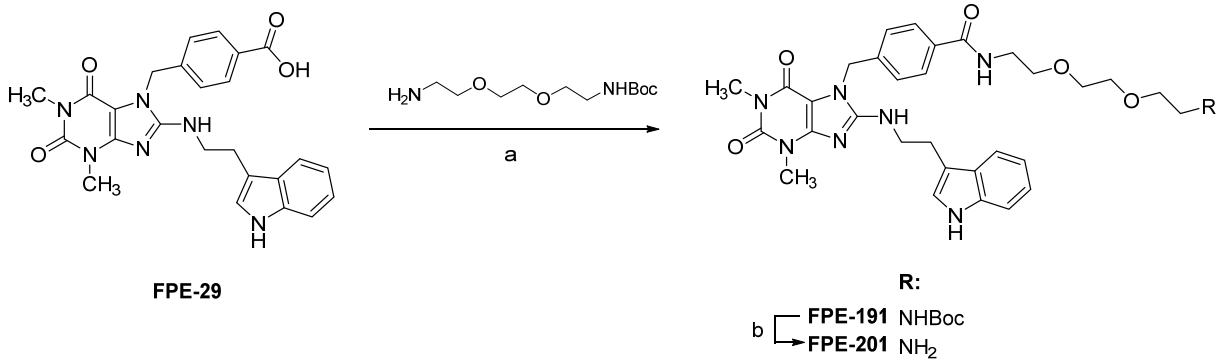

*Scheme 32. Synthesis of compounds **FPE-191** and **FPE-201**. Conditions: **a)** $POCl_3$, pyridine, RT, 12h; **b)** HCl 4N in dioxane, MeOH, 0°C to RT, 24h.*

Ether formation from **FPE-13** often resulted in low yields and debenzylation side-products (Scheme 4), therefore, considering the improvement in the activity obtained going from compound **FPE-29** (free carboxylic acid) to **FPE-76** (amide) (Figure 18), and the easy accessibility of this building block (cheap starting materials, straight-forward reactions), amide coupling with diamine linkers was performed

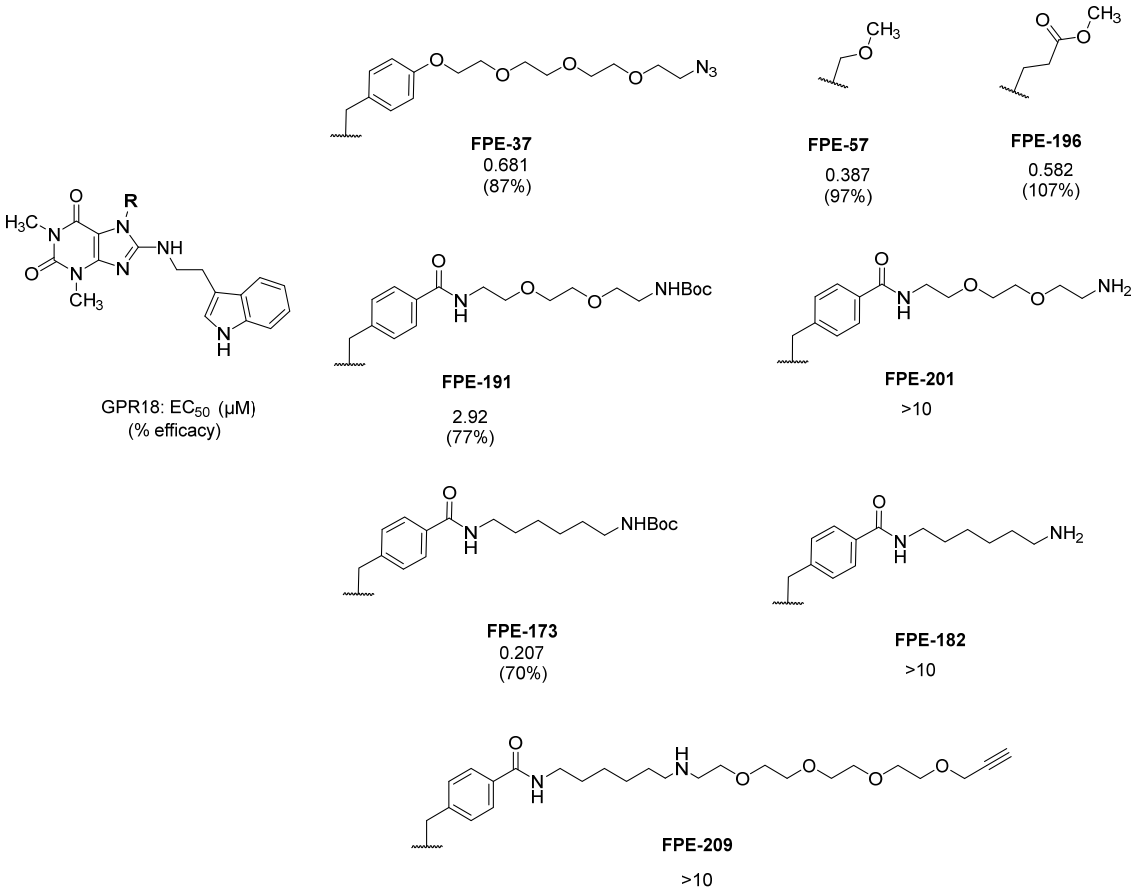

*Figure 32. Biological evaluation of compounds **FPE-37, FPE-191, FPE-201, FPE-196, FPE-173, FPE-182, FPE-209** bearing different linkers.*

Already **FPE-191** shows a 4-fold decrease in activity compared to **FPE-37** and this loss is even more pronounced when more hydrophilicity is introduced in the molecule with a free NH_2 in compound **FPE-201** (Figure 32). Thus, the idea was to attach a "double linker" consisting of a small hydrocarbon chain (4-5 carbons) and a PEG chain as shown in *Figure 33*.

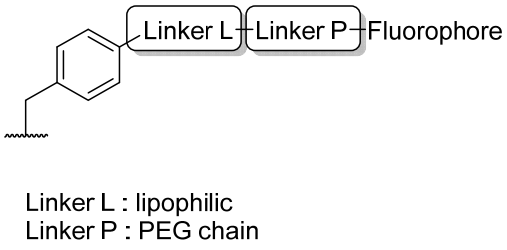

Figure 33. "Double linker" strategy.

The small hydrocarbon chain will probably be more compatible with the lipophilic area and lead to a more tolerated derivative, while providing more length for the PEG linker to eventually protrude on the extracellular side.

As shown in Scheme 33, a first attempt using the methyl ester of 5-bromopentanoic acid, was not successful as far as the alkylation of **FPE-13** is concerned.

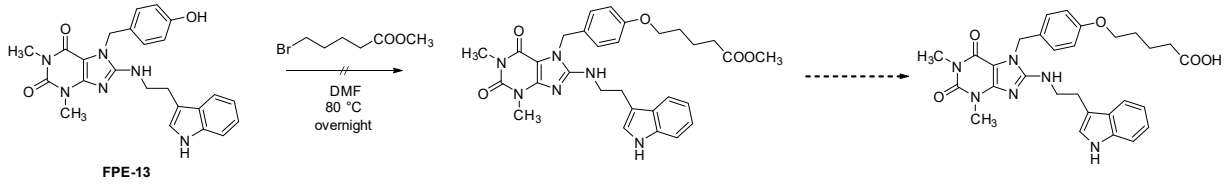

*Scheme 33. Attempt of introducing a lipophilic linker via ether formation on **FPE-13.***

Since the amide coupling looked like a more straightforward strategy, it is tried on **FPE-29** with hexamethylenediamine Boc-protected on one side, as shown in *Scheme 34*. The corresponding product, **FPE-173,** underwent Boc deprotection to achieve **FPE-182** with a free amino group. The latter was able to react as a nucleophile on the tosylated PEG linker **FPE-207** to achieve **FPE-209**.

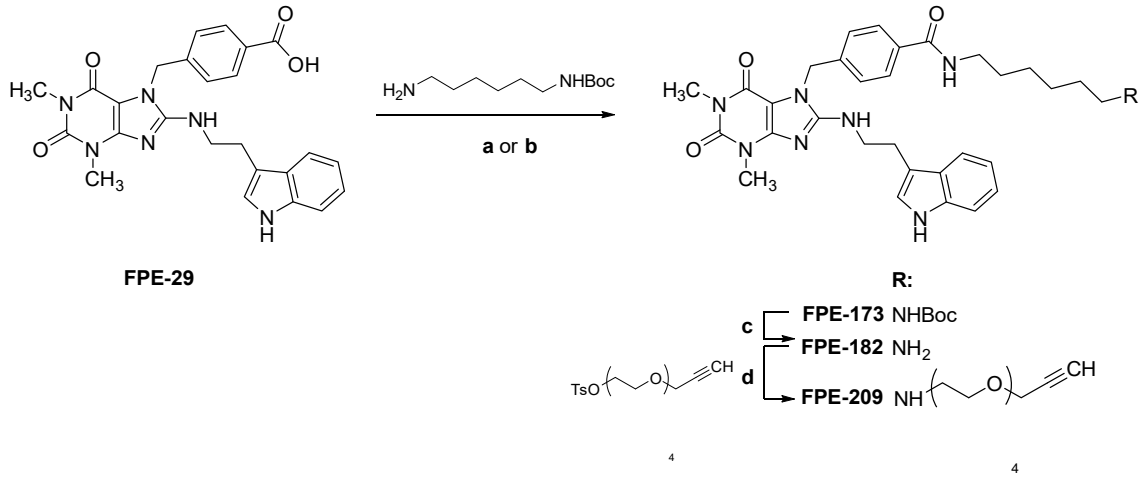

*Scheme 34. Synthesis of compounds **FPE-173, FPE-182 and FPE-209** to test the double-linker strategy. Conditions: **a)** $POCl_3$, pyridine, RT, 12h; **b)** DIPEA, COMU, DMF, RT, 12h; **c)** HCl 4N in dioxane, MeOH, 0°C to RT, 24h; c) K_2CO_3, DMF dry, RT to 80°C, 18h. COMU: (1-Cyano-2-ethoxy-2-oxoethylidenaminooxy)dimethylamino-morpholino-carbenium hexafluorophosphate.*

As seen in Figure 32 and as expected, **FPE-173** shows a 14-fold increase in activity compared to the pegylated counterpart **FPE-191**. In both cases, removal of the Boc group and the presence of a free amine leads to a total loss in activity. This is also true when a PEG chain is introduced in **FPE-209**.

A direct attachment of linker + fluorophore to *N*7 had been attempted in the past with compound **NBOG75**, but resulted in a molecule that despite its moderate activity, had great solubility problems (Figure 34). Therefore, maybe a longer, more hydrophilic chain will be a good alternative to continue.

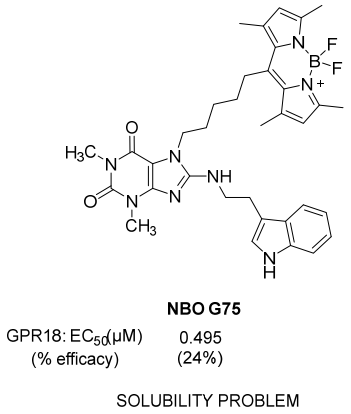

*Figure 34. Biological evaluation of **NBOG75** featuring a direct connection between a BODIPY fluorophore on N7.*

Compound **FPE-196** was synthesized according to strategy IV, as shown in Scheme 35. A first attempt to hydrolyze the ester with the specified conditions was not successful, but it is a great starting point for further development.

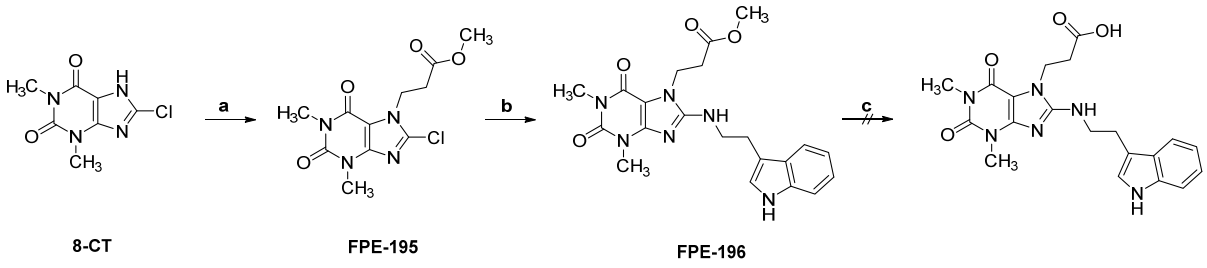

*Scheme 35. Synthesis of **FPE-196** and attempt to hydrolyze the ester. Conditions: **a)** methyl 3-bromopropanoate, K_2CO_3, DMF, RT, 2.5 h; **b)** Tryptamine, DIPEA, NMP, 145°C, 18h; c) **)** LiOH · H_2O, THF, RT, 12h.*

With an EC_{50} value of 0.582 μM, **FPE-196** may open up new possibilities for the future attachment of fluorophores.

In a similar manner, compound **FPE-57** was synthesized with a common methylenemethoxy (MOM) protecting group on *N*7. This compound was designed to serve both as it is and as a building block for future modifications, specifically to prevent interference with the NH group at position 7 while modifying the indolylethylamino portion of the molecule. The synthesis was carried out as shown in Scheme 36.

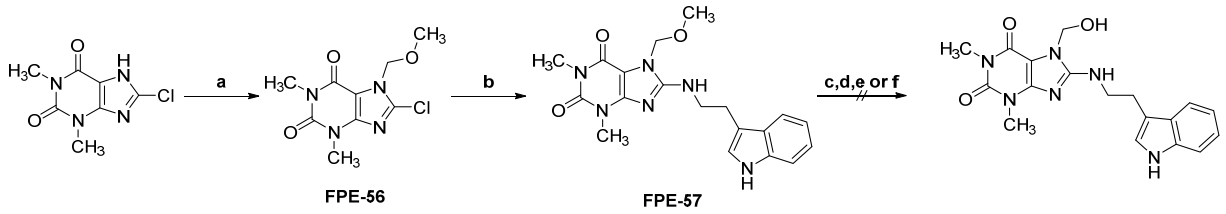

*Scheme 36. Synthesis of **FPE-57**. Conditions: a) MOM-chloride, DMF, K2CO3, RT, 12h; b) tryptamine, DIPEA, NMP, 145°C, 12h; c-f: see Table 9. MOM: Methoxymethyl.*

*N*7 was alkylated using MOM-chloride to produce **FPE-56**,[146] which was then coupled with tryptamine to yield the desired MOM-protected compound, **FPE-57**. Of all the strategies tested to act on the MOM group, only the demethylation conditions previously used to obtain **FPE-13** were successful (Table 9, reaction f). However, this method resulted in the complete removal of the MOM group, producing **FPE-179**, but with a very low yield of only 7%.

Table 9. Reactions conditions used on FPE-57.

Reaction	Conditions	Comments
c	HCl 4M, MeOH, RT, overnight	No go
d	4M HCl/dioxane, 90°C, overnight	No go
e	Pd/C, H_2, RT, 5h	No go
f	BBr_3, DMF, 5°C, 3h	Full removal of MOM (7% yield)

A more efficient strategy needs to be used if a demethylation is desired.

In the meantime, **FPE-57** was biologically evaluated and showed nearly a 2-fold decrease in potency compared to its non-oxygenated counterpart, **MZ1411** (Table 3).

This suggests that introducing a more polar atom can interfere with the optimal interactions typically formed by a small, non-polar, lipophilic moiety like a propyl group. However, the MOM group is still smaller and more flexible than the methyl butyrate group of **FPE-196**, which might allow better accommodation within the receptor's binding site, potentially leading to a more effective interaction.

3.1.1.8 Design of a fluorescent ligand — triazole-based linkers

The advent of click chemistry has made triazole-based linkers popular due to their relative rigidity. The copper-catalyzed azide–alkyne cycloaddition (CuAAC) between an alkyne and an azide forms a 1,4-disubstituted 1,2,3-triazole, serving as a linker and enhancing solubility. To optimize the conditions and check for tolerability of such moieties in the binding pocket, compound **FPE-144** was first synthesized, as shown in *Scheme 37*.

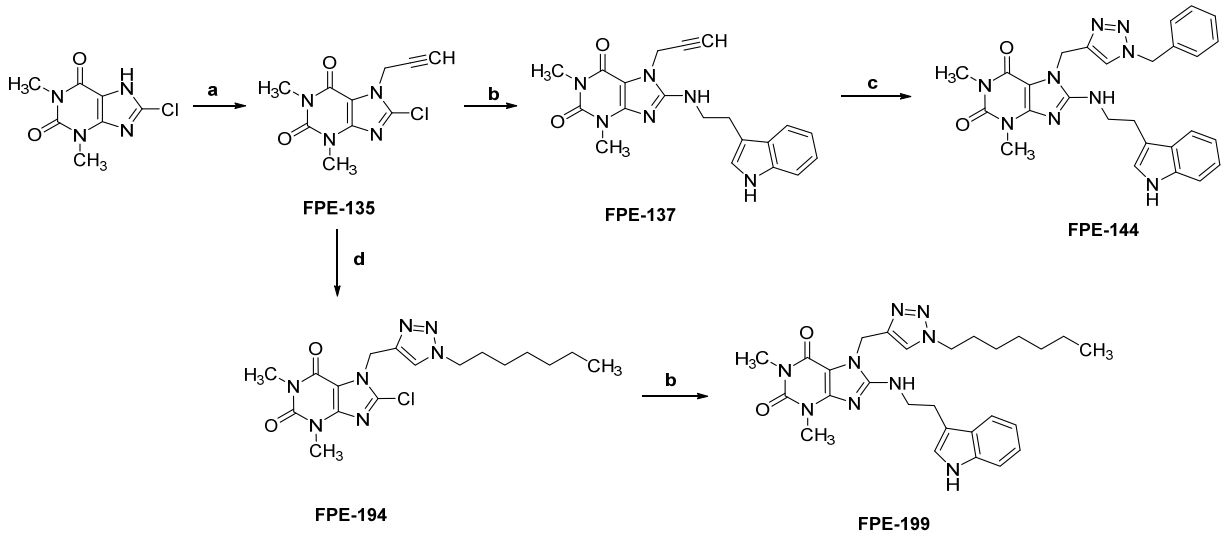

*Scheme 37. Synthesis of compounds **FPE-144** and **FPE-199** bearing a triazole linker. Conditions: **a)** K_2CO_3, DMF, RT, 2.5 h; **b)** tryptamine, DIPEA, NMP, 145°C, 18h; **c)** see Table 10, entry 1; **d)** see Table 10, entry 4.*

Firstly, **MZ1432** was resynthesized and then subjected to classical click chemistry conditions as detailed in Table 10, entry 1, yielding **FPE-144**.[147] Due to long reaction times and low yields, further optimization attempts were made, as shown in entry 2. Despite the consumption of the starting material, only by-products were formed. Less harsh conditions may be tried, e.g. with 2,2'-bipyridine as for the Chan-Lam-Evans coupling reaction. After $CuSO_4$ is reduced to Cu(I) by a reducing agent like sodium ascorbate, 2,2'-bipyridine forms a stable complex with Cu(I). 2,2'-bipyridine in conjunction with $CuSO_4$ and a reducing agent could be a robust and efficient catalytic

system, leveraging the stability and reactivity of the Cu(I)-bipyridine complex to achieve high yields and selectivity in the synthesis of 1,2,3-triazoles.[148,149]

Attempts were made using microwave irradiation with the corresponding bromide and sodium azide. This one-pot, copper-catalyzed azide formation/click reaction would generate the desired organic azide in situ, avoiding handling large amounts of these toxic compounds and utilizing the high availability of alkyl bromides in our group.

Initially, the reaction between **FPE-137** and *p*-chlorobenzyl bromide (the substituent of the lead compound) in the presence of the catalyst system $CuSO_4 \cdot 5H_2O$ and sodium ascorbate was not successful (Table 10, entry 3).

Simultaneously, the catalyst system $CuSO_4 \cdot 5H_2O$ and metallic Cu according to Appukkuttan et *al.* was tried (Table 10, entry 4).[150] The reaction was conducted on the building block **FPE-135**, bearing already a propargyl group, due to the limited availability of the final compound **FPE-137,** using 7-bromobenzene to test longer alkyl chains and a double linker in this position. As shown in Scheme 32, this successfully led to **FPE-194**, which then underwent tryptamine coupling to produce the final compound **FPE-199**.

The two successful strategies, with and without microwave irradiation, were then employed to generate compounds containing a BODIPY fluorophore. The reaction between **FPE-190** and **FPE-BOD3**, which already had an azide group (Table 10, entry 5), was unsuccessful despite extending the reaction time to 48 hours. Next, microwave-assisted one-pot copper-catalyzed azide formation/click reaction conditions were tried using **FPE-BOD** with a bromo instead of an azido function. This also failed to yield the desired compound after 20 minutes. Extending the reaction time to 40 minutes resulted in damage to the fluorophore (Table 10, entry 6). A final effort (Table 10, entry 7) with **FPE-209** and **FPE-BOD** confirmed that 20 minutes was sufficient for azide formation but not for triazole formation. These experiments were valuable in understanding the fine-tuning required for fluorophore attachment. Rather than using high temperatures and longer times, it is better to employ less harsh conditions, potentially using alternative catalyst systems and improved purification techniques to achieve higher yields.

Table 10. Attempts and optimization of the click-chemistry reaction conditions. See text for details. Trypt: tryptamine.

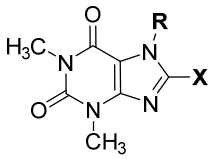

Entry	R	Reagent	Conditions	Yield
1 **X = Trypt**		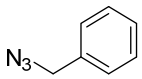	$CuSO_4 \cdot 5H_2O$, sodium ascorbate, H_2O/*t*BuOH 1:1, 60°C, 24h	20 %
2 **X = Trypt**		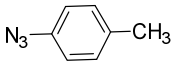	$CuSO_4 \cdot 5H_2O$, sodium ascorbate, DMF, MW "Dynamic Mode", 110°C → 150°C, 1.5h	-
3 **X = Trypt**		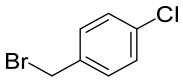	$CuSO_4 \cdot 5H_2O$, sodium ascorbate, H_2O/*t*BuOH 1:1, NaN_3 MW "Fixed Power" 100W, 125°C,1h	-
4 **X = Cl**		$Br(CH_2)_6CH_3$	NaN_3, $CuSO_4 \cdot 5H_2O$, Cu(0), MW "Fixed Power" 100W, 125°C, 20'	13%
5 **X = Trypt**	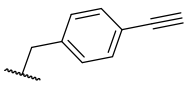	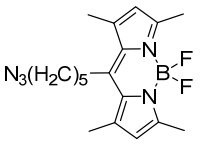	$CuSO_4 \cdot 5H_2O$, sodium ascorbate, H_2O/*t*BuOH 1:1, RTto 60°C, 48h	-
6 **X = Trypt**		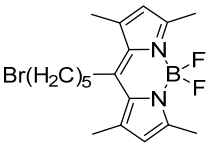	NaN_3, $CuSO_4 \cdot 5H_2O$, Cu(0), MW "Fixed Power" 100W, 125°C, 40'	-
7 **X = Trypt**	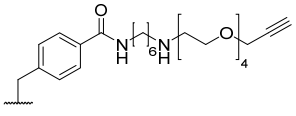	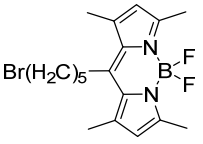	NaN_3, $CuSO_4 \cdot 5H_2O$, Cu(0), MW "Fixed Power" 100W, 125°C, 20'	-

To check for suitability of a triazole moiety in this position, **FPE-144** and **FPE-199** were biologically assessed (Figure 35). With an EC_{50} value of 0.619 µM, **FPE-144** is not ideal indicating that bulkier moieties (e.g., fluorophores) may not be tolerated in this position. However, the longer and more flexible alkyl chain in **FPE-199** led to a 2.5-fold higher activity. This is promising for future attempts to attach a fluorophore.

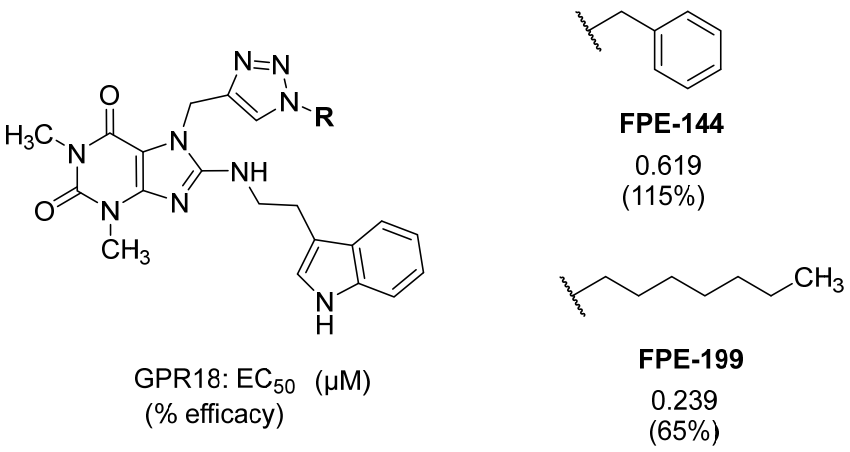

*Figure 35. Biological evaluation of triazole-bearing compounds **FPE-144** and **FPE-199**.*

3.1.2 Scaffold modifications

While the primary focus of this research was directed towards improving potency via substitutions on *N*7 and designing a fluorescent probe, scaffold modification of the xanthine core was pursued as a secondary goal. Nonetheless, these modifications would provide valuable insights into the SAR and contribute to the overall understanding of how potential lead compounds interact with the target receptor.

3.1.2.1 Attempts to achieve a 9-deaza core

A modification that seemed interesting was the generation of xanthine core structure derivatives starting from the corresponding 9-deazaxanthine scaffold. This alteration is particularly intriguing because replacing the nitrogen atom at position 9 with a carbon can significantly impact the electronic properties and hydrogen bonding potential of the molecule, potentially leading to differences in receptor binding and selectivity. This specific modification has been explored also in other projects, e.g. developing antiviral and anticancer molecules and adenosine receptor antagonists.[151–153] Synthesis is shown in Scheme 38.

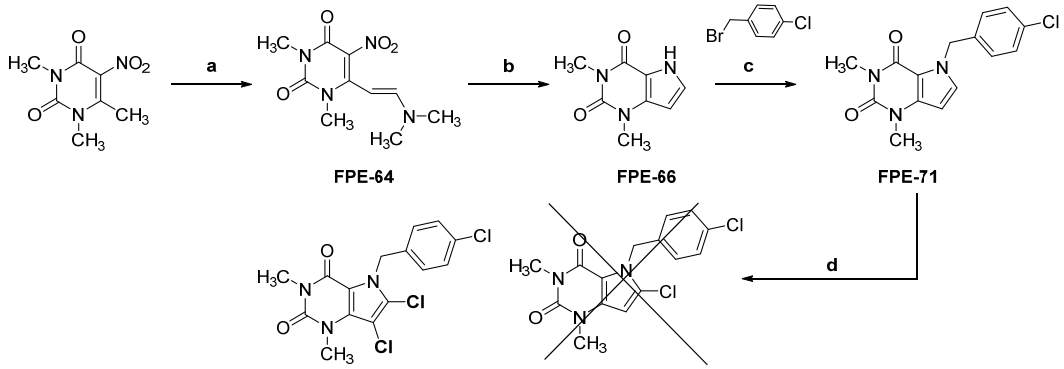

Scheme 38. Attempt at the synthesis of the 9-deazaxanthine scaffold. Conditions: ***a)*** *DMF-DEA, Dry DMF, RT, 2.5h;* ***b)*** *Pd/C, H_2, MeOH, RT, 2h;* ***c)*** *K_2CO_3, DMF, RT, 2.5h;* ***d)*** *NCS, THF, RT, 16h.*

According to literature, the synthesis began with the reaction of 1,3,6-trimethyl-5-nitro uracil with DMF-diethylacetal (DMF-DEA) to achieve **FPE-64**.[154] This reaction introduced a dimethylaminovinyl group that is crucial for the subsequent cyclization step. The latter happened via hydrogenation over palladium/carbon to obtain **FPE-66**. Alkylation with *p*-chlorobenzyl bromide (substituent of the lead compound) gave **FPE-71**. The latter underwent validated strategy I conditions, but long reaction times necessary for the full conversion of the starting material

resulted in a compound chlorinated on both *C*8 and C9. It was therefore not possible to proceed with the following step.

Other strategies avoiding the chlorination step can be tried in the future, as the one proposed below in Scheme 39.

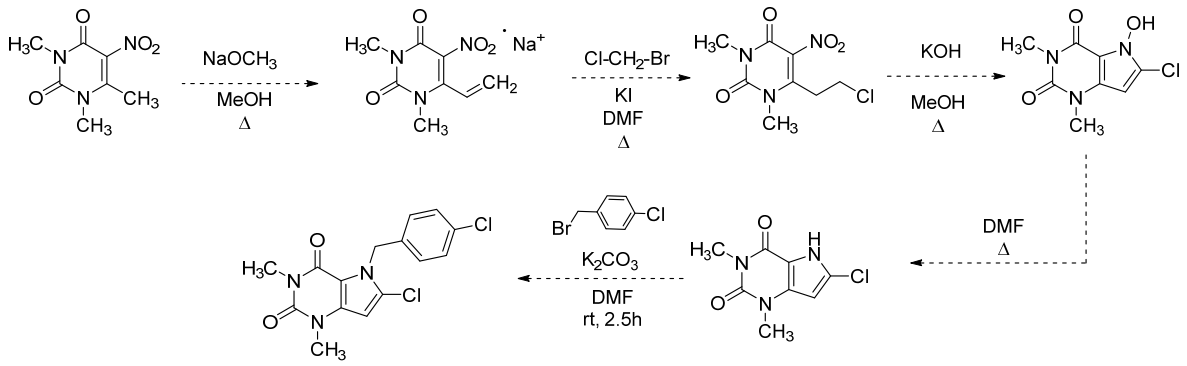

Scheme 39. Proposed strategy for the synthesis of the 9-deazaxanthine derivative.

Another possible approach would be the synthesis of the corresponding 9-deazaxanthine brominated at position *C*8 exploiting malonate chemistry as shown by Bartoccini et *al.* [155]

3.1.2.2 Attempts to synthesize a thionated xanthine core

Modifying the xanthine core by converting its carbonyl groups into thiocarbonyl groups represents a strategic approach in drug design. This will help understanding the actual relevance of each oxygen and assessing whether a thiocarbonyl could be more effective (for example regarding the nature of hydrogen bond formation: thio groups being weak H-bond acceptors in contrast to carbonyl groups.[156,157]

For the *C*6 carbonyl, some literature suggested the possibility of selectively converting it in a thiocarbonyl most likely due the different electronic environment around this carbonyl.[158] The carbonyl carbon at *C*6 may be more electrophilic due to electronic effects from adjacent groups and aromatic stabilization, making it more prone to nucleophilic attack by thionation reagents. The different approaches are depicted in Scheme 40.

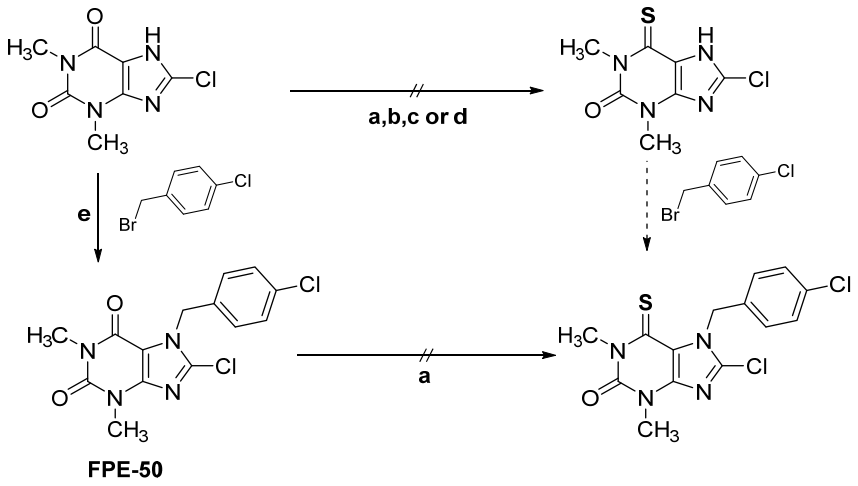

Scheme 40. Attempts at the conversion of the carbonyl at C6 into a thiocarbonyl. Conditions: ***a)*** *Lawesson's reagent, toluene, reflux, 30h;* ***b)*** *Lawesson's reagent, THF, reflux, 48h;* ***c:*** *P_2S_5, pyridine, 115°C;* ***d)*** *Lawesson's reagent, microwave 60W to 100W, 13 min;* ***e)*** *K_2CO_3, RT, 2.5h*

Lawesson's reagent (LR) is a very effective mild thionating agent, which upon heating generates two reactive dithiophosphine ylides. Using LR directly on 8-chlorotheophylline did not lead to the desired product with none of the tried conditions (*Scheme 40*), including the microwave-assisted one[159]. Initially this was thought to be due to the presence of a free NH group, which could interfere with LR, leading to its ring-opening.[160] Therefore, the following approach involved the resynthesis of the building block **FPE-50** via alkylation of 8-chlorotheophylline with 1-(bromomethyl)-4-chlorobenzene. This underwent the same thionating conditions, but still no product was achieved.

Finally, P_2S_5 was tried instead, which could allow better compatibility with the substrate and the exploration of a different set of conditions (e.g. pyridine at higher temperatures) that could potentially overcome the limitations encountered with LR. Unfortunately, even this approach was not successful.

Considering that the selective conversion of the *C*6 carbonyl to a thiocarbonyl in theophylline has been documented in literature,[161] maybe the presence of the chlorine in position *C*8 can alter the electronic environment around the adjacent positions, potentially making the carbonyl less reactive towards thionation. A final strategy could be the usage of theophylline itself as reported in literature, proceeding with chlorination of *C*8.[159]

A completely different method was employed to convert the carbonyl at *C*2. As depicted in Scheme 41, initial attempts to open the ring of compound **FPE-50** unexpectedly yielded a series of side

products, with **FPE-53-F1** being the most predominant one. Featuring a hydroxy group at position 8, it presents a promising candidate for further investigation into linker modifications between the xanthine scaffold and the indole moiety (as discussed in Section 3.1.3). Attempts to alkylate this hydroxy group under the described conditions were unsuccessful. Future efforts will focus on alternative ring-opening strategies, potentially followed by ring closure (e.g., using 1,1′-thiocarbonyldiimidazole) and coupling with tryptamine.

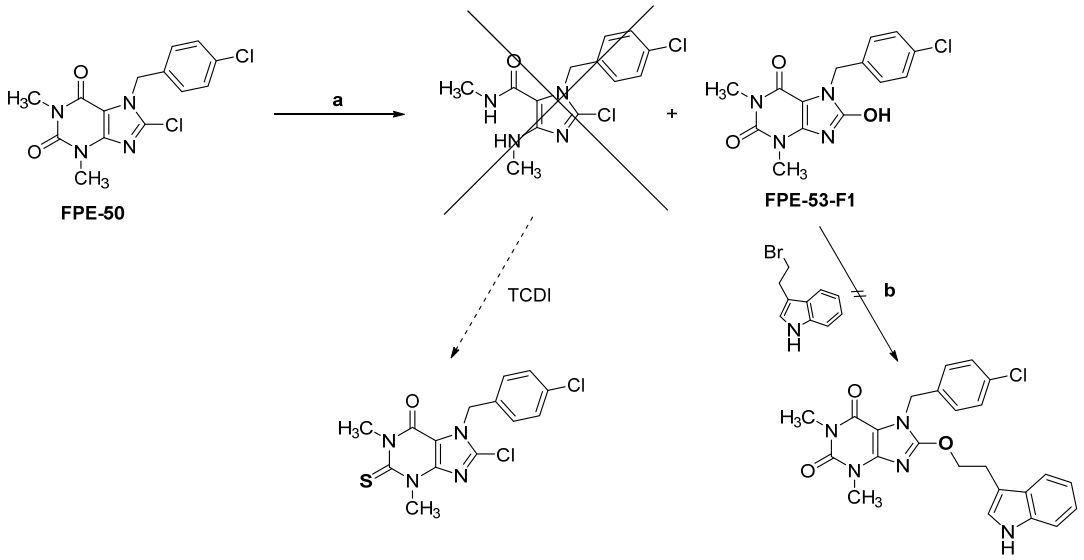

Scheme 41. Conversion attempts of the carbonyl at C2 into a thiocarbonyl. Conditions: ***a)*** *2N NaOH, dioxane, 90°C, 4h;* ***b)*** *K_2CO_3, DMF, RT, 12h.*

The subsequent strategy aimed at building the core by scratch in an 8 step procedure (Scheme 42).[162] Firstly 6-amino-1,3-dimethyl-2-thiouracil was synthesized reacting 1,3-dimethylthiourea and cyanoacetic acid in acetic anhydride under microwave irradiation. After having obtained this building block, the steps of strategy I were followed: nitrosation (**FPE-MP5**), conversion of the nitroso group to amino (**FPE-MP6**), formation of a Schiff base with *p*-chlorobenzaldehyde (**FPE-MP7**), followed by its reduction (**FPE-MP9**) and ring closure with triethyl orthoformate (**FPE-MP10**). When trying to synthesize the compound bearing a chlorine at position *C*8, the validated chlorination procedure with NCS proved unsuccessful.

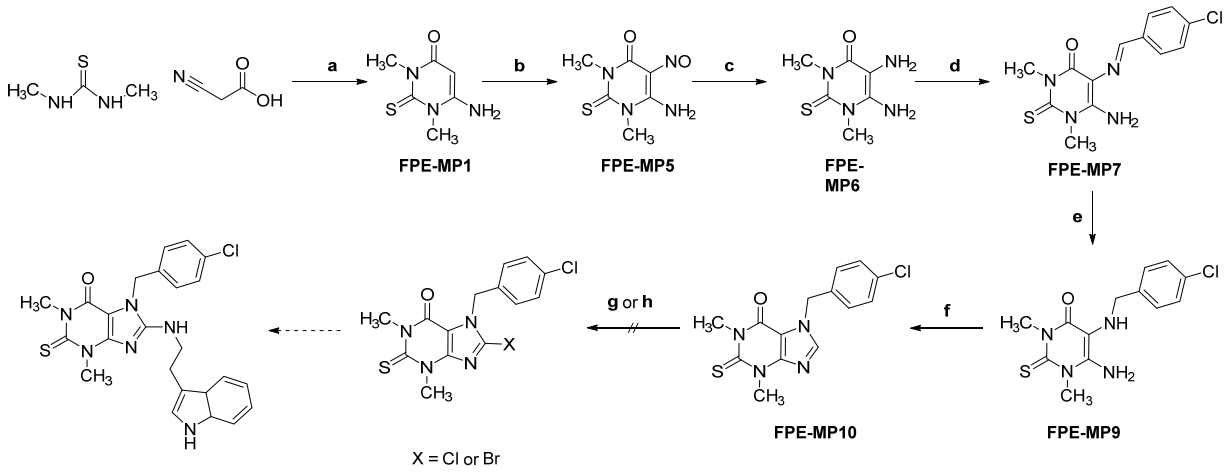

Scheme 42. 8-step synthesis plan to achieve a thiocarbonyl at position 2 of the xanthine core. Conditions: ***a)*** *acetic anhydride, microwave 200W, 70°C, 2h;* ***b)*** *$NaNO_2$, 50% CH_3COOH_{aq} at 65°C, 10 min; c) $Na_2S_2O_3$, 12.5% NH_4OH_{aq} at 70°C, 10 min;* ***d)*** *p-chlorobenzaldeyde, H_2O, CH_3COOH, 15 min;* ***e)*** *$NaBH_3CN$, DCM, MeOH, CH_3COOH, 15 min;* ***f)*** *TEOF, 145°C, 5h;* ***g)*** *NCS, THF, RT, 16h;* ***h)*** *Br_2, acetic acid in water, RT,15 min.*

N-Chloro succinimide is known to possess mild oxidative properties due to the nature of the N-Cl bond. This very likely led to a fast oxidation of the thiocarbonyl group in position 2, which caused desulfurization. Therefore, another strategy to obtain bromination at milder conditions (room temperature and short reaction time) was tried, but did not yield the desired compound either. Both attempts (chlorination and bromination) were constantly checked via TLC-MS showing the very rapid desulfurization. This was confirmed by LC-MS and NMR analyses.

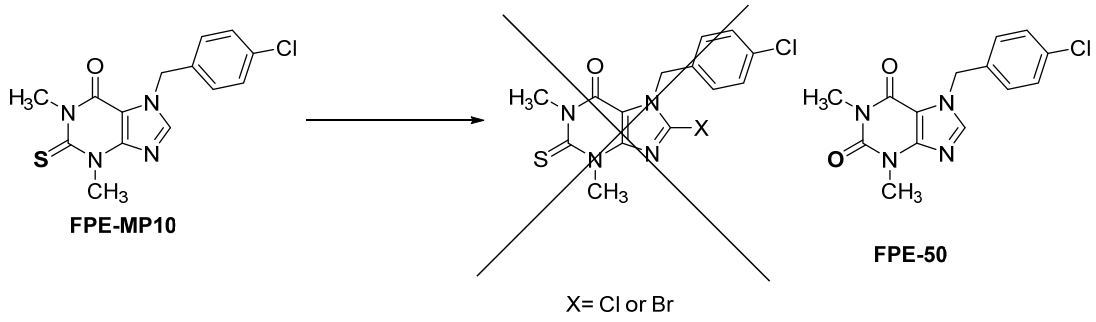

Scheme 43. Desulfurization of ***FPE-MP10*** *leading to* ***FPE-50***

Finally, due to the numerous synthetic challenges encountered, further pursuit of these scaffold modifications was deprioritized in favor of higher-priority goals.

3.1.3 Modifications on the indole and the ethylamino linker

Up to date all modifications on the tryptamine moiety have not resulted in any activity improvement (Chapter 2,

Table 5). However, given the indole's versatility and its common presence in bioactive compounds, additional exploration was conducted to complete the SAR studies and gain a deeper understanding of the ligand's behavior in the binding pocket.

3.1.3.1 Bioisosteric replacement of the indole ring

Firstly, thiophene- and 7-azaindole-containing substituents were tried given the immediate availability of the starting materials — the corresponding carbaldehydes.

As shown in Scheme 44, first of all, the corresponding carbaldehyde underwent Henry reaction with nitromethane and ammonium acetate yielding **FPE-MP17** and **FPE-MP14**.[163] Reduction of both the nitro group and the double bond was performed with $LiAlH_4$ to obtain **FPE-MP18** in the first case. Surprisingly, for the 7-azaindole, the desired intermediate was not the main product of the reaction, whilst several side products were formed. Given the small scale of the reaction, purification was not possible. Another attempt, with milder conditions and scaling up of the quantitiy may lead to the expected compound.

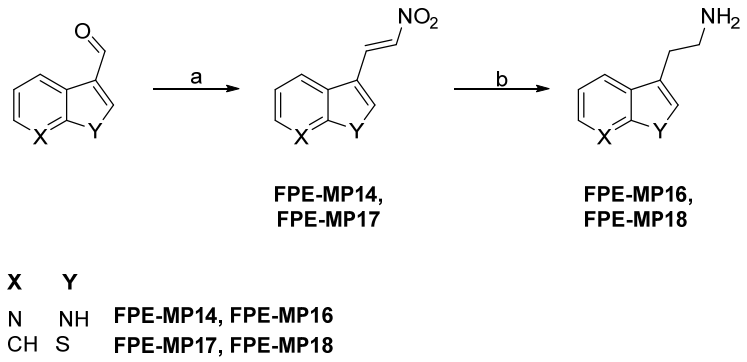

Scheme 44. Synthesis of tryptamine analogues. Conditions: ***a)*** *CH_3NO_2, $CH_3COO^-NH_4^+$, 110°C, 12h;* ***b)*** *$LiAlH_4$, THF, 0°C to RT, 12 h;* ***c)*** *Tryptamine, DIPEA, NMP, 145°C, 18h.*

Finally, **FPE-MP18** was used for the standard tryptamine coupling onto the building block **FPE-50**, to obtain **FPE-MP19**. Similarly, using commercially available benzofuran tryptamine analogue, compound **FPE-203** was made (Scheme 45).

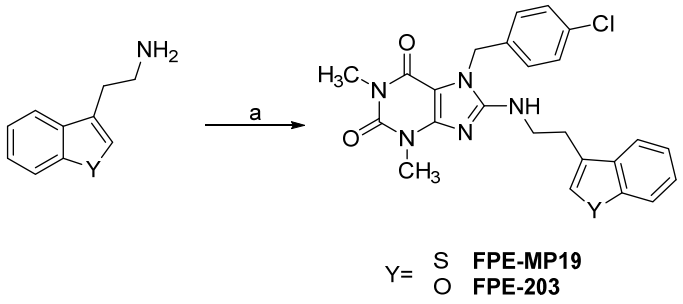

*Scheme 45. Synthesis of **FPE-MP19** and **FPE-203**. Conditions: **a)** Tryptamine, DIPEA, NMP, 145°C, 18h.*

Before proceeding with other attempts for the azaindole synthesis and the introduction of other bioisosteres, compounds were biologically evaluated (Figure 36).

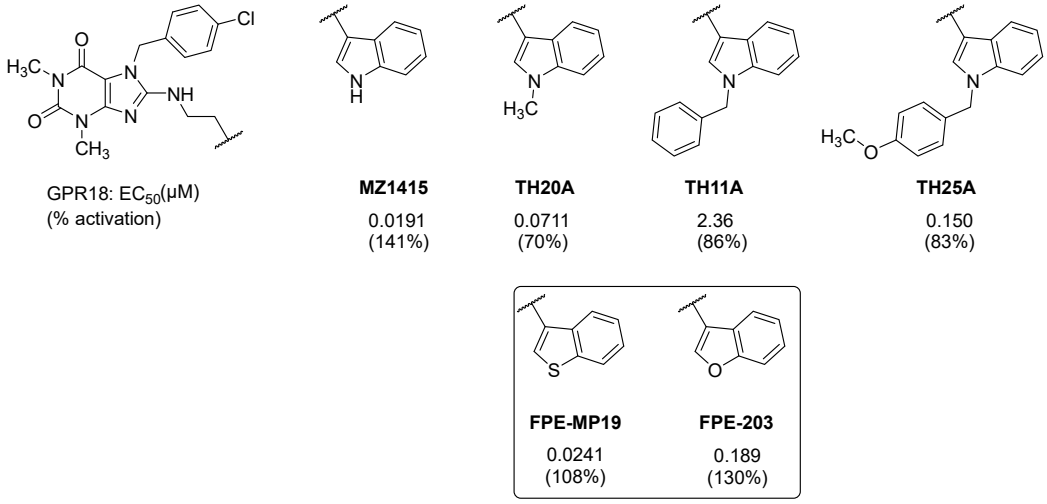

*Figure 36. Biological evaluation of **FPE-MP19, FPE-203** and related previously synthesized compounds.*

As reported in our recent publication, the indole portion of the molecule appears to bind in a lipophilic cavity of the receptor forming H-bond interactions with Tyr264 and π-π stacking with both Tyr264 and Phe248.[88] Methylation of the indole NH group (**TH20A**) disrupts this critical hydrogen bond, resulting in a decrease in binding affinity. However, the indole ring still maintains some favorable interactions with the binding site residues due to its aromatic nature and partial retention of π-π stacking capabilities.

Both sulfur and oxygen are isosteres, but sulfur's greater polarizability and ability to engage in van der Waals or π-π interactions with hydrophobic residues like Ile175 and Leu255, likely make it more effective in mimicking the indole's interaction profile (**FPE-MP19**). In contrast, the benzofuran's oxygen atom does not facilitate a direct hydrogen bond, and its higher

electronegativity disrupts the electron density and interaction dynamics within the binding pocket, leading to a more substantial loss in potency (**FPE-203**).

Larger substitutions are generally not favoured (**TH11A)** although **TH25A** bearing a *p*-methoxybenzyl group is tolerated and may pave the way for fluorophore attachment.

These results suggest that while the hydrogen bond is important, other interactions (e.g., π-π stacking, hydrophobic contacts) also contribute to the overall binding affinity.

3.1.3.2 Changes in the ethylamino linker

The ethylamino linker, connecting the xanthine core to the indole moiety, has not been extensively explored in terms of SAR. Preliminary findings indicated that the NH group in this linker is crucial for activity, as methylation of the NH group led to a complete loss of activity in **TH20B** (*Figure 37*). To confirm the importance of the NH group and to explore alternative linker modifications, a series of derivatives was synthesized. These modifications aim to provide a better understanding of how changes to the linker influence the overall biological activity and binding properties of these compounds.

To explore the effects of removing the NH group in the linker, we transitioned from a linker with an amino group to a purely carbon-based linker. Initially, a 3-carbon chain was tested to maintain the same 3-atom distance, aiming to investigate how the absence of the NH group influences the molecule's binding interactions with the receptor. Subsequently, a shorter 2-carbon chain was tested to examine the influence of linker length which has an impact on the geometry and spatial orientation of the substituent.

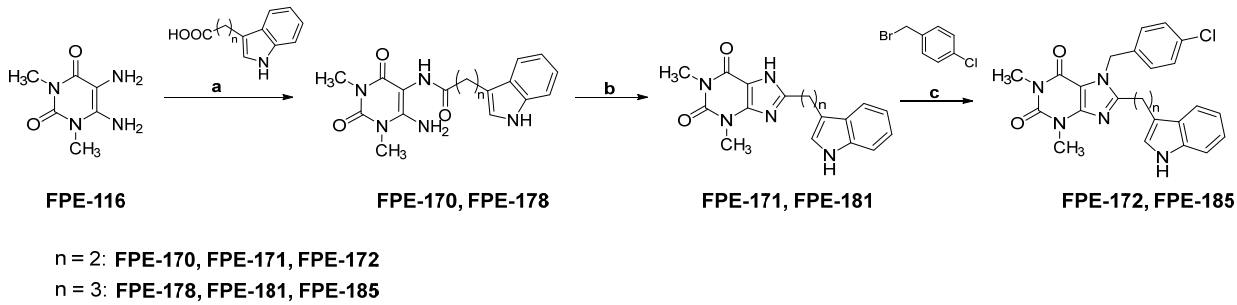

*Scheme 46. Synthesis of compounds **FPE-172** and **FPE-175** bearing carbon-based linkers. Conditions: **a)** DIPEA, COMU, DMF, RT, 30 mins; **b)** $NaOH_{aq.sol.}$ 2N, 80°C, 10 mins; **c)** K_2CO_3, DMF, RT, 2.5h.*

As shown in

Scheme 46, the reaction began with the 5,6-diaminouracil derivative **FPE-116**, where the NH_2 group at position 6 underwent amide bond formation with an indole-bearing carboxylic acid, resulting in compounds **FPE-170** and **FPE-178**.[164] Subsequent ring closure under strong basic conditions yielded **FPE-171** and **FPE-181**. Finally, alkylation of *N*7 with the desired alkyl bromide provided the final compounds **FPE-172** and **FPE-185**.

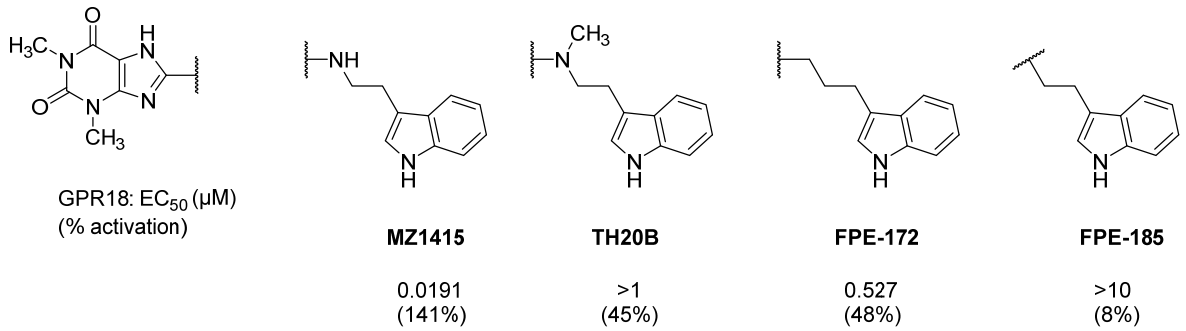

*Figure 37. Biological evaluation of **FPE-172** and **FPE-185** and related compounds.*

Replacing the ethylamino group in the lead compound **PSB-KK-1415** with a 3-carbon chain in **FPE-172** resulted in a 28-fold decrease in activity, although it was still tolerated. In contrast, **FPE-185** showed no activity. Reducing the linker length can restrict movement and bring connected functional groups closer together, potentially affecting binding interactions and overall activity.

These findings underscore the importance of the NH group in the linker as well as the critical role of linker length.

An attempt to replace nitrogen with oxygen, as shown in Scheme 41, was unsuccessful under mild conditions.

Another approach involved the use of tryptophol. Anticipating the need for harsher conditions, it was deemed necessary to protect the indole NH to prevent side reactions with the chlorine at position 8 of the xanthine core. However, the initial reaction according to literature did not yield the desired product, resulting in Boc-protection of both the NH and OH groups.[165] Further optimization of the reaction conditions is required before proceeding with the subsequent steps outlined in Scheme 47.

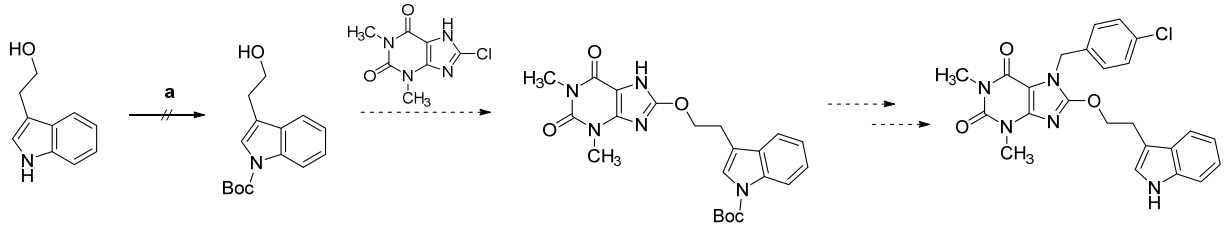

Scheme 47. Proposed reaction pathway to obtain an oxygen containing linker. Conditions: ***a)*** *Bu_4NHSO_4, Boc_2O,NaOH, DCM, 0°C to RT, 5h.*

These modifications on the indole moiety and the ethylamino linker have been important to advance our understanding of the molecular interactions within the binding pocket, underscoring the significance of the NH group and the optimal distance for maintaining activity. These findings will guide future design strategies for more potent and selective molecules.

3.2 Synthesis of antagonists for GPR183

3.2.1 Benzoic acid amides

In the quest for GPR18 ligands, it was fortuitously discovered that **FPE48B** exhibited antagonistic effects on the closely related GPR183 receptor (synthesis in Scheme *14*). Notably, **FPE48B** shares structural similarities with previously identified GPR183 antagonists, providing a valuable foundation for the search for potent antagonists.

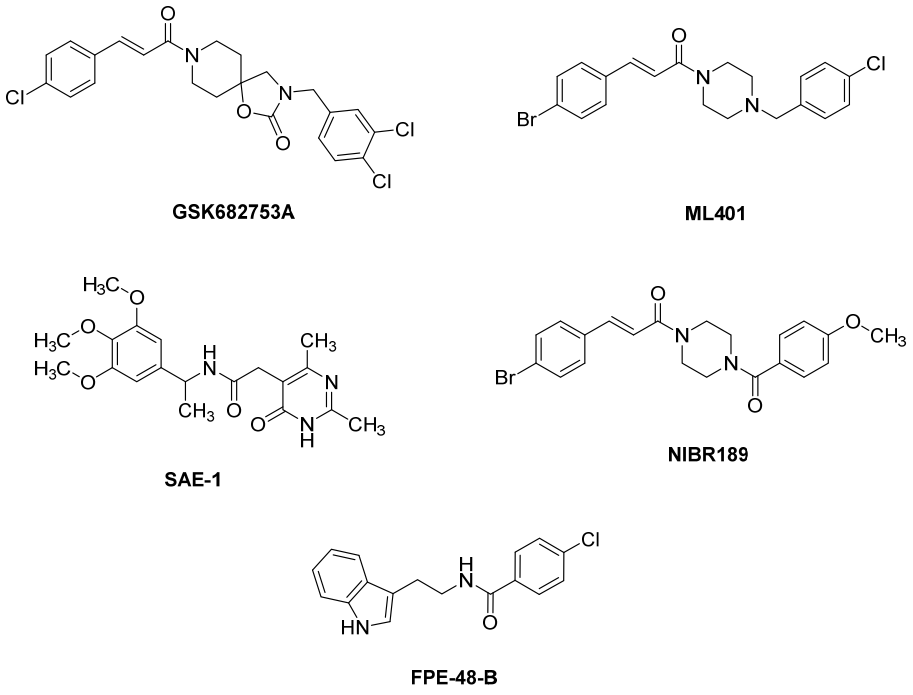

*Figure 38. Analysis of structural features of known GPR183 antagonists for SAR transfer in the **FPE-48B** scaffold.*

To refine our design of antagonists for GPR183, structural motifs identified in established antagonists, such as the presence of one or more methoxy group(s), *p*-bromophenyl and 3,4-dichlorophenyl were incorporated into the **FPE-48B** scaffold to enhance antagonistic potency (Figure *38*). Thus, our structural modifications were based on proven structural elements. The synthesized compounds (*Scheme 48*) were biologically evaluated in cellular β-arrestin recruitment assays.

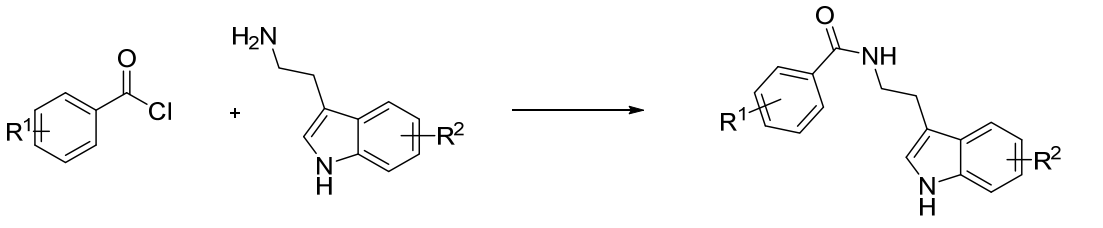

FPE-150, FPE-151, FPE-152, FPE-156,FPE-157,FPE-158, FPE-ML23

	R^1	R^2
FPE-150	4-Cl	5-OMe
FPE-151	-	-
FPE-152	-	5-OMe
FPE-156	3,4-Cl	-
FPE-157	3,4-Cl	5-OMe
FPE-158	3,4-OMe	-
FPE-ML23	Br	-

Scheme 48. Synthesis of benzoic acid amides. Conditions: Et_3N, DCM, 3h.

This synthesis consisted of a one-step amide formation between tryptamine and a suitable carboxylic acid chloride. The nucleophilic acyl substitution reaction was performed under basic conditions to neutralize the hydrochloric acid produced during the reaction, which can otherwise shift the equilibrium towards the reagents.

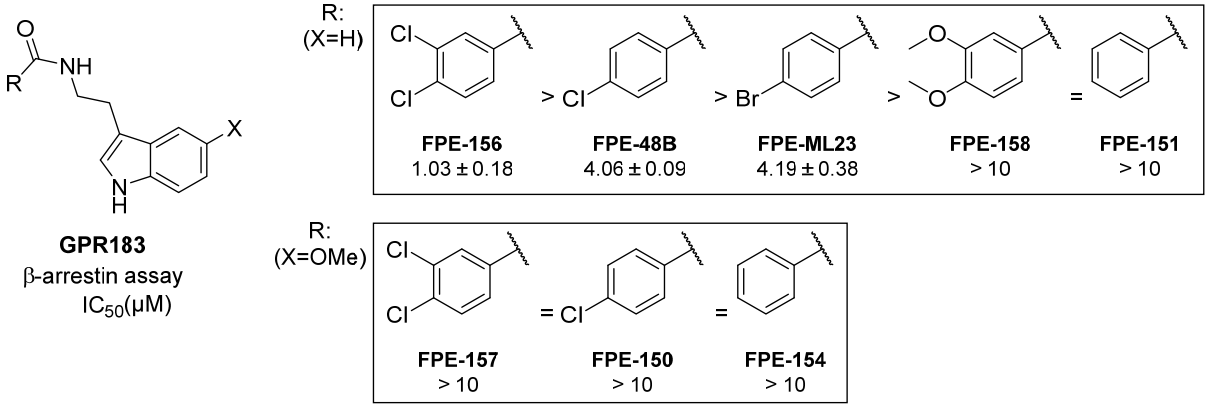

Figure 39. Biological evaluation of benzoic acid amides. Compounds were initially tested at a concentration of 10 μM. Effects were normalized to the signal induced by 0.1 μM 7α,25-hydroxycholesterol (7α,25-OHC, for GPR183). Data shown are means of three independent experiments performed in duplicates).

As shown in Figure 39, our studies revealed that incorporating a methoxy group at the 5-position of the indole significantly diminished the biological activity of the compounds. Among those bearing a naked indole moiety, modifications on the phenyl portion showed that halogen substituents, particularly 3,4-dichloro- and 4-chloro-benzamide, significantly enhance activity,

likely due to increased lipophilicity and favorable electronegativity. 4-Bromobenzamide was slightly less effective, suggesting that optimal size and electronegativity are crucial. In contrast, while many potent synthetic ligands for GPR183 feature one or more methoxy groups, 3,4-dimethoxybenzamide lacked substantial activity. This indicates that a different binding mode may apply for this scaffold, where electron-donating methoxy groups do not favor interactions with the receptor. Similarly, the unsubstituted benzamide was also inactive, underscoring that electron-withdrawing halogen atom in specific positions are essential for potent antagonistic activity.

3.2.2 Cinnamic acid amides

The cinnamoyl moiety is a component of known GPR183 antagonists such as GSK682753A, NIBR189, and ML401 (Figure 38). The synthesis of cinnamic acid amides was achieved by an amide coupling reaction between tryptamine and variously substituted cinnamic acids in the presence of triethylamine and T3P as the carboxylic acid activator. Due to the nature of the starting material, commercially available only as an E/Z mixture, **FPE-ML25** resulted in a mixture of E- and Z-configurated isomers.

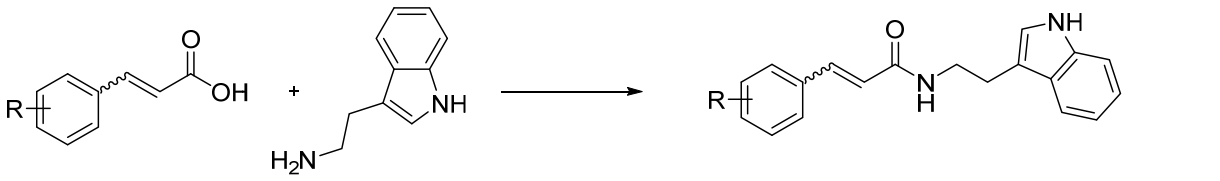

FPE-ML25, FPE-ML26, FPE-ML27, FPE-ML29, FPE-ML31, FPE-ML32, FPE-ML33

	R	isomer
FPE-ML25	2-F,4-Br	E/Z
FPE-ML26	4-Cl	E
FPE-ML27	4-CF_3	E
FPE-ML29	3-Cl	E
FPE-ML31	3,4-Cl	E
FPE-ML32	-	E
FPE-ML33	4-Br	E

Scheme 49. Synthetic pathway of cinnamic acid containing ligands for GPR183. Conditions: Et_3N, T3P, DCM, 12h, RT.

After the reaction, impurities such as unreacted acids, residual coupling reagents, and acidic by-products may still be present. Treatment with $NaHCO_3$ in an aqueous work-up resulted in a cleaner organic phase and thereby facilitated the purification process, although the overall yield was generally low.

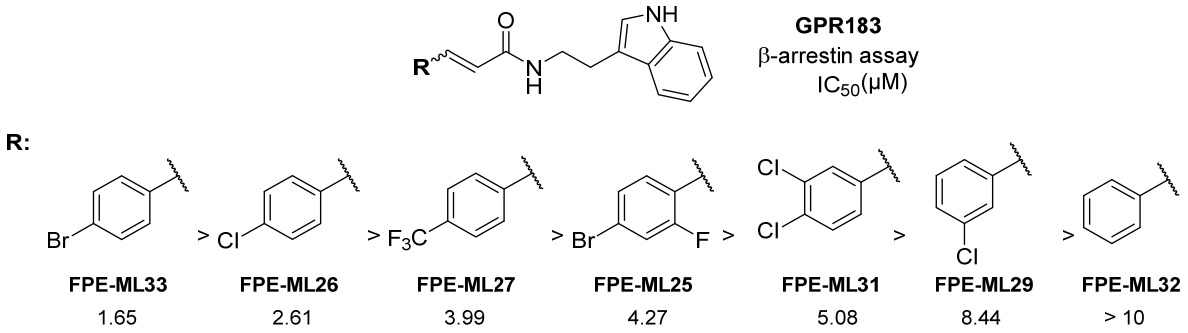

Figure 40. Biological evaluation of cinnamic acid amides. Compounds were initially tested at a concentration of 10 μM. Effects were normalized to the signal induced by 0.1 μM 7α,25-hydroxycholesterol (7α,25-OHC, for GPR183). Data shown are means of three independent experiments performed in duplicates.

As shown in *Figure 40*, the SAR analysis of variously substituted cinnamic acid amides revealed that halogen substituents at the *para*-position significantly enhanced antagonist potency at GPR183. Specifically, compounds with 4-bromo or 4-chloro substitution (**FPE-ML33** and **FPE-ML26**) exhibited the highest activity, likely due to the favorable size, lipophilicity, and ability to engage in specific interactions with the receptor. The 4-trifluoromethyl group in **FPE-ML27**, while also enhancing potency, was less effective than Cl- or Br-substitution, suggesting that lipophilicity and steric factors play a more dominant role than electronegativity alone. Moderate activity was observed with 2-F,4-Br and 3,4-dichloro substitutions (**FPE-ML25** and **FPE-ML31**), indicating that while halogens are beneficial, their optimal positioning is crucial, as also shown for the lower activity of **FPE-ML29**. In contrast, the absence of substituents in **FPE-ML32** led to a loss in antagonistic activity, underscoring the importance of specific structural modifications for effective receptor binding. Overall, the most potent antagonists for GPR183 are those with properly placed halogen substituents at the *para*-position, improving receptor interaction.

Further investigation is needed to fully elucidate the SARs of these cinnamic acid amides. Future studies will also explore modifications on the indole moiety to enhance antagonistic activity at GPR183.

3.2.3 Piperazine derivatives

As explained in Chapter 2, piperazine, a component of well-known antagonists such as NIBR51 and NIBR127, was incorporated into our ligand design. We synthesized these compounds systematically: initially forming amides on one nitrogen of the piperazine ring (Series A), then on

the other nitrogen (Series B), and finally on both sides of the ring (Series C) to evaluate the antagonistic activity of the new derivatives.

3.2.3.1 Series A

For these ligands the synthetic strategy depended on the availability of properly substituted piperazines. If this was the case, the synthesis was performed in a one-pot reaction – amide coupling with indole-3-propionic acid and the appropriately substituted piperazine which was catalyzed by T3P and triethylamine. This strategy was used only for compound **FPE-ML24** as shown in Scheme 50.

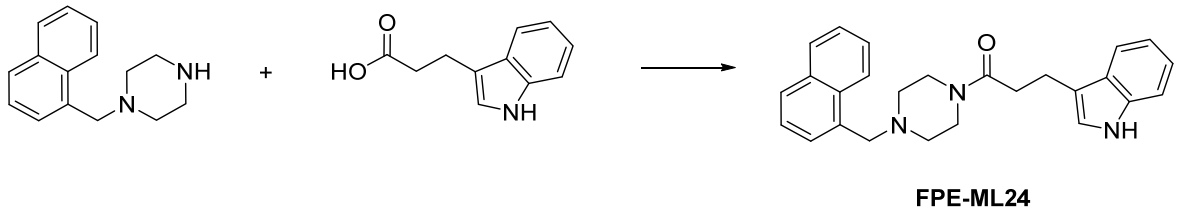

FPE-ML24

*Scheme 50. Synthesis of **FPE-ML24**. Conditions : Et_3N, T3P, DCM, 12h, RT.*

For other compounds, in which the indolyethyl moiety remained unchanged , it seemed more useful to synthesize the building block **FPE-ML35** first. This was achieved via amide coupling of indole-3-propionic acid and *N*-Boc-protected piperazine in the presence of carbonyldiimidazole (CDI) to yield **FPE-ML35**. Subsequently, Boc-deprotection mediated by trifluoroacetic acid (TFA) led to **FPE-ML30** (Scheme 51).

The appropriate benzyl bromide was used for alkylation at the free NH group of piperazine yielding **FPE-ML39, FPE-ML40, FPE-ML47**. Residues were chosen based on the structures of known antagonists and active compounds from the benzoic acid and cinnamic acid amides series (3.2.1 and 3.2.2).

As shown in Figure 41, none of the synthesized compounds in this series showed activity, thus synthesis of further derivatives of this series was not pursued.

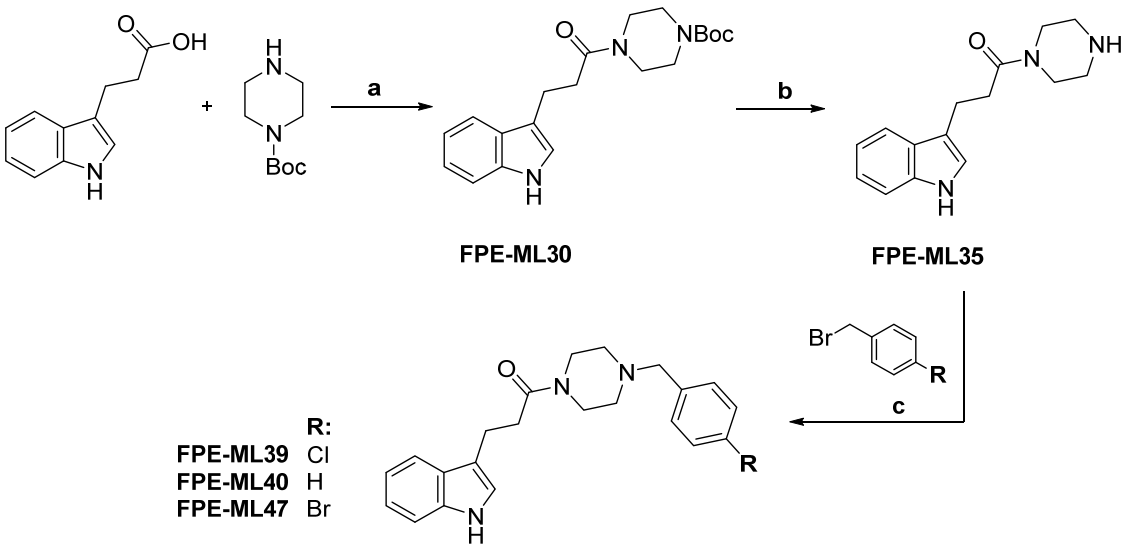

Scheme 51. Synthesis of piperazine derivatives (series A). Conditions: ***a)*** *1,1'-Carbonyldiimidazole, THF, 2.5h, RT;* ***b)*** *DCM, TFA, 0.5h, RT;* ***c)*** *K_2CO_3, acetone, 2h, 50°C.*

3.2.3.2 Series B

Synthesis of series B began by reducing the carboxylic acid in indole-3-propionic acid using $LiAlH_4$, yielding **FPE-ML43**. This intermediate was tosylated to produce **FPE-ML48**, which has a suitable leaving group to allow the compound's reaction with the free NH of Boc-protected piperazine. The alkylation led to **FPE-ML49**, which was then deprotected with trifluoroacetic acid TFA to yield **FPE-ML50**.[166,167]

This last intermediate served as a starting point for amide coupling with either carboxylic acids or acyl chlorides, depending on the desired substitution. For coupling with carboxylic acids, we used a combination of coupling reagents, namely 1-ethyl-3-(3'-dimethylaminopropyl)carbodiimide hydrochloride/hydroxybenzotriazole (EDC·HCl/HOBt). In the case of coupling with acid chlorides, the amide bond formation occurred via nucleophilic acyl substitution following deprotonation of the amine by a base.

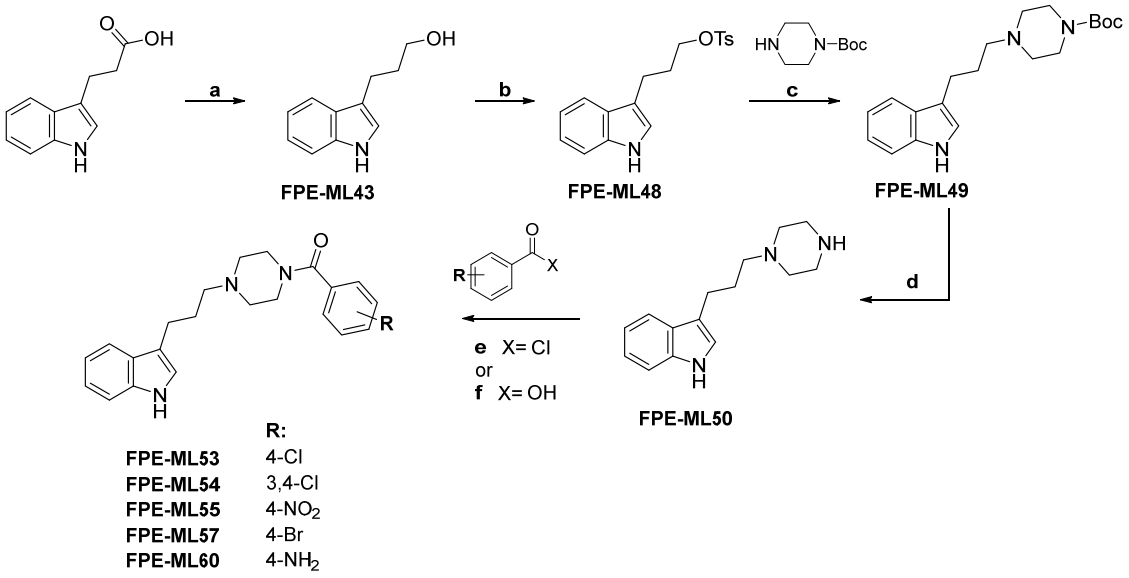

Scheme 52. Synthesis of piperazine derivatives (series B). Conditions: ***a)*** *$LiAlH_4$, dry THF, 12h, RT; b) TsCl, DMAP, 12h, RT;* ***c)*** *K_2CO_3, acetonitrile, 6h, 80°C; d) TFA, DCM, 0.5h, RT;* ***e)*** *Et_3N, DCM, 5h, 0°C; f) HOBt, EDC·HCl, acetone, 2-4h, Argon, RT.*

The reaction mechanism is shown in Scheme 53.

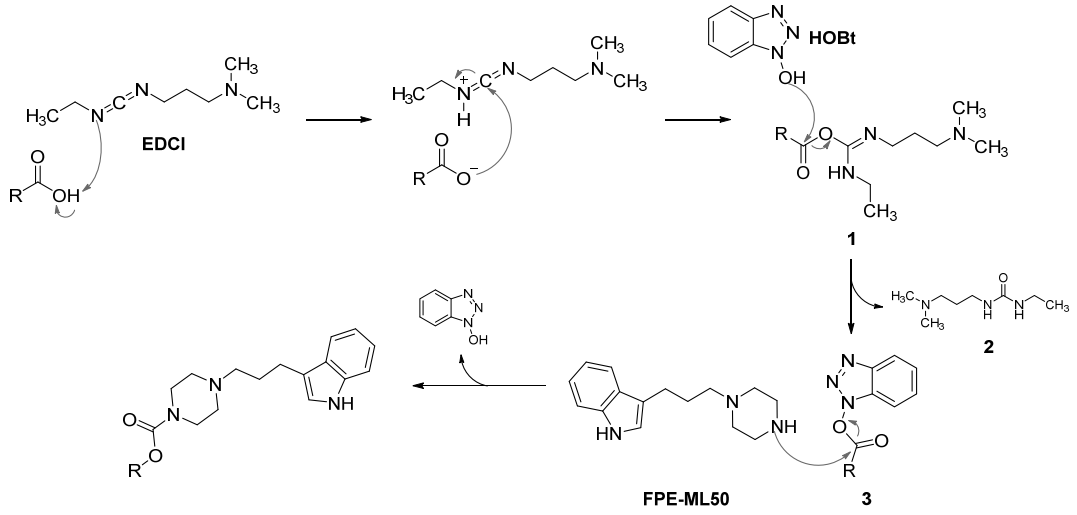

Scheme 53. Reaction mechanism of amide coupling using 1-ethyl-3-(3'-dimethylaminopropyl)carbodiimide (EDCI) and hydroxybenzotriazole (HOBt). ***1****: corresponding O-acylisourea;* ***2****: corresponding urea by-product;* ***3****: corresponding OBt ester.*

The addition of a few drops of Et_3N ensured that the amine in **FPE-ML50** remained in its nucleophilic, unprotonated form. The nucleophilic nitrogen of the amine then attacked the carbonyl carbon of the HOBt ester (compound 3), whose depletion was monitored via TLC-MS, forming a transient tetrahedral intermediate that rapidly collapsed to expel HOBt and yield the desired amide

bond. However, due to the formation of various by-products during the reaction, the yields were generally low.

3.2.3.3 Series C

To finally assess whether having an amide bond on both sides of the piperazine ring as seen in NIBR189 is beneficial, series C was designed.

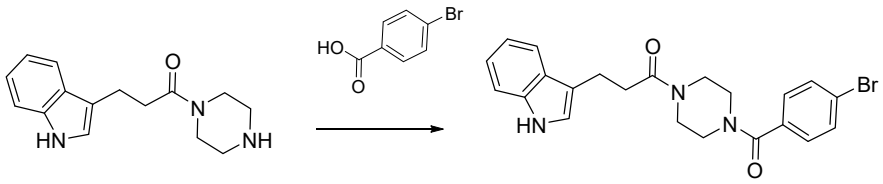

*Scheme 54. Synthesis of **FPE-ML61**. Conditions : HOBt, EDC·HCl, acetone, Et_3N, 4h, Argon, RT.*

The building block **FPE-ML35** previously synthesized (Scheme 51), was reacted with 4-bromo-benzoic acid in the presence of the coupling agents EDC-HCl/HOBt. Also, this time, the addition of a few drops of Et_3N ensured the successful progress of the reaction.

3.2.3.4 Biological evaluation

Results of the biological evaluations of piperazine derivatives are reported in Figure 41.

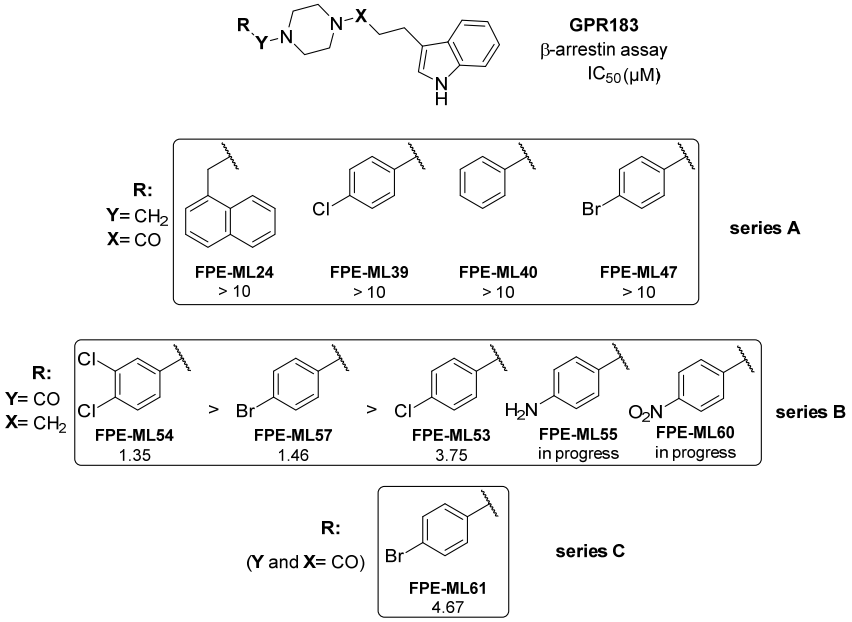

Figure 41. Biological evaluation of piperazine derivatives as inhibitors of GPR183.

None of the compounds of series A showed any biological activity, while ligands of series B were potent inhibitors of GPR183. This difference may stem from the orientation of the amide group relative to the piperazine ring, with series B positioning the amide in a way that better aligns with key receptor interactions, optimizing binding affinity and inhibitory activity compared to series A. In series B, the intermediate potency of the 4-bromophenyl substitution (**FPE-ML57**) compared to 3,4-dichlorophenyl (**FPE-ML54**) and 4-chlorophenyl (**FPE-ML53**) can be attributed to bromine's larger size and its moderate electron-withdrawing properties. The 3,4-dichlorophenyl group likely benefits from the combined effects of two electron-withdrawing chlorine atoms at both *meta*- and *para*-position, leading to stronger interactions with the receptor. In contrast, the 4-chlorophenyl group, with only one chlorine atom, exerts a weaker electron-withdrawing effect, resulting in lower potency. Bromine, being larger than chlorine and a bit less electron-withdrawing, provides an intermediate effect on potency. Ongoing testing of the 4-nitrophenyl and 4-aminophenyl analogs (**FPE-ML55, FPE-ML60**) will provide further insights into the influence of electron-withdrawing and electron-donating groups on potency. The 3-fold loss in potency observed when an amide bond is introduced on both nitrogens of the piperazine ring (**FPE-ML61**) could be due to reduced flexibility and altered electronic properties. Thus, the SAR transfer from NIBR189 did not lead to a highly potent compound, suggesting the possibility of a different binding mode.

4 SUMMARY

This work presents advancements in the design, synthesis, and biological evaluation of small molecule ligands targeting two related G protein-coupled receptors, GPR18 and GPR183, which are implicated in immunoregulation and inflammatory pathways, making them attractive drug discovery targets. The focus is on the structure-activity relationships (SAR) of these receptors. For GPR18, detailed SAR analysis identified potent, selective xanthine-based agonists that will serve as crucial tools for studying the receptor's roles in physiology and pathology. Meanwhile, insights into the SAR of GPR183 were gained across several antagonist classes, including benzoic acid amides, cinnamic acid amides, and piperazine derivatives. This foundational work lays the groundwork for developing optimized ligands in future drug discovery efforts.

Together, the novel compounds developed in these two sub-projects will contribute to expanding the toolkit for studying GPCRs in the context of inflammation and immune regulation, ultimately advancing therapeutic strategies for related diseases.

GPR18

For GPR18, starting from the recently published **PSB-KK1415** (EC_{50} = 0.0191 µM),[88] the exploration of the SARs centered around the xanthine core and its *N*7 position modifications.

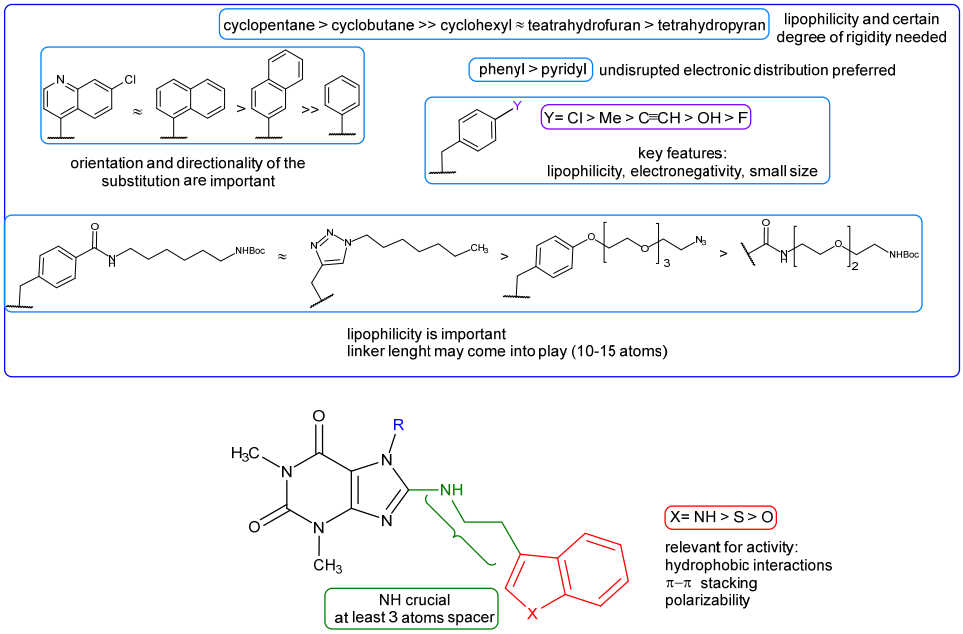

Figure 42. SAR summary for indolylethylaminoxanthines as GPR18 agonists.

Five multi-step synthetic strategies were implemented that led to a wide range of new compounds, allowing for a comprehensive evaluation of the impact of various substituents on potency and efficacy.

As shown in Figure 42, SAR analysis confirmed that at the N7 position, specific structural motifs, such as benzyl rings substituted in the *para* position with small, lipophilic, and electronegative groups, were generally favored, resulting in highly potent compounds. Substitutions with fused aromatic systems, like 1-naphthyl or 7-chloroquinoline, further enhanced potency compared to simpler aromatic groups, emphasizing the critical role of both lipophilicity and structural rigidity. The reduced potency of 2-naphthyl and phenyl substitutions suggests that molecular orientation and directionality are also key factors influencing activity.

Bioisosteric replacements of the benzyl ring with other aromatic systems, such as pyridine, failed to improve potency, likely due to disruptions in electronic distribution. Likewise, sp3-rich rings, particularly those containing polar heteroatoms like oxygen, did not enhance potency. However, smaller, more rigid groups such as cyclopentylmethyl and cyclobutylmethyl outperformed bulkier ones like cyclohexylmethyl, indicating that some degree of structural rigidity improves receptor binding by preventing misalignment.

Optimization of the linker further revealed that PEGylated chains were suboptimal, while alkyl linkers with moderate flexibility were better tolerated. Notably, linkers up to 15 atoms in length performed more effectively than longer ones, suggesting that balance between flexibility and length is crucial for optimal interaction.

Significant insights were also obtained regarding other ligand components. Modifications in the ethylamino linker (Figure 42, green) indicated that the NH group is essential, and that at least a 3-atom spacer is necessary between the xanthine and indole moieties for effective interaction. Substitutions on the indole ring demonstrated that certain moieties, such as benzothiophene, can mimic the interaction profile of indole and exhibit comparable activity.

Additionally, advancements in the Chan-Lam-Evans coupling and click-chemistry techniques opened new avenues for further functionalization of the ligands. The optimization of reaction conditions for the synthesis of various BODIPY dyes was also successfully achieved, paving the

way for their application in future studies, particularly when attached to the most promising pharmacophore-linker combinations.

Importantly, several synthesized compounds were highlighted for their potential use as tool compounds, particularly for developing fluorescence- or radio-labeled ligands. As shown in Figure 43, these include compounds with appropriate functional groups for linker/fluorophore attachment and compounds equipped with different types of linkers, which demonstrated that bulky substitutions are tolerated.

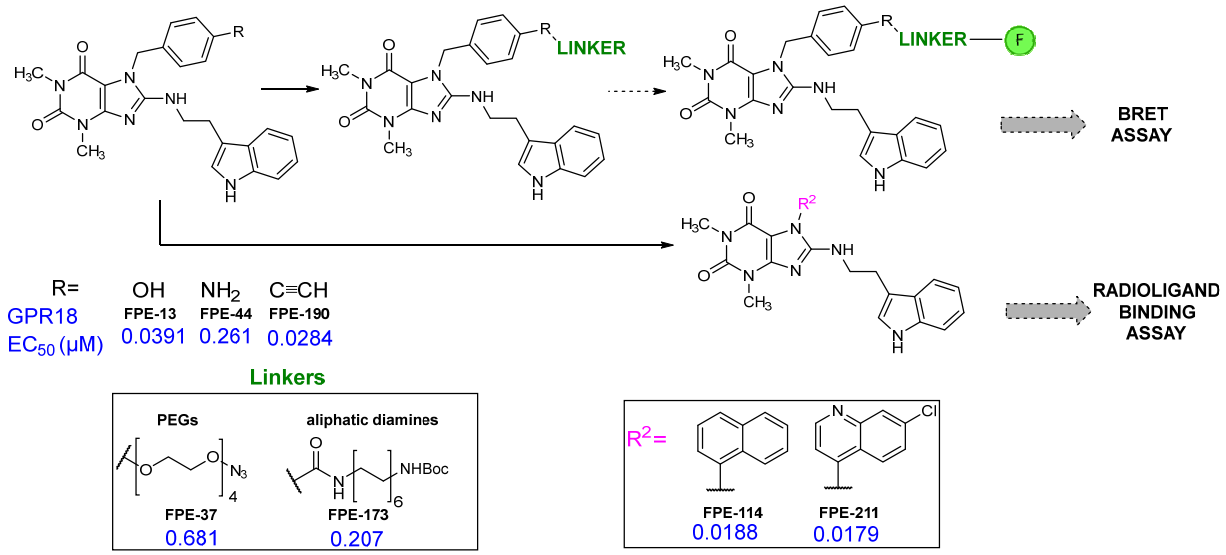

Figure 43. Road to fluorescence- or radio-labeled ligands for GPR18. Some of the best performing compounds are shown as examples.

The next steps could include more rational design of derivatives using molecular modeling, a focus on partial agonists/antagonists, modifications on the xanthine core and scaffold hopping, and a focus on fluorescence-labeled compounds in order to establish binding assays. Synthesis of new classes of derivatives could start from the newly discovered compounds **FPE-114** and **FPE-211** to improve potency.

The newly developed tool compounds will be highly useful to study the (patho)physiological roles of this still enigmatic receptor, and may contribute to validating it as a novel drug target.

GPR183

Starting from the hit compound **FPE-48B** and published GPR183 antagonists, this research focused on designing antagonists for GPR183, evaluating three chemical classes: benzoic acid amides, cinnamic acid amides, and piperazine derivatives.

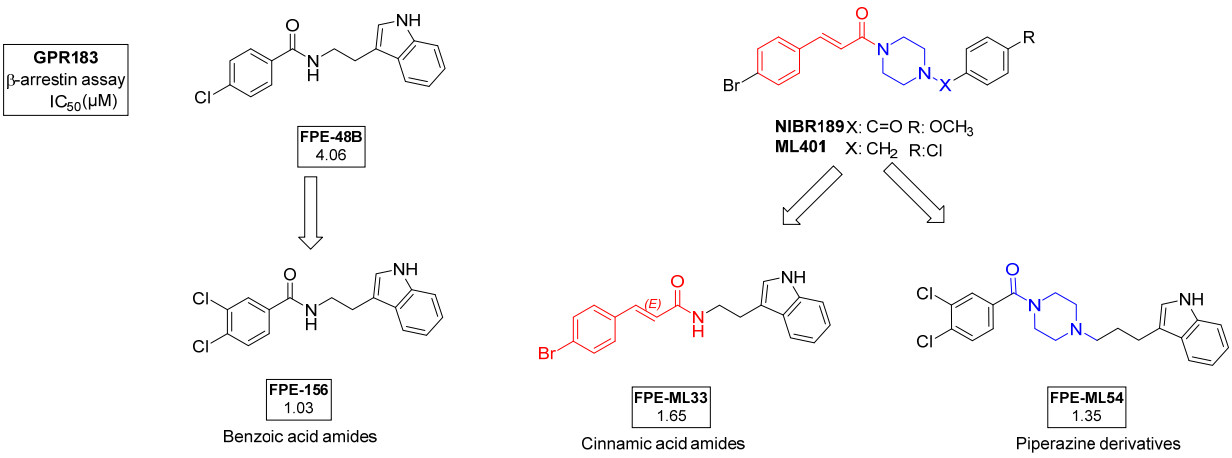

Figure 44. Overview of the most active GPR183 antagonists per class.

As shown in Figure 44, key findings revealed that halogen substitutions, particularly in the *para* position of the phenyl moiety on the opposite side of the indole, consistently enhanced potency across all classes. For instance, the 3,4-dichlorophenyl substitution significantly improved activity in both the benzoic acid amides and piperazine derivatives, with the best compounds being **FPE-156** (IC_{50} = 1.03 μM) and **FPE-ML54** (IC_{50} = 1.35 μM), respectively.

In the cinnamic acid amide series, an intriguing difference was observed, where the *p*-bromo substitution led to the highest activity, as exemplified by **FPE-ML33** (IC_{50} = 1.65 μM). This suggests a unique binding mode in this class, distinct from the other two series.

Moreover, the orientation of the amide group was critical for piperazine derivatives, where compounds with the amide positioned opposite to tryptamine exhibited markedly higher potency. The SAR across these classes pointed towards halogen-based modifications as the most promising approach, while electron-donating groups such as methoxy generally resulted in lower potency.

Therefore, starting from the hit compound **FPE-48B** a 4-fold increase in potency was achieved in this benzoic acid amides class, while information on known antagonists NIBR189 and ML401 was used to drive the design of two other classes, cinnamic acid amides and piperazine derivatives, with compounds showing potency in the low micromolar range

Future optimization should focus on fine-tuning substituents and exploring bioisosteric replacements, leveraging the structural insights gained.

In conclusion, while the current series of compounds requires further optimization, the new structural insights provide a solid foundation for future drug discovery efforts for GPR183 antagonists.

5 EXPERIMENTAL

5.1 Materials and methods

Starting materials, reagents and solvents were used as purchased from ABCR, Alfa Aesar, Sigma-Aldrich, Activate Scientific, or Fluorochem. The progress of the reactions was monitored by thin-layer chromatography (TLC, Merck, 0,2 mm silica gel 60 F254) followed by analytical LC-MS. Column chromatography was performed on silica gel, 0.060−0.200 mm, pore diameter ca. 6 nm. All synthesized compounds were finally dried in *vacuum* at 8-12 Pa (0.08−0.12 mbar). ^{1}H and ^{13}C NMR data were collected either on a Bruker Avance 500 MHz NMR spectrometer at 500 MHz (^{1}H) or 126 MHz (^{13}C) or on a Bruker Ascend 600 MHz NMR spectrometer at 600 MHz (^{1}H) or 151 MHz (^{13}C). DMSO-d_6 was employed as a solvent at 303 K, unless otherwise noted. Chemical shifts are reported in parts per million (ppm) relative to the deuterated solvents (DMSO-d_6), ^{1}H: 2.49 ppm, 1^{3}C: 39.70 ppm; ($CDCl_3$) ^{1}H: 7.25 ppm, ^{13}C: 77.17 ppm; coupling constants J are given in Hertz and spin multiplicities are given as s (singlet), d (doublet), t (triplet), q (quartet), m (multiplet), dd (doublet of doublets), dt (doublet of triplets), ddd (doublet of doublets of doublets). The purities of isolated final products were determined by HPLC coupled to a diode array detector (DAD) measuring UV absorption from 200 to 950 nm, and an electrospray ionization (ESI) mass spectrometer (Applied Biosystems API 2000 LCMS/MS, HPLC Agilent 1100) using a Phenomenex Luna 3 µ C18 column (50 mm × 2.00 mm). The compounds were dissolved at a concentration of 1.0 mg/mL in acetonitrile containing 2 mM ammonium acetate. Then, 10 μL of the sample were injected into an HPLC column, and elution was performed with a gradient of

water/acetonitrile (containing 2 mM ammonium acetate) from 90:10 to 0:100 for 20 min at a flow rate of 300 μL/min, starting the gradient after 10 min. The purity of the final compounds was in all cases ≥ 95% unless otherwise stated. HRMS were recorded with one of the following methods:

1. micrOTOF-Q mass spectrometer (Bruker) with ESI-source coupled with an HPLC Dionex Ultimate 3000 (Thermo Scientific) using an EC 50/2 Nucleodur C18 Gravity 3 µm column (MachereyNagel). The column temperature was 425°C. Ca. 1 µL of a 1 mg/mL solution of the sample in acetonitrile was injected and a flow rate of 0.3 mL/min was used. HPLC was started with a solution of acetonitrile in water (10:90), containing 2 mM CH_3COONH_4. The gradient was started after 1 min reaching 100% acetonitrile within 9 min and then flushed with this concentration for another 5 min;
2. LTQ Orbitrap Velos mass spectrometer (Thermo Fisher Scientific, Bremen, Germany) by direct infusion nano spray (TriVersa NanoMate, Advion, Harlow, UK). Chips with 4 µm nozzles were used with 1.6 kV in positive mode or 1.2 kV negative mode with 0.3 psi pressure. MS spectra were recorded in the Orbitrap mass analyzer with a resolution of 60,000. A lock mass (polysiloxane $[M+H]^+$, 445.120024 m/z) was used for internal calibration when available. The resulting mass error was typically <1 ppm. Data were manually inspected in Xcalibur software (Thermo Fisher Scientific). Averaged m/z values of several spectra were compared to theoretical values of the analytes.

M.p.s were measured on a M.p. apparatus (BÜCHI M.p. B-545) and are uncorrected.

Reactions carried under microwave irradiation were performed in a Discover 2.0 microwave reactor, CEM Corp., USA.

^{13}C NMR data for select molecules are reported with peak assignments to their respective carbons. These examples were chosen to illustrate the typical carbon NMR assignments of the scaffold, providing a reference for the interpretation of other related compounds within the study.

5.2 Synthesis of ligands for GPR18

5.2.1 General procedures (GPs)

General procedure A for the synthesis of N^6-substituted 5,6-diamino uracil derivatives via reductive amination

5,6-Diaminouracil (2.5 mmol, 1 eq) was put into a 50 ml round-bottomed flask and dissolved in water. Acetic acid (0.04 ml) was then added under stirring followed by the corresponding benzhaldheyde (6.9 mmol, 2.7 eq) over 15 minutes at RT . After all the reagent was added, the mixture was kept stirring some more minutes and then it was cooled down in an ice bath. The mixture was then filtered under reduced pressure and the product washed with cold water, followed by cold water/acetonitrile 50:50 and finally with just cold acetonitrile. The product was let dry overnight and used without further purification for the next step. To a suspension of the corresponding Schiff´s base (1.8 mmol, 1 eq) in DCM (4 ml) and MeOH (4 ml) it was added glacial acetic acid (1.8 mmol, 1 eq) followed by $NaBH_3CN$ (1.9 mmol, 1.1 eq). The reaction mixture was stirred at RT for 2 h. After this time, additional glacial acetic acid (0.18 mmol, 0.1 eq) and $NaBH_3CN$ (0.19 mmol, 0.11 eq) were added and the reaction mixture was further stirred overnight. The reaction was monitored via TLC and when no further improvement was detected, the reaction mixture was concentrated under reduced pressure and the precipitated was filtered, washed with cold methanol and dried under *vacuum*.

General procedure B for the synthesis of N^6-substituted 5,6-diamino uracil derivatives via S_NAr

6-Amino-5-bromo-1,3-dimethyluracil (0.85 mmol, 1 eq) was dissolved in dry DMF (2 ml) and Et_3N (3.4 mmol, 4 eq) was added. The mixture was stirred at RT for 30 mins. Corresponding amine (0.95 mmol, 1.1 eq) was then added and the mixture was stirred at 120°C for 24h. When no further improvement was detected via TLC monitoring, the reaction was quenched with ice-cold water. The mixture was then extracted with EtOAc and the combined organic layers were dried over $MgSO_4$ and concentrated under *vacuum.*

General procedure C for the ring closure of the N^6-substituted 5,6-diaminouracil derivatives

The appropriate amine (1.07 mmol, 1 eq) was weighed into a sealed vial and suspended into triethylorthoformate (3.5 mL). The mixture was heated under stirring at 145°C for 5 hours. When

monitoring trough TLC did not show further improvement, the mixture was cooled down and filtered, washed with diethyl ether and dried under *vacuum*.

General procedure D for the Chan-Lam-Evans coupling on theophylline

Theophylline (0.47 mmol, 1 eq), corresponding boronic acid or its pinacol ester (0.94 mmol, 2 eq) and Na_2CO_3 (0.1 g, 0.94 mmol , 2 eq), were suspended in dichoroethane. Afterwards a suspension of $Cu(OAc)_2$ (0.47 mmol, 1 eq) and 2′-2′-bipyridine (0.47 mmol, 1 eq) in hot dicholoroethane was added. The mixture in stirred at 70°C overnight. When no further improvement was detected, it was let cool down to RT and quenched with HCl 1N (≈20 ml). The organic layer was separated from the aqueous phase which was then extracted with DCM. Combined organic layers are washed with brine, dried over $MgSO_4$ and concentrated under *vacuum*. Purification achieved with flash column chromatography on silica gel.

General procedure E for the C8 chlorination of the *N*7-substituted theophylline derivatives

NCS (0.9 mmol, 1.3 eq) was added to a solution of the corresponding *N*7-substituted theophylline (200 mg, 0.69 mmol) in THF (3 ml) and the mixture was stirred at RT for 16h. The reaction was monitored by TLC and when no further improvement was detected, the mixture was concentrated under *vacuum* and the solid washed with water filtered and further dried under reduced pressure.

General procedure F for the alkylation of 8-chlorotheophylline

8-Chlorotheophylline (1 eq) and K_2CO_3 (1.2 eq) were weighed into a round-bottomed flask and dissolved in dry DMF. The mixture was stirred at RT for 30 minutes. Afterwards, the corresponding alkyl or arylalkyl bromide (1.2 eq) was added and the mixture was kept under stirring at RT for further 2-16 hours. Unless otherwise stated, purification is achieved via precipitation in ice-cold water followed by filtration under *vacuum*.

General procedure G for the tryptamine coupling

The corresponding *N*7 alkylated 8-chlorotheophylline (1 eq) and tryptamine (2 eq) were weighed into a sealed tube and dissolved in NMP. DIPEA (3.5 eq) was then added and the mixture was heated up to 145°C under stirring and kept overnight. After completion, the solvent was removed under *vacuum* and water was added. An extraction with EtOAc was performed and the combined organic layers are dried over $MgSO_4$ and concentrated in *vacuum*. Purification achieved with flash column chromatography on silica gel.

General procedure H for the tryptamine coupling under microwave conditions

In a 20 mL microwave vial, 8-chlorotheophylline (1 eq). tryptamine (2 eq) and DIPEA (3.5 eq) were dissolved in NMP (3 mL). The reaction mixture was stirred at 195°C for 22 min under microwave irradiation (Dynamic Mode). When no further improvement was detected, resulting precipitates were washed with ice-cold water, filtrated under reduced pressure and dried overnight.

General procedure I for the demethylation of methoxy groups

Methoxylated compound (1 eq) was weighed into a round-bottomed flask and dissolved in DCM (3 mL). The mixture was stirred and cooled to 5°C with an ice bath. Then a 1 M solution of BBr_3 in DCM (4 eq) was added dropwise over 10 minutes. The reaction was kept stirring for 3 hours. Afterwards it was quenched with methanol dropwise. Water was then added paying attention to the formation of clusters of the BBr_3 complex (sonicating when necessary) and adjusting the pH to 9 with a saturated aqueous solution of $NaHCO_3$. An extraction was then performed with DCM. The organic phase was further washed with a saturated solution of $NaHCO_3$, dried over $MgSO_4$, filtered and concentrated in *vacuum*.

5.2.2 Synthesis of intermediates and finished products for the study of position *N*7

5.2.2.1 Synthesis of building blocks and alkylating reagents

6-Amino-5-bromo-1,3-dimethylpyrimidine-2,4(1*H*,3*H*)-dione (FPE-96)

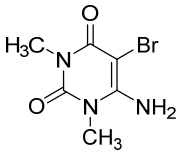

6-Amino-1,3-dimethyluracil (5 g, 32 mmol, 1 eq) and NBS (5.98 g, 34 mmol, 1.05 eq) are dissolved in ACN (30 ml). The mixture is stirred at reflux for 1.5 hours. It is then cooled down to RT and filtered. The remaining solid is washed with water. **Yield**: 5.85 g, 25 mmol, 78%. **LC-MS** (m/z): 234.0 ($[M+H]^+$); **purity** by HPLC-UV (220 – 400 nm)-ESI-MS: 99.2%; **^{1}H NMR (**500 MHz**,** DMSO-d_6**)** δ 7.00 (s, 2H, NH_2), 3.35 (d, J =1.4 Hz, 3H, CH_3), 3.15 (d, J =1.4 Hz, 3H, CH_3); **^{13}C NMR** (126 MHz, DMSO-d_6) δ 157.95, 151.78, 150.49, 70.77, 31.15, 28.63.

4-(Bromomethyl)-*N*-propylbenzenesulfonamide (FPE-11), CAS 1308718-63-9

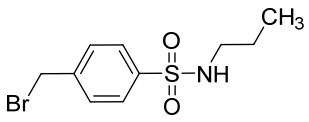

4-(Bromomethyl)benzenesulfonylchloride (500 mg, 1.8 mmol) was put into a sealed vial and dissolved in DCM (1.5 ml). Afterwards, propylamine (0.4 mL) was carefully added under stirring and the mixture was stirred at RT for 20 hours. When no further improvement was detected, water was added and an extraction with DCM was performed. The combined organic extract was further washed with water: HCl 1N 50:50 and dried over $MgSO_4$. The solvent was removed under reduced pressure. **Yield:** 300 mg, 1.12 mmol, 62%.

4-Ethynylbenzyl 4-methylbenzenesulfonate (FPE-ML65)

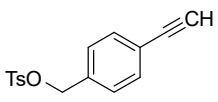

In a 100 mL round-bottomed flask, tosyl chloride (0.865 g, 4.54 mmol, 3 eq) and potassium hydroxide (0.849 g, 15.1 mmol, 10 eq) were added to the solution of (4-ethynylphenyl)methanol (0.200 g, 1.51 mmol, 1 eq) in THF (20 mL).The reaction mixture was stirred at RT overnight. Resulting precipitates were filtrated under reduced pressure and filtrated was concentrated under reduced pressure. **Yield:** 200 mg, 0.698 mmol, 46.2 %; **LC-MS (m/z)**: 304.2 ($[M+ H_2O+H]^+$); **purity** by HPLC-UV (220 – 400 nm)-ESI-MS: 77.3%. This compound is used without further purification.

1-(4-Methoxyphenyl)ethan-1-ol (FPE-80)[169] **, CAS 3319-15-1**

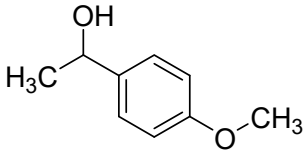

Methylmagnesium bromide (3 M in THF, 47.7 mmol, 1.3 eq) was added dropwise to a cold solution of 4-methoxybenzaldheyde (5g, 37 mmol, 1 eq) in dry THF (70 mL) under Argon. The reaction was stirred for 10 minutes, let warm up to RT and stirred for further 3 hours. The reaction was quenched with a saturated solution of NH_4Cl and extracted with EtOAc. The organic phase was dried over $MgSO_4$ and concentrated under *vacuum*. Purification is achieved with column chromatography (EtOAc in Cyclohexane 0 to 30%) to give a yellow oil. **Yield**: 3.5 g, 23 mmol, 62%; **LC-MS (m/z)**: 135.0 ($[M+H]^+$); **purity** by HPLC-UV (220 – 400 nm)-ESI-MS: 86.4%.

***tert*-Butyl 2-bromo-2-(4-chlorophenyl)acetate (FPE-168), CAS 138646-94-3**

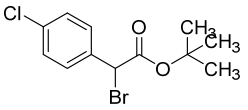

A double-necked round-bottomed flask was flushed with argon and then charged with 2-bromo-2-(4-chlorophenyl)acetic acid (0.5 g, 2 mmol, 1 eq), *tert*-butylacetate (9 mL) and $HClO_4$ (0.05 mL). The mixture was stirred at RT overnight. When no further improvement was detected, the reaction was quenched with a saturated aqueous solution of $NaHCO_3$ and extracted with Et_2O. Organic layers were combined, dried over $MgSO_4$ and concentrated under *vacuum.* **Yield**: 361 mg, 1.18 mmol, 60%; **M.p.:** 120°C**; ^{1}H NMR** (600 MHz, DMSO-d_6) δ 7.59 – 7.56 (m, 2H, Ar-H_{benzyl}), 7.48 – 7.45 (m, 2H, Ar-H_{benzyl}), 5.80 (s, 1H, C*H*COO), 1.41 (s, 9H, 3xCH_3); **^{13}C NMR** (151 MHz, DMSO-d_6) δ 166.65, 135.52, 133.65, 130.50 (2C), 128.69(2C), 82.76, 46.86, 27.27 (3C); **LC-MS (m/z)**: 305.0 ($[M-H]^-$); **purity** by HPLC-UV (220 – 400 nm)-ESI-MS: 97.2%.

5.2.2.2 Synthesis of 6-amino-5-((aryl/alkyl)amino)-1,3-dimethylpyrimidine-2,4(1H,3H)-diones

6-Amino-5-(cyclopropylamino)-1,3-dimethylpyrimidine-2,4(1*H*,3*H*)-dione (FPE-97)

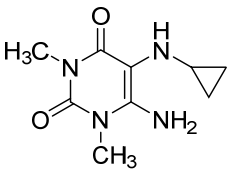

FPE-96 (0.2 g, 0.85 mmol, 1 eq) is dissolved in a mixture of cyclopropylamine (1.7 ml) and water (0.5 ml). The reaction is stirred at 75°C for 5 hours. It is then cooled down to RT and extracted with EtOAc. The organic layers are combined, dried over $MgSO_4$ and concentrated under *vacuum*. Purification with flash column chromatography (methanolic ammonia 7 N in DCM 0% to 10%). **Yield**: 25 mg, 0.12 mmol, 12%; **LC-MS** (m/z): 211.0 ($[M+H]^+$); **purity** by HPLC-UV (220 – 400 nm)-ESI-MS: 81.2%. Crude used without further purification.

6-Amino-5-((2-chloro-4-methoxybenzyl)amino)-1,3-dimethylpyrimidine-2,4(1*H*,3*H*)-dione (FPE-118)

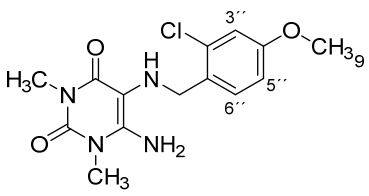

Synthesis according to **GPA**. Purification was achieved via recrystallization in cold MeOH. **Yield**: 200 mg, 0.62 mmol, 62%; **M.p**.: 199°C; **^{1}H NMR** (600 MHz, DMSO-d_6) δ 7.43 (d, J =8.5 Hz, 1H, C6′′-H), 6.99 (d, J = 2.6 Hz, 1H, C3′′-H), 6.88 (dd, J = 8.5, 2.6 Hz, 1H, C5′′-H), 6.37 (s, 2H, NH_2), 3.87 – 3.81 (m, 2H, NH*CH*$_2$), 3.76 (s, 3H, OCH_3), 3.27 (s, 3H, N3CH_3), 3.12 (s, 3H, N1CH_3); **^{13}C NMR** (151 MHz, DMSO-d_6) δ 160.31, 158.80, 151.76, 150.31, 133.36, 131.35, 129.55, 114.25, 112.87, 96.33, 55.43, 48.55, 29.89, 27.28; **LC-MS (m/z)**: 325.1 ([M+H]$^+$); **purity** by HPLC-UV (220 – 400 nm)-ESI-MS: 77.9%.

5.2.2.3 Synthesis of 7-alkyl/arylalkyl-1,3-dimethyl-3,7-dihydro-1H-purine-2,6-diones

7-Cyclopropyl-1,3-dimethyl-3,7-dihydro-1*H*-purine-2,6-dione (FPE-99)

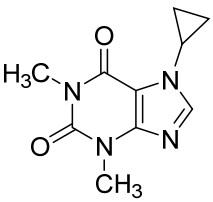

Synthesis according to **GP D**. Purification with flash column chromatography on silica gel (MeOH in DCM 0 to 5%). **Yield:** 83 mg, 0.38 mmol, 34%; **M.p.:** 188°C; **^{1}H NMR** (600 MHz, DMSO-d_6) δ 8.06 (s, 1H, C8H), 3.73 – 3.65 (m, 1H, *N*7CH), 3.40 (s, 3H, N3CH_3), 3.23 (s, 3H, N1CH_3), 1.10 – 0.99 (m, 4H, $H_{cyclopropyl}$); **^{13}C NMR** (151 MHz, DMSO-d_6) δ 154.06, 150.98, 148.39, 141.41, 107.51, 29.33, 28.49, 27.56, 6.61 (2C); **LC-MS (m/z)**: 221.0 ([M+H]$^+$); **purity** by HPLC-UV (220 – 400 nm)-ESI-MS: 98.3%.

1,3-Dimethyl-7-(naphthalen-1-yl)-3,7-dihydro-1*H*-purine-2,6-dione (FPE-110 step I)

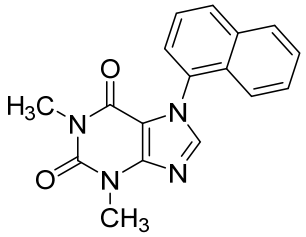

Synthesis according to **GP D**. Purification with flash column chromatography on silica gel (MeOH in DCM 0 to 5%). **Yield:** 29 mg, 0.09 mmol, 10%; **M.p.:** 224°C; **^{1}H NMR (**600Mhz**,** DMSO-d_6**)** δ 8.35 (s, 1H, C8H)), 8.15 (ddd, J = 7.2, 2.6, 0.8 Hz, 1H, $H_{naphtyl}$), 8.11 – 8.08 (m, 1H, $H_{naphtyl}$), 7.67 – 7.64 (m, 2H, $H_{naphtyl}$), 7.62 (ddd, J = 8.1, 6.9, 1.2 Hz, 1H, $H_{naphtyl}$), 7.54 (ddd, J = 8.2, 6.8, 1.3 Hz, 1H, $H_{naphtyl}$), 7.39 (dd, J = 8.5, 1.0 Hz, 1H, $H_{naphtyl}$), 3.56 (s, 3H, N3CH_3), 3.13 (s, 3H, N1CH_3); **^{13}C NMR** (151 MHz, DMSO-d_6) δ 153.47, 151.10, 148.58, 143.67, 133.35, 131.59, 129.77, 129.64, 128.08, 127.65, 126.78, 125.22, 125.18, 121.93,

108.41, 29.61, 27.5; **LC-MS (m/z)**: 307.1 ([M+H]$^+$); **purity** by HPLC-UV (220 – 400 nm)-ESI-MS: 91.0%.

7-(2-Chloro-4-methoxybenzyl)-1,3-dimethyl-3,7-dihydro-1*H*-purine-2,6-dione (FPE-120)

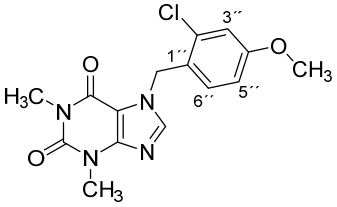

Synthesis according GPC. **Yield**: 149 mg, 0.44 mmol, 72%; **M.p.**: 177°C; **^{1}H NMR** (600 MHz, DMSO-*d*$_6$) δ 8.08 (s, 1H, C8H), 7.09 (d, *J* = 2.6 Hz, 1H, 3´´-H), 7.07 (d, *J* = 8.7 Hz, 1H, 6´´-H), 6.89 (dd, *J* = 8.6, 2.6 Hz, 1H, 5´´-H), 5.52 (s, 2H, *N*7CH$_2$), 3.76 (s, 3H, OCH$_3$), 3.44 (s, 3H, N3CH$_3$), 3.20 (s, 3H, N1CH$_3$); **^{13}C NMR** (151 MHz, DMSO-*d*$_6$) δ 159.54, 154.18, 150.86, 148.28, 142.65, 132.58, 130.03, 125.61, 114.62, 113.40, 105.91, 55.49, 46.43, 39.92, 29.31, 27.38; **LC-MS (m/z)**: 335.1 ([M+H]$^+$); **purity** by HPLC-UV (220 – 400 nm)-ESI-MS: 90.0%.

7-(1-(4-Methoxyphenyl)ethyl)-1,3-dimethyl-3,7-dihydro-1*H*-purine-2,6-dione (FPE-127)

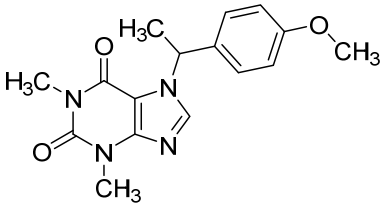

Synthesis according to GPC. **Yield** 47.2 mg, 0.15 mmol, 88%; **LC-MS (m/z)**: 315.1 ([M+H]$^+$); **purity** by HPLC-UV (220 – 400 nm)-ESI-MS: 94.9%. Crude used without further purification.

1,3-Dimethyl-7-(naphthalen-2-yl)-3,7-dihydro-1*H*-purine-2,6-dione (FPE-133)

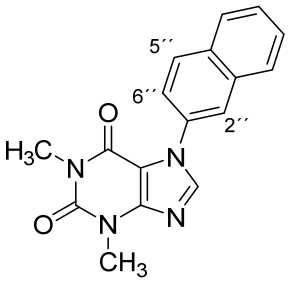

Synthesis according to **GP D**. Purification with flash column chromatography on silica gel (MeOH in DCM 0 to 5%). **Yield:** 70 mg, 0.23 mmol, 10%; **M.p.:** 226°C; **^{1}H NMR** (500 MHz, DMSO-*d*$_6$) δ 8.46 (s, 1H, C8H), 8.15 (d, *J* = 2.2 Hz, 1H, 2´´-H), 8.07 (d, *J* = 8.8 Hz, 1H, 5´´-H), 8.05 – 7.98 (m, 2H, Ar-H$_{naphtyl}$), 7.69 (dd, *J* = 8.8, 2.2 Hz, 1H, 6´´-H), 7.63 (dt, *J* = 6.2, 3.4 Hz, 2H, Ar-H$_{naphtyl}$), 3.53 (s, 3H, N3CH$_3$), 3.23 (s, 3H, N1CH$_3$); **^{13}C NMR** (126 MHz, DMSO-d$_6$) δ 153.74, 150.94, 149.27, 142.94, 132.42, 132.38, 132.30, 128.53, 128.01, 127.67, 127.05, 126.95, 123.70, 123.15, 106.42, 29.60, 27.78; **LC-MS (m/z)**: 305.0 ([M+H]$^+$); **purity** by HPLC-UV (220 – 400 nm)-ESI-MS: 98.0%.

1,3-Dimethyl-7-phenyl-3,7-dihydro-1*H*-purine-2,6-dione (FPE-134)

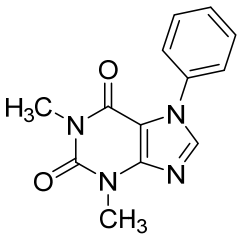

Synthesis according to **GP D**. Purification with flash column chromatography on silica gel (MeOH in DCM 0 to 5%). **Yield:** 70 mg, 0.27 mmol, 13%; **M.p.:** 225°C; **^{1}H NMR** (500 MHz, DMSO-*d*$_6$) δ 8.36 (s, 1H,C8H), 7.63 – 7.47 (m, 5H, Ar-H$_{phenyl}$), 3.50 (s, 3H,N3CH$_3$), 3.22 (s, 3H, N1CH$_3$); **^{13}C NMR** (126 MHz, DMSO-d$_6$) δ 153.64, 150.90, 149.21, 142.71, 134.79, 128.87, 128.48, 125.12, 106.17, 29.55, 27.75; **LC-MS (m/z)**: 257.1 ([M+H]$^+$); **purity** by HPLC-UV (220 – 400 nm)-ESI-MS: 99.9%.

1,3-Dimethyl-7-(quinolin-4-yl)-3,7-dihydro-1*H*-purine-2,6-dione (FPE-193)

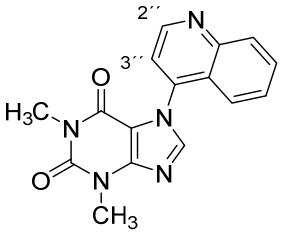

Synthesis according to **GP D**. Purification with flash column chromatography on silica gel (MeOH in DCM 0 to 3%). **Yield:** 7 mg, 0.23 mmol, 30%; **M.p.:** 204°C ; **^{1}H NMR** (600 MHz, DMSO-*d*$_6$) δ 9.09 (d, *J* = 4.5 Hz, 1H, 2´´-H), 8.47 (s, 1H, C8H), 8.19 (d, *J* = 8.4 Hz, 1H, Ar-H$_{quinolyl}$), 7.88 (ddd, *J* = 8.3, 6.6, 1.6 Hz, 1H, Ar-H$_{quinolyl}$), 7.73 (d, *J* = 4.5 Hz, 1H, 3´´-H), 7.67 – 7.55 (m, 2H, Ar-H$_{quinolyl}$), 3.56 (s, 3H, N3CH$_3$), 3.14 (s, 3H, N1CH$_3$); **^{13}C NMR** (151 MHz, DMSO-*d*$_6$) δ 153.54, 151.10, 150.64, 148.96, 148.53, 143.47, 139.48, 130.45, 129.21, 128.17, 124.27, 122.63, 119.51, 108.10, 29.76, 27.67; **LC-MS (m/z)**: 308.1 ([M+H]$^+$); **purity** by HPLC-UV (220 – 400 nm)-ESI-MS: 97.9%.

7-(7-Chloroquinolin-4-yl)-1,3-dimethyl-3,7-dihydro-1*H*-purine-2,6-dione (FPE-204)

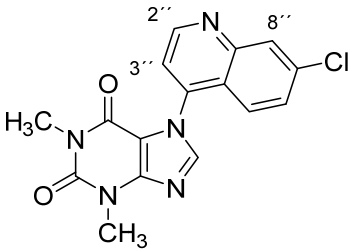

Synthesis according to **GP D**. Purification with flash column chromatography on silica gel (MeOH in DCM 0 to 3%). **Yield:** 95 mg, 0.28 mmol, 24%; **M.p.:** 177°C ; **^{1}H NMR** (600 MHz, DMSO-*d*$_6$) δ 9.13 (d, *J* = 4.6 Hz, 1H, C2´´-H), 8.48 (s, 1H, C8-H), 8.27 (d, *J* = 2.0 Hz, 1H, C8´´-H), 7.77 (d, *J* = 4.5 Hz, 1H, C3´´-H), 7.72 – 7.65 (m, 2H, Ar-H$_{quinolyl}$), 3.56 (s, 3H, N3CH$_3$), 3.14 (s, 3H, N1CH$_3$); **^{13}C NMR** (151 MHz, DMSO-*d*$_6$) δ 153.54, 152.13, 151.05, 149.03, 148.80, 143.44, 139.67, 135.11, 128.59, 127.78, 125.12, 122.95, 119.83, 108.03, 29.74, 27.66; **LC-MS (m/z)**: 342.0 ([M+H]$^+$); **purity** by HPLC-UV (220 – 400 nm)-ESI-MS: 93.1%.

8-Chloro-7-cyclopropyl-1,3-dimethyl-3,7-dihydro-1H-purine-2,6-dione (FPE-111)

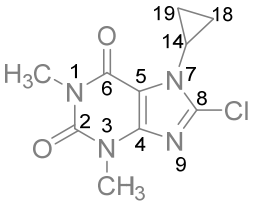

Synthesis according to **GP E**. Purification with flash column chromatography on silica gel (MeOH in DCM 0 to 5%). **Yield:** 42 mg, 0.16 mmol, 35%; **M.p.:** 245°C; **^{1}H NMR** (600 MHz, DMSO-d_6) δ 3.37 (m, 4H, N3CH_3 and N7*CH*), 3.22 (s, 3H, N1CH_3), 1.22 – 1.05 (m, 4H, $H_{cyclopropyl}$); **^{13}C NMR** (151 MHz, DMSO-d_6) δ 152.97 (C6), 150.79 (C2), 146.62 (C4), 140.06 (C8), 108.79 (C5), 29.56 (CH_3), 27.91 (CH_3), 27.37 (C14), 8.82 (2 C, C18 and C19); **LC-MS (m/z)**: 255.2 ([M+H]$^+$); **purity** by HPLC-UV (220 – 400 nm)-ESI-MS: 100%.

8-Chloro-1,3-dimethyl-7-(naphthalen-1-yl)-3,7-dihydro-1*H*-purine-2,6-dione (FPE-110 step II)

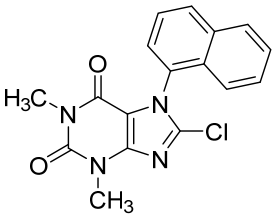

Synthesis according to **GP E**. Crude use without further purification. **LC-MS (m/z)**: 341.00 ([M+H]$^+$); **purity** by HPLC-UV (220 – 400 nm)-ESI-MS: < 20%. Used without further purification.

8-Chloro-7-(2-chloro-4-methoxybenzyl)-1,3-dimethyl-3,7-dihydro-1*H*-purine-2,6-dione (FPE-121)

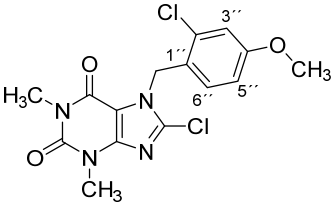

Synthesis according to **GP E**. **Yield** 95 mg, 0.26 mmol, 60%; **M.p.:** 180°C ; **^{1}H NMR** (600 MHz, DMSO-d_6) δ 7.12 (d, J = 2.5 Hz, 1H, 6′′-H), 6.85 (dd, J = 8.7, 2.6 Hz, 1H, 5′′-H), 6.73 (d, J = 8.7 Hz, 1H, 3′′-H), 5.55 (s, 2H, N7CH_2), 3.76 (s, 3H, OCH_3), 3.43 (s, 3H, N3CH_3), 3.20 (s, 3H, N1CH_3); **^{13}C NMR** (151 MHz, DMSO-d_6) δ 159.45, 153.69, 150.67, 146.85, 138.26, 131.81, 128.23, 124.44, 114.77, 113.79, 107.56, 55.62, 55.62, 45.81, 29.57, 27.60; **LC-MS (m/z)**: 369.1 ([M+H]$^+$); **purity** by HPLC-UV (220 – 400 nm)-ESI-MS: 99.5%.

8-Chloro-7-(4-methoxyphenethyl)-1,3-dimethyl-3,7-dihydro-1*H*-purine-2,6-dione (FPE-91 II)

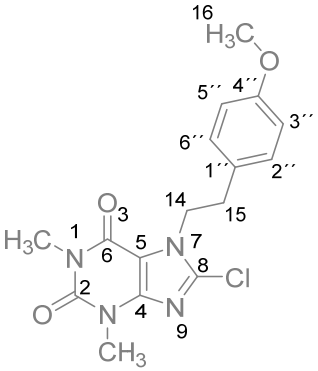

Synthesis according to **GP E**. **Yield:** 22 mg, 0.063 mmol, 49%; **M.p.:** 156°C; **^{1}H NMR (**500 MHz**,** DMSO-d_6**)** δ 7.04 (d, J = 8.17 Hz, 2H, Ar-H_{benzyl}), 6.82 (d, J = 8.33 Hz, 2H, Ar-H_{benzyl}), 4.40 (t, J = 7.09 Hz, 2H, N7CH_2), 3.71 (s, 3H, OCH_3), 3.38 (s, 3H, N3CH_3), 3.25 (s, 3H, N1CH_3), 2.97 (t, J = 7.09 Hz, 2H, CH_2CH_2); **^{13}C NMR (126 MHz, DMSO)** δ 157.97 (C4′′), 153.45 (C6), 150.52 (C2), 146.57 (C4), 137.49 (C8), 129.67 (2C, CH_{Ar}), 128.66 (C1′′), 113.71 (2C, CH_{Ar}), 106.81 (C5), 54.81 (C16), 47.25 (C14), 34.48 (C15), 29.32 (1C, CH_3), 27.48 (1C, CH_3); **LC-MS (m/z)**: 349.1 ([M+H]$^+$); **purity** by HPLC-UV (220 – 400 nm)-ESI-MS: 98.7%

8-Chloro-1,3-dimethyl-7-phenyl-3,7-dihydro-1*H*-purine-2,6-dione (FPE-136)

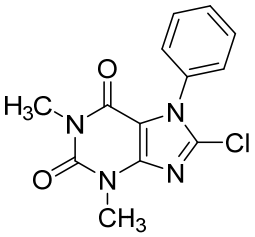

Synthesis according to **GP E**. **Yield:** 55 mg, 0.19 mmol, 76%; **M.p.:** decomposed at 250°C; **^{1}H NMR** (600 MHz, DMSO-d_6) δ 7.59 – 7.56 (m, 3H, Ar-H_{benzyl}), 7.52 (dd, J = 6.8, 2.9 Hz, 2H, Ar-H_{benzyl}), 3.47 (s, 3H, N3CH_3), 3.17 (s, 3H, N1CH_3); **^{13}C NMR** (151 MHz, DMSO-d_6) δ 152.79, 150.65, 146.89, 138.21, 133.64, 129.80, 129.05 (2C), 127.49 (2C), 108.70, 29.61, 27.67; **LC-MS (m/z)**: 291.0 ([M+H]$^+$); **purity** by HPLC-UV (220 – 400 nm)-ESI-MS: 90.2%.

8-Chloro-1,3-dimethyl-7-(naphthalen-2-yl)-3,7-dihydro-1*H*-purine-2,6-dione (FPE-140)

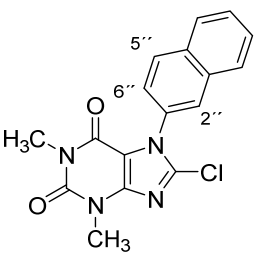

Synthesis according to **GP E**. **Yield:** 22 mg, 0.063 mmol, 49%; **M.p.:** 195°C; ^{1}H NMR (600 MHz, DMSO-d_6) δ 8.14 (d, J = 2.1 Hz, 1H, 2′′-H), 8.11 (d, J = 8.7 Hz, 1H, 5′′-H), 8.07 (d, J = 7.3 Hz, 1H, Ar-$H_{napthyl}$), 8.04 (d, J = 7.2 Hz, 1H, Ar-$H_{napthyl}$), 7.70 – 7.64 (m, 2H, Ar-$H_{napthyl}$), 7.60 (dd, J = 8.7, 2.1 Hz, 1H, 6′′-H), 3.50 (s, 3H, N1CH_3), 3.17 (s, 3H, N3CH_3); **^{13}C NMR** (151 MHz, DMSO-d_6) δ 152.89, 150.68, 146.96, 138.43, 132.92, 132.34, 131.10, 128.87, 128.22, 127.79, 127.60, 127.17, 126.52, 124.91, 108.92, 29.67, 27.68; **LC-MS (m/z)**: 341.0 ([M+H]$^+$); **purity** by HPLC-UV (220 – 400 nm)-ESI-MS: 100%.

8-Chloro-1,3-dimethyl-7-(quinolin-4-yl)-3,7-dihydro-1*H*-purine-2,6-dione (FPE-206)

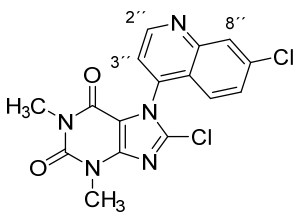

Synthesis according to **GP E**. **Yield:** 45 mg, 0.12 mmol, 45%; **M.p.:** 187°C; **^{1}H NMR** (600 MHz, DMSO-*d*$_6$) δ 9.20 (d, *J* = 4.5 Hz, 1H, C2´´-H), 8.31 (d, *J* = 1.9 Hz, 1H, C8´´-H), 7.89 (d, *J* = 4.5 Hz, 1H, C3´´-H), 7.73 – 7.63 (m, 2H, Ar-H$_{quinolyl}$), 3.52 (s, 3H, N3CH$_3$), 3.12 (s, 3H, N1CH$_3$); **^{13}C NMR** (151 MHz, DMSO-*d*$_6$) δ 152.76, 152.40, 150.73, 148.98, 147.44, 138.53, 138.41, 135.49, 129.17, 128.10, 124.69, 122.99, 121.42, 109.79, 29.84, 27.67; **LC-MS (m/z)**: 376.2 ([M+H]$^+$); **purity** by HPLC-UV (220 – 400 nm)-ESI-MS: 99.8%.

8-Chloro-7-(4-methoxybenzyl)-1,3-dimethyl-3,7-dihydro-1*H*-purine-2,6-dione (FPE-8)

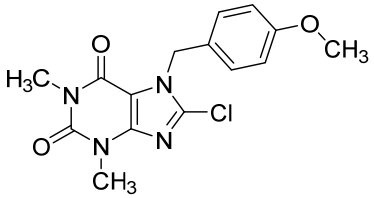

Synthesized according to **GP F**. Purification by flash column chromatography on silica gel (MeOH in DCM 0 to 5%); **Yield** 667 mg, 1.99 mmol, 85.5%; **M.p.** 179°C; **^{1}H NMR** (600 MHz, DMSO-*d*$_6$): δ 7.28 (d, *J* = 8.66 Hz, 2H, Ar-H$_{benzyl}$), 6.91 (d, *J* = 8.66 Hz, 2H, Ar-H$_{benzyl}$), 5.45 (s, 2H, N7CH$_2$), 3.72 (s, 3H, -OCH$_3$), 3.39 (s, 3H, N3CH$_3$), 3.24 (s, 3H, N1CH$_3$); **^{13}C NMR** (151 MHz, DMSO-*d*$_6$) δ 159.03, 153.87, 150.63, 146.82 , 137.63, 129.01 (2C), 127.40, 114.13 (2C), 107.15, 55.09, 47.98, 29.51, 27.67; **LC-MS (m/z)**: 447.3 ([M+H]$^+$); **purity** by HPLC-UV (220 – 400 nm)-ESI-MS: 97.7%.

8-Chloro-7-(4-hydroxybenzyl)-1,3-dimethyl-3,7-dihydro-1*H*-purine-2,6-dione (FPE-16)

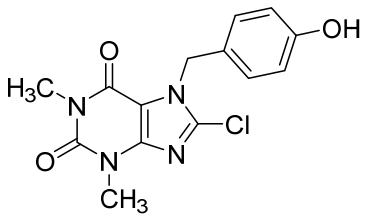

Synthesis according to **GP I**. Purification by flash column chromatography on silica gel (MeOH in DCM 3 to 5%). **Yield**: 30 mg, 0.093 mmol, 62%; **M.p.:** 196°C; **^{1}H NMR** (600 MHz, DMSO-*d*$_6$): δ 9.49 (s, 1H, -OH), 7.16 (d, *J* = 8.46 Hz, 2H, Ar-H$_{benzyl}$), 6.72 (d, *J* = 8.47 Hz, 2H, Ar-H$_{benzyl}$), 5.39 (s, 2H, N7CH$_2$), 3.38 (s, 3H, N3CH$_3$), 3.24 (s, 3H, N1CH$_3$); **^{13}C NMR** (151 MHz, DMSO-*d*$_6$) δ 157.14, 153.71, 150.47, 146.62, 137.45, 128.96 (2C), 125.53, 115.27 (2C), 106.97, 47.97, 29.35, 27.52; **LC-MS (m/z)**: 321.0 ([M+H]$^+$); **purity** by HPLC-UV (220 – 400 nm)-ESI-MS: 93.7%.

8-Chloro-7-(2-fluoroethyl)-1,3-dimethyl-3,7-dihydro-1*H*-purine-2,6-dione (FPE-17B)

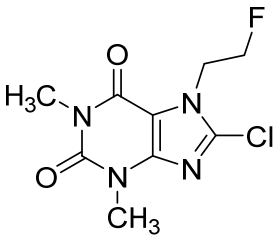

FPE 16 (25 mg, 0.075 mmol, 1 eq) and Cs_2CO_3 (73 mg, 0.23 mmol,3 eq) were weighed into a sealed vial and dissolved in DMF (1 ml) under stirring for 15 minutes. Afterwards, 1-bromo-2-fluoroethane (0.01 mL, 0.113 mmol, 1.5 eq) was added and the mixture was heated up to 60°C and stirred for 2.5 hours. When no further improvement was detected, the reaction was quenched with ice-cold water to achieve precipitation followed by filtration. The crude was used without further purification for the next step. **Yield**: 20 mg, 32.5%; **LC-MS (m/z)**: 261.1 ($[M+H]^+$); **purity** by HPLC-UV (220 – 400 nm)-ESI-MS: 75.9%. The compound was used without further purification to the next step.

4-((8-Chloro-1,3-dimethyl-2,6-dioxo-1,2,3,6-tetrahydro-7*H*-purin-7-yl)methyl)-*N*-propylbenzenesulfonamide (FPE-14)

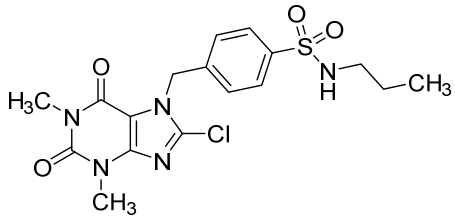

Synthesis according to **GP F**. **Yield:** 103.8 mg, 0.224 mmol, 32%; **M.p.** 181°C; **^{1}H NMR (**600Mhz**,** DMSO-d_6**)**: δ 7.77 (d, J = 8.32 Hz, 2H, Ar-H_{benzyl}), 7.59 (t, J = 5.73 Hz, 1H, ,SO_2NH), 7.45 (d, J = 8.31 Hz, 2H, Ar-H_{benzyl}), 5.63 (s, 2H, N7CH_2), 3.42 (s, 3H, N3CH_3), 3.23 (s, 3H, N1CH_3), 2.68 (td, J = 5.48, 6.93 Hz, 2H, *CH_2*CH_2CH_3), 1.36 (q, J = 7.25 Hz, 2H, CH_2*CH_2*CH_3), 0.78 (t, J = 7.38 Hz, 3H, CH_2CH_2*CH_3*). **^{13}C NMR** (151 MHz, DMSO-d_6) δ 154.26, 151.07, 147.29, 140.70, 140.06, 138.36, 128.15, 127.34, 107.82, 48.38, 44.72, 31.07, 28.07, 22.80, 11.48; **LC-MS (m/z)**: 426.1 ($[M+H]^+$); **purity** by HPLC-UV (220 – 400 nm)-ESI-MS: 97.6%.

Methyl 4-((8-chloro-1,3-dimethyl-2,6-dioxo-1,2,3,6-tetrahydro-7*H*-purin-7-yl) methyl) benzoate (FPE-26)

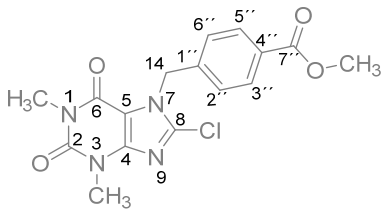

Synthesis according **GP F**. **Yield**: 982 mg, 2.71 mmol, 97%; **M.p**: 210°C; **^{1}H NMR (**600Mhz**,** DMSO-d_6**)** δ 7.94 (d, J = 8.30 Hz, 2H, Ar-H_{benzyl}), 7.39 (d, J = 8.31 Hz, 2H, Ar-H_{benzyl}), 5.63 (s, 2H, N7CH_2), 3.84 (s, 3H, -OCH_3), 3.41 (s, 3H, N3CH_3), 3.22 (s, 3H, N1CH_3); **^{13}C NMR** (151 MHz, DMSO-d_6) δ 165.79 (C7''), 153.83 (C6), 150.66 (C2), 146.86 (C4), 140.63 (C1''), 137.97 (C8), 129.62 (2C, CH_{Ar}),

129.24 (C4''), 127.30 (2C, CH_{Ar}), 107.39 (C5), 52.17 (-O-CH_3), 48.13 (C14), 29.56 (1C, -CH_3), 27.66 (1C, CH_3); **LC-MS (m/z)**: 363.0 ([M+H]$^+$); **purity** by HPLC-UV (220 – 400 nm)-ESI-MS: 96.1%.

8-Chloro-1,3-dimethyl-7-(pyridin-4-ylmethyl)-3,7-dihydro-1*H*-purine-2,6-dione (FPE-28)

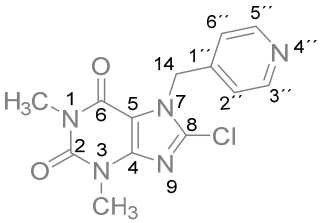

Synthesis according to **GP F**. White solid. **Yield**: 135 mg, 0.44 mmol, 31%; **M.p.:** 170°C**; ^{1}H NMR (**600Mhz**,** DMSO-d_6**):** δ 8.56 – 8.54 (m, 2H, Ar-H_{benzyl}), 7.21 (d, J = 6.14 Hz, 2H, Ar-H_{benzyl}), 5.58 (s, 2H, N7CH_2), 3.42 (s, 3H, N3CH_3), 3.21 (s, 3H, N1CH_3); **^{13}C NMR** (151 MHz, DMSO-d_6) δ 154.23 (C6), 151.10 (C2), 150.47 (2C, C3'' and C5''), 147.30 (C4), 144.62 (C1''), 138.45 (C8), 122.02 (2C, C2'' and C6''), 47.82 (C14), 31.07 (1C, CH_3), 28.04 (1C, CH_3)**; LC-MS (m/z)**: 305.9 ([M+H]$^+$); **purity** by HPLC-UV (220 – 400 nm)-ESI-MS: 99.5%.

8-Chloro-7-((6-chloropyridin-3-yl)methyl)-1,3-dimethyl-3,7-dihydro-1*H*-purine-2,6-dione (FPE-32)

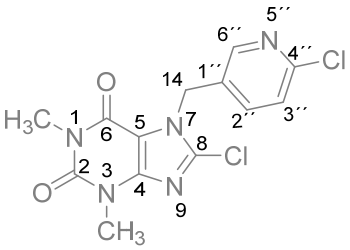

Synthesis according to **GP F. Yield**: 677 mg, 0.2 mmol, 71%; **M.p.**: 173°C **^{1}H NMR (**600Mhz**,** DMSO-d_6**)** : δ 8.44 (dd, J = 0.75, 2.51 Hz, 1H, C6''-H), 7.77 (dd, J = 2.57, 8.31 Hz, 1H, C2''-H), 7.53 (dd, J = 0.69, 8.37 Hz, 1H,C3''-H), 5.58 (s, 2H, N7CH_2), 3.40 (s, 3H, N3CH_3), 3.23 (s, 3H, N1CH_3). **^{13}C NMR** (151 MHz, DMSO-d_6) δ 154.05 (C6), 150.78 (C2), 150.12 (C6''), 149.23 (C4''), 147.05 (C4), 139.14 (C2''), 137.90 (C8), 130.94, 124.61 (C3''), 107.41 (C5), 45.61 (C14), 29.68 (1C, -CH_3), 27.80 (1C, -CH_3)**; LC-MS (m/z)**: 339.9 ([M+H]$^+$); **purity** by HPLC-UV (220 – 400 nm)-ESI-MS: 86.2%.

8-Chloro-7-((5-chloropyridin-2-yl)methyl)-1,3-dimethyl-3,7-dihydro-1*H*-purine-2,6-dione (FPE-34)

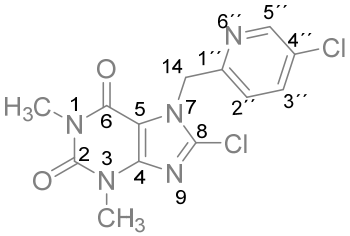

Synthesis according to **GP F**. **Yield:** 75 mg, 0.22 mmol, 79%; **M.p.:** 201°C**; ^{1}H NMR (**600MHz**,** DMSO-d_6**):** δ 8.53 (d, J = 2.39 Hz, 1H, C5''-H), 7.96 (dd, J = 2.52, 8.42 Hz, 1H, C2''-H), 7.46 (d, J = 8.42 Hz, 1H, C3''-H), 5.65 (s, 2H, N7CH_2), 3.42 (s, 3H, N3CH_3), 3.18 (s, 3H, N1CH_3). **^{13}C NMR** (151 MHz, DMSO-d_6) δ 153.94 (C6), 153.13 (C1''), 150.88 (C2), 148.14 (C5''), 146.95 (C4), 139.04 (C3''), 137.22 (C8), 130.65 (C4''), 123.31 (C2''), 107.71 (C5), 49.36 (C14), 29.80 (1C, -CH_3), 27.82 (1C, -CH_3); **LC-MS (m/z)**: 339.8 ([M+H]$^+$); **purity** by HPLC-UV (220 – 400 nm)-ESI-MS: 96.8%.

8-Chloro-1,3-dimethyl-7-(4-nitrobenzyl)-3,7-dihydro-1*H*-purine-2,6-dione (FPE-38)

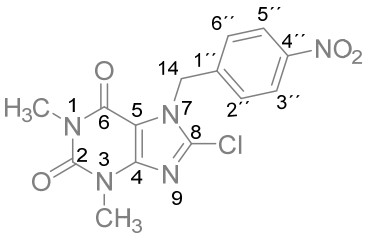

Synthesis according to **GP F. Yield**: 1.8 g, 5.15 mmol, 55%. **M.p.** 186°C; ^{1}H NMR (500 MHz, DMSO-d_6) δ 8.22 (d, J = 8.8 Hz, 2H, Ar-H_{benzyl}), 7.52 (d, J = 8.6 Hz, 2H, Ar-H_{benzyl}), 5.69 (s, 2H, N7CH_2), 3.42 (s, 3H, N3CH_3), 3.22 (s, 3H, N1CH_3); ^{13}C NMR (126 MHz, DMSO-d_6) δ 165.34, 153.78, 150.61, 147.15, 146.88, 142.72, 137.97, 128.21, 123.85, 107.34, 47.82, 41.10, 29.52, 27.59; **LC-MS (m/z)**: 349.9([M+H]$^+$); **purity** by HPLC-UV (220 – 400 nm)-ESI-MS: 96.2%.

8-Chloro-7-(3-chloro-4-methoxybenzyl)-1,3-dimethyl-3,7-dihydro-1*H*-purine-2,6-dione (FPE-41)

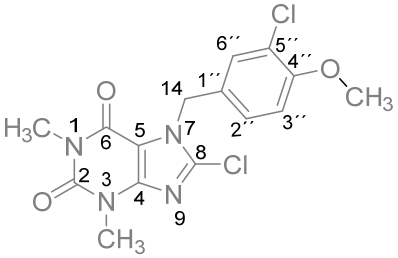

Synthesis according to **GP F**. **Yield** 876 mg, 2.12 mmol, 91%; **M.p.:** 174°C; **^{1}H NMR (**600MHz**,** DMSO-d_6**)** δ 7.42 (d, J = 2.20 Hz, 1H, C6''-H), 7.26 (dd, J = 2.20, 8.61 Hz, 1H, C2''-H), 7.10 (d, J = 8.58 Hz, 1H, C3''-H), 5.42 (s, 2H, -N7CH_2), 3.82 (s, 3H, -OCH_3), 3.36 (s, 3H, N3CH_3), 3.22 (s, 3H, N1CH_3); **^{13}C NMR** (151 MHz, DMSO-d_6) δ 154.45 (C4''), 153.95 (C6), 150.66 (C2), 146.90 (C4), 137.77 (C8), 129.23 (1C, $C_{Aromatic}$), 128.55($C_{Aromatic}$), 127.89 ($C_{Aromatic}$), 121.23 (C5''), 113.03 (C3''), 107.21 (C5), 56.27 (-OCH_3), 47.50 (C14), 29.59 (1C, CH_3), 27.75 (1C, CH_3); **LC-MS (m/z)**: 369.0 ([M+H]$^+$); **purity** by HPLC-UV (220 – 400 nm)-ESI-MS: 98.4%.

8-Chloro-7-(4-chlorobenzyl)-1,3-dimethyl-3,7-dihydro-1H-purine-2,6-dione (FPE-50)

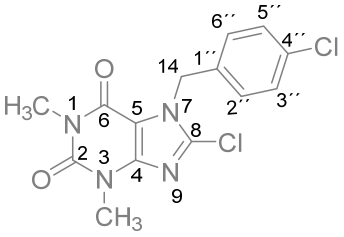

Synthesis according to **GP F. Yield**: 0.810 g, 2.4 mmol, quantitative. **M.p.** 218°C; ^{1}H NMR (500 MHz, DMSO-d_6) δ 7.42 (d, J = 8.5 Hz, 2H, Ar-H$_{benzyl}$), 7.31 (d, J = 8.5 Hz, 2H, Ar-H$_{benzyl}$), 5.52 (s, 2H, N7CH$_2$), 3.39 (s, 3H, N3CH$_3$), 3.22 (s, 3H, N1CH$_3$); ^{13}C NMR (126 MHz, DMSO-d$_6$) δ 153.80, 150.59, 146.81, 137.76, 134.35, 132.70, 129.15, 128.71, 107.22, 47.72, 29.48, 27.59; **LC-MS (m/z):** 339.0 ([M+H]$^+$); **purity** by HPLC-UV (220 – 400 nm)-ESI-MS: 99.0%.

8-Chloro-7-(methoxymethyl)-1,3-dimethyl-3,7-dihydro-1*H*-purine-2,6-dione (FPE-56)

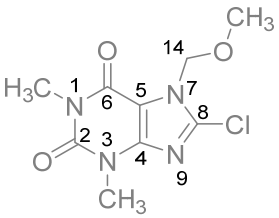

8-Chlorotheophylline (1g, 4.66 mmol, 1 eq) is weighed in a 50-ml round-bottomed flask and dissolved in DMF (6 ml). K$_2$CO$_3$ (0.77 g, 5.6 mmol, 1.2 eq) is then added and the mixture is stirred at RT for 30 minutes. The mixture is then cooled to -10/-15°C with a ice/acetone bath and chloromethyl methyl ether (0.42 ml, 5.6 mmol, 1.2 eq) is added dropwise. The mixture is let warm again to RT and stirred overnight. When no further improvement was detected, the reaction was quenched with ice-cold water to achieve precipitation. The precipitate is collected with filtration under *vacuum*. **Yield:** 1.135 g, 4.4 mmol, 94.4%; **^{1}H NMR (**600MHz**,** DMSO-d_6**)** δ 5.61 (s, 2H, N7CH$_2$), 3.40 (s, 3H, N3CH$_3$), 3.32 (s, 3H, OCH$_3$), 3.23 (s, 3H, N1CH$_3$). **^{13}C NMR** (151 MHz, DMSO-d_6) δ 153.61 (C6), 150.61 (C2), 146.74 (C4), 138.70 (C8), 107.46 (C5), 75.36 (C14), 56.28 (-O-CH$_3$), 29.59 (1C, -CH$_3$), 27.66 (1C, CH$_3$); **LC-MS (m/z)**: 259.0 ([M+H]$^+$); **purity** by HPLC-UV (220 – 400 nm)-ESI-MS: 98.6%.

7-(4-Aminobenzyl)-8-chloro-1,3-dimethyl-3,7-dihydro-1*H*-purine-2,6-dione (FPE-68)

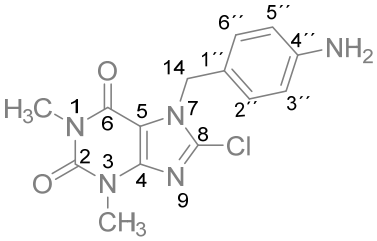

FPE-38 (0.49 g, 1.4 mmol, 1 eq) was dissolved in EtOH (5 mL). SnCl$_2$ was then carefully added and the mixture was stirred at 70°C for 1.5 hours. Ice cold water was added to the mixture and an extraction with EtOAc was performed. The organic phase was dried over MgSO$_4$ and concentrated under *vacuum* to give the product as a yellow solid. **Yield**: quantitative; **M.p.:** 192°C; **^{1}H NMR (**600MHz**,** DMSO-d_6) δ 7.03

(d, J = 8.46 Hz, 2H, Ar-H_{benzyl}), 6.50 (d, J = 8.43 Hz, 2H, Ar-H_{benzyl}), 5.30 (s, 2H, N7-CH_2), 5.11 (s, 2H, NH_2), 3.37 (s, 3H, N3CH_3), 3.24 (s, 3H, N1CH_3); **^{13}C NMR** (151 MHz, DMSO-d_6) δ 153.97 (C6), 150.75 (C2), 148.83 (C4´´), 146.87 (C4), 137.63 (C8), 128.95 (2 C, C2´´ and C6´´), 122.30 (C1´´) , 113.84 (2C, C3´´ and C5´´), 107.20 (C5), 48.58 (C14), 29.62 (1C, CH_3), 27.81 (1C, CH_3); **LC-MS (m/z)**: 320.0 ([M+H]$^+$); **purity** by HPLC-UV (220 – 400 nm)-ESI-MS: 78.8%.

_N_-(4-((8-Chloro-1,3-dimethyl-2,6-dioxo-1,2,3,6-tetrahydro-7_H_-purin-7-yl)methyl)phenyl) methanesulfonamide (FPE-69)

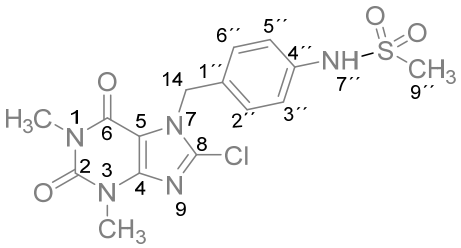

FPE-68 (0.253 g, 0.79 mmol, 1 eq) and methane sulfonyl chloride (0.18 g, 1.58 mmol, 2 eq) were dissolved in DCM (5 ml) and the mixture was stirred at RT for 24 h. When no improvement was detected, solvent was evaporated and the crude was partitioned between water and EtOAc. The combined organic layers were dried over $MgSO_4$ and concentrated under *vacuum*. Purification with flash column chromatography on silica gel (MeOH in DCM 0 to 5%). **Yield:** 130 mg, 0.33 mmol, 41%; **M.p.**: 126°C; **^{1}H NMR (**600MHz**,** DMSO-d_6**)** 9.77 (s, 1H, $NHSO_2$), 7.28 (d, J = 8.55 Hz, 2H, Ar-H_{benzyl}), 7.17 (d, J = 8.59 Hz, 2H, Ar-H_{benzyl}), 5.48 (s, 2H, N7CH_2), 3.39 (s, 3H, N3CH_3), 3.24 (s, 3H, N1CH_3), 2.98 (s, 3H, SO_2CH_3).**^{13}C NMR** (151 MHz, DMSO-d_6) δ 153.84 (C6), 150.63 (C2), 146.80 (C4), 138.18 (C8), 137.72 (C4´´), 130.68 (C1´´), 128.45 (2C, CH_{Ar}), 119.80 (2C, CH_{Ar}), 107.22 (C5), 47.94 (C14), 29.51 (1C, -CH_3), 27.65 (1C, CH_3). **LC-MS (m/z)**: 398.0 ([M+H]$^+$); **purity** by HPLC-UV (220 – 400 nm)-ESI-MS: 94.9%.

7-(4-Acetylbenzyl)-8-chloro-1,3-dimethyl-3,7-dihydro-1_H_-purine-2,6-dione (FPE-75)

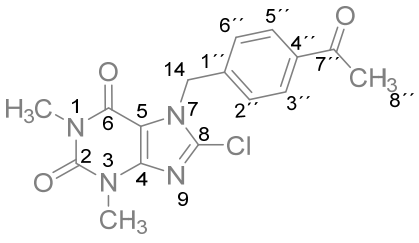

Synthesis according to **GP F**. **Yield:** quantitative**; M.p.**: 223°C; **^{1}H NMR (**600MHz**,** DMSO-d_6**)** δ 7.93 (d, J = 8.29 Hz, 2H; Ar-H_{benzyl}), 7.38 (d, J = 8.27 Hz, 2H, Ar-H_{benzyl}) , 5.62 (s, 2H, N7CH_2), 3.41 (s, 3H, N3CH_3), 3.22 (s, 3H, N1CH_3), 2.55 (s, 3H, $COCH_3$); **^{13}C NMR** (151 MHz, DMSO-d_6) δ 197.37 (C7''), 153.80 (C6), 150.62 (C2), 146.84 (C4), 140.38 (C8), 137.92 (1C, C_{Ar}), 136.38 (1C, C_{Ar}), 128.64 (2C, CH_{Ar}), 127.19 (2C, CHAr), 107.34 (C5), 48.13 (C14), 29.54 (1C, CH_3), 27.62 (1C,

CH3), 26.68 (C8´´); **LC-MS (m/z)**: 347.1 ([M+H]$^+$); **purity** by HPLC-UV (220 – 400 nm)-ESI-MS: 93.0%.

8-Chloro-1,3-dimethyl-7-(4-nitrophenethyl)-3,7-dihydro-1*H*-purine-2,6-dione (FPE-90)

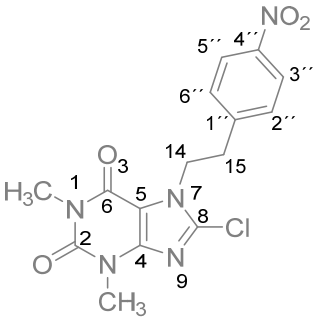

Synthesis according to **GP F**. Further purification achieved with column chromatography on silica gel (2% MeOH in DCM). **Yield:** 87 mg, 0.24 mmol, 13%; **M.p.:** 181°C; **^{1}H NMR (**500 MHz**,** DMSO-*d*$_6$**)** δ 8.12 (d, *J* = 8.49 Hz, 2H, Ar-H$_{benzyl}$), 7.42 (d, *J* = 8.62 Hz, 2H, Ar-H$_{benzyl}$), 4.50 (t, *J* = 6.86 Hz, 2H, N7CH$_2$), 3.37 (s, 3H, N3CH$_3$), 3.24 (s, 3H, N1CH$_3$), 3.21 (t, *J* = 6.94 Hz, 2H, CH$_2$*CH$_2$*). **^{13}C NMR (126 MHz, DMSO) δ** 153.49 (C6), 150.54 (C2), 146.65 (C4), 146.36 (1C, C$_{Ar}$), 145.25 (1C, C$_{Ar}$), 137.49 (1C, C$_{Ar}$), 130.23(2C, CH$_{Ar}$), 123.32 (2C, CH$_{Ar}$), 106.87 (C5), 46.46 (C14), 35.04 (C15), 29.35 (1C, CH$_3$) , 27.50 (1C, CH$_3$); **LC-MS (m/z)**: 364.1 ([M+H]$^+$); **purity** by HPLC-UV (220 – 400 nm)-ESI-MS: 99.4%.

8-Chloro-7-(cyclohexylmethyl)-1,3-dimethyl-3,7-dihydro-1*H*-purine-2,6-dione (FPE-106)

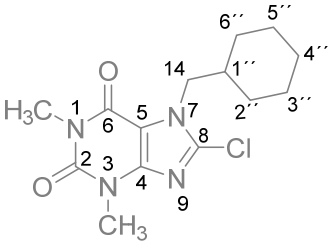

Synthesis according to **GP F**. **Yield:** 105 mg, 0.34 mmol, 72%; **M.p.:** 96°C; **^{1}H NMR (**600MHz**,** DMSO-*d*$_6$**)** δ 4.10 (d, *J* = 7.4 Hz, 2H, N7CH$_2$), 3.39 (s, 3H, N3CH$_3$), 3.23 (s, 3H, N1CH$_3$), 1.83 (ttt, *J* = 11.1, 7.3, 3.6 Hz, 1H, N7CH$_2$*CH*), 1.69 – 1.65 (m, 2H, H$_{cyclohexyl}$), 1.62 – 1.59 (m, 2H, H$_{cyclohexyl}$), 1.53 (d, *J* = 11.3 Hz, 2H, H$_{cyclohexyl}$), 1.17 – 1.11 (m, 3H, H$_{cyclohexyl}$), 1.06 – 0.99 (m, 2H, H$_{cyclohexyl}$); **^{13}C NMR** (151 MHz, DMSO-*d*$_6$) δ 153.47, 146.58, 137.66, 107.39, 51.22, 39.92, 37.87, 29.39 (2C), 29.35, 27.50, 25.52, 24.90 (2C); **LC-MS (m/z)**: 311.2 ([M+H]$^+$); **purity** by HPLC-UV (220 – 400 nm)-ESI-MS: 97.5%.

8-Chloro-7-(3-fluorobenzyl)-1,3-dimethyl-3,7-dihydro-1*H*-purine-2,6-dione (FPE-131)

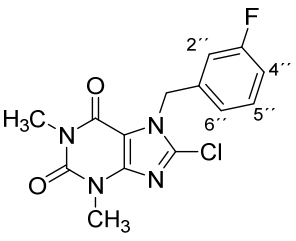

Synthesis according to **GP F**. **Yield:** quantitative; **M.p.:** 150°C; ^{1}H NMR (500 MHz, DMSO-*d*$_6$) δ 7.41 (td, *J* = 7.8, 6.0 Hz, 1H, Ar-H$_{benzyl}$), 7.18 – 7.08 (m, 3H, Ar-H$_{benzyl}$), 5.55 (s, 2H, N7CH$_2$), 3.40 (s, 3H, N3CH$_3$), 3.23 (s, 3H, N1CH$_3$) ^{13}C NMR (126 MHz, DMSO-d$_6$) δ 162.96, 161.01, 153.68, 150.45, 146.66, 137.90 (d, *J$_{C,F}$* = 7.5 Hz), 137.64, 130.67 (d, *J$_{C,F}$*

= 8.4 Hz), 122.99 (d, $J_{C,F}$ = 2.9 Hz), 114.70 (d, $J_{C,F}$ = 20.9 Hz), 113.93 (d, $J_{C,F}$ = 22.2 Hz), 107.13, 47.63, 29.33, 27.45; **LC-MS (m/z)**: 323.1([M+H]$^+$); **purity** by HPLC-UV (220 – 400 nm)-ESI-MS: 99.6%.

8-Chloro-1,3-dimethyl-7-(prop-2-yn-1-yl)-3,7-dihydro-1*H*-purine-2,6-dione (FPE-135)

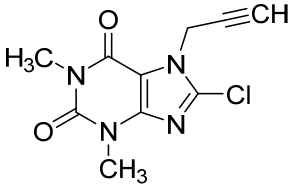

Synthesis according to **GP F** but reaction time was extended to 24h. **Yield:** quantitative; **M.p.:** 160°C; ^{1}H NMR (500 MHz, DMSO-d_6) δ 5.18 (d, J = 2.5 Hz, 2H, N7CH$_2$), 3.53 (t, J = 2.5 Hz, 1H, CH), 3.39 (s, 3H, N3CH$_3$), 3.23 (s, 3H, N1CH$_3$)**; ^{13}C NMR** (126 MHz, DMSO-d$_6$) δ 153.62, 150.57, 146.64, 137.76, 106.67, 76.60, 35.01, 29.51, 27.58; **LC-MS (m/z)**: 253.0 ([M+H]$^+$); **purity** by HPLC-UV (220 – 400 nm)-ESI-MS: 99.8%.

8-Chloro-7-(4-(hydroxymethyl)benzyl)-1,3-dimethyl-3,7-dihydro-1*H*-purine-2,6-dione (FPE-145)

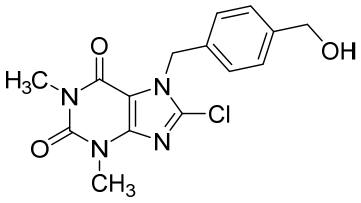

Synthesis according to **GP F**. **Yield**: 326 mg, 0.976 mmol, 94%; **M.p.:** 187°C**; ^{1}H NMR** (500 MHz, DMSO-d_6) δ 7.29 (d, J = 8.3 Hz, 2H, Ar-H$_{benzyl}$), 7.24 (d, J = 8.2 Hz, 2H, Ar-H$_{benzyl}$), 5.51 (s, 2H, N7CH$_2$), 5.14 (t, J = 5.7 Hz, 1H, CH$_2$*OH*), 4.46 (d, J = 5.7 Hz, 2H, *CH$_2$*OH), 3.40 (s, 3H, N3CH$_3$), 3.23 (s, 3H, N1CH$_3$); **^{13}C NMR** (126 MHz, DMSO-d$_6$) δ 153.81, 150.62, 146.79, 142.43, 137.76, 133.70, 127.01 (2C), 126.78 (2C), 107.25, 62.47, 48.25, 29.50, 27.63; **LC-MS (m/z)**: 335.1 ([M+H]$^+$); **purity** by HPLC-UV (220 – 400 nm)-ESI-MS: 99.4%.

8-Chloro-1,3-dimethyl-7-(naphthalen-2-ylmethyl)-3,7-dihydro-1*H*-purine-2,6-dione (FPE-147)

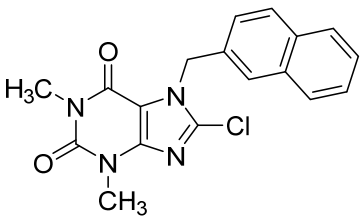

Synthesis according to **GP F**. **Yield**: 343 mg, 0.96 mmol, 94%; **M.p.:** 195°C; **^{1}H NMR** (500 MHz, DMSO-d_6) δ 7.91 (m, 3H, Ar-H$_{naphtyl}$), 7.75 (s, 1H, Ar-H$_{naphtyl}$), 7.52 (dd, J = 6.2, 3.3 Hz, 2H, Ar-H$_{naphtyl}$), 7.44 (d, J = 8.5 Hz, 1H, Ar-H$_{naphtyl}$), 5.71 (s, 2H, N7CH$_2$), 3.42 (s, 3H, N3CH$_3$), 3.24 (s, 3H, N1CH$_3$); ^{13}C NMR (126 MHz, DMSO-d$_6$) δ 153.86, 150.65, 146.83, 137.94, 132.94, 132.69, 132.37, 128.48, 127.77, 127.51,

126.45, 126.30, 125.78, 124.89, 107.43, 48.59, 29.53, 27.64; **LC-MS (m/z)**: 355.1([M+H]$^+$); **purity** by HPLC-UV (220 – 400 nm)-ESI-MS: 90.7%.

***tert*-Butyl 2-(8-chloro-1,3-dimethyl-2,6-dioxo-1,2,3,6-tetrahydro-7*H*-purin-7-yl)-2-(4-chlorophenyl)acetate (FPE-169)**

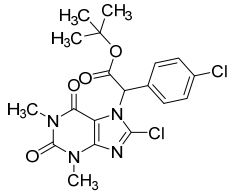

Synthesis according to **GP F**. **Yield**: 150 mg, 0.34 mmol, 35%; **M.p.:** 180°C ; **^{1}H NMR** (500 MHz, DMSO-*d*$_6$) δ 7.49 – 7.42 (m, 4H, Ar-H$_{benzyl}$), 6.97 (s, 1H, *CH*CO), 3.41 (s, 3H, N3CH$_3$), 3.22 (s, 3H, N1CH$_3$), 1.41 (s, 9H, 3xCH$_3$); **^{13}C NMR** (126 MHz, DMSO-d$_6$) δ 164.33, 153.76, 150.50, 146.80, 138.15, 133.26, 132.63, 130.51 (2C), 128.32 (2C), 107.26, 83.55, 61.10, 29.56, 27.71, 27.47 (3C); **LC-MS (m/z)**: 437.1 ([M-H]$^-$); **purity** by HPLC-UV (220 – 400 nm)-ESI-MS: 94.5%.

8-Chloro-7-(4-ethynylbenzyl)-1,3-dimethyl-3,7-dihydro-1H-purine-2,6-dione (FPE-189)

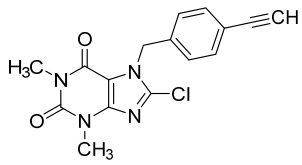

Synthesis according to **GP F**. **Yield**: 350 mg, 1.07 mmol, 95%; **M.p.:** 186°C; **^{1}H NMR** (500 MHz, DMSO-*d*$_6$) δ 7.47 (d, *J* = 8.2 Hz, 2H, Ar-H$_{benzyl}$), 7.28 (d, *J* = 8.2 Hz, 2H, Ar-H$_{benzyl}$), 5.55 (s, 2H, N7CH$_2$), 4.20 (s, 1H,C≡CH), 3.40 (s, 3H, N3CH$_3$), 3.22 (s, 3H, N1CH$_3$); ^{13}C NMR (126 MHz, DMSO-d$_6$) δ 153.79, 150.59, 146.81, 137.82, 136.12, 132.03 (2C), 127.43 (2C), 121.38, 107.27, 82.88, 81.12, 48.07, 29.48, 27.59; **LC-MS (m/z)**: 329.1 ([M+H]$^+$); **purity** by HPLC-UV (220 – 400 nm)-ESI-MS: 96.8%.

3-(8-Chloro-1,3-dimethyl-2,6-dioxo-1,2,3,6-tetrahydro-7*H*-purin-7-yl)propyl acetate (FPE-195)

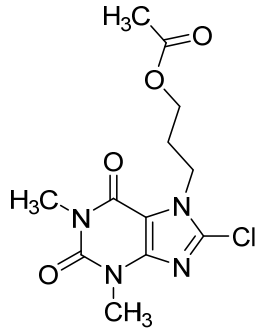

Synthesis according to **GP F**. **Yield**: 70 mg, 0.22 mmol, 96%; **M.p.:** 182°C ; **^{1}H NMR** (600 MHz, DMSO-*d*$_6$) δ 4.35 (t, *J* = 6.7 Hz, 2H, N7CH$_2$), 3.99 (t, *J* = 6.0 Hz, 2H, CH$_2$O), 3.39 (s, 3H, N3CH$_3$), 3.23 (s, 3H, N1CH$_3$), 2.09 (p, *J* = 6.4 Hz, 2H, N7CH$_2$*CH$_2$*), 1.95 (s, 3H, COCH$_3$), **^{13}C NMR** (151 MHz, DMSO-*d*$_6$) δ 170.18, 153.58, 150.64, 146.98, 137.72, 107.28, 60.92, 43.22, 40.06, 29.48, 28.31, 27.64, 20.53; **LC-MS (m/z)**: 315.0 ([M+H]$^+$); **purity** by HPLC-UV (220 – 400 nm)-ESI-MS: 94.3%.

8-Chloro-7-(4-chlorophenethyl)-1,3-dimethyl-3,7-dihydro-1*H*-purine-2,6-dione (FPE-ML13)

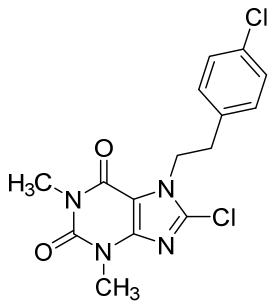

Synthesis according to **GP F**, with reaction time 24h and temperature risen to 50°C. **Yield:** 1.63 g, 4.63 mmol, 99.3 %; **M.p.:** 193°C; **^{1}H NMR** (600 MHz, DMSO-*d*$_6$) δ: 7.32 (d, *J* = 8.0 Hz, 2H, Ar-H$_{benzyl}$), 7.15 (d, *J* = 8.2 Hz, 2H,Ar-H$_{benzyl}$), 4.44 (t, *J* = 6.9 Hz, 2H, N7CH$_2$), 3.38 (s, 3H, N3CH$_3$), 3.25 (s, 3H, N1CH$_3$), 3.05 (t, *J* =6.9 Hz, 2H, N7CH$_2$*CH$_2$*); **^{13}C NMR** (151 MHz, DMSO-*d*$_6$) δ δ. 153.6, 150.7, 146.8 , 137.7, 136.1, 131.5, 130.8 (2C), 128.4 (2C), 107.0, 47.1, 34.8, 29.5, 27.7; **LC-MS (m/z)**: 353.0 ([M+H]$^+$); **purity** by HPLC-UV (220 – 400 nm)-ESI-MS: 92.4%.

8-Chloro-1,3-dimethyl-7-(pyridin-3-ylmethyl)-3,7-dihydro-1*H*-purine-2,6-dione (FPE-ML21)

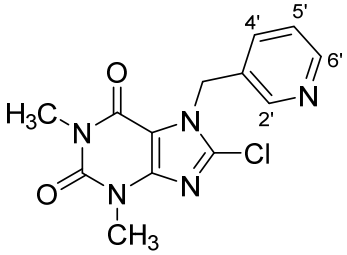

Synthesis according to **GP F**. **Yield**: 150 mg, 0.491 mmol, 21%; **M.p.:** 176°C; **^{1}H NMR** (600 MHz, DMSO-*d*$_6$) δ 8.59 (d, *J* = 2.3 Hz, 1 H, C2′-H), 8.53 (d, *J* = 4.8 Hz, 1 H, C6′-H), 7.70 (t, *J* = 7.9 Hz, 1H, C4′-H), 7.39 (dd, *J* = 7.9 Hz, 4.8 Hz, 1 H, C5′-H), 5.58 (s, 2 H, N7CH$_2$), 3.40 (s, 3H, N3-CH$_3$), 3.32 (s, 3H, N1-CH$_3$). **^{13}C NMR** (151 MHz, DMSO-*d*$_6$) δ 150.7, 149.3, 148.7, 146.9, 137.8, 135.2, 131.2, 123.9, 107.3, 46.2, 29.3, 27.7; **LC-MS (m/z)**: 306.1 ([M+H]$^+$); **purity** by HPLC-UV (220 – 400 nm)-ESI-MS: 95.4%.

8-Chloro-1,3-dimethyl-7-((tetrahydro-2*H*-pyran-4-yl)methyl)-3,7-dihydro-1*H*-purine-2,6-dione (FPE-MP2)

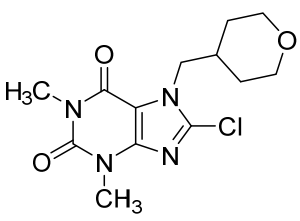

Synthesis according to **GP F**, but pushed to 70°C overnight. **Yield:** 362 mg, 1.16 mmol, 83%**; M.p.:** 201°C; **^{1}H NMR** (500 MHz, DMSO-*d*$_6$) δ 4.15 (d, *J* = 7.4 Hz, 2H, N7CH$_2$), 3.82 (ddd, *J* = 11.5, 4.5, 1.9 Hz, 2H, CH$_{2\ tetrahydropyranyl}$), 3.38 (s, 3H, N3CH$_3$), 3.24 – 3.19 (m, 5H, N1CH$_3$ and CH$_{2tetrahydropyranyl}$), 2.08 (th, *J* = 11.4, 3.7 Hz, 1H, CH$_{tetrahydropyranyl}$), 1.45 – 1.41 (m, 2H, CH$_{2tetrahydropyranyl}$), 1.35 – 1.26 (m, 2H, CH$_{2tetrahydropyranyl}$); **^{13}C NMR** (126 MHz,

DMSO-d_6) δ 153.58, 150.60, 146.69, 137.78, 107.48, 66.31, 50.76, 35.45, 29.48, 29.43, 27.58; ; **LC-MS (m/z)**: 312.1 ([M+H]$^+$); **purity** by HPLC-UV (220 – 400 nm)-ESI-MS: 99.8%.

8-Chloro-1,3-dimethyl-7-((tetrahydrofuran-2-yl)methyl)-3,7-dihydro-1*H*-purine-2,6-dione (FPE-MP13)

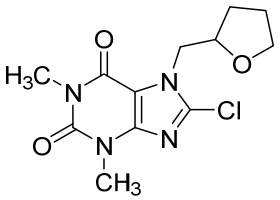

Synthesis according to **GP F**. **Yield**: 157.3 mg, 0.527 mmol, 38 %; **M.p.:** 197°C; **^{1}H NMR** (600 MHz, DMSO-d_6) δ 4.31 (d, J = 10.0 Hz, 1H, $H_{tetrahydrofuranyl}$), 4.25 – 4.18 (m, 2H, N7CH_2), 3.77 (td, J = 7.7, 6.3 Hz, 1H, $H_{tetrahydrofuranyl}$), 3.63 (td, J = 7.8, 6.1 Hz, 1H, $H_{tetrahydrofuranyl}$), 3.39 (s, 3H, N3CH_3), 3.23 (s, 3H, N1CH_3), 1.98 (ddt, J = 12.3, 8.6, 6.3 Hz, 1H), 1.94 – 1.87 (m, 1H, $H_{tetrahydrofuranyl}$), 1.86 – 1.79 (m, 1H, $H_{tetrahydrofuranyl}$), 1.68 (ddt, J = 11.7, 8.3, 5.7 Hz, 1H, $H_{tetrahydrofuranyl}$); **^{13}C NMR** (151 MHz, DMSO-d_6) δ 153.70, 150.64, 146.67, 138.30, 107.24, 76.48, 67.25, 49.36, 40.06, 29.50, 29.49, 28.15, 27.64, 24.92; **LC-MS (m/z)**: 298.0 ([M+H]$^+$); **purity** by HPLC-UV (220 – 400 nm)-ESI-MS: 99.0%.

8-Chloro-7-((1-heptyl-1*H*-1,2,3-triazol-4-yl)methyl)-1,3-dimethyl-3,7-dihydro-1*H*-purine-2,6-dione (FPE-194)

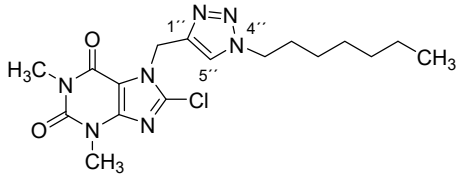

FPE-135 (0.139 g, 0.55 mmol, 1.1 eq), 1-bromoheptane (0.078 mL, 0.5 mmol, 1 eq), NaN_3 (0.035 g, 0.55 g, 1.1 eq), were suspended in 2 ml of a water and *tert*butyl alcohol mixture (1:1). Sodium ascorbate (0.1 mmol, 100 µL of a freshly prepared 1M solution in water) was then added, followed by Cu (0) powder (25 mg). The mixture was stirred under microwave irradiation at 125°C and 100 W for 20 minutes. When no further improvement was detected, it was diluted with 10 mL of ice-cold water and the obtained solid was filtered and further washed with water, 5 mL of HCl 0.25 N and finally with Et_2O. It was further purified with preparative TLC (EtOAc : cyclohexane 2:8). **Yield:** 27 mg, 0.068 mmol, 13%; **M.p.:** 160°C; **^{1}H NMR** (600 MHz, DMSO-d_6) δ 8.09 (s, 1H, C5′′-H), 5.57 (s, 2H, N7CH_2), 4.30 (t, J = 7.1 Hz, 2H, N4′′-CH_2), 3.39 (s, 3H, N3CH_3), 3.23 (s, 3H, N1CH_3), 1.76 (p, J = 7.2 Hz, 2H, $CH_{2\text{-pentyl}}$), 1.27 – 1.11 (m, 8H, 4 x $CH_{2\text{-pentyl}}$), 0.83 (t, J = 7.0 Hz, 3H, CH_2*CH_3*); **^{13}C NMR** (151 MHz, DMSO-d_6) δ 153.66, 150.62, 146.69, 141.19 (C1′′), 137.92, 123.51(C5′′), 107.05, 49.37,

40.91, 31.00, 29.56, 29.50, 27.90, 27.61, 25.65, 21.87, 13.82; **LC-MS (m/z)**: 394.2 ([M+H]$^+$); **purity** by HPLC-UV (220 – 400 nm)-ESI-MS: 78.1%.

8-Chloro-1,3-dimethyl-7-tosyl-3,7-dihydro-1*H*-purine-2,6-dione (FPE-87)

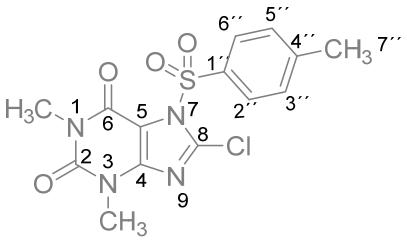

8-Chlorotheopylline (0.5 g, 2.33 mmol, 1 eq) and tosylchloride (0.578 g, 3.03 mmol, 1.3 eq) were dissolved in MeCN (10 ml). Et_3N (0.65 ml, 4.66 mmol, 2 eq) was then added dropwise. The mixture was stirred at reflux for 4h. After completion, solvent was removed under *vacuum* and the crude was partitioned between water and DCM. Organic layers were combined, dried over $MgSO_4$ and concentrated under *vacuum*. Purification with flash column chromatography on silica gel (EtOAc in DCM 3 to 10%) followed by recrystallization in MeOH. **Yield:** 142 mg, 0.39 mmol, 17%; **M.p**.: decomposed at 235°C; **^{1}H NMR (**600MHz**,** DMSO-*d*$_6$**)** δ 7.48 (d, *J* = 8.07 Hz, 2H, Ar-H$_{benzyl}$), 7.12 (d, *J* = 7.84 Hz, 2H, Ar-H$_{benzyl}$), 3.38 (s, 3H, N3CH$_3$), 3.22 (s, 3H, N1CH$_3$), 2.29 (s, 3H, CH$_3$); **^{13}C NMR** (151 MHz, DMSO-*d*$_6$) δ 153.39 (C6), 150.71 (C2), 146.96 (C4), 145.30 (C8), 137.61 (1C, C$_{Ar}$), 136.19 (1C, C$_{Ar}$), 127.93 (2C, CH$_{Ar}$), 125.34 (2C, CH$_{Ar}$), 107.73 (C5), 29.68 (1C, CH$_3$), 27.61 (1C, CH$_3$), 20.62 (C7′′); **LC-MS (m/z)**: 368.9 ([M+H]$^+$); **purity** by HPLC-UV (220 – 400 nm)-ESI-MS: 90.6%.

5.2.2.5 Synthesis of 8-((2-(1H-indol-3-yl)ethyl)amino)-7-alkyl/arylalkyl-1,3-dimethyl-3,7-dihydro-1H-purine-2,6-diones

8-((2-(1*H*-Indol-3-yl)ethyl)amino)-1,3-dimethyl-3,7-dihydro-1*H*-purine-2,6-dione (FPE-179)

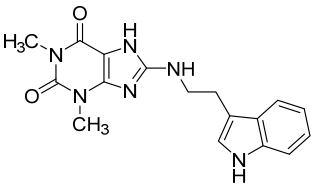

Synthesis according to **GPI** starting from **FPE-57** (**Yield**: 23 mg, 0.065 mmol, 7 %) or **GP H** (**Yield:** 200 mg, 0.59 mmol, 63% with **GP H**; **M.p.:** 295°C; **^{1}H NMR** (600 MHz, DMSO-*d*$_6$) δ 11.40 (s, 1H, N7H), 10.81 (s, 1H, NH$_{indole}$), 7.59 (dd, *J* = 7.8, 1.1 Hz, 1H, Ar-H), 7.34 (d, *J* = 8.2 Hz, 1H, Ar-H), 7.17 (d, *J* = 2.3 Hz, 1H, Ar-H), 7.11 (t, *J* = 5.9 Hz, 1H, *NH*CH$_2$), 7.07 (ddd, *J* = 8.2, 6.9, 1.2 Hz, 1H, Ar-H), 6.98 (ddd, *J* = 7.9, 6.9, 1.0 Hz, 1H, Ar-H), 3.55 – 3.48 (m, 2H, NH*CH$_2$*CH$_2$), 3.37 (s, 3H, N3CH$_3$), 3.19 (s, 3H, N1CH$_3$), 2.94 (t, *J* = 7.5 Hz, 2H, NHCH$_2$*CH$_2$*); **^{13}C NMR** (151 MHz, DMSO-*d*$_6$) δ 154.71, 152.25, 151.22, 149.44, 136.18, 127.20, 122.78, 120.88, 118.33, 118.17, 111.49, 111.31, 101.24, 42.92, 29.48, 27.38, 25.20; **LC-MS (m/z)**: 339.2

([M+H]$^+$); **purity** by HPLC-UV (220 – 400 nm)-ESI-MS: 97.6%; **HRMS (ESI, m/z)** calcd for $C_{17}H_{18}N_6O_2$ [M + H]$^+$, 339.1564; found, 339.1561.

8-(((2-(1*H*-Indol-3-yl)ethyl)amino)methyl)-7-(4-methoxybenzyl)-1,3-dimethyl-3,7-dihydro-1*H*-purine-2,6-dione (FPE-9)

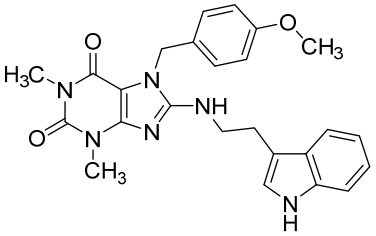

Synthesis according to **GP G**. Purification achieved via recrystallization in cold MeOH. **Yield:** 667 mg, 1.45 mmol, 81%. **M.p.:** 159°C; **^{1}H NMR** (300 MHz, DMSO-*d*$_6$) δ 10.78 (s, 1H, NH_{indole}), 7.63 (d, *J* = 7.6 Hz, 1H, Ar-H), 7.30 - 7.38 (m, 2H, Ar-H_{benzyl} and *NH*CH_2), 7.20 (t, *J* = 7.9 Hz, 1H, Ar-H), 7.10 (d, *J* = 2.3 Hz, 1H, Ar-H), 7.05 (td, *J* = 7.6, 1.2 Hz, 1H, Ar-H), 6.93 - 7.00 (m, 1H, Ar-H), 6.78 - 6.84 m, 2H, Ar-H_{benzyl}), 6.73 (d, *J* = 7.6 Hz, 1H, Ar-H), 5.24 (s, 2H, N7CH_2), 3.68 (s, 3H, -OCH_3), 3.55 - 3.63 (m, 2H, NH*CH*$_2$$CH_2$), 3.39 (s, 3H, N3$CH_3$), 3.15 (s, 3H, N1$CH_3$), 2.96 (t, *J* = 7.6 Hz, 2H, $NHCH_2$*CH*$_2$); ^{13}C NMR (DMSO-*d*$_6$) δ ppm: 159.7, 154.3, 153.2, 151.5, 149.4, 139.0, 136.7, 130.1, 127.7, 123.3, 121.4, 119.5, 118.8, 118.7, 113.6, 112.9, 112.0, 111.8, 101.7, 55.4, 45.6, 43.8, 29.7, 27.7, 25.9; **LC-MS (m/z)**: 334.9 ([M+H]$^+$); **purity** by HPLC-UV (220 – 400 nm)-ESI-MS: 97.7%.

8-(((2-(1*H*-Indol-3-yl)ethyl)amino)methyl)-7-(4-hydroxybenzyl)-1,3-dimethyl-3,7-dihydro-1*H*-purine-2,6-dione (FPE-13)

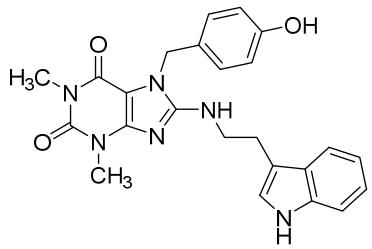

Synthesis according to **GP I.** Purification by flash column chromatography on silica gel (MeOH in DCM 3 to 5%).**Yield:** 36 mg, 0.08 mmol, 37%**; M.p.:** 120°C; **^{1}H NMR** (600 MHz, DMSO-*d*$_6$) δ 10.80 (s, 1H, NH_{indole}), 9.33 (s, 1H, -OH), 7.65 (d, *J* = 7.86 Hz, 1H, Ar-H), 7.34 (d, *J* = 8.08 Hz, 1H, Ar-H_{benzyl}), 7.28 (t, *J* = 5.71 Hz, 1H, *NH*CH_2), 7.13 (d, *J* = 2.21 Hz, 1H, Ar-H), 7.10 – 7.05 (m, 3H, Ar-H), 6.99 (t, *J* = 1.05, 6.93, 7.90 Hz, 1H, Ar-H), 6.67 (d, *J* = 8.53 Hz, 2H, Ar-H), 5.15 (s, 2H, N7CH_2), 3.62 – 3.58 (m, 2H, NH*CH*$_2$$CH_2$), 3.39 (s, 3H, N3$CH_3$), 3.18 (s, 3H, N1$CH_3$), 2.98 (t, *J* = 7.53 Hz, 2H, $NHCH_2$*CH*$_2$); **^{13}C NMR** (151 MHz, DMSO-*d*$_6$) δ 156.91, 153.84, 152.95, 151.17 , 149.07, 136.45, 128.93 (2C), 127.48, 127.44, 123.00, 121.10, 118.52, 118. 40, 115.33 (2C), 111.71, 111.56, 101.36, 44.97, 43.52, 29.45, 27.41, 25.64; **LC-MS (m/z)**: 445.1 ([M+H]$^+$); **purity** by HPLC-UV (220 –

400 nm)-ESI-MS: 95.6%; **HRMS (ESI, m/z)** calcd for $C_{24}H_{24}N_6O_3$ $[M + Na]^+$, 467.1802; found, 467.1786.

4-((8-((2-(1*H*-Indol-3-yl)ethyl)amino)-1,3-dimethyl-2,6-dioxo-1,2,3,6-tetrahydro-7*H*-purin-7-yl)methyl)-*N*-propylbenzenesulfonamide (FPE-15)

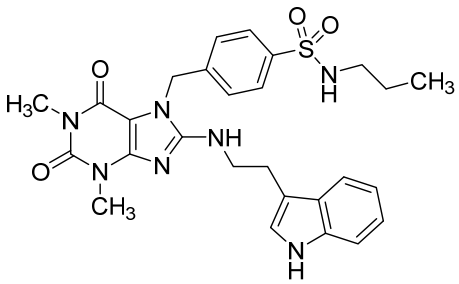

Synthesis according to **GP G**. Purification by flash column chromatography on silica (MeOH in DCM 0 to 2%) followed by recrystallization in cold MeOH. **Yield**: 52 mg, 0.09 mmol, 38%; **M.p.** 240°C; **^{1}H-NMR** (600 MHz, DMSO-d_6) δ 10.82 (s, 1H, NH_{indole}), 7.72 (d, J = 8.29 Hz, 2H, Ar-H_{benzyl}), 7.63 (d, J = 7.86 Hz, 1H Ar-H), 7.53 (t, J = 5.06 Hz, 1H, SO_2NH), 7.40 (t, J = 5.66 Hz, 1H, *NH*CH_2), 7.34 (d, J = 8.28 Hz, 2H, Ar-H_{benzyl}), 7.13 (d, J = 2.36 Hz, 1H, Ar-H), 7.06 (t, J = 7.58 Hz, 1H, Ar-H), 6.98 (t, J = 7.44 Hz, 1H, Ar-H), 5.37 (s, 2H, N7-CH_2), 3.61 (dt, J = 6.19, 8.23 Hz, 2H, NH*CH*$_2$$CH_2$), 3.42 (s, 3H, N3-$CH_3$), 3.16 (s, 3H, N1-$CH_3$), 2.98 (t, J = 7.52 Hz, 2H, NHCH$_2$*CH*$_2$), 2.66 (q, J = 6.36 Hz, 2H, *CH*$_2$$CH_2CH_3$), 1.36 (h, J = 7.31 Hz, 2H, CH_2*CH*$_2$$CH_3$), 0.78 (t, J = 7.36 Hz, 3H, CH_2CH_2*CH*$_3$).**^{13}C NMR** (151 MHz, DMSO-d_6) δ 154.01, 152.92, 151.17, 149.15, 141.70, 139.79, 136.42, 127.55 (2C), 127.43, 126.86 (2C), 122.97, 121.07, 118.47, 118.38, 111.68, 111.52, 101.39, 45.20, 44.49, 43.51, 29.47, 27.35, 25.52, 22.60, 11.26; **LC-MS (m/z)**: 550.5 ($[M+H]^+$); **purity** by HPLC-UV (220 – 400 nm)-ESI-MS: 97.6%; **HRMS (ESI, m/z)** calcd for $C_{27}H_{31}N_7O_4S$ $[M + Na]^+$, 572.2050; found, 572.1957.

8-((2-(1*H*-Indol-3-yl)ethyl)amino)-7-(2-fluoroethyl)-1,3-dimethyl-3,7-dihydro-1*H*-purine-2,6-dione (FPE-22)

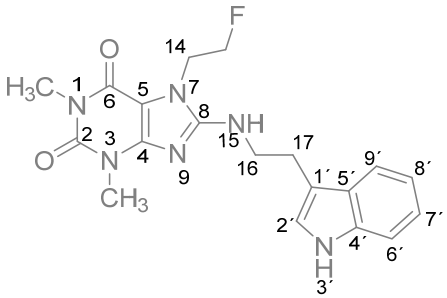

Synthesis according to **GP G**. Purification with flash column chromatography on silica (MeOH in DCM 0 to 5%). **Yield:** 8.2 mg, 0.021 mmol, 56%; **M.p.**: decomposition at 230°C**; ^{1}H NMR** (600 MHz, DMSO-d_6) δ 10.81 (d, J = 2.41 Hz, 1H, NH_{indole}), 7.64 (d, J = 7.84 Hz, 1H, Ar-H), 7.35 – 7.29 (m, 2H, Ar-H and *NH*CH_2), 7.16 (d, J = 2.39 Hz, 1H, Ar-H), 7.06 (t, J = 7.51 Hz, 1H, Ar-H), 6.98 (t, J = 7.41 Hz, 1H, Ar-H), 4.63 (dt, $J_{H,H}$ = 5.02, $J_{H,F}$ =47.2 Hz, 2H, -CH_2-F), 4.36 (dt, $J_{H,H}$ = 5.05, $J_{H,F}$ = 24.47 Hz, 2H, N7-CH_2)*, 3.61 – 3.56 (m, 2H, NH*CH*$_2$$CH_2$),

3.40 (s, 3H, N3-CH_3), 3.30 (s, 3H, N1-CH_3), 2.99 (t, J = 7.54 Hz, 2H, $NHCH_2CH_2$); **^{13}C NMR** (151 MHz, DMSO-d_6) δ 154.20, 151.15, 149.04, 136.38, 127.43, 122.91, 121.03, 118.44, 118.34, 111.73, 111.51, 101.49, 81.86 (d, $J_{C,F}$ = 168.2 Hz), 42.93 (d, $J_{C,F}$ = 20.8 Hz), 29.40, 27.35, 25.49; **LC-MS (m/z)**: 385.1 ($[M+H]^+$); **purity** by HPLC-UV (220 – 400 nm)-ESI-MS: 98.5%; **HRMS (ESI, m/z)** calcd for $C_{19}H_{21}FN_6O_2$ $[M + Na]^+$, 407.1602; found, 407.1554.

8-Chloro-7-(4-(2-fluoroethoxy)benzyl)-1,3-dimethyl-3,7-dihydro-1*H*-purine-2,6-dione (FPE-23)

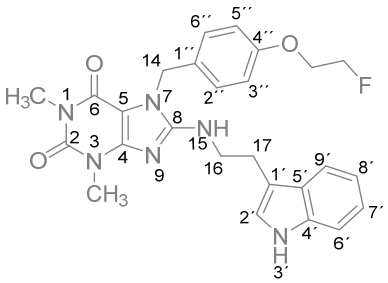

Synthesis according to **GPI.** Purification was achieved with preparative TLC (3% MeOH in DCM). **Yield:** 5 mg, 0.010 mmol, 93%; **M.p**: decomposed at 230°C; **^{1}H NMR** (600 MHz, DMSO-d_6) δ 10.82 (s, 1H, -NH_{indole}), 7.64 (d, J = 7.87 Hz, 1H, Ar-H), 7.37 – 7.32 (m, 2H, Ar-H and $NHCH_2$); 7.19 (d, J = 8.31 Hz, 2H, Ar-H_{benzyl}), 7.14 – 7.12 (m, 1H, Ar-H), 7.07 (t, J = 7.50 Hz, Ar-H), 6.98 (t, J = 7.42 Hz, 1H, Ar-H), 6.87 (d, J = 8.29 Hz, 2H, Ar-H_{benzyl}), 5.20 (s, 2H, -N7-CH_2), 4.71 (dt, $J_{H,H}$ = 3.48, $J_{H,F}$ = 47.85 Hz, 2H, -CH_2-F), 4.18 (dt, $J_{H,H}$ = 3.73, $J_{H,F}$ = 30.14 Hz, 2H, -O-CH_2-), 3.64 – 3.58 (m, 2H, -NHCH_2CH_2), 3.39 (s, 3H, N3-CH_3), 3.17 (s, 3H, N1-CH_3), 2.99 (t, J = 7.41 Hz, 2H, -$NHCH_2CH_2$); **^{13}C NMR** (151 MHz, DMSO-d_6) δ 157.47 (C4''), 153.68 (C6), 152.76 (C8), 150.98 (C2), 148.92 (C4), 136.27 (C4'), 129.62 (C1''), 128.97 (2C, C2'' and C6''), 127.26 (C5'), 122.84 (C2'), 120.87 (C7'), 118.32 (C9'), 118.19 (C8'), 114.41 (2C, C3'' and C5''), 111.50 (C6'), 111.34 (C1'), 101.12 (C5), 81.95 (d, $J_{C,F}$ = 166.4 Hz, 1C, CH_2-F), 43.82 (d, $J_{C,F}$ = 215.0 Hz, 1C,-O-CH_2-), 44.67 (C14), 43.24 (C17), 29.25(1C, CH_3), 27.19(1C, CH_3), 25.35 (C16); **LC-MS (m/z)**: 491.4 ($[M+H]^+$); **purity** by HPLC-UV (220 – 400 nm)-ESI-MS: ≥90%; **HRMS (ESI, m/z)** calcd for $C_{26}H_{27}FN_6O_3$ $[M + Na]^+$ 513.2021; found, 513.1983.

Methyl 4-((8-((2-(1*H*-indol-3-yl)ethyl)amino)-1,3-dimethyl-2,6-dioxo-1,2,3,6-tetrahydro-7*H*-purin-7-yl)methyl)benzoate (FPE-27)

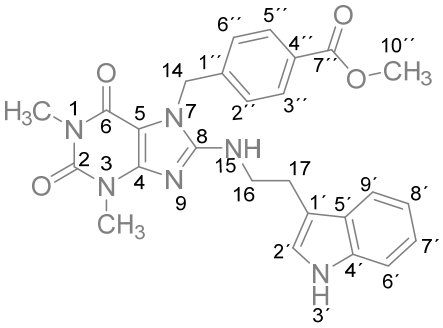

Synthesis according to **GP G**. Purification with flash column chromatography on silica gel (MeOH in DCM 0 to 5%). **Yield:** 448 mg, 0.92 mmol, 37%; **M.p.:** 208°C; **^{1}H NMR (**500 MHz**,** DMSO-*d*$_6$**)** δ 10.78 (s, 1H, NH$_{indole}$), 7.88 (d, *J* = 8.31 Hz, 2H, Ar-H$_{benzyl}$), 7.62 (dd, *J* = 1.05, 7.96 Hz, 1H, Ar-H), 7.38 – 7.31 (m, 2H, *NH*CH$_2$ and Ar-H), 7.27 (d, *J* = 8.30 Hz, 2H, Ar-H$_{benzyl}$), 7.11 (d, *J* = 2.31 Hz, 1H, Ar-H), 7.06 (ddd, *J* = 1.18, 6.96, 8.15 Hz, 1H, Ar-H), 6.97 (ddd, *J* = 1.00, 6.93, 7.90 Hz, 1H, Ar-H), 5.36 (s, 2H, N7CH$_2$), 3.83 (s, 3H, -OCH$_3$), 3.61 (dt, *J* = 6.13, 7.98 Hz, 2H, NH*CH$_2$*CH$_2$), 3.41 (s, 3H, N3CH$_3$), 3.15 (s, 3H, N1CH$_3$), 2.98 (dd, *J* = 6.53, 8.33 Hz, 2H, NHCH$_2$*CH$_2$*); **^{13}C NMR** (126 MHz, DMSO-*d*$_6$**)**: δ 165.97 (C7''), 153.87 (C6), 152.73 (C8), 151.00 (C2), 148.96 (C4), 142.51 (C1''), 136.26 (C4'), 129.37 (2C, C2'' and C6''), 128.64 (1C, C$_{Ar}$), 127.27 (1C, C$_{Ar}$), 127.01 (2C, C3'' and C5''), 122.77 (C2'), 120.88 (C7'), 118.28 (C9'), 118.19 (C8'), 111.50 (C6'), 111.35 (C5'), 101.23 (C1'), 52.07 (C10''), 45.18 (C14), 43.29 (C16), 29.28 (1C, -CH$_3$), 27.15 (1C, -CH$_3$), 25.33 (C17); **LC-MS (m/z)**: 487.1 ([M+H]$^+$); **purity** by HPLC-UV (220 – 400 nm)-ESI-MS: 98.2%.

4-((8-((2-(1*H*-Indol-3-yl)ethyl)amino)-1,3-dimethyl-2,6-dioxo-1,2,3,6-tetrahydro-7*H*-purin-7-yl)methyl)benzoic acid (FPE-29)

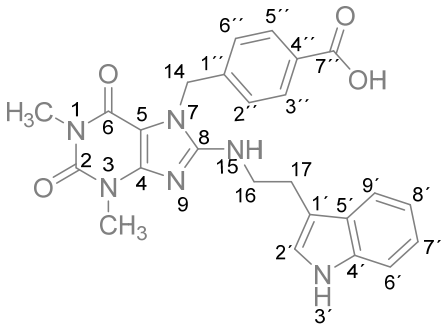

In a 50 mL round-bottomed flask, **FPE-27** (33 mg, 0.68 mmol, 1 eq) was dissolved in 4 mL of THF, then 50% aqueous solution of LiOH · H$_2$O (0.12 g, 2.72 mmol, 4 eq) was added dropwise. The mixture was kept stirring overnight at RT. When no improvement was detected, water was added and the pH adjusted to 1-2 with HCl 1N, achieving precipitation. The precipitate was filtered under reduced pressure and washed with Et$_2$O to give the wanted compoud. **Yield**: 219 mg, 0.46 mmol, 68%; **M.p.:** 195°C**; ^{1}H NMR** (500 MHz, DMSO-*d*$_6$) δ 10.79 (s, 1H, NH$_{indole}$), 7.86 (d, *J* = 8.23 Hz, 2H, Ar-H$_{benzyl}$), 7.63 (d, *J* = 7.87 Hz, 1H, Ar-H), 7.36 (t, *J* = 5.71 Hz, 1H, *NH*CH$_2$), 7.33 (d, *J* = 8.11 Hz, 1H, Ar-H), 7.24 (d, *J* = 8.29 Hz, 2H, Ar-H$_{benzyl}$), 7.11 (d, *J* = 2.31 Hz, 1H, Ar-H), 7.06

(ddd, *J* = 1.19, 6.95, 8.13 Hz, 1H, Ar-H), 6.97 (ddd, *J* = 0.94, 0.94, 1.02, 5.82, 5.96 Hz, 1H, Ar-H), 5.35 (s, 2H, N7CH_2), 3.60 (dt, *J* = 5.95, 7.98 Hz, 2H, NH*CH_2*CH_2), 3.41 (s, 3H, N3CH_3), 3.15 (s, 3H, N1CH_3), 2.98 (t, *J* = 7.46 Hz, 2H, NHCH$_2$*CH_2*); **^{13}C NMR** (126 MHz, DMSO-d$_6$) δ 166.85 (C7''), 153.54 (C6), 152.41 (C8), 150.68 (C2), 148.62 (C4), 141.28 (C1''), 135.93 (C4'), 129.15 (2C, C3'' and C5''), 126.93 (C4''), 126.43 (2C, C2'' and C46'), 122.46 (C2'), 120.55 (C7'), 117.96 (C9'), 117.86 (C8'), 111.18 (C6'), 111.03 (C1'), 100.93 (C5), 44.86 (C14), 43.00 (C16), 28.96 (1C, -CH_3), 26.84 (1C, CH_3), 25.02 (C17); **LC-MS (m/z)**: 487.1 ([M+H]$^+$); **purity** by HPLC-UV (220 – 400 nm)-ESI-MS: 98.2%.

8-((2-(1*H*-Indol-3-yl)ethyl)amino)-1,3-dimethyl-7-(pyridin-4-ylmethyl)-3,7-dihydro-1H-purine-2,6-dione (FPE-30)

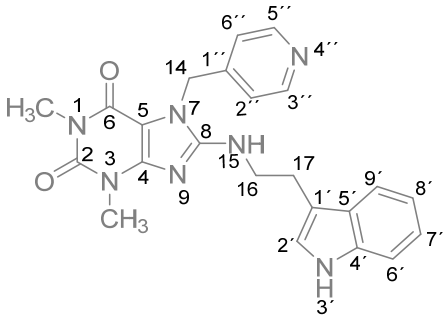

Synthesis according to **GP G**. Purification with flash column chromatography on silica gel (MeOH in DCM 0 to 5%). **Yield:** 35.2 mg, 0.08 mmol, 28%; **M.p.:** 217°C; **^{1}H NMR** (600 MHz, DMSO-*d*$_6$) δ 10.79 (s, 1H, NH$_{indole}$), 8.47 (d, *J* = 4.76 Hz, 2H, Ar-H$_{benzyl}$), 7.63 (d, *J* = 7.84 Hz, 1H, Ar-H), 7.39 (t, *J* = 5.64 Hz, 1H, *NH*CH$_2$), 7.34 (d, *J* = 8.08 Hz, 1H, Ar-H), 7.10 (d, *J* = 2.36 Hz, 1H, Ar-H) , 7.09 – 7.04 (m, 3H, Ar-H$_{benzyl}$ and Ar-H), 6.97 (t, *J* = 7.45 Hz, 1H, Ar-H), 5.32 (s, 2H, N7CH_2), 3.61 (q, *J* = 6.96 Hz, 2H, NH*CH_2*CH_2), 3.42 (s, 3H, N3CH_3), 3.15 (s, 3H, N1CH_3), 2.99 (t, *J* = 7.36 Hz, 2H, NHCH$_2$*CH_2*). **^{13}C NMR** (151 MHz, DMSO-*d*$_6$) δ 154.08 (C6) , 152.90 (C8), 151.17 (C2), 149.90 (2C,C3'' and C5''), 149.15 (C4), 146.14 (C1''), 136.43 (C4'), 127.43 (C5'), 123.02 (1C,r), 121.80 (2C, C2'' and C6'') 121.06(C7'), 118.47 (C9'), 118.37(C8'), 111.65 (C6'), 111.53(C1'), 101.36(C5), 44.69 (C14), 43.42 (C16), 29.48 (1C, CH_3), 27.31 (1C, CH_3), 25.43 (C17); **LC-MS (m/z)**: 430.0 ([M+H]$^+$); **purity** by HPLC-UV (220 – 400 nm)-ESI-MS: 96.4%; **HRMS (ESI, m/z)** calcd for $C_{23}H_{23}N_7O_2$ [M + Na]$^+$, 452.1805; found, 452.1755.

-((8-((2-(1*H*-Indol-3-yl)ethyl)amino)-1,3-dimethyl-2,6-dioxo-1,2,3,6-tetrahydro-7*H*-purin-7-yl)methyl)-*N*-propylbenzamide (FPE-31)

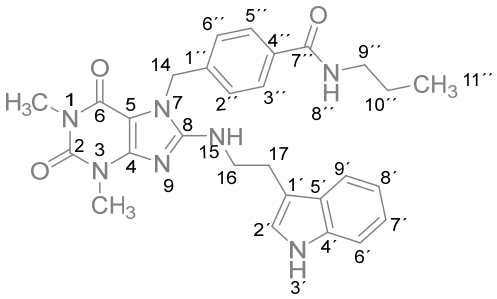

FPE-29 (0.2 g, 0.42 mmol, 1.1 eq) and T3P (50% solution *wt* in DCM, 266 mg, 0.42 mmol, 1.1 eq) were dissolved in 1 mL of DCM and the solution is stirred at 0°C. Afterwards a solution of propylamine (0.03 mL, 0.378 mmol, 1 eq) and Et_3N (0.1 mL, 0.76 mmol, 2 eq) in DCM (1 mL) was added dropwise. The reaction mixture was kept stirring overnight at RT. Afterwards, an extraction was performed with EtOAc and a saturated aqueous solution of $NaHCO_3$. The organic phase was dried over $MgSO_4$ and concentrated under *vacuum*. Purification with flash column chromatography on silica gel (MeOH in DCM 0 to 5%) **Yield:** 10 mg, 0.019 mmol, 5%**; M.p.:** 263°C; **^{1}H NMR** (600 MHz, DMSO-d_6) δ 10.80 (s, 1H, NH_{indole}), 8.35 (t, J = 5.72 Hz, 1H, CONH), 7.75 (d, J = 8.25 Hz, 2H, Ar-H_{benzyl}), 7.64 (d, J = 7.83 Hz, 1H, Ar-H), 7.40 (t, J = 5.70 Hz, 1H, *NH*CH_2), 7.34 (d, J = 8.06 Hz, 1H, Ar-H), 7.24 (d, J = 8.01 Hz, 2H, Ar-H_{benzyl}), 7.13 – 7.11 (m, 1H, Ar-H), 7.06 (t, J = 6.94 Hz, 1H, Ar-H), 6.98 (t, J = 7.38 Hz, 1H, Ar-H), 5.33 (s, 2H, N7CH_2), 3.64 – 3.57 (m, 2H, NH*CH_2*CH_2), 3.41 (s, 3H, N3CH_3), 3.20 (q, J = 6.86 Hz, 2H, , *CH_2*CH_2CH_3), 3.16 (s, 3H, N1CH_3), 2.98 (t, J = 7.54 Hz, 2H, NHCH$_2$*CH_2*), 1.51 (dt, J = 7.31 Hz, 2H, CH_2*CH_2*CH_3), 0.87 (t, J = 7.38 Hz, 3H, CH_2CH_2*CH_3*); **^{13}C NMR** (151 MHz, DMSO-*d_6*) δ 165.89 (C7’’), 153.84 (C6) , 152.73 (C8), 150.99 (C2), 148.96 (C4), 139.96 (C1’’), 136.25 (C4’), 133.92 (C4’’), 127.31 (2C, C2’’ and C6’’), 127.24 (C5’), 126.68 (2C, C3’’ and C5’’), 122.79 (C2’), 120.88 (C7’), 118.29 (C9’), 118.19(C8’), 111.49 (C6’), 111.35 (C1’), 101.21 (C5), 45.11 (C14), 43.33 (1C, C16), 40.90 (C9’’), 29.28 (1C, CH_3), 27.16 (1C, CH_3), 25.40 (C17), 22.35 (C10’’), 11.39 (C11’’); **LC-MS (m/z)**: 514.2. ($[M+H]^+$); **purity** by HPLC-UV (220 – 400 nm)-ESI-MS: 93.8%; **HRMS (ESI, m/z)** calcd for $C_{28}H_{31}N_7O_3$ $[M + Na]^+$, 536.2381; found, 536.3360.

8-((2-(1*H*-Indol-3-yl)ethyl)amino)-7-((6-chloropyridin-3-yl)methyl)-1,3-dimethyl-3,7-dihydro-1*H*-purine-2,6-dione (FPE-33)

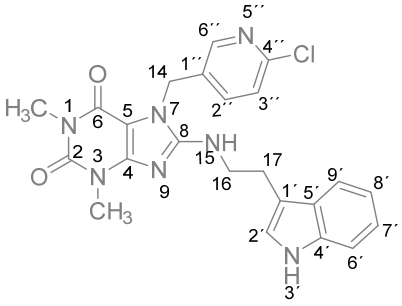

Synthesis according to **GP G**. Purification with flash column chromatography on silica gel (MeOH in DCM 0 to 3%). **Yield:** 28 mg, 0.06 mmol, 33%; **M.p.**: 244°C **^{1}H NMR** (600 MHz, DMSO-d_6) δ 10.80 (s, 1H, , NH_{indole}), 8.36 (d, J = 2.47 Hz, 1H, C6′′-H), 7.62 (d, J = 7.83 Hz, 1H, Ar-H), 7.58 (dd, J = 2.52, 8.34 Hz, 1H, C2’’-H), 7.47 (t, J = 5.65 Hz, 1H, *NH*CH_2), 7.42 (d, J = 8.26 Hz, 1H, C3’’-H), 7.34 (d, J = 8.09 Hz, Ar-H), 7.14 – 7.12 (m, 1H, Ar-H), 7.06 (t, J = 6.91 Hz, 1H, Ar-H), 6.97 (t, J = 6.88 Hz, 1H, Ar-H), 5.30 (s, 2H, N7CH_2), 3.65 – 3.58 (m, 1H, NH*CH_2*CH_2), 3.39 (s, 3H, N3CH_3), 3.17 (s, 3H, N1CH_3), 2.99 (t, J = 7.46 Hz, 2H, NHCH$_2$*CH_2*); **^{13}C NMR** (151 MHz, DMSO-d_6) δ 153.84 (C6), 153.00 (C8), 151.14(C2), 149.53 (CH_{Ar}), 149.28 (CH_{Ar}), 149.07(C4), 138.79 (1C, l), 136.44 (C4’), 132.49 (C1’’), 127.42 (C5’), 124.37 (C3’’), 122.98 (C2’), 121.07(C7’), 118.46(C9’), 118.38(1C, C8’), 111.67(C6’), 111.54 (C1’), 101.15(C5), 43.49 (C14), 42.63(C16), 29.46(1C, CH_3), 27.37(1C, CH_3), 25.49 (C17); **LC-MS (m/z)**: 464.0 ([M+H]$^+$); **purity** by HPLC-UV (220 – 400 nm)-ESI-MS: 94.8%; **HRMS (ESI, m/z)** calcd for $C_{46}H_{44}Cl_2N_{14}O_4$ [2M + Na]$^+$, 949.2939; found, 949.2859.

8-((2-(1*H*-Indol-3-yl)ethyl)amino)-7-((5-chloropyridin-2-yl)methyl)-1,3-dimethyl-3,7-dihydro-1*H*-purine-2,6-dione (FPE-35)

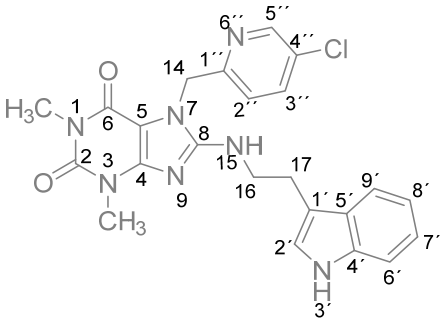

Synthesis according to **GP G**. Purification with flash column chromatography (MeOH in DCM 0% to 3%). **Yield:** 15.4 mg, 0.03 mmol, 51%; **M.p.:** 207°C; **^{1}H NMR** (600 MHz, DMSO-d_6) δ 10.79 (s, 1H, NH_{indole}), 8.51 (d, J = 2.52 Hz, 1H, C5’’-H), 7.85 (dd, J = 2.57, 8.44 Hz, 1H, C3’’-H), 7.62 (d, J = 7.88 Hz, 1H, Ar-H), 7.33 (d, J = 8.09 Hz, 1H, Ar-H), 7.29 (t, J = 5.65 Hz, 1H, *NH*CH_2), 7.13 (d, J = 2.23 Hz, 1H, Ar-H), 7.09 (d, J = 8.46 Hz, 1H, C2’’-H), 7.06 (t, J = 8.02 Hz, 1H, Ar-H), 6.97 (t, J = 7.01 Hz, 1H, Ar-H), 5.37 (s, 2H, N7CH_2), 3.59 (dd, J = 6.63, 13.78 Hz, 1H, NH*CH_2*CH_2), 3.42 (s, 3H, N3CH_3), 3.13 (s, 3H, N1CH_3), 2.97 (t, J = 7.42 Hz, 2H, NHCH$_2$*CH_2*); **^{13}C NMR** (151 MHz, DMSO-d_6) δ 155.11 (C1’), 154.43 (C6), 152.86(C8), 151.15 (C2), 149.01(C4), 147.79 (C5’’), 136.91 (C3’’),

136.39 (C4'), 129.89 (C4''), 127.43 (C5'), 123.01 (C2'), 122.28 (C2''), 121.03 (C7'), 118.45 (C9'), 118.34 (C8'), 111.67(C6'), 111.50 (C5'), 101.56 (C5), 46.80 (C14), 43.46 (C16), 29.46 (1C, CH_3), 27.26 (1C, CH_3), 25.40 (C17); **LC-MS (m/z)**: 464.0 ($[M+H]^+$); **purity** by HPLC-UV (220 – 400 nm)-ESI-MS: 98.4%; **HRMS (ESI, m/z)** calcd for $C_{23}H_{22}ClN_7O_2$ $[M + Na]^+$, 486.1416; found, 486.1397.

8-((2-(1*H*-Indol-3-yl)ethyl)amino)-7-(4-(2-(2-(2-(2-azidoethoxy)ethoxy)ethoxy)ethoxy)benzyl)-1,3-dimethyl-3,7-dihydro-1*H*-purine-2,6-dione (FPE-37)

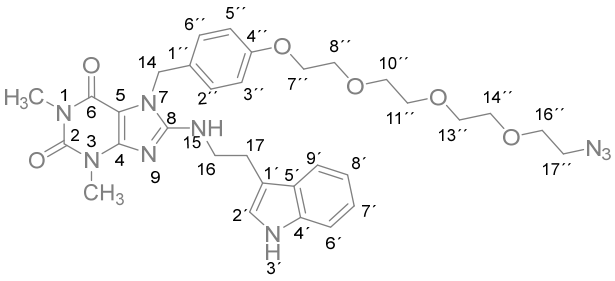

FPE-13 (0.03 g, 0.07 mmol, 1 eq) and K_2CO_3 (0.011 g, 0.08 mmol, 1.2 eq) were weighed into a sealed tube and dissolved in DMF (2 mL). The mixture was stirred at RTfor 30 minutes. Then the alkylating agent **TH055** (0.04 g, 0.1 mmol, 1.4 eq) was added and the temperature was raised to 80°C. The reaction was stirred for 7 hours and when no further progress was detected with the TLC, it was stopped. Solvent was removed under reduced pressure and an extraction with EtOAc and water was performed. The organic phase was further washed with a saturated aqueous solution of $NaHCO_3$, dried over $MgSO_4$ and concentrated under *vacuum*. A purification with flash column chromatography on silica gel (MeOH in DCM 5 to 10%) was followed by a recrystallization in cold MeOH. **Yield:** 5 mg, 0.008 mmol, 11%; **M.p**.: 248°C; **^{1}H NMR** (600 MHz, DMSO-d_6): δ 10.81 (s, 1H, NH_{indole}), 7.64 (d, J = 7.85 Hz, 1H, Ar-H), 7.36 – 7.31 (m, 2H, Ar-H and *NH*CH_2), 7.17 (d, J = 8.61 Hz, 2H, Ar-H_{benzyl}), 7.13 (d, J = 2.22 Hz, 1H, Ar-H), 7.07 (t, J = 6.97 Hz, 1H, Ar-H), 6.98 (t, J = 6.92 Hz, 1H, Ar-H), 6.84 (d, J = 8.65 Hz, 2H, Ar-H_{benzyl}), 5.20 (s, 2H, N7CH_2), 4.03 (t, J = 4.64 Hz, 2H, -C7''-H_2), 3.71 (t, J = 4.63 Hz, 2H, -C8''-H_2), 3.64 – 3.58 (m, 2H, NH*CH_2*CH_2), 3.59 – 3.55 (m, 4H, H_{PEG}), 3.55 – 3.52 (m, 6H, H_{PEG}), 3.39 (s, 3H, N3CH_3), 3.36 (t, J = 4.64, 2H, CH_2*CH_2*N_3), 3.17 (s, 3H, N1CH_3), 2.98 (t, J = 7.44 Hz, 2H, NHCH_2*CH_2*); **^{13}C NMR** (151 MHz, DMSO-d_6) δ : δ 158.21 (C4''), 154.08 (C6), 153.18 (C8), 151.39 (C2), 149.33 (C4), 136.68 (C4'), 129.51 (C1''), 129.17 (2C, C2'' and C6''), 127.67 (C5'), 123.25 (C2'), 121.29 (C7'), 118.73 (C9'), 118.60 (C8'), 114.75 (2C, C3'' and C5''), 111.91 (C6'), 111.76 (C5'), 101.53 (C5), 70.27 (1C, $C_{Aliphatic}$), 70.21 (1C, $C_{Aliphatic}$), 70.19 (1C, $C_{Aliphatic}$), 70.07 (1C, $C_{Aliphatic}$),

69.61 (1C, $C_{Aliphatic}$), 69.29 (1C, $C_{Aliphatic}$), 67.47 (1C, $C_{Aliphatic}$), 50.37 (1C, $C_{Aliphatic}$), 45.10 (C14), 43.66 (C16), 29.65 (1C, -CH_3), 27.60 (1C, CH_3), 25.77 (C17); **LC-MS (m/z)**: 646.6 ($[M+H]^+$); **purity** by HPLC-UV (220 – 400 nm)-ESI-MS: 95.7%; **HRMS (ESI, m/z)** calcd for $C_{32}H_{39}N_9O_6$ $[M + Na]^+$, 668.2916; found, 668.2911.

8-((2-(1*H*-indol-3-yl)ethyl)amino)-1,3-dimethyl-7-(4-nitrobenzyl)-3,7-dihydro-1*H*-purine-2,6-dione (FPE-40)

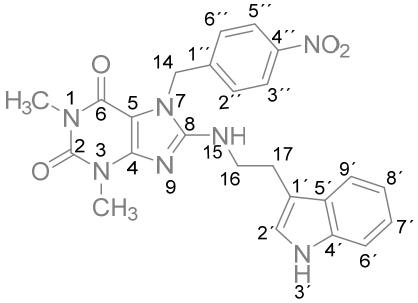

Synthesis according to **GP G**. Purification with flash column chromatography on silica gel (MeoH in DCM 0 to 5%) followed by recrystallization in MeOH. **Yield:** 223 mg, 0.47 mmol, 16%. **M.p.** 199°C; ^{1}H NMR (500 MHz, DMSO-d_6) δ 10.78 (d, J =1.15 Hz, 1H, NH_{indole}), 8.09 - 8.12 (m, 2H, Ar-H_{benzyl}), 7.59 (d, J =8.02 Hz, 1H, Ar-H), 7.41 (t, J =5.58 Hz, 1H, *NH*CH_2), 7.34 (d, J =8.88 Hz, 2H, Ar-H_{benzyl}), 7.30 (d, J =8.02 Hz, 1H, Ar-H), 7.08 (d, J =2.29 Hz, 1H, Ar-H), 7.00 - 7.05 (m, 1H, Ar-H), 6.91 - 6.95 (m, 1H, Ar-H), 5.37 (s, 2H, N7CH_2), 3.56 - 3.61 (m, 2H, NH*CH_2*CH_2), 3.37 (s, 3H, N3CH_3), 3.11 (s, 3H, N1CH_3), 2.96 (t, J =7.16 Hz, 2H, NHCH$_2$*CH_2*); **LC-MS (m/z)**:474.1 ($[M+H]^+$); **purity** by HPLC-UV (220 – 400 nm)-ESI-MS: 95.9%.

8-((2-(1*H*-Indol-3-yl)ethyl)amino)-7-(3-chloro-4-methoxybenzyl)-1,3-dimethyl-3,7-dihydro-1*H*-purine-2,6-dione (FPE-42)

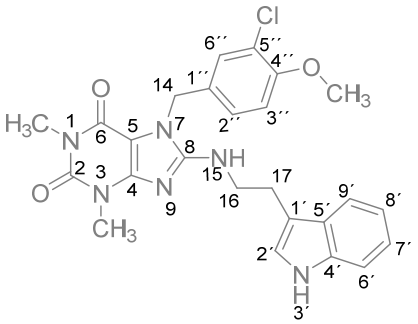

Synthesis according to **GP G**. Purification with flash column chromatography on silica gel (MeOH in DCM 0 to 3%). **Yield:** 81 mg, 1.51 mmol, 78%, **M.p.:** 123°C; **^{1}H NMR** (600 MHz, DMSO-d_6): δ 10.80 (s, 1H, NH_{indole}), 7.64 (d, J = 7.86 Hz, 1H, Ar-H), 7.40 – 7.36 (m, 2H, *NH*CH2and C6’′-H), 7.34 (d, J = 8.10 Hz, 1H, Ar-H), 7.15 – 7.12 (m, 2H, C2’’-H and C2’-H), 7.07 (t, J = 6.95 Hz, 1H, Ar-H), 7.02 (d, J = 8.57 Hz, 1H, C3’’-H), 6.98 (t, J = 6.95 Hz, 1H, Ar-H), 5.20 (s, 2H, -N7CH_2), 3.81 (s, 3H, -OCH_3), 3.62 (dd, J = 6.58, 13.99 Hz, 1H, NH*CH_2*CH_2), 3.39 (s, 3H, N3CH_3), 3.18 (s, 3H, N1CH_3), 2.99 (t, J = 7.50 Hz, 2H, NHCH$_2$*CH_2*); **^{13}C NMR** (151 MHz, DMSO-d_6) δ : δ154.11 (C4’’), 153.90 (C6), 153.07 (C8),

151.23 (C2), 149.26 (C4), 136.54 (C4'), 130.45 (1C, $C_{Ar''}$), 129.21 (1C, $C_{Ar''}$), 127.64 (1C, C_{Ar}), 127.52 (1C, C_{Ar}), 123.05 (C2'), 121.17 (1C, C_{Ar}), 121.30 (1C, C_{Ar}), 118.56 (C9'), 118.47 (C8'), 113.07 (C3''), 111.77 (C6'), 111.63 (C1'), 101.30 (C5), 56.35, 55.14, 44.51, 43.56, 40.33, 29.53, 27.48, 25.69; **LC-MS (m/z)**: 493.1 ($[M+H]^+$); **purity** by HPLC-UV (220 – 400 nm)-ESI-MS: 97.0%; **HRMS (ESI, m/z)** calcd for $C_{50}H_{50}Cl_2N_{12}O_6$ $[2M + H]^+$, 1007.3246; found, 1007.3154.

8-((2-(1*H*-Indol-3-yl)ethyl)amino)-7-(3-chloro-4-hydroxybenzyl)-1,3-dimethyl-3,7-dihydro-1*H*-purine-2,6-dione (FPE-43)

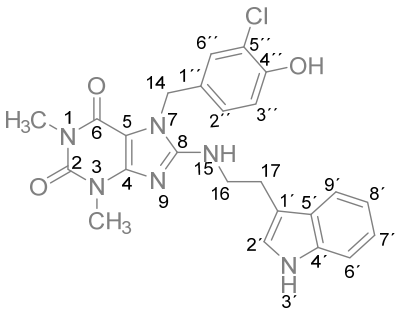

Synthesis according to **GPI**. Purification with flash column chromatography on silica gel (MeOH in DCM 0 to 5%). **Yield:** 208 mg, 0.44 mmol, 36%; **M.p.:** 203°C; **^{1}H NMR** (600 MHz, DMSO-*d*$_6$): δ 10.79 (s, 1H, NH_{indole}), 10.12 (s, 1H, -OH), 7.65 (d, *J* = 7.80 Hz, 1H, Ar-H), 7.36 – 7.33 (m, 2H, *NH*CH_2 and Ar-H), 7.31 (d, *J* = 2.12 Hz, 1H, C6''-H), 7.15 (d, *J* = 2.30 Hz, 1H, Ar'-H), 7.07 (t, *J* = 7.75 Hz, 1H, Ar-H) 7.03 (dd, *J* = 2.12, 8.46 Hz, 1H, C2''-H), 6.98 (t, *J* = 7.41 Hz, 1H, Ar-H), 6.89 (d, *J* = 8.36 Hz, 1H, C3''-H), 5.16 (s, 2H, N7CH_2), 3.61 (dt, *J* = 5.97, 8.16 Hz, 2H, NH*CH_2*CH_2), 3.39 (s, 3H, N3CH_3), 3.18 (s, 3H, N1CH_3), 2.98 (t, *J* = 7.58 Hz, 2H, NHCH$_2$*CH_2*); **^{13}C NMR** (151 MHz, DMSO-*d*$_6$) δ : δ 153.75 (C6), 152.93 (C8), 152.54 (C4''), 151.11 (C2), 149.07 (C4), 136.40 (C4'), 129.09 (1C, $C_{Ar''}$), 128.92(1C, $C_{Ar''}$), 127.38 (1C, C_{Ar}), 127.34 (1C, C_{Ar}), 122.86 (C2'), 121.04 (C7'), 119.53 (C5''), 118.42 (C9'), 118.34 (C8'), 116.79 (C3''), 111.67 (C6'), 111.51 (C5'), 101.23 (C5), 44.44 (C14), 43.52 (C16), 29.39 (1C, CH_3), 27.36 (1C, CH_3), 25.64 (C17); **LC-MS (m/z)**: 479.1 ($[M+H]^+$); **purity** by HPLC-UV (220 – 400 nm)-ESI-MS: 96.6%; **HRMS (ESI, m/z)** calcd for $C_{48}H_{46}$ $Cl_2N_{12}O_6$ $[2M + Na]^+$, 979.2933; found, 979.2846.

8-((2-(1*H*-Indol-3-yl)ethyl)amino)-7-(4-aminobenzyl)-1,3-dimethyl-3,7-dihydro-1*H*-purine-2,6-dione (FPE-44)

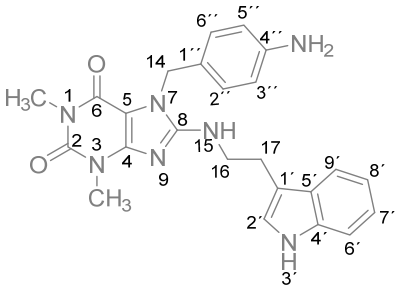

FPE-40 (0.223 g, 0.47 mmol) was dissolved into MeOH and transferred to a suitable flask. Pd/C (27.88 g) was then added. Argon was flushed into the flask before getting the hydrogen flow. The reaction was kept stirring under H_2 for 7 hours. Afterwards, it was stopped, the solution was further diluted with

EtOAc, to ensure the complete solubility, and filtered through celite under reduce pressure. A purification with flash column chromatography on silica gel was performed (MeOH in DCM 5 to 15%). **Yield:** 82 mg, 0.19 mmol, 39%; **M.p.:** 137°C; **^{1}H NMR (**600MHz**,** DMSO-*d*$_6$**) δ** 10.79 (s, 1H, NH_{indole}), 7.66 (d, *J* = 6.86 Hz, 1H, Ar-H), 7.35 (d, *J* = 8.09 Hz, 1H, Ar-H), 7.20 (t, *J* = 5.72 Hz, 1H, *NH*CH_2), 7.13 (d, *J* = 2.27 Hz, 1H, Ar-H), 7.07 (ddd, *J* = 1.13, 6.97, 8.09 Hz, 1H, Ar-H), 7.00 – 6.95 (m, 3H, 1 Ar-H_{indole} and 2 Ar-H_{benzyl}), 6.47 (d, *J* = 8.45 Hz, 2H, Ar-H_{benzyl}), 5.08 (s, 2H, N7CH_2), 4.98 (s, 2H, -NH_2), 3.60 (m, 2H, NH*CH_2*CH_2), 3.38 (s, 3H, N3CH_3), 3.19 (s, 3H, N1CH_3), 2.98 (t, *J* = 7.29, 7.76 Hz, 2H, NHCH$_2$*CH_2*);**^{13}C NMR** (151 MHz, DMSO-*d*$_6$) δ 153.61 (C6), 152.76 (C8), 150.99 (C2), 148.80 (C4), 148.01 (C4''), 136.27 (C4'), 128.43 (2C, C2'' and C6''), 127.26 (C5'), 123.98 (C1''), 122.76 (C2'), 120.89 (C7'), 118.32 (C9'), 118.20 (C8'), 113.65 (2C, C3'' and C5''), 111.56 (C6'), 111.35 (C1'), 101.24 (C5), 45.00 (C14), 43.37 (C16), 29.21 (1C, CH_3), 27.21 (1C, CH_3), 25.52 (C17); **LC-MS (m/z)**: 444.2 ($[M+H]^+$); **purity** by HPLC-UV (220 – 400 nm)-ESI-MS: 100%; **HRMS (ESI, m/z)** calcd for $C_{24}H_{25}N_7O_2$ $[M + Na]^+$, 466.1962; found, 466.1926.

N-(4-((8-((2-(1*H*-indol-3-yl)ethyl)amino)-1,3-dimethyl-2,6-dioxo-1,2,3,6-tetrahydro-7*H*-purin-7-yl)methyl)phenyl)acetamide (FPE-45)

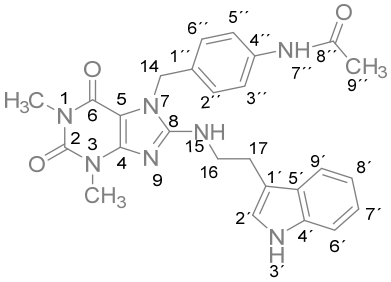

FPE-44 (0.062 g, 0.14 mmol, 1 eq) was suspended in DCM (10 mL). Acetic anhydride was then added and the mixture was stirred at RT for 1h. The solvent was removed under reduced pressure and the crude partitioned between a saturated aqueous solution of Na_2CO_3 and EtOAc. The organic phase was dried over $MgSO_4$ and concentrated under v*acuum*. Purification was achieved with flash colum chromatography on islica gel (MeoH in DCM 0 to 5%), followed by recrystallization in DCM. **Yield**: 3 mg, 6 ·10^{-3} mmol,, 4%; **M.p.:** 167°C; **^{1}H NMR (**600MHz**,** DMSO-*d*$_6$**)** δ 10.77 (s, 1 H, NH_{indole}), 9.89 (s, 1H, NHCO), 7.65 (d, *J* = 6.66 Hz, 1 H, Ar-H), 7.47 (d, *J* = 8.54 Hz, 2H, Ar-H_{benzyl}), 7.34 (d, *J* = 8.16 Hz, Ar-H), 7.31 (t, *J* = 5.74 Hz, 1H, *NH*CH_2), 7.15 (d, *J* = 8.52 Hz, 2H, Ar-H_{benzyl}), 7.11 (d, *J* = 2.24 Hz, 1H, Ar-H), 7.06 (ddd, *J* = 1.15, 6.97, 8.15 Hz, 1H, Ar-H), 6.98 (ddd, *J* = 1.03, 6.96, 7.97 Hz, 1H, Ar-H), 5.22 (s, 2H, N7CH_2), 3.61 – 3.57 (m, 2H, NH*CH_2*CH_2),3.40 (s, 3H, N3CH_3), 3.17 (s, 3H, N1CH_3), 2.97 (t, *J* = 7.34 Hz, 2H, NHCH$_2$*CH_2*), 2.01 (s, 3H, $COCH_3$). **^{13}C NMR** (151 MHz, DMSO-*d*$_6$) δ 167.78 (C8''), 153.31 (C6),

152.34 (C8), 150.58 (C2), 148.46 (C4), 138.02 (C4''), 135.81 (C4'), 131.16 (C1''), 127.10 (2C, C2'' and C6''), 126.82 (C5′), 122.32 (C2'), 120.46 (C7'), 118.76 (C3'' and C5''), 117.88 (C9'), 117.77 (C8'), 111.09 (C6'), 110.93 (C1'), 100.82 (C5), 44.46 ((C14), 42.95 (C16), 28.83(1C, CH_3), 26.77 (1C, CH_3), 25.03 (C17), 23.46 (C9''); **LC-MS (m/z)**: 486.3 ($[M+H]^+$); **purity** by HPLC-UV (220 – 400 nm)-ESI-MS: 95.9%; **HRMS (ESI, m/z)** calcd for $C_{26}H_{27}N_7O_3$ $[M + Na]^+$, 508.2024; found, 508.2068.

8-((2-(1*H*-Indol-3-yl)ethyl)amino)-7-(methoxymethyl)-1,3-dimethyl-3,7-dihydro-1*H*-purine-2,6-dione (FPE-57)

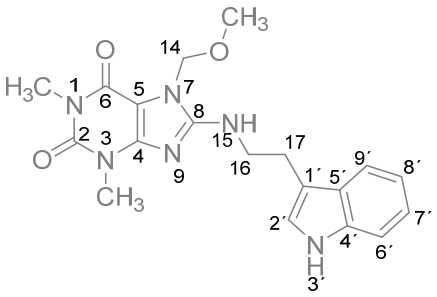

Synthesis according to **GP G**. Purification achieved via precipitation in cold MeOH. **Yield**: 614 mg, 1.6 mmol, 38%; **M.p.:** 203; **^{1}H NMR (**500 MHz**,** DMSO-*d*$_6$**)** δ 10.78 (s, 1H, NH_{indole}), 7.65 (dd, *J* = 1.02, 7.86 Hz, 1H, Ar-H), 7.40 (t, *J* = 5.70 Hz, 1H, *NH*CH_2), 7.33 (d, *J* = 8.06 Hz, 1H, Ar-H), 7.17 (d, *J* = 2.28 Hz, 1H, Ar-H), 7.06 (ddd, *J* = 1.19, 6.92, 8.07 Hz, 1H, Ar-H), 6.98 (ddd, *J* = 1.03, 7.01, 7.93 Hz, 1H, Ar-H), 5.41 (s, 2H, N7-CH_2), 3.61 (ddd, *J* = 5.66, 7.25, 8.53 Hz, 2H, NH*CH*$_2$$CH_2$), 3.40 (s, 3H, N3$CH_3$), 3.23 (s, 3H, N1$CH_3$), 3.19 (s, 3H, OCH_3), 3.01 (dd, *J* = 6.94, 8.20 Hz, 2H, NHCH$_2$*CH*$_2$); **^{13}C NMR (126 MHz, DMSO)** δ 154.60 (C6), 152.72 (C8), 151.12 (C2), 149.16 (C4), 136.38 (C4′), 127.42 (C5′), 122.91 (C2′), 121.02 (C7′), 118.46 (C9′), 118.32 (C8′), 111.66 (C6′), 111.47 (C1′), 101.56 (C5), 72.79 (C14), 55.42 (OCH_3),43.45 (C16), 29.46 (1C, CH_3), 27.34 (1C, CH_3), 25.43 (C17); **LC-MS (m/z)**: 383.1 ($[M+H]^+$); **purity** by HPLC-UV (220 – 400 nm)-ESI-MS: 97.3%; **HRMS (ESI, m/z)** calcd for $C_{19}H_{22}N_6O_3$ $[M + H]^+$, 383.183; found, 383.241.

***N*-(4-((8-((2-(1*H*-indol-3-yl)ethyl)amino)-1,3-dimethyl-2,6-dioxo-1,2,3,6-tetrahydro-7*H*-purin-7-yl)methyl)phenyl)methanesulfonamide (FPE-72)**

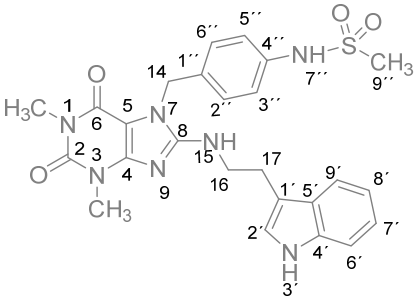

Synthesis according to **GP B.** Purification with flash colum chromatography on silica gel (MeOH in DCM 0 to 5%). **Yield.** 7 mg, 0.013 mmol, 4%; **M.p.:** 178°C; **^{1}H NMR (**600MHz**,** DMSO-*d*$_6$**)** δ 10.77 (s, 1 H, NH_{indole}), 9.89 (s, 1H, $NHSO_2$), 7.65 (d, *J* = 6.66 Hz, 1 H, Ar-H), 7.47 (d, *J* = 8.54 Hz, 2H, Ar-H_{benzyl}), 7.34 (d, *J* = 8.16 Hz, Ar-H), 7.31 (t, *J* = 5.74 Hz, 1H,

NHCH_2), 7.15 (d, *J* = 8.52 Hz, 2H, Ar-H_{benzyl}), 7.11 (d, *J* = 2.24 Hz, 1H, Ar-H), 7.06 (ddd, *J* = 1.15, 6.97, 8.15 Hz, 1H, Ar-H), 6.98 (ddd, *J* = 1.03, 6.96, 7.97 Hz, 1H, Ar-H), 5.22 (s, 2H, N7CH_2), 3.61 – 3.57 (m, 2H, NH*CH₂*CH_2),3.40 (s, 3H, N3CH_3), 3.17 (s, 3H, N1CH_3), 2.97 (t, *J* = 7.34 Hz, 2H, NHCH₂*CH₂*), 2.01 (s, 3H, SO_2CH_3). **^{13}C NMR** (151 MHz, DMSO-*d₆*) δ 153.87 (C6), 152.91 (C8), 151.13, (C2) 149.05 (C4), 137.64 (C4´´), 136.38 (C4´), 132.72 (C1´´), 128.26 (2C, C2´´and C6´´), 127.40 (C5´), 122.90 (C2´), 121.03 (C7´), 120.16 (2 C, C3´´ and C5´´), 118.44 (C9´), 118.34 (C8´), 111.66 (C6´), 111.50 (C1´), 101.34 (C5), 44.89 (C14), 43.50 (C16), 40.20 (C9´´), 29.39 (1C, CH_3), 27.30 (1C, CH_3), 25.56 (C17); **LC-MS (m/z)**: 522.6 ([M+H]$^+$); **purity** by HPLC-UV (220 – 400 nm)-ESI-MS: 96.4%; **HRMS (ESI, m/z)** calcd for $C_{25}H_{27}N_7O_4S$ [M + H]$^+$,522.1918; found, 522.1926.

8-((2-(1*H*-indol-3-yl)ethyl)amino)-7-(4-acetylbenzyl)-1,3-dimethyl-3,7-dihydro-1*H*-purine-2,6-dione (FPE-76)

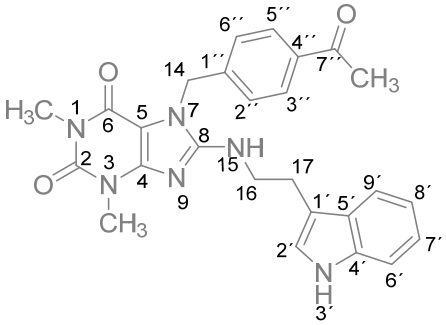

Synthesis according to **GP G.** Purification with flash column chromatography on silica gel(MeOH in DCM 0 to 5%). **Yield:** 200 mg, 0.42 mmol, 25%; **M.p.:** 213.5°C; **^{1}H NMR (**500 MHz**,** DMSO-*d₆*) **δ** 10.79 (s, 1H, NH_{indole}), 7.87 (d, *J* = 8.16 Hz, 2H, Ar-H_{benzyl}), 7.64 (d, *J* = 7.86 Hz, 1H, Ar-H), 7.38 (t, *J* = 5.65 Hz, 1H, *NH*CH_2), 7.35 (d, *J* = 8.09 Hz, 1H, Ar-H), 7.28 (d, *J* = 8.32 Hz, 2H, Ar-H_{benzyl}), 7.12 (d, *J* = 2.28 Hz, 1H, Ar-H), 7.07 (dd, *J* = 6.93, 8.13 Hz, 1H, Ar-H), 6.98 (t, *J* = 7.43 Hz, 1H, Ar-H), 5.36 (s, 2H, N7CH_2), 3.66 – 3.59 (m, 2H, NH*CH₂*CH_2), 3.42 (s, 3H, N3CH_3), 3.16 (s, 3H, N1CH_3), 3.00 (t, *J* = 7.43 Hz, 2H, NHCH₂*CH₂*), 2.54 (s, 3H, $COCH_3$), **^{13}C NMR (126 MHz, DMSO) δ** 197.55 (C7´´), 154.00 (C6), 152.86 (C8), 151.12 (C2), 149.10 (C4), 142.45 (C1´´), 136.40 (C4´), 136.04 (C4´´), 128.54 (2C, CH_{Ar}), 127.41 (C5´), 127.13 (2C, CH_{Ar}), 122.94 (C2´), 121.01 (C7´), 118.43 (C9´), 118.32 (C8´), 111.63 (C6´), 111.47 (C1´), 101.33 (C5), 45.31 (C14), 43.41 (C16), 29.42 (1C, CH_3), 27.29 (1C, CH_3), 26.82 (C8´´), 25.46 (C17); **LC-MS (m/z)**: 471.3 ([M+H]$^+$); **purity** by HPLC-UV (220 – 400 nm)-ESI-MS: 97.9%; **HRMS (ESI, m/z)** calcd for $C_{26}H_{26}N_6O_3$ [M + H]$^+$, 471.2139; found, 471.2142.

8-((2-(1*H*-indol-3-yl)ethyl)amino)-1,3-dimethyl-7-(4-nitrophenethyl)-3,7-dihydro-1*H*-purine-2,6-dione (FPE-92)

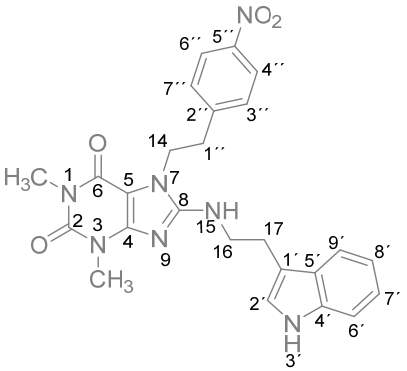

Synthesis according to **GP G**. Purification with preparative TLC (2% MeOH in DCM). **Yield:** 5 mg, 0.01 mmol, 5%; **M.p.**: 110°C; ^{1}H NMR (500 MHz, DMSO-d_6) δ 10.79 (s, 1H, NH_{indole}), 8.16 (d, J = 8.7 Hz, 2H, Ar-H_{benzyl}), 7.61 (d, J = 7.8 Hz, 1H, Ar-H), 7.46 (d, J = 8.6 Hz, 2H, Ar-H_{benzyl} 7.34 (d, J = 8.1 Hz, 1H, Ar-H), 7.21 (t, J = 5.7 Hz, *NH*CH_2), 7.15 (d, J = 2.4 Hz, 1H, Ar-H), 7.06 (ddd, J = 8.2, 6.9, 1.1 Hz, 1H, Ar-H), 7.02 – 6.95 (m, 1H, Ar-H), 4.26 (t, J = 7.7 Hz, 2H, N7CH_2), 3.57 – 3.51 (m, 2H, , NH*CH*$_2$$CH_2$), 3.40 (s, 3H, N3$CH_3$), 3.20 (s, 3H, N1$CH_3$), 3.07 – 3.00 (m, 2H, N7CH_2*CH*$_2$), 2.90 (t, J = 7.6 Hz, 2H, NHCH$_2$*CH*$_2$); **^{13}C NMR (126 MHz, DMSO) δ** 153.72, 153.03, 151.35, 149.19, 146.62, 146.57, 136.56, 130.60, 127.60, 123.66, 123.03, 121.22, 118.57, 118.52, 111.89, 111.69, 101.45, 43.57, 43.38, 35.31, 29.60, 27.55, 25.64; **LC-MS (m/z)**: 488.1 ([M+H]$^+$); **purity** by HPLC-UV (220 – 400 nm)-ESI-MS: 97.0%; **HRMS (ESI, m/z)** calcd for $C_{25}H_{25}N_7O_4$ [M + H]$^+$, 488.204; found, 487.965.

8-((2-(1*H*-indol-3-yl)ethyl)amino)-7-(4-methoxyphenethyl)-1,3-dimethyl-3,7-dihydro-1*H*-purine-2,6-dione (FPE-93)

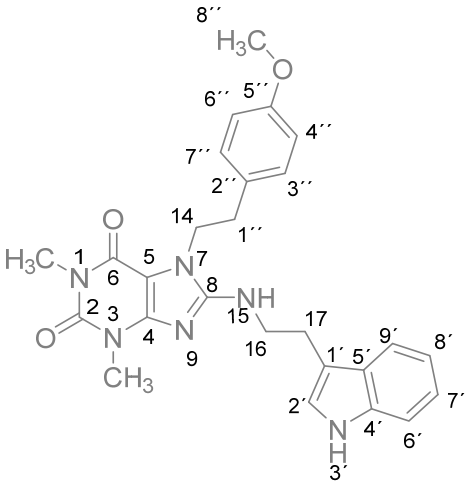

Synthesis according to **GP G**. Purification with flash column chromatography on silica gel (MeOH in DCM 0 to 7%) followed by preparative TLC (5% MeOH in DCM); **Yield:** 2 mg, 0.004 mmol, 8%; **M.p.:** 198°C**; ^{1}H NMR (**500 MHz**,** DMSO-d_6**)** δ 10.80 (s, 1H, NH_{indole}), 7.64 (d, J = 7.9 Hz, 1H, ArH), 7.34 (d, J = 8.1 Hz, 1H, Ar-H), 7.17 (d, J = 2.3 Hz, 1H, Ar-H), 7.14 (d, J = 8.6 Hz, 2H, Ar-H_{benzyl}), 7.07 (t, J = 7.7 Hz, 1H, Ar-H), 7.01 – 6.97 (m, 1H, Ar-H), 6.86 (d, J = 8.6 Hz, 2H, Ar-H_{benzyl}), 4.21 – 4.11 (m, 2H, N7CH_2), 3.71 (s, 3H, OCH_3), 3.60 – 3.52 (m, 2H, NH*CH*$_2$$CH_2$), 3.41 (s, 3H, N3$CH_3$), 3.21 (s, 3H, N1$CH_3$), 2.97 – 2.91 (m, 2H, N7CH_2*CH*$_2$), 2.84 – 2.79 (m, 2H, NHCH$_2$*CH*$_2$); **^{13}C NMR** (151 MHz, DMSO-d_6) δ 157.93, 153.36, 152.70, 151.05,

148.80, 136.25, 129.86 (2C), 129.79, 127.31, 122.71, 120.90, 118.32, 118.19, 113.71 (2C), 111.67, 111.36, 101.19, 55.00, 43.93, 43.30, 34.32, 29.27, 27.23, 25.38; **LC-MS (m/z)**: 473.3 ($[M+H]^+$); **purity** by HPLC-UV (220 – 400 nm)-ESI-MS: 97.7%; **HRMS (ESI, m/z)** calcd for $C_{26}H_{28}N_6O_3$ $[M + H]^+$, 473.2296; found, 473.2294.

8-((2-(1*H*-indol-3-yl)ethyl)amino)-7-(cyclohexylmethyl)-1,3-dimethyl-3,7-dihydro-1*H*-purine-2,6-dione (FPE-107)

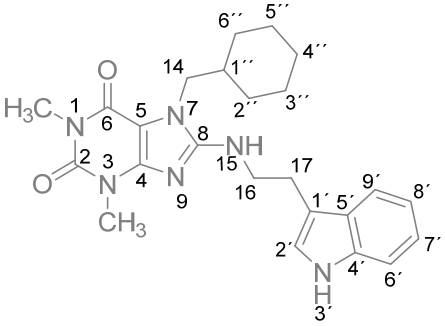

Synthesis according to **GP G**. Purification with flash column chromatography on silica gel (MeOH in DCM 0 to 3%) followed by preparative TLC (3% MeOH in DCM). **Yield**: 20 mg, 0.046 mmol, 16%; **M.p.:** 205°C**;** **^{1}H NMR** (600 MHz, DMSO-d_6) δ 10.80 (s, 1H, NH_{indole}), 7.64 (d, J = 1.1 Hz, 1H, Ar-H), 7.33 (d, J = 8.1 Hz, 1H, Ar-H), 7.15 (d, J = 2.2 Hz, 1H, Ar-H), 7.08 – 7.02 (m, 2H, Ar-H and *NH*CH_2), 6.98 (ddd, J = 7.9, 7.0, 1.0 Hz, 1H, Ar-H), 3.83 (d, J = 7.5 Hz, 2H, N7CH_2), 3.63 – 3.56 (m, 2H, NH*CH_2*CH_2), 3.39 (s, 3H, N3CH_3), 3.17 (s, 3H, N1CH_3), 2.99 (dd, J = 8.3, 6.6 Hz, 2H, NHCH$_2$*CH_2*), 1.72 (ddd, J = 11.3, 7.6, 3.6 Hz, 1H, N7CH_2*CH*), 1.66 – 1.62 (m, 2H, $H_{cyclohexyl}$), 1.60 – 1.58 (m, 1H, $H_{cyclohexyl}$), 1.46 (d, J = 12.1 Hz, 2H, $H_{cyclohexyl}$), 1.12 – 1.05 (m, 3H, $H_{cyclohexyl}$), 0.95 (qd, J = 11.8, 3.7 Hz, 2H, $H_{cyclohexyl}$); **^{13}C NMR** (151 MHz, DMSO-d_6) δ 153.41, 152.26, 148.23, 135.97, 127.02, 122.47, 120.57, 118.03, 117.88, 111.34, 111.05, 101.54, 47.54, 43.03, 39.78, 36.98, 29.09 (2C), 28.93, 26.89, 25.65, 25.12, 24.87 (2C); **LC-MS (m/z)**: 435.3 ($[M+H]^+$); **purity** by HPLC-UV (220 – 400 nm)-ESI-MS: 98.6%; **HRMS (ESI, m/z)** calcd for $C_{24}H_{30}N_6O_2$ $[M + H]^+$, 435.250; found, 435.089.

8-((2-(1*H*-indol-3-yl)ethyl)amino)-7-cyclopropyl-1,3-dimethyl-3,7-dihydro-1*H*-purine-2,6-dione (FPE-112)

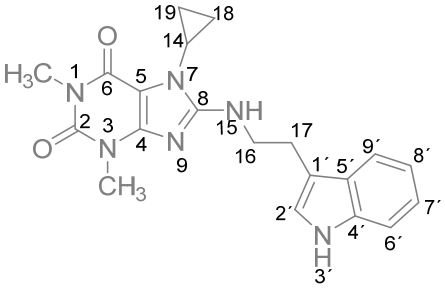

Synthesis according to **GP G**. Purification with flash column chromatography on silica gel (MeOH in DCM 0 to 2%). **Yield:** 18 mg, 0.048 mmol, 32%; **M.p.:** 233°C; **^{1}H NMR** (600 MHz, DMSO-d_6) δ 10.80 (s, 1H, 1H, NH_{indole}), 7.66 (d, J = 7.9 Hz, 1H, , Ar-H), 7.34 (d, J = 8.1 Hz, 1H, Ar-H), 7.18 (d, J = 2.3 Hz, 1H, Ar-H), 6.98 (t, J = 7.2 Hz, 1H, Ar-H),

7.07 (ddd, *J* = 8.1, 6.9, 1.2 Hz, 1H, Ar-H), 6.85 (t, *J* = 5.9 Hz, 1H, *NH*CH_2), 3.62 (dt, *J* = 7.8, 5.8 Hz, 2H, NH*CH_2*CH_2), 3.38 (s, 3H, N3CH_3), 3.18 (s, 3H, N1CH_3), 3.02 (t, *J* = 7.6 Hz, 2H, NHCH_2*CH_2*), 2.90 (tt, *J* = 9.9, 5.1 Hz, 1H, N7CH), 1.05 – 1.00 (m, 2H, $H_{cyclopropyl}$), 0.84 – 0.80 (m, 2H, $H_{cyclopropyl}$); **^{13}C NMR** (151 MHz, DMSO-*d_6*) δ 154.56 (C6), 151.72 (C2), 150.77 (C8), 148.33 (C4), 135.98 (C4′), 127.05 (C5′), 122.46 (C2′), 120.63 (C7′), 118.09 (C8′), 117.90 (C6′), 111.37 (C1′), 111.08 (C1′), 101.93 (C5), 43.09 (C16), 28.91 (1C, CH_3), 27.08 (1C, CH_3), 25.12 (C17), 23.61 (C14), 8.45 (2 C, C18 and C19); **LC-MS (m/z)**: 379.2 ([M+H]$^+$); **purity** by HPLC-UV (220 – 400 nm)-ESI-MS: 96.9%; **HRMS (ESI, m/z)** calcd for $C_{20}H_{22}N_6O_2$ [M + H]$^+$, 379.188; found, 379.183.

8-((2-(1*H*-indol-3-yl)ethyl)amino)-1,3-dimethyl-7-(naphthalen-1-yl)-3,7-dihydro-1*H*-purine-2,6-dione (FPE-114)

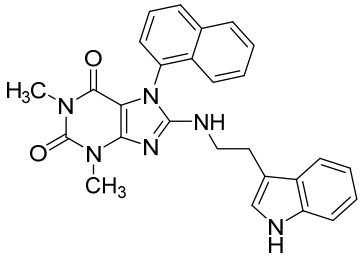

Synthesis according to **GP G**. Purification with flash column chromatography on silica gel (MeOH in DCM 0 to 5%). **Yield:** 10 mg, 0.022 mmol, 6%; **M.p.**; 190°C; **^{1}H NMR** (600 MHz, DMSO-*d_6*) δ 10.75 (d, *J* = 1.8 Hz, 1H, NH_{indole}), 8.09 (dd, *J* = 19.0, 8.2 Hz, 2H, Ar-H), 7.65 – 7.57 (m, 3H, Ar-H), 7.57 – 7.49 (m, 2H, Ar-H), 7.38 – 7.28 (m, 2H, Ar-H), 7.08 – 7.02 (m, 2H, Ar-H), 6.95 (ddd, *J* = 7.9, 6.9, 1.0 Hz, 1H, Ar-H_{indole}), 6.66 (t, *J* = 5.8 Hz, 1H, Ar-H_{indole}), 3.54 – 3.48 (m, 5H, N3CH_3 and NH*CH_2*CH_2), 3.05 (s, 3H, N1CH_3), 2.92 (dd, *J* = 8.8, 6.4 Hz, 2H, NHCH_2*CH_2*); **^{13}C NMR** (151 MHz, DMSO-*d_6*) δ 154.36, 151.78, 151.08, 149.41, 136.19, 134.00, 130.47, 130.43, 129.53, 128.24, 127.28, 127.07, 126.51, 125.75, 122.70, 122.22, 120.83, 118.34, 118.12, 111.50, 111.29, 103.80, 43.26, 29.45, 27.12, 25.28, **LC-MS (m/z)**: 465.3 ([M+H]$^+$); **purity** by HPLC-UV (220 – 400 nm)-ESI-MS: 95.5%; **HRMS (ESI, m/z)** calcd for $C_{27}H_{24}N_6O_2$ [M + H]$^+$, 465.203; found, 465.038.

8-((2-(1*H*-indol-3-yl)ethyl)amino)-7-(2-chloro-4-methoxybenzyl)-1,3-dimethyl-3,7-dihydro-1*H*-purine-2,6-dione (FPE-122)

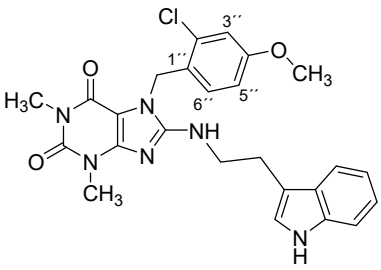

Synthesis according to **GP G**. Purification with flash column chromatography on silica gel (MeOH in DCM 0 to 3%). **Yield**: 22 mg, 0.044 mmol, 17%; **M.p**.: 226°C; **^{1}H NMR** (500 MHz, DMSO-d_6) δ 10.77 (s, 1H, NH_{indole}), 7.63 (d, J = 7.8 Hz, 1H, Ar-H), 7.37 – 7.29 (m, 2H, Ar-H), 7.17 – 7.02 (m, 3H, 2 Ar-H and *NH*CH_2), 6.97 (ddd, J = 8.0, 7.0, 1.1 Hz, 1H, Ar-H_{indole}), 6.79 (dd, J = 8.7, 2.6 Hz, 1H, 5´´-H), 6.42 (d, J = 8.7 Hz, 1H, 6´´-H), 5.28 (s, 2H, N7CH_2), 3.74 (s, 3H, OCH_3), 3.63 – 3.56 (m, 2H, NH*CH_2*CH_2), 3.45 (s, 3H, N3CH_3), 3.12 (s, 3H, N1CH_3), 2.98 (t, J = 7.4 Hz, 2H, NHCH$_2$*CH_2*); **^{13}C NMR** (126 MHz, DMSO-d_6) δ 158.75, 153.99, 152.39, 150.82, 148.77, 136.05, 131.31, 127.09, 126.46, 126.00, 122.61, 120.67, 118.09, 117.98, 114.67, 113.05, 111.31, 111.14, 100.95, 55.39, 43.08, 43.05, 29.12, 26.88, 25.11; **LC-MS (m/z)**: 493.3 ([M+H]$^+$); **purity** by HPLC-UV (220 – 400 nm)-ESI-MS: 97.7%; **HRMS (ESI, m/z)** calcd for $C_{25}H_{25}ClN_6O_3$ $[M + H]^+$, 493.1749; found, 493.1748.

8-((2-(1*H*-indol-3-yl)ethyl)amino)-7-(2-chloro-4-hydroxybenzyl)-1,3-dimethyl-3,7-dihydro-1*H*-purine-2,6-dione (FPE-125)

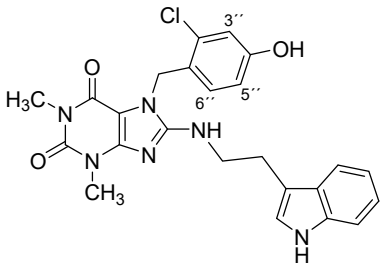

Synthesis according to **GP I**. Purification by flash column chromatography on silica gel (MeOH in DCM 3 to 5%). **Yield** 15.4 mg, 0.03 mmol, 30%; **M.p.** 221°C; **^{1}H NMR** (600 MHz, DMSO-d_6) δ 10.78 (d, J = 1.7 Hz, 1H, NH_{indole}), 9.79 (s, 1H, OH), 7.64 (d, J = 7.9 Hz, 1H), 7.35 – 7.28 (m, 2H, Ar-H), 7.12 (d, J = 2.3 Hz, 1H, Ar-H), 7.06 (ddd, J = 8.2, 7.0, 1.2 Hz, 1H, Ar-H), 6.97 (ddd, J = 8.0, 6.9, 1.1 Hz, 1H, Ar-H), 6.87 (d, J = 2.4 Hz, 1H, 6´´H), 6.64 (dd, J = 8.5, 2.4 Hz, 1H, 5´´-H), 6.33 (d, J = 8.5 Hz, 1H, 3´´-H), 5.24 (s, 2H, N7CH_2), 3.62 – 3.56 (m, 2H, NH*CH_2*CH_2), 3.44 (s, 3H, N3CH_3), 3.12 (s, 3H, N1CH_3), 2.97 (dd, J = 8.6, 6.5 Hz, 2H, NHCH$_2$*CH_2*); **^{13}C NMR** (151 MHz, DMSO-d_6) δ 157.21, 154.17, 152.57, 151.01, 148.93, 136.24, 131.18, 127.26, 126.68, 124.37, 122.76, 120.88, 118.30, 118.18, 115.99, 114.51, 111.52, 111.35, 101.19, 43.31, 43.25, 29.31, 27.09, 25.38; **LC-MS (m/z)**: 479.2 ([M+H]$^+$); **purity** by HPLC-UV

(220 – 400 nm)-ESI-MS: 94.5%; **HRMS (ESI, m/z)** calcd for $C_{24}H_{23}ClN_6O_3$ $[M + H]^+$, 479.1593; found, 479.1597.

8-((2-(1*H*-Indol-3-yl)ethyl)amino)-7-(3-fluorobenzyl)-1,3-dimethyl-3,7-dihydro-1*H*-purine-2,6-dione (FPE-132)

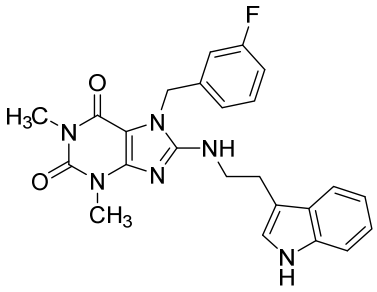

Synthesis according to **GP G**. Purification by flash column chromatography on silica gel (MeOH in DCM 1 to 7%); **Yield** 120 mg, 0.27 mmol, 27%; **M.p.** 271°C; **^{1}H NMR** (600 MHz, DMSO-*d*$_6$) δ 10.78 (br, 1H, NH_{indole}), 7.37 (t, *J* = 5.7 Hz, 1H, Ar-H), 7.36 – 7.32 (m, 2H, Ar-H and *NH*CH_2), 7.10 (d, *J* = 2.3 Hz, 1H, Ar-H), 7.09 (d, *J* = 2.6 Hz, 1H, Ar-H), 7.08 – 7.04 (m, 2H, Ar-H), 7.01 (d, *J* = 7.9 Hz, 1H, Ar-H), 6.98 (ddd, *J* = 8.0, 7.0, 1.0 Hz, 1H, Ar-H), 5.30 (s, 2H, N7CH_2), 3.63 – 3.59 (m, 2H, , NH*CH*$_2$$CH_2$), 3.41 (s, 3H, N3$CH_3$), 3.17 (s, 3H, , N1$CH_3$), 2.98 (t, *J* = 7.5 Hz, 2H, NHCH$_2$*CH*$_2$); **^{13}C NMR** (151 MHz, DMSO-*d*$_6$) δ 162.91, 161.29, 152.78, 150.98, 148.97, 139.87 (d, $J_{C,F}$ = 7.2 Hz), 136.25, 130.52 (d, $J_{C,F}$ = 8.1 Hz), 127.23, 122.99 (d, $J_{C,F}$ = 2.1 Hz), 122.76, 120.88, 118.27, 118.18, 114.16 (d, $J_{C,F}$ = 21.3 Hz), 113.89 (d, $J_{C,F}$ = 22.0 Hz), 111.48, 111.35, 101.15, 44.80, 43.31, 29.27, 27.18, 25.38; **LC-MS (m/z)**: 447.3 ([M+H]$^+$); **purity** by HPLC-UV (220 – 400 nm)-ESI-MS: 97.7%; **HRMS (ESI, m/z)** calcd for $C_{24}H_{23}FN_6O_2$ $[M + H]^+$, 447.1939; found, 447.1937.

8-((2-(1*H*-indol-3-yl)ethyl)amino)-1,3-dimethyl-7-(prop-2-yn-1-yl)-3,7-dihydro-1*H*-purine-2,6-dione (FPE-137)

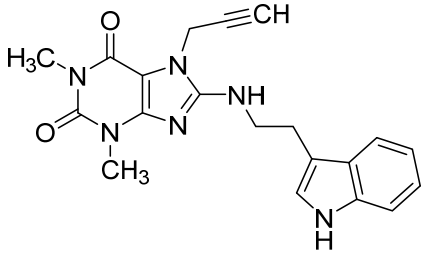

Synthesis according to **GP G**. Purification by flash column chromatography on silica gel (MeOH in DCM 0 to 5%); **Yield** 120 mg, 0.27 mmol, 27%; **M.p.**: 168°C; ^{1}H NMR (300 MHz, DMSO-*d*$_6$) δ 10.79 (s, 1H, NH_{indole}), 7.65 (d, *J* =7.62 Hz, 1H, Ar-H), 7.44 (t, *J* =5.57 Hz, 1H, *NH*CH_2), 7.33 (d, *J* =8.21 Hz, 1H, Ar-H), 7.18 (d, *J* =1.76 Hz, 1H, Ar-H), 7.02 - 7.09 (m, 1H, Ar-H), 6.95 - 7.01 (m, 1H, Ar-H), 4.91 (d, *J* =2.34 Hz, 2H, N7CH_2), 3.56 - 3.64 (m, 2H, NH*CH*$_2$), 3.37 (s, 3H, N3CH_3), 3.29 (t, *J* =2.05 Hz, 1H, N7CH$_2$C*CH*), 3.17 (s, 3H, N1CH_3), 2.99 (t, *J* =7.33 Hz, 2H, NHCH$_2$*CH*$_2$); **^{13}C NMR** (DMSO-*d*$_6$) δ 154.3, 153.2, 151.4, 149.5, 136.7, 127.7, 123.3, 121.4, 118.8, 118.7, 111.9,

111.8, 101.1, 78.9, 75.8, 43.8, 32.8, 29.7, 27.6, 25.9; **LC-MS (m/z)**: 377.2 ([M+H]$^+$); **purity** by HPLC-UV (220 – 400 nm)-ESI-MS: 75.4%.

8-((2-(1*H*-indol-3-yl)ethyl)amino)-1,3-dimethyl-7-phenyl-3,7-dihydro-1*H*-purine-2,6-dione (FPE-138)

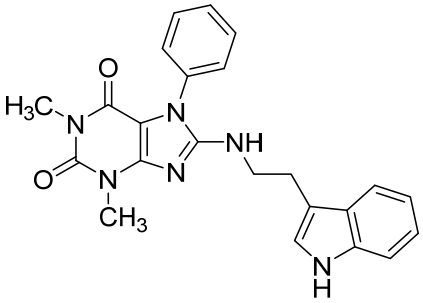

Synthesis according to **GP G**. Purification by flash column chromatography on silica gel (MeOH in DCM 0 to 7%); **Yield** 25 mg, 0.06 mmol, 33%; **M.p.** 239°C; **^{1}H NMR** (500 MHz, DMSO-d_6) δ 10.77 (s, 1H, NH_{indole}), 7.64 (d, J = 7.8 Hz, 1H, Ar-H), 7.53 – 7.43 (m, 3H, 2 Ar-H_{benzyl} and *NH*CH_2), 7.36 – 7.30 (m, 3H, Ar-H_{benzyl}), 7.13 (d, J = 2.3 Hz, 1H, Ar-H), 7.06 (ddd, J = 8.1, 6.9, 1.2 Hz, 1H, Ar-H), 6.98 (ddd, J = 7.9, 7.0, 1.0 Hz, 1H, Ar-H), 6.75 (t, J = 5.8 Hz, 1H, Ar-H), 3.56 (ddd, J = 9.0, 7.5, 5.8 Hz, 2H, NH*CH*$_2$$CH_2$), 3.47 (s, 3H, N3$CH_3$), 3.13 (s, 3H, N1$CH_3$), 2.98 (dd, J = 8.7, 6.4 Hz, 2H, NHCH$_2$*CH*$_2$); ^{13}C NMR (126 MHz, DMSO-d$_6$) δ 153.58, 151.87, 150.97, 149.42, 136.21, 133.94, 129.08, 128.24, 127.40, 127.30, 122.67, 120.85, 118.36, 118.13, 111.59, 111.30, 102.43, 43.42, 29.34, 27.23, 25.20; **LC-MS (m/z)**: 415.3 ([M+H]$^+$); **purity** by HPLC-UV (220 – 400 nm)-ESI-MS: 97.0%; **HRMS (ESI, m/z)** calcd for $C_{23}H_{22}N_6O_2$ [M + H]$^+$, 415.1877; found, 415.1875.

8-((2-(1*H*-indol-3-yl)ethyl)amino)-1,3-dimethyl-7-(naphthalen-2-yl)-3,7-dihydro-1*H*-purine-2,6-dione (FPE-142)

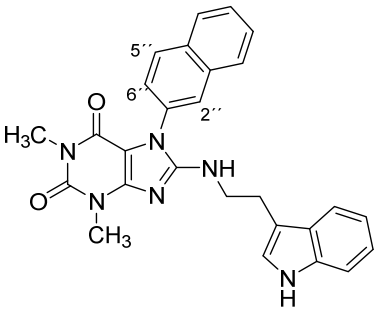

Synthesis according to **GP G**. Purification by flash column chromatography on silica gel (MeOH in DCM 0 to 5%) followed by preparative TLC (DCM : MeOH 95:5); **Yield** 5 mg, 0.011 mmol, 10%; **M.p.**: 180°C; **^{1}H NMR** (600 MHz, DMSO-d_6) δ 10.79 (s, 1H, NH_{indole}), 8.02 (d, J = 8.7 Hz, 1H, Ar-H, 5′′-H), 7.99 – 7.93 (m, 1H, Ar-H), 7.89 (d, J = 2.1 Hz, 1H, 2′′-H), 7.61 (m, 3H, Ar-H), 7.42 (dd, J = 8.6, 2.1 Hz, 1H, 6′′-H), 7.33 (d, J = 8.1 Hz, 1H, Ar-H), 7.14 (d, J = 2.3 Hz, 1H, Ar-H_{indole}), 7.10 – 7.03 (m, 1H, Ar-H, *NH*CH_2), 7.02 – 6.91 (m, 2H, Ar-H_{indole}), 3.59 – 3.53 (m, 2H, NH*CH*$_2$$CH_2$), 3.49 (s, 3H, N3$CH_3$), 3.13 (s, 3H, N1$CH_3$), 2.98 (t, J = 7.5 Hz, 2H, NHCH$_2$*CH*$_2$); **^{13}C NMR** (151 MHz, DMSO-d_6) δ 153.82, 151.98, 151.03, 149.54, 136.22, 132.87,

132.45, 131.50, 128.77, 128.16, 127.58, 127.36, 126.84, 126.60, 126.07, 125.69, 122.74, 120.86, 118.37, 118.17, 111.65, 111.34, 102.65, 43.46, 30.66, 29.43, 27.26, 25.17. **LC-MS (m/z)**: 465.2 ($[M+H]^+$); **purity** by HPLC-UV (220 – 400 nm)-ESI-MS: 94.3%; **HRMS (ESI, m/z)** calcd for $C_{27}H_{24}N_6O_2$ $[M + H]^+$ 465.2034; found, 465.2036.

8-((2-(1*H*-indol-3-yl)ethyl)amino)-7-(4-(hydroxymethyl)benzyl)-1,3-dimethyl-3,7-dihydro-1*H*-purine-2,6-dione (FPE-146)

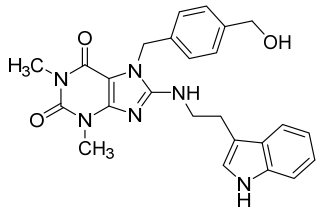

Synthesis according to **GP G**. Purification by flash column chromatography on silica gel (MeOH in DCM 0 to 7%) followed by recrystallization in DCM. **Yield**: 241 mg, 0.526 mmol, 55%; **M.p.:**128°C; **^{1}H NMR** (500 MHz, DMSO-d_6) δ 10.77 (s, 1H, NH_{indole}), 7.65 (d, J = 7.7 Hz, 1H, Ar-H), 7.34 (d, J = 8.1 Hz, 1H, Ar-H), 7.31 (t, J = 5.7 Hz, 1H, *NH*CH_2), 7.24 (d, J = 8.2 Hz, 2H, Ar-H_{benzyl}), 7.16 (d, J = 8.1 Hz, 2H, Ar-H_{benzyl}), 7.10 (d, J = 2.3 Hz, 1H, Ar-H), 7.07 (ddd, J = 8.1, 6.9, 1.2 Hz, 1H, Ar-H), 6.98 (ddd, J = 8.1, 6.9, 1.2 Hz, 1H, Ar-H), 5.27 (s, 2H, N7CH_2), 5.10 (t, J = 5.6 Hz, 1H, CH_2*OH*), 4.45 (d, J = 5.5 Hz, 2H, *CH_2*OH), 3.65 – 3.56 (m, 2H, NH*CH_2*CH_2), 3.40 (s, 3H, N3CH_2), 3.17 (s, 3H, N1CH), 2.98 (t, J = 7.5 Hz, 2H, NHCH_2*CH_2*); **^{13}C NMR** (126 MHz, DMSO-d_6) δ 153.75, 152.71, 150.96, 148.86, 141.59, 136.22, 135.36, 127.22, 126.81 (2C), 126.58 (2C), 122.75, 120.84, 118.27, 118.16, 111.47, 111.31, 101.21, 62.61, 45.08, 43.29, 29.22, 27.15, 25.37; **LC-MS (m/z)**: 459.3 ($[M+H]^+$); **purity** by HPLC-UV (220 – 400 nm)-ESI-MS: 98.3%; **HRMS (ESI, m/z)** calcd for $C_{25}H_{26}N_6O_3$ $[M + H]^+$, 459.2139; found, 459.2137.

8-((2-(1*H*-indol-3-yl)ethyl)amino)-1,3-dimethyl-7-(naphthalen-2-ylmethyl)-3,7-dihydro-1*H*-purine-2,6-dione (FPE-148)

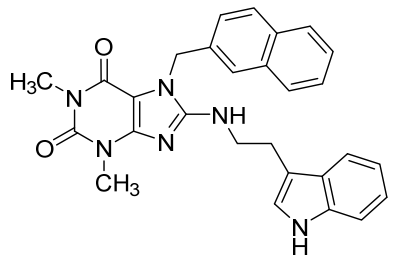

Synthesis according to **GP G**. Purification by flash column chromatography on silica gel (MeOH in DCM 0 to 7%) followed by preparative TLC (DCM : MeOH 95:5). **Yield**: 0.2, 0.42 mmol, 45%; **M.p**.: 191°C; **^{1}H NMR** (600 MHz, DMSO-d_6) δ 10.78 (d, J = 2.5 Hz, 1H, NH_{indole}), 7.89 – 7.79 (m, 3H, Ar-$H_{naphtyl}$), 7.67 (s, 1H, Ar-$H_{naphtyl}$), 7.64 (dd, J = 8.0, 1.1 Hz, 1H), 7.49 (dt, J = 6.2, 3.4 Hz, 2H, Ar-$H_{naphtyl}$), 7.41 (t, J = 5.7 Hz, 1H, *NH*CH_2), 7.36 (d, J = 8.5, 1H, Ar-H), 7.34 (d, J = 8.2 Hz, 1H, Ar-H), 7.14 (d, J = 2.3

Hz, 1H, Ar-H), 7.06 (ddd, *J* = 8.2, 7.0, 1.1 Hz, 1H, Ar-H), 6.97 (ddd, *J* = 7.9, 6.9, 1.0 Hz, 1H, Ar-H), 5.46 (s, 2H, N7CH_2), 3.63 (ddd, *J* = 8.8, 7.2, 5.6 Hz, 2H, NH*CH_2*CH_2), 3.42 (s, 3H, N3CH_3), 3.16 (s, 3H, N1CH_3), 2.99 (dd, *J* = 8.6, 6.5 Hz, 2H, NHCH_2*CH_2*); **^{13}C NMR** (151 MHz, DMSO-*d_6*) δ 153.89, 152.77, 151.00, 148.93, 136.25, 134.73, 132.71, 132.18, 128.10, 127.69, 127.47, 127.25, 126.27, 125.93, 125.25, 125.21, 122.72, 120.88, 118.30, 118.18, 111.54, 111.34, 101.36, 45.52, 43.32, 29.28, 27.17, 25.45; **LC-MS (m/z)**: 479.3 ([M+H]$^+$); **purity** by HPLC-UV (220 – 400 nm)-ESI-MS: 93.3%; **HRMS (ESI, m/z)** calcd for $C_{28}H_{26}N_6O_2$ [M + H]$^+$, 479.2190; found,479.2191.

8-((2-(1*H*-indol-3-yl)ethyl)amino)-7-(4-ethynylbenzyl)-1,3-dimethyl-3,7-dihydro-1*H*-purine-2,6-dione (FPE-190)

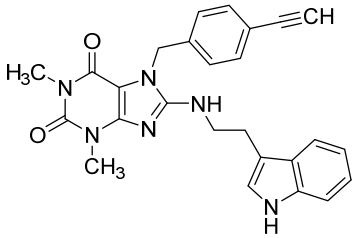

Synthesis according to **GP G**. Purification by flash column chromatography on silica gel (MeOH in DCM 0 to 5%). **Yield**: 250 mg, 0.55 mmol, 53%; **M.p.:** 202°C; **^{1}H NMR** (500 MHz, DMSO-*d_6*) δ 10.80 (d, *J* = 2.6 Hz, 1H, NH_{indole}), 7.63 (d, *J* = 7.8 Hz, 1H, Ar-H), 7.41 (d, *J* = 8.2 Hz, 2H, Ar-H_{benzyl}), 7.39 – 7.32 (m, 2H, Ar-H and *NH*CH_2), 7.18 (d, *J* = 8.2 Hz, 2H, Ar-H_{benzyl}), 7.12 (d, *J* = 2.3 Hz, 1H, Ar-H), 7.07 (ddd, *J* = 8.1, 7.0, 1.2 Hz, 1H, Ar-H), 7.01 – 6.93 (m, 1H, Ar-H), 5.29 (s, 2H, N7CH_2), 4.15 (s, 1H, C≡CH), 3.66 – 3.53 (m, 2H, NH*CH_2*CH_2), 3.40 (s, 3H, N3CH_3), 3.16 (s, 3H, N1CH_3), 2.98 (t, *J* = 7.4 Hz, 2H, NHCH_2*CH_2*); **^{13}C NMR** (126 MHz, DMSO-d_6) δ 153.77, 152.70, 150.94, 148.90, 137.92, 136.23, 131.75 (2C), 127.22, 127.19 (2C), 122.75, 120.82, 120.66, 118.24, 118.14, 111.47, 111.29, 101.13, 83.17, 80.68, 45.03, 43.24, 29.20, 27.10, 25.29; **LC-MS (m/z)**: 453.3 ([M+H]$^+$); **purity** by HPLC-UV (220 – 400 nm)-ESI-MS: 97.4%; **HRMS (ESI, m/z)** calcd for $C_{26}H_{24}N_6O_2$ [M + H]$^+$, 453.2034; found, 453.2038.

3-(8-((2-(1*H*-indol-3-yl)ethyl)amino)-1,3-dimethyl-2,6-dioxo-1,2,3,6-tetrahydro-7*H*-purin-7-yl)propyl acetate (FPE-196)

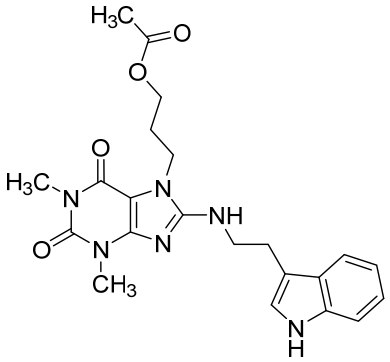

Synthesis according to **GP G**. Purification by flash column chromatography on silica gel (MeOH in DCM 0 to 5%). **Yield**: 30 mg, 0.068 mmol, 35%; **M.p.:** 186°C; **^{1}H NMR** (500 MHz, DMSO-*d*$_6$) δ 10.80 (s, 1H, NH$_{indole}$), 7.64 (dd, *J* = 7.8, 1.1 Hz, 1H, Ar-H), 7.37 – 7.31 (m, 1H, Ar-H), 7.22 – 7.15 (m, 2H, Ar-H and *NH*CH$_2$), 7.06 (ddd, *J* = 8.1, 6.9, 1.2 Hz, 1H, Ar-H), 6.98 (ddd, *J* = 7.9, 7.0, 1.0 Hz, 1H, Ar-H), 4.10 (t, *J* = 6.8 Hz, 2H, N7CH$_2$), 3.96 (t, *J* = 6.3 Hz, 2H, CH$_2$O), 3.65 – 3.55 (m, 2H, NH*CH$_2$*CH$_2$), 3.40 (s, 3H, N3CH$_3$), 3.18 (s, 3H, N1CH$_3$), 2.99 (dd, *J* = 8.7, 6.5 Hz, 2H, NHCH$_2$*CH$_2$*), 1.95 (m, 5H, COCH$_3$ and N7CH$_2$*CH$_2$*); ^{13}C NMR (126 MHz, DMSO-d$_6$) δ 170.19, 153.52, 152.61, 150.98, 148.71, 136.23, 127.27, 122.68, 120.84, 118.24, 118.15, 111.61, 111.32, 101.36, 61.20, 43.36, 29.17, 27.98, 27.13, 25.39, 20.52; **LC-MS (m/z)**: 439.2 ([M+H]$^+$); **purity** by HPLC-UV (220 – 400 nm)-ESI-MS: 97.7%; **HRMS (ESI, m/z)** calcd for $C_{22}H_{26}N_6O_4$ [M + H]$^+$, 439.2088; found, 439.2093.

8-((2-(1*H*-indol-3-yl)ethyl)amino)-7-((1-heptyl-1*H*-1,2,3-triazol-4-yl)methyl)-1,3-dimethyl-3,7-dihydro-1*H*-purine-2,6-dione (FPE-199)

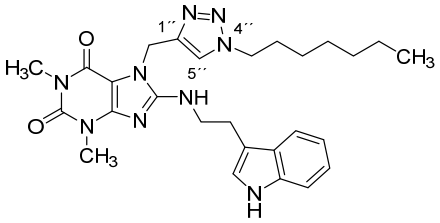

Synthesis according to **GP G**. Purification by flash column chromatography on silica gel (MeOH in DCM 0 to 5%). **Yield**: 20 mg, 0.04 mmol, 57%; **M.p.:** 233°C; **^{1}H NMR** (600 MHz, DMSO-*d*$_6$) δ 10.79 (s, 1H, NH$_{indole}$), 7.82 (s, 1H, C5´´-H), 7.64 (d, *J* = 7.8 Hz, 1H, Ar-H), 7.37 – 7.31 (m, 2H, Ar-H and *NH*CH$_2$), 7.15 (d, *J* = 2.2 Hz, 1H, Ar-H), 7.06 (ddd, *J* = 8.1, 6.9, 1.1 Hz, 1H, Ar-H), 7.01 – 6.94 (m, 1H, Ar-H), 5.35 (s, 2H, N7CH$_2$), 4.27 (t, *J* = 7.0 Hz, 2H, *CH$_2$*CH$_3$), 3.60 (dt, *J* = 7.9, 5.7 Hz, 2H), 3.40 (s, 3H, N3CH$_3$), 3.18 (s, 3H, N1CH$_3$), 2.99 – 2.94 (m, 2H, NH*CH$_2$*CH$_2$), 1.73 (p, *J* = 7.2 Hz, 2H, CH$_{2\text{-pentyl}}$), 1.19 (dddd, *J* = 22.5, 15.6, 11.2, 7.8 Hz, 8H, 4x CH$_{2\text{-pentyl}}$), 0.80 (t, *J* = 6.9 Hz, 3H, CH$_2$*CH$_3$*); **^{13}C NMR** (151 MHz, DMSO-*d*$_6$) δ 153.85, 152.72, 151.02, 148.85, 142.67 (C1´´), 136.23, 127.24, 122.84, 122.72 (C5´´), 120.88, 118.27, 118.18, 111.52, 111.34, 101.13, 49.25, 43.36, 37.96, 31.03, 29.66, 29.24, 27.95, 27.15, 25.70, 25.44, 21.88, 13.81; **LC-MS (m/z)**:

518.4 ([M+H]$^+$); **purity** by HPLC-UV (220 – 400 nm)-ESI-MS: 94.6%; **HRMS (ESI, m/z)** calcd for $C_{27}H_{35}N_9O_2$ [M + H]$^+$ 518.2986; found, 518.2998.

8-((2-(1*H*-indol-3-yl)ethyl)amino)-7-(7-chloroquinolin-4-yl)-1,3-dimethyl-3,7-dihydro-1*H*-purine-2,6-dione (FPE-211)

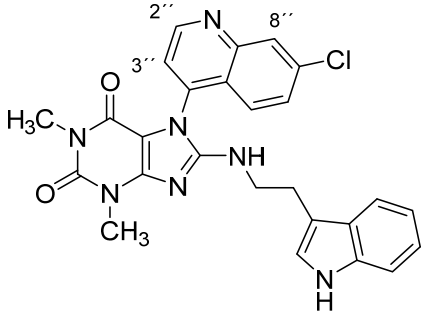

Synthesis according to **GP G**. Purification by flash column chromatography on silica gel (MeOH in DCM 0 to 5%), followed by preparative TLC (5% MeOH in DCM). **Yield**: quantitative; **M.p.:** 140°C; **^{1}H NMR** (600 MHz, DMSO-*d*$_6$) δ 10.78 (s, 1H, NH$_{indole}$), 9.07 (d, *J* = 4.5 Hz, 1H, C2′′-H), 8.23 (d, *J* = 1.8 Hz, 1H, C8′′-H), 7.66 – 7.55 (m, 4H, 3 Ar-H and *NH*CH$_2$), 7.33 (d, *J* = 8.0 Hz, 1H, Ar-H), 7.10 (d, *J* = 2.2 Hz, 1H, Ar-H), 7.09 – 7.00 (m, 2H, Ar-H), 6.96 (t, *J* = 7.4 Hz, 1H, Ar-H$_{indole}$), 3.56 – 3.49 (m, 5H, N3CH$_3$ and NH*CH$_2$*CH$_2$), 3.07 (s, 3H, N1CH$_3$), 2.94 (td, *J* = 7.4, 4.0 Hz, 2H, NHCH$_2$*CH$_2$*); **^{13}C NMR** (151 MHz, DMSO-*d*$_6$) δ 153.89, 152.43, 151.80, 151.02, 149.95, 149.34, 139.11, 136.20, 134.74, 128.25, 127.88, 127.28, 125.11, 124.29, 122.83, 121.93, 120.85, 118.25, 118.17, 111.39, 111.33, 103.48, 43.33, 29.54, 27.19, 25.02; **LC-MS (m/z)**: 500.1 ([M+H]$^+$); **purity** by HPLC-UV (220 – 400 nm)-ESI-MS: 98.5%; **HRMS (ESI, m/z)** calcd for $C_{26}H_{22}ClN_7O_2$ [M + H]$^+$, 500.1596; found, 500.1597.

8-((2-(1*H*-indol-3-yl)ethyl)amino)-7-(4-chlorophenethyl)-1,3-dimethyl-3,7-dihydro-1*H*-purine-2,6-dione (FPE-ML15)

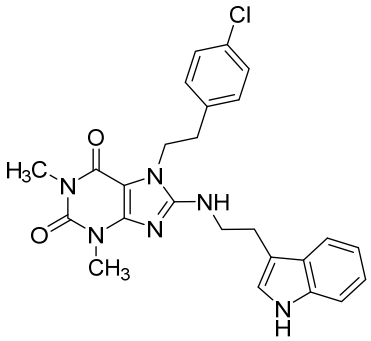

Synthesis according to **GP G**. Purification by flash column chromatography on silica gel (MeOH in DCM 0 to 5%). **Yield**: 1.10 g, 4.56 mmol, 98.5%; **M.p.**: 120°C; **^{1}H NMR** (600 MHz, DMSO-*d*$_6$) δ: 10.81 (s, 1 H, NH$_{indole}$), 7.64 (d, *J* = 7.8 Hz, 1 H, Ar-H), 7.34 (m, 3 H, 2 x Ar-H$_{benzyl}$ and *NH*CH$_2$), 7.22 (d, *J* = 8.4 Hz, 2 H, Ar-H$_{benzyl}$), 7.16 (m, 2H, Ar-H), 7.06 (ddd, *J* = 8.1 Hz, 6.9 Hz, 1.1 Hz, 1 H,Ar-H), 6.98 (ddd, *J* = 8.0 Hz, 6.9 Hz, 1.0 Hz, 1 H, Ar-H), 4.22-4.16 (m, 2 H, N7CH$_2$), 3.58-3.51 (m, 2 H, NH*CH$_2$*CH$_2$), 3.40 (s, 3 H, N3CH$_3$), 3.20 (s, 3 H, N1-CH$_3$), 2.93 (dd, *J* = 8.8 Hz, 6.4 Hz, 2 H, N7CH$_2$CH$_2$), 2.90-2.85 (m, 2 H, NHCH$_2$*CH$_2$*); **^{13}C NMR** (151 MHz, DMSO-*d*$_6$) δ 153.3, 152.7, 151.0, 148.8, 136.9, 136.2, 131.1, 130.8 (2C), 128.2

(2C), 127.3, 122.7, 120.9, 118.3, 118.2, 111.6, 111.4, 101.1, 43.5, 43.3, 34.5, 27.2, 25.3, 20.7; **LC-MS (m/z)**: 477.3 ([M+H]$^+$); **purity** by HPLC-UV (220 – 400 nm)-ESI-MS: 99.1%; **HRMS (ESI, m/z)** calcd for $C_{25}H_{25}ClN_6O_2$ [M + H]$^+$, 477.1800; found, 477.1802.

8-((2-(1*H*-indol-3-yl)ethyl)amino)-1,3-dimethyl-7-(pyridin-3-ylmethyl)-3,7-dihydro-1*H*-purine-2,6-dione (FPE-ML22)

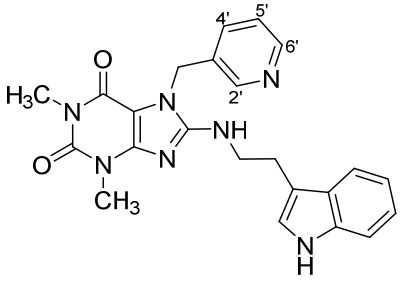

Synthesis according to **GP G**. Purification by flash column chromatography on silica gel (MeOH in DCM 0 to 5%). **Yield**: 26 mg, 0.061 mmol, 12.5%; **M.p**.: 259°C ; **^{1}H NMR** (600 MHz, DMSO-*d*$_6$) δ: 10.79 (d, *J* = 2.4 Hz, 1 H, NH_{indole}), 8.53 (d, *J* = 2.3 Hz, 1 H, C2′-H), 8.47 (dd, *J* = 4.8 Hz, 1.6 Hz, 1 H, C6′-H), 7.64 (d, *J* = 7.9 Hz, 1 H, C4′-H), 7.54 (t, *J* = 8.0 Hz, 2.0 Hz, 1 H, Ar-H), 7.45 (t, *J* = 5.7 Hz, Ar-H), 7.39-7.22 (m, 2H, C5′-H and Ar-H), 7.12-7.03 (m, 2 H, Ar-H and *NH*CH_2), 6.98 (ddd, *J* = 8.0 Hz, 6.9 Hz, 1.0 Hz, Ar-H), 5.32 (s, 2H, N7CH_2), 3.62 (dt, *J* = 7.8 Hz, 6.1 Hz, 2 H, NH*CH*$_2$$CH_2$), 3.40 (s, 3 H, N3$CH_3$), 3.17 (s, 3 H, 3N1$CH_3$), 2.89 (t, *J* = 7.5 Hz, 2 H, NHCH$_2$*CH*$_2$); **^{13}C NMR** (151 MHz, DMSO-*d*$_6$) δ 153.7, 152.8, 151.0, 149.0, 148.7, 148.6, 136.3, 134.8, 132.7, 127.2, 123.6, 122.8, 120.9, 118.3, 118.2, 111.5, 111.4, 101.1, 54.9, 43.3, 29.3, 27.2, 23.4; **LC-MS (m/z)**: 430.3 ([M+H]$^+$); **purity** by HPLC-UV (220 – 400 nm)-ESI-MS: 95.4%; **HRMS (ESI, m/z)** calcd for $C_{23}H_{23}N_7O_2$ [M + H]$^+$, 430.1986; found, 430.1984.

8-((2-(1*H*-indol-3-yl)ethyl)amino)-1,3-dimethyl-7-((tetrahydro-2*H*-pyran-4-yl)methyl)-3,7-dihydro-1*H*-purine-2,6-dione (FPE-MP3)

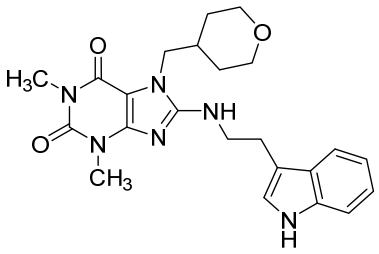

Synthesis according to **GP G**. Purification by flash column chromatography on silica gel (MeOH in DCM 0 to 7%). **Yield**: 335 mg, 0.769 mmol, 68%; **M.p**.: 226°C; **NMR** (500 MHz, DMSO-*d*$_6$) δ 10.80 (s, 1H, NH_{indole}), 7.64 (d, *J* = 7.8 Hz, 1H, Ar-H), 7.34 (d, *J* = 8.1 Hz, 1H, Ar-H), 7.15 (d, *J* = 2.3 Hz, 1H,Ar-H), 7.10 (t, *J* = 5.7 Hz, 1H, *NH*CH_2), 7.06 (ddd, *J* = 8.1, 6.9, 1.2 Hz, 1H, Ar-H), 6.98 (ddd, *J* = 8.0, 7.0, 1.0 Hz, 1H, Ar-H), 3.88 (d, *J* = 7.5 Hz, 2H, N7-CH_2), 3.78 (dt, *J* = 9.4, 2.6 Hz, 2H, $CH_{2tetrahydropyranyl}$), 3.64 – 3.59 (m, 2H, $CH_{2tetrahydropyranyl}$), 3.40 (s, 3H, N3CH_3), 3.18 (s, 3H, N1CH_3), 3.13 (dd, *J* = 11.6, 2.3 Hz, 2H, NHC*H*$_2$$CH_2$), 3.01 (t, *J* = 7.3 Hz, 2H, NH-CH_2C*H*$_2$), 1.94 (ddp, *J* =

11.3, 7.5, 3.7 Hz, 1H, $CH_{tetrahydropyranyl}$), 1.33 (dd, *J* = 13.6, 3.5 Hz, 2H, $CH_{2tetrahydropyranyl}$), 1.28 – 1.19 (m, 2H, $CH_{2tetrahydropyranyl}$); **^{13}C NMR** (126 MHz, DMSO-*d*$_6$) δ 153.67, 152.54, 150.95, 148.56, 136.23, 127.29, 122.74, 120.80, 118.25, 118.12, 111.58, 111.29, 101.70, 66.44, 47.24, 43.21, 34.77, 29.35, 29.16, 27.13, 25.27 ; **LC-MS (m/z)**: 436.2 ($[M+H]^+$); **purity** by HPLC-UV (220 – 400 nm)-ESI-MS: 99.8%; **HRMS (ESI, m/z)** calcd for $C_{23}H_{28}N_6O_3$ $[M + H]^+$, 437.2296; found,437.2299.

8-((2-(1*H*-indol-3-yl)ethyl)amino)-1,3-dimethyl-7-((tetrahydrofuran-2-yl)methyl)-3,7-dihydro-1*H*-purine-2,6-dione (FPE-MP15)

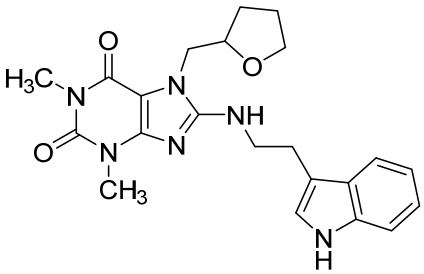

Synthesis according to **GP H**.**Yield**: 100 mg, 0.237 mmol, 45%; **M.p**.: 225°C; **^{1}H NMR** (600 MHz, DMSO-*d*$_6$) δ 10.81 (s, 1H, NH_{indole}), 7.64 (dd, *J* = 7.9, 1.1 Hz, 1H, Ar-H), 7.34 (d, *J* = 8.1 Hz, 1H, Ar-H), 7.18 (d, *J* = 2.3 Hz, 1H, Ar-H), 7.07 (ddd, *J* =8.0, 6.9, 1.1 Hz, 1H, Ar-H), 6.98 (ddd, *J* =8.0, 6.9, 1.0 Hz, 1H, Ar-H), 6.94 (t, *J* =5.7 Hz, 1H, *NH*CH_2), 4.14 – 3.98 (m, 3H, N7CH_2 and $H_{tetrahydrofuranyl}$), 3.66 (dt, *J* = 8.0, 6.7 Hz, 1H, $H_{tetrahydrofuranyl}$), 3.60 (q, *J* = 6.8 Hz, 2H, NH*CH_2*CH_2), 3.54 (td, *J* = 7.8, 6.1 Hz, 1H, $H_{tetrahydrofuranyl}$), 3.40 (s, 3H, N3CH_3), 3.18 (s, 3H, N1CH_3), 2.99 (t, *J* = 7.4 Hz, 2H, NHCH$_2$*CH_2*), 1.88 – 1.70 (m, 3H, 3 x $H_{tetrahydrofuranyl}$), 1.57 (ddt, *J* = 11.8, 7.7, 6.4 Hz, 1H, $H_{tetrahydrofuranyl}$); **^{13}C NMR** (151 MHz, DMSO-*d*$_6$) δ 154.12, 152.73, 150.95, 148.56, 136.26, 127.26, 122.83, 120.88, 118.30, 118.17, 111.49, 111.33, 101.74, 76.84, 67.18, 46.18, 43.27, 29.23, 27.93, 27.18, 25.31, 24.98; **LC-MS (m/z)**: 422.1 ($[M+H]^+$); **purity** by HPLC-UV (220 – 400 nm)-ESI-MS: 99.0 %; **HRMS (ESI, m/z)** calcd for $C_{22}H_{26}N_6O_3$ $[M + H]^+$, 423.2139; found, 423.2139.

***tert*-butyl (6-(4-((8-((2-(1*H*-indol-3-yl)ethyl)amino)-1,3-dimethyl-2,6-dioxo-1,2,3,6-tetrahydro-7*H*-purin-7-yl)methyl)benzamido)hexyl)carbamate (FPE-173)**

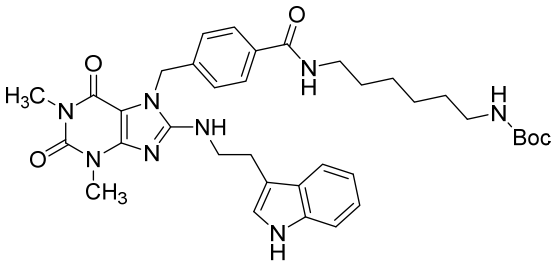

FPE-29 (1 g, 2.11 mmol, 1 eq) and tert-butyl (6-aminohexyl)carbamate hydrochloride (0.586 g, 2.32 mmol, 1.1 eq) were dissolved in pyridine (5 mL) and stirred at 0°C. Afterwards, $POCl_3$ (0.22 mL, 2.32 mmol, 1.1 eq) is carefully added dropwise. The

mixture is allowed to warm up to RT and stirred overnight. After no improvement was detected, it was quenched with a saturated aqueous solution of $NaHCO_3$ and extracted with EtOAc 3 times. Organic layers were combined, dried over $MgSO_4$ and concentrated under *vacuum*. Purification achieved with flash column chromatography on silica gel (MeOH in DCM 0 to 5%). **Yield:** 710 mg, 1.06 mmol, 50%;

or

FPE-29 (0.077 g, 0.16 mmol, 1.1 eq) and tert-butyl (6-aminohexyl)carbamate hydrochloride (0.031 g, 0.145 mmol, 1 eq). DIPEA (0.015 mL, 0.16 mmol, 1.1 eq) and COMU (0.1 g, 0.23 mmol, 1.6 eq) were dissolved in DMF (2 mL) and stirred at RT overnight. It is afterwards stirred at 50°C for further 2 hours. When no further improvement was detected, extraction was performed with EtOAC and water. Organic layers were combined, dried over $MgSO_4$ and concentrated under *vacuum*. Purification achieved with column chromatography on silica gel (MeOH in DCM 5%). **Yield:** 60 mg, 0.09 mmol, 56%;

M.p.: 182°C; **^{1}H NMR** (600 MHz, DMSO-*d*$_6$) δ 10.79 (d, *J* = 2.3 Hz, 1H, NH_{indole}), 8.33 (t, *J* = 5.7 Hz, 1H, CONH), 7.74 (d, *J* = 8.3 Hz, 2H, Ar-H_{benzyl}), 7.64 (d, *J* = 7.8 Hz, 1H, Ar-H), 7.39 (t, *J* = 5.7 Hz, 1H, C8-NH), 7.34 (d, *J* = 8.1 Hz, 1H, Ar-H), 7.24 (d, *J* = 8.2 Hz, 2H, Ar-H_{benzyl}), 7.12 (d, *J* = 2.2 Hz, 1H, Ar-H), 7.06 (ddd, *J* = 8.1, 6.9, 1.1 Hz, 1H, Ar-H), 6.98 (ddd, *J* = 7.8, 6.9, 1.0 Hz, 1H, Ar-H), 6.73 (t, *J* = 5.8 Hz, 1H, NHBoc), 5.33 (s, 2H, N7CH_2), 3.65 – 3.56 (m, 2H, C8-NH*CH_2*CH_2), 3.41 (s, 3H, N3CH_3), 3.22 (q, *J* = 6.6 Hz, 2H, CONH*CH_2*), 3.16 (s, 3H, N1CH_3), 2.98 (t, *J* = 7.6 Hz, 2H, C8-NHCH_2*CH_2*), 2.88 (q, *J* = 6.6 Hz, 2H, *CH_2*NHBoc), 1.48 (p, *J* = 7.6, 7.2 Hz, 2H, $CH_{2\text{-hexyl}}$), 1.35 (m, 11H, 3x CH_3 and 1x $CH_{2\text{-hexyl}}$), 1.26 (ttd, *J* = 14.9, 8.7, 8.0, 2.9 Hz, 4H, 2x $CH_{2\text{-hexyl}}$); **^{13}C NMR** (151 MHz, DMSO-*d*$_6$) δ 165.85, 155.54, 153.84, 152.72, 150.98, 148.95, 139.95, 136.24, 133.92, 127.30 (2C), 127.23, 126.67(2C), 122.78, 120.88, 118.29, 118.19, 111.49, 111.34, 101.21, 77.24, 45.11, 43.34, 40.06, 39.06, 29.41, 29.27, 29.07, 28.24 (3C), 27.16, 26.13, 25.98, 25.41; **LC-MS (m/z)**: 671.6 ($[M+H]^+$); **purity** by HPLC-UV (220 – 400 nm)-ESI-MS: 98.4%; **HRMS (ESI, m/z)** calcd for $C_{36}H_{46}N_8O_5$ $[M + H]^+$, 671.3664; found, 671.3666.

4-((8-((2-(1*H*-indol-3-yl)ethyl)amino)-1,3-dimethyl-2,6-dioxo-1,2,3,6-tetrahydro-7*H*-purin-7-yl)methyl)-*N*-(6-aminohexyl)benzamide hydrochloride (FPE-182)

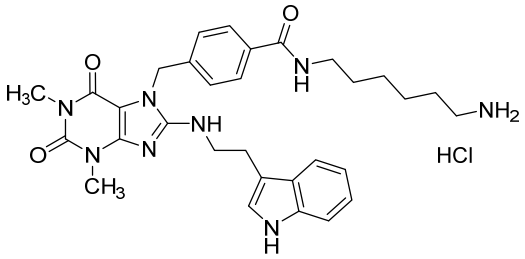

FPE-173 (700 mg, 1 mmol, 1 eq) was dissolved in MeOH 7 mL) and stirred at 0°C for 10 minutes. HCl 4N in dioxane (2 mL, 8 mmol, 8 eq) was then added dropwise. The mixture was allowed to warm to RT and stirred for 24 hours. Solvent was afterwards removed under *vacuum* and the obtained solid was recrystallized from Et_2O. **Yield**: 450mg, 0.74 mmol, 70%; **M.p.:** decomposed at 188°C; **^{1}H NMR** (600 MHz, DMSO-*d*$_6$) δ 10.83 (d, *J* = 2.7 Hz, 1H, NH_{indole}), 8.41 (t, *J* = 5.7 Hz, 1H, CONH), 7.76 (d, *J* = 8.3 Hz, 4H, Ar-H_{benzyl} and NH_2), 7.64 (d, *J* = 7.8 Hz, 1H, Ar-H), 7.46 (t, *J* = 5.7 Hz, 1H, C8-NH), 7.34 (d, *J* = 8.1 Hz, 1H, Ar-H), 7.25 (d, *J* = 8.0 Hz, 2H, Ar-H_{benzyl}), 7.12 (d, *J* = 2.2 Hz, 1H, Ar-H), 7.08 – 7.03 (m, 1H, Ar-H), 6.98 (t, *J* = 7.4 Hz, 1H, Ar-H), 5.34 (s, 2H, N7CH_2), 3.62 – 3.57 (m, 2H, C8-NH*CH_2*CH_2), 3.41 (s, 3H, N3CH_3)*, 3.24 (q, *J* = 6.6 Hz, 2H, CONH*CH_2*), 3.16 (s, 3H, N1CH_3), 2.98 (t, *J* = 7.6 Hz, 2H, C8-NHCH_2*CH_2*), 2.75 (td, *J* = 7.5, 5.5 Hz, 2H, *CH_2*NH_2), 1.51 (dq, *J* = 13.7, 7.1 Hz, 4H, 2x $CH_{2\text{-hexyl}}$), 1.32 (ddd, *J* = 12.7, 8.4, 4.6 Hz, 4H, 2x $CH_{2\text{-hexyl}}$); **^{13}C NMR** (151 MHz, DMSO-*d*$_6$) δ 165.88, 153.87, 152.73, 150.99, 148.98, 140.03, 136.25, 133.85, 127.33 (2C), 127.23, 126.74 (2C), 122.80, 120.88, 118.30, 118.19, 111.48, 111.37, 101.20 45.12, 43.34, 38.94, 38.69, 29.29, 28.90, 27.17, 26.89, 25.89, 25.47, 25.41; **LC-MS** (m/z): 605.6 ([M-H]$^-$); **purity** by HPLC-UV (220 – 400 nm)-ESI-MS: 98.0%; **HRMS** (ESI, m/z) calcd for $C_{31}H_{38}N_8O_3$ $[M + H]^+$, 571.3140; found, 571.3152. *partially overlaps with the shifted water peak

***tert*-butyl (2-(2-(2-(4-((8-((2-(1*H*-indol-3-yl)ethyl)amino)-1,3-dimethyl-2,6-dioxo-1,2,3,6-tetrahydro-7*H*-purin-7-yl)methyl)benzamido)ethoxy)ethoxy)ethyl)carbamate (FPE-191)**

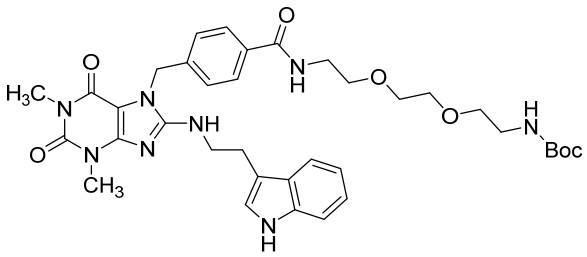

FPE-29 (0.4 g, 0.85 mmol, 1 eq) and tert-butyl (2-(2-(2-aminoethoxy)ethoxy)ethyl)carbamate (0.23 g, 0.93 mmol, 1.1 eq) were dissolved in pyridine (5 mL) and stirred at 0°C. Afterwards, $POCl_3$ (0.086 mL, 0.93 mmol, 1.1 eq) is carefully added dropwise. The mixture is allowed to warm up to RT and stirred overnight. After no improvement was detected, it was quenched with a saturated aqueous solution of $NaHCO_3$ and

extracted with EtOAc 3 times. Organic layers were combined, dried over $MgSO_4$ and concentrated under *vacuum*. Purification achieved with flash column chromatography on silica gel (MeOH in DCM 0 to 5%). **Yield:** 150 mg, 0.21 mmol, 25%; **M.p.**: 120°C; **^{1}H NMR** (600 MHz, DMSO-*d*$_6$) δ 10.78 (d, *J* = 1.7 Hz, 1H, NH_{indole}), 8.42 (t, *J* = 5.7 Hz, 1H, CONH), 7.76 (d, *J* = 8.3 Hz, 2H, Ar-H_{benzyl}), 7.64 (d, *J* = 7.9 Hz, 1H, Ar-H), 7.38 (t, *J* = 5.7 Hz, 1H, *NH*CH_2), 7.34 (d, *J* = 8.1 Hz, 1H, Ar-H), 7.25 (d, *J* = 8.1 Hz, 2H, Ar-H_{benzyl}), 7.12 (d, *J* = 2.2 Hz, 1H, Ar-H), 7.06 (ddd, *J* = 8.2, 7.0, 1.2 Hz, 1H, Ar-H), 6.98 (ddd, *J* = 7.9, 6.9, 1.0 Hz, 1H, Ar-H), 6.72 (t, *J* = 5.3 Hz, 1H, *NH*Boc), 5.33 (s, 2H, N7CH_2), 3.60 (dt, *J* = 7.9, 5.7 Hz, 2H, NH*CH*$_2$$CH_2$), 3.53 – 3.47 (m, 6H, 3x $CH_{2\text{-PEG}}$), 3.42 – 3.35 (m, 7H, N3CH_3 and 2x $CH_{2\text{-PEG}}$), 3.16 (s, 3H, N1CH_3), 3.04 (q, *J* = 6.0 Hz, 2H, $CH_{2\text{-PEG}}$), 2.98 (t, *J* = 7.5 Hz, 2H, NHCH$_2$*CH*$_2$), 1.35 (s, 9H, 3x CH_3); **^{13}C NMR** (151 MHz, DMSO-*d*$_6$) δ 166.07, 155.56, 153.85, 152.74, 151.00, 148.96, 140.14, 136.26, 133.58, 127.37(2C), 127.25, 126.71 (2C), 122.79, 120.90, 118.30, 118.21, 111.50, 111.36, 101.23, 77.56, 69.56, 69.46, 69.15, 68.91, 45.12, 43.35, 40.06, 39.17, 29.29, 28.19 (3C), 27.17, 25.42; **LC-MS (m/z)**: 703.9 ([M+H]$^+$); **purity** by HPLC-UV (220 – 400 nm)-ESI-MS: 98.9%; **HRMS (ESI, m/z)** calcd for $C_{36}H_{46}N_8O_7$ [M + H]$^+$, 703.3562; found,703.3566.

4-((8-((2-(1*H*-indol-3-yl)ethyl)amino)-1,3-dimethyl-2,6-dioxo-1,2,3,6-tetrahydro-7*H*-purin-7-yl)methyl)-*N*-(2-(2-(2-aminoethoxy)ethoxy)ethyl)benzamide hydrochloride (FPE-201)

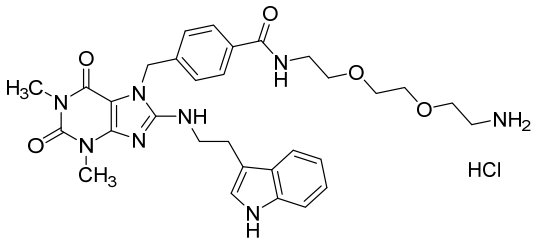

FPE-191 (123 mg, 0.18 mmol, 1 eq) was dissolved in MeOH (3 mL) and stirred at 0°C for 10 minutes. HCl 4N in dioxane (0.28 mL, 1.1 mmol, 6 eq) was then added dropwise. The mixture was allowed to warm to RT and stirred for 24 hours. Solvent was afterwards removed under *vacuum* and the obtained solid was recrystallized from Et_2O. **Yield**: 78 mg, 0.13 mmol, 70%; **M.p.:** 198°C; **^{1}H NMR** (600 MHz, DMSO-*d*$_6$) δ 10.85 (d, *J* = 2.2 Hz, 1H, NH_{indole}), 8.52 (t, *J* = 5.7 Hz, 1H, CONH), 7.92 (s.br., 3H, NH_3^+), 7.78 (d, *J* = 8.3 Hz, 2H,Ar-H_{benzyl}), 7.64 (d, *J* = 7.8 Hz, 1H, Ar-H), 7.49 (t, *J* = 5.4 Hz, 1H, *NH*CH_2), 7.34 (d, *J* = 8.1 Hz, 1H, Ar-H), 7.26 (d, *J* = 8.1 Hz, 2H, Ar-H_{benzyl}), 7.12 (d, *J* = 2.2 Hz, 1H, Ar-H), 7.06 (ddd, *J* = 8.1, 6.9, 1.2 Hz, 1H, Ar-H), 6.97 (ddd, *J* = 8.0, 6.9, 1.0 Hz, 1H, Ar-H), 5.35 (s, 2H, N7CH_2), 3.63 – 3.51 (m, 10H, NH*CH*$_2$$CH_2$ and 4x $CH_{2\text{-PEG}}$), 3.41 (d, *J* = 5.5 Hz, 5H, N3CH_3 and $CH_{2\text{-PEG}}$), 3.15 (s, 3H, N1CH_3), 2.98 (t, *J* = 7.5 Hz, 2H, NHCH$_2$*CH*$_2$), 2.93 (q, *J* = 5.5 Hz, 2H, $CH_{2\text{-PEG}}$); **^{13}C NMR** (151 MHz,

DMSO-*d*$_6$) δ 166.06, 153.86, 152.73, 150.98, 148.96, 140.21, 136.25, 133.50, 127.38 (2C), 127.23, 126.78 (2C), 122.80, 120.86, 118.29, 118.17, 111.46, 111.36, 101.19, 69.67, 69.43, 68.87, 66.59, 45.12, 43.32, 38.50, 38.42, 29.29, 27.17, 25.39; **LC-MS (m/z)**: 603.5 ([M+H]$^+$); **purity** by HPLC-UV (220 – 400 nm)-ESI-MS: 98.9%; **HRMS (ESI, m/z)** calcd for $C_{31}H_{38}N_8O_5$ [M + H]$^+$, 603.3038; found, 603.3062.

4-((8-((2-(1*H*-indol-3-yl)ethyl)amino)-1,3-dimethyl-2,6-dioxo-1,2,3,6-tetrahydro-7*H*-purin-7-yl)methyl)-*N*-(4,7,10,13-tetraoxa-16-azadocos-1-yn-22-yl)benzamide (FPE-209)

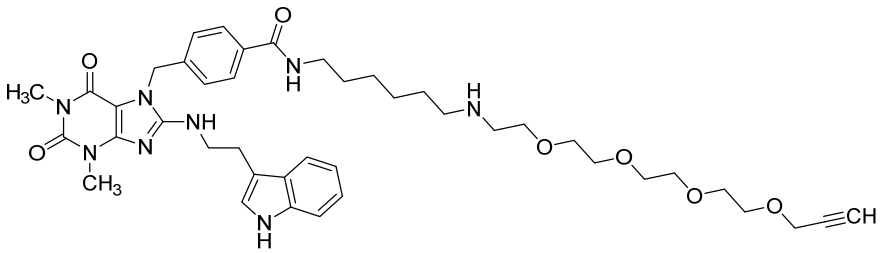

A round-bottomed flask is flushed with argon and then it is charged with **FPE-182** (180 mg, 0.3 mmol, 1 eq), K_2CO_3 (50 mg, 0.36 mmol, 1.2 eq) and dry DMF and the mixture is stirred at RT for 30 mins. Then propargyl-PEG4-bromide (106 mg, 0.36 mmo, 1.2 eq) is added and the mixture is stirred at RT overnight. When checked no much improvement was detected, therefore temperature is raised at 80°C and the mixture stirred for additional 6 hours. When no further improvement was detected, it was allowed to warm up to RT and an extraction was performed with water and EtOAc. Organic layers were combined, dried over $MgSO_4$ and concentrated in *vacuum*. Purification was achieved with flash column chromatography on silica gel (MeOH in DCM 0 to 7%). **Yield**: 25 mg, 0.032 mmol, 11%; **M.p.**: 236°C; **^{1}H NMR** (600 MHz, DMSO-*d*$_6$) δ 10.79 (d, *J* = 2.4 Hz, 1H, NH_{indole}), 8.33 (t, *J* = 5.7 Hz, 1H, CONH — exchanges with D_2O), 7.74 (d, *J* = 8.0 Hz, 2H, Ar-H_{benzyl}), 7.64 (d, *J* = 7.9 Hz, 1H, Ar-H), 7.39 (t, *J* = 5.6 Hz, 1H, *NH*CH_2 — exchanges with D_2O), 7.33 (d, *J* = 8.1 Hz, 1H, Ar-H), 7.24 (d, *J* = 8.0 Hz, 2H, Ar-H_{benzyl}), 7.12 (d, *J* = 2.2 Hz, 1H, Ar-H), 7.06 (t, *J* = 7.5 Hz, 1H, Ar-H), 6.98 (t, *J* = 7.4 Hz, 1H, Ar-H), 5.33 (s, 2H, N7CH_2), 4.13 (d, *J* = 2.4 Hz, 2H, *CH_2*C≡CH), 3.60 (q, *J* = 7.8, 7.2 Hz, 2H, NH*CH_2*CH_2), 3.56 – 3.46 (m, 12H, N3CH_3 and 4 x CH_{2PEG} and C≡CH), 3.46 – 3.37 (m, 6H, 3x CH_{2PEG}), 3.22 (q, *J* = 6.6 Hz, 2H, CONH*CH_2*), 3.16 (s, 3H, N1CH_3), 2.98 (t, *J* = 7.5 Hz, 2H, NHCH$_2$*CH_2*), 2.66 – 2.60 (m, 2H, *CH_2*NHCH$_2$), 1.49 (q, *J* = 6.9 Hz, 2H, $CH_{2\text{-hexyl}}$), 1.38 (t, *J* = 6.9 Hz, 2H, $CH_{2\text{-hexyl}}$), 1.33 – 1.20 (m, 4H, 2x $CH_{2\text{-hexyl}}$)*; **^{13}C NMR** (151 MHz, DMSO-*d*$_6$) δ 165.83, 153.84, 152.73, 150.98, 148.95, 139.94, 136.24, 133.92, 127.30 (2C), 127.23, 126.67(2C), 122.77, 120.87, 118.29, 118.19, 111.49, 111.34, 101.20, 80.29, 77.01, 70.00, 69.73,

69.57, 69.46, 68.48, 57.45, 49.22, 48.74, 45.10, 43.33, 40.18, 40.06, 29.49, 29.27, 29.10, 27.15, 26.55, 26.42, 25.40; **LC-MS** (m/z): 785.9 ([M-H]$^+$); **purity** by HPLC-UV (220 – 400 nm)-ESI-MS: 99.4%; **HRMS** (ESI, m/z) calcd for $C_{42}H_{56}N_8O_7$ [M + H]$^+$, 785.4345; found, 785.4342. *In the D_2O exchanged ^{1}H NMR, due to the shift of the ppms of water and DMSO and simplification of the multiplicity it is possible to see the signal: 2.45 (t, *J* = 7.5 Hz, 2H, NH*CH*$_2$CH$_2$O), while it remains difficult to clearly identify CH$_2$*NH*CH$_2$ both in DMSO and D_2O exchanged.

8-((2-(1*H*-indol-3-yl)ethyl)amino)-7-((1-benzyl-1*H*-1,2,3-triazol-4-yl)methyl)-1,3-dimethyl-3,7-dihydro-1*H*-purine-2,6-dione (FPE-144)

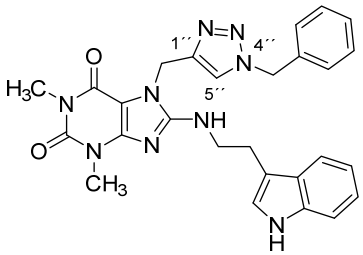

FPE-137 (0.38 g, 1 mmol, 1 eq) and benzylazide (150 µL, 1.3 mmol, 1.3 eq) were suspended in 4 ml of a water and tertbutyl alcohol mixture (1:1). Sodium ascorbate (0.1 mmol, 100 µL of a freshly prepared 1M solution in water) was then added, followed by copper (II) sulfate pentahydrate (5 mg, 0.02 mmol, 0.02 eq, in 70 µL of water). The mixture is stirred at 60°C for 24h. When no further improvement was detected, the reaction was allowed to warm to RT and quenched by the addition of ice-cold water achieving precipitation. This crude was then further purified by flash column chromatography on silica gel (EtOAc in cyclohexane 0 to 20%) **. Yield:** 40 mg, 0.079 mmol, 8%, **M.p.** 216°C; **^{1}H NMR** (600 MHz, DMSO-*d*$_6$) δ 10.79 (s, 1H, NH$_{indole}$), 7.94 (s, 1H, 5´´-H), 7.64 (d, *J* = 7.8 Hz, 1H, Ar-H), 7.39 – 7.22 (m, 7H, 6 Ar-H and *NH*CH$_2$), 7.15 (d, *J* = 2.3 Hz, 1H, Ar-H$_{indole}$), 7.07 (ddd, *J* = 8.1, 6.9, 1.1 Hz, 1H, Ar-H$_{indole}$), 6.98 (td, *J* = 7.4, 7.0, 1.0 Hz, 1H, Ar-H$_{indole}$), 5.54 (s, 2H, N4´´-*CH*$_2$), 5.35 (s, 2H, N7CH$_2$), 3.58 (ddd, *J* = 9.2, 7.6, 5.7 Hz, 2H, NH*CH*$_2$CH$_2$), 3.39 (s, 3H, N3CH$_3$), 3.17 (s, 3H, N1CH$_3$), 2.95 (dd, *J* = 8.8, 6.5 Hz, 2H, NHCH$_2$*CH*$_2$); **^{13}C NMR** (151 MHz, DMSO-*d*$_6$) δ * δ 153.83, 152.70, 150.99, 148.84, 143.04 (C1´´), 136.23, 135.99, 128.65 (2C), 128.06, 127.87 (2C), 127.23, 123.14, 122.73 (C5´´), 120.89, 118.28, 118.18, 111.51, 111.35, 101.12, 52.68, 43.35, 37.95, 29.23, 27.15, 25.45; **LC-MS (m/z)**: 510.4 ([M+H]$^+$); **purity** by HPLC-UV (220 – 400 nm)-ESI-MS: 97.9%; **HRMS (ESI, m/z)** calcd for $C_{27}H_{27}N_9O_2$ [M + H]$^+$, 510.2360; found, 510.2362. *triazole carbons assigned on the basis of the overlap with **FPE-199.**

5.2.3 Synthesis of intermediates for xanthine scaffold modifications

6-(2-(Dimethylamino)vinyl)-1,3-dimethyl-5-nitropyrimidine-2,4(1*H*,3*H*)-dione (FPE-64)[154]

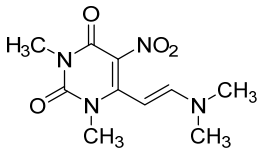

1,3,6-trimethyl-5-nitropyrimidine-2,4(1*H*,3*H*)-dione (0.5 g, 2.5 mmol, 1 eq) was suspended in dry DMF (2 mL). DMF diethylacetal (0.55 g, 3.75 mmol, 1.5 eq), was then added and the mixture stirred at RT for 2.5 hours. Addition of diethyl ether led to precipitation of a deep orange solid. **Yield**: 126 mg, 0.5 mmol, 20%; **LC-MS (m/z)**: 254.8 ([M+H]$^+$); **purity** by HPLC-UV (220 – 400 nm)-ESI-MS: 99.0%.

1,3-Dimethyl-1,5-dihydro-2*H*-pyrrolo[3,2-d]pyrimidine-2,4(3*H*)-dione (FPE-66)[154]

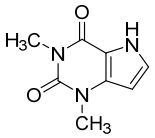

To a suspension of **FPE-64** (0.120 g, 0.47 mmol, 1 eq) in MeOH (5 mL), Pd/C (10 mg) was added under Argon. The mixture was stirred at RT for 2 hours under H_2 atmosphere. The mixture was treated with 15% aq. NaOH and was then filtered over celite and washed with MeOH. Treatment with conc. HCl released the free acid. Purification was achieved by flash column chromatography (MeOH in DCM 0 to 3%). **Yield:** 35 mg, 0.19 mmol, 41%; %; **LC-MS (m/z)**: 180.0 ([M+H]$^+$); **purity** by HPLC-UV (220 – 400 nm)-ESI-MS: 81.0%.

5-(4-Chlorobenzyl)-1,3-dimethyl-1,5-dihydro-2*H*-pyrrolo[3,2-d]pyrimidine-2,4(3*H*)-dione (FPE-71)

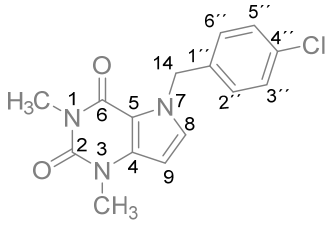

Synthesis according to **GP F**. **Yield:** 25 mg, 0.083 mmol, 44%. **^{1}H NMR (**600MHz**,** DMSO-d_6) δ 7.49 (d, J = 2.88 Hz, 1H, C8-H), 7.37 (m, 2H, Ar), 7.24 (dd, J = 5.01, 8.41 Hz, 2H, Ar), 6.22 (d, J = 2.93 Hz, 1H, C9-H)), 5.51 (s, 2H, N7-CH), 3.37 (s, 3H, CH_3), 3.20 (s, 3H, CH_3); **^{13}C NMR** (151 MHz, DMSO-d_6) δ Analysis hindered by impurities and low signal-to-noise ratio. **LC-MS (m/z)**: 303.9 ([M+H]$^+$); **purity** by HPLC-UV (220 – 400 nm)-ESI-MS: 73.0%.

6-amino-1,3-dimethyl-2-thioxo-2,3-dihydropyrimidin-4(1*H*)-one (FPE-MP1)

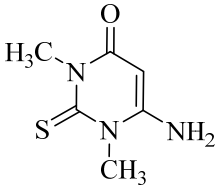

To a stirred solution of 1,3-dimethylthiourea (1.000 g, 9.615 mmol, 1 eq.) in acetic anhydride (10 mL) was added cyanoacetic acid (0.817 g, 9.615 mmol, 1 eq.), and the resulting mixture was transferred into a sealed vessel and heated by microwave irradiation at 70°C (200W) for 2 hours. The reaction mixture was concentrated and the resulting oily residue was diluted with H_2O (20 mL) and treated with an aqueous solution of NaOH 4N until pH 10. An orange precipitate was formed and it was collected by filtration. **Yield:** 0.906 g, 6.22 mmol, 65 %**; M.p.:** 136°C; **LC-MS (2022-11-02)** (m/z)**:** 171.0 ($[M+H]^+$); **purity** by HPLC-UV (220 – 400 nm)-ESI-MS: 96.1%; **^{1}H NMR** (500 MHz, DMSO-d_6) δ 7.01 (s, 2H –NH_2), 5.03 (s, 1H, -CH), 3.75 (s, 3H, -CH_3), 3.52 (s, 3H, -CH_3); **^{13}C NMR** (126 MHz, DMSO-d_6) δ 177.12, 159.17, 154.84, 79.40, 37.10, 34.86.

6-amino-5-((4-chlorobenzyl)amino)-1,3-dimethyl-2-thioxo-2,3-dihydropyrimidin -4(1*H*)-one (FPE-MP9)

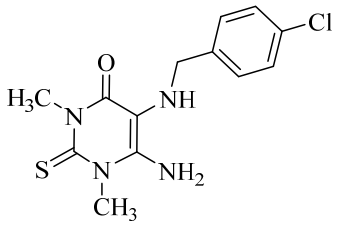

Synthesis according to **GPA** using **FPE-MP1**. **Yield:** 248.9 mg, 0.799 mmol, 44%; **M.p.**: 175°C; **LC-MS (m/z):** 310.8 ($[M+H]^+$); **purity** by HPLC-UV (220 – 400 nm)-ESI-MS: 94.0%; **^{1}H NMR** (500 MHz, DMSO-d_6) δ 7.42 (d, J = 8.5 Hz, 2H), 7.34 (d, J = 8.4 Hz, 2H), 6.65 (s, 2H), 3.88 (d, J = 6.4 Hz, 2H), 3.80 (s, 3H), 3.58 (s, 3H); **^{13}C NMR** (126 MHz, DMSO-d_6) δ 174.23, 158.21, 151.23, 139.35, 131.21, 130.11, 127.85, 101.50, 50.04, 38.00, 35.18

7-(4-chlorobenzyl)-1,3-dimethyl-2-thioxo-1,2,3,7-tetrahydro-6*H*-purin-6-one (FPE-MP10)

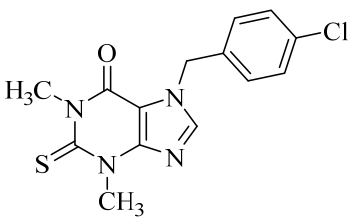

Synthesis according to **GP C**. **Yield**: 215.5 mg, 0.672 mmol, 84 %; **LC-MS (m/z):** 320 ($[M+H]^+$); **purity** by HPLC-UV (220 – 400 nm)-ESI-MS: 99.1%; **M.p.**: 214°C; **^{1}H NMR** (600 MHz, DMSO-d_6) δ 8.43 (s, 1H), 7.41 (d, J = 8.5 Hz, 2H), 7.36 (d, J = 8.5 Hz, 2H), 5.53 (s, 2H), 3.86 (s, 3H), 3.65 (s, 3H); **^{13}C NMR** (151 MHz, DMSO-d_6) δ 174.76, 153.02, 148.79, 143.40, 135.69, 132.62, 129.40, 128.65, 109.03, 48.55, 36.69, 34.59.

5.2.4 Synthesis of intermediates and finished products for the study of the indolylethylamino moiety

_N_-(6-amino-1,3-dimethyl-2,4-dioxo-1,2,3,4-tetrahydropyrimidin-5-yl)-4-(1_H_-indol-3-yl)butanamide (FPE-170)

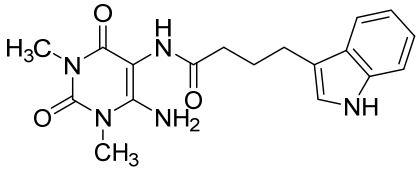

To a solution of 4-(1*H*-indol-3-yl)butanoic acid (65 mg, 0.32 mmol, 1.1 eq) in DMF was added COMU (137 mg, 0.32 mmol, 1 eq) and the mixture was stirred at RT for 10 minutes. Afterwards a solution of **FPE-116** (50 mg. 0.29 mmol, 1 eq) and DIPEA (0.03 mL, 0.32 mmol, 1.1 eq) in DMF was added dropwise. The mixture is further stirred at RT for 30 minutes. When no improvement was detected, the crude was partitioned between H_2O and EtOAc. Organic layers were combined, dried over $MgSO_4$ and concentrated in *vacuum*. **Yield**: 80 mg, 0.23 mmol, 77% ; **M.p.:** 187°C; **^{1}H NMR** (500 MHz, DMSO-d_6) δ 10.73 (d, J = 2.2 Hz, 1H, NH_{indole}), 8.28 (s, 1H, NHCO), 7.54 (dd, J = 7.9, 1.2 Hz, 1H, Ar-H), 7.33 (d, J = 8.1 Hz, 1H, Ar-H), 7.13 (d, J = 2.2 Hz, 1H, Ar-H), 7.05 (ddd, J = 8.1, 7.0, 1.2 Hz, 1H, Ar-H), 6.96 (ddd, J = 8.0, 7.0, 1.0 Hz, 1H, Ar-H), 6.50 (s, 2H, NH_2), 3.30 (s, 3H, N3CH_3), 3.11 (s, 3H, N1CH_3), 2.73 (t, J = 7.5 Hz, 2H, $COCH_2CH_2CH_2$), 2.31 (t, J = 7.5 Hz, 2H, $COCH_2CH_2CH_2$), 1.91 (p, J = 7.6 Hz, 2H, $COCH_2CH_2CH_2$); **^{13}C NMR** (126 MHz, DMSO-d_6) δ 172.81, 159.24, 151.94, 150.51, 136.25, 127.19, 122.19, 120.66, 118.32, 117.95, 114.30, 111.18, 87.71, 35.00, 29.89, 27.41, 25.84, 24.30; **LC-MS (m/z)**: 354.2 ($[M+H]^+$); **purity** by HPLC-UV (220 – 400 nm)-ESI-MS: 100%.

8-(3-(1*H*-indol-3-yl)propyl)-1,3-dimethyl-3,7-dihydro-1*H*-purine-2,6-dione (FPE-171)

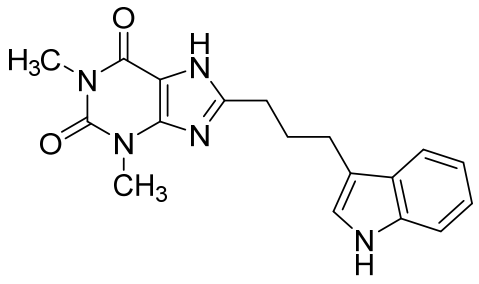

FPE-170 (0.08 g, 0.23 mmol, was dissolved in 4N NaOH (2 mL). The mixture was stirred at 70°C for 10 minutes. The crude was then extracted with EtOAc, Organic layers were combined, dried over $MgSO_4$ and concentrated in *vacuum*. **Yield**: 43 mg, 0.12 mmol, 52%; **M.p**.:178°C; **^{1}H NMR** (600 MHz, DMSO-d_6) δ 13.15 (s, 1H, N7-H), 10.76 (s, NH_{indole}), 7.51 (d, J = 7.8 Hz, 1H, Ar-H), 7.33 (d, J = 8.1 Hz, 1H, Ar-H), 7.13 (d, J = 2.2 Hz, 1H, Ar-H), 7.07 – 7.03 (m, 1H, Ar-H), 6.99 – 6.93 (m, 1H, Ar-H), 3.58 – 3.52 (m, 2H,

CH$_2$CH$_2$CH$_2$), 3.42 (s, 3H, N3CH$_3$), 3.22 (s, 3H, N1CH$_3$), 3.09 – 3.04 (m, 2H, CH$_2$CH$_2$*CH*$_2$), 2.07 (p, *J* = 7.6 Hz, 2H, CH$_2$*CH*$_2$CH$_2$); **^{13}C NMR** (151 MHz, DMSO-*d*$_6$) δ analysis hindered by impurities and low signal-to-noise ratio; **LC-MS (m/z)**: 338.2 ([M+H]$^+$); **purity** by HPLC-UV (220 – 400 nm)-ESI-MS: 90.3%.

8-(3-(1*H*-indol-3-yl)propyl)-7-(4-chlorobenzyl)-1,3-dimethyl-3,7-dihydro-1*H*-purine-2,6-dione (FPE-172)

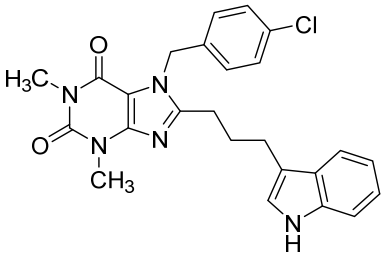

Synthesis according to **GP F**. **Yield**: 20 mg, 0.041 mmol, 35%; **M.p.:** 170°C; **^{1}H NMR** (600 MHz, DMSO-*d*$_6$) δ 10.77 (s, 1H, NH$_{indole}$), 7.45 (d, *J* = 7.9 Hz, 1H, Ar-H), 7.33 (dd, *J* = 8.1, 5.1 Hz, 3H, 2 Ar-H$_{benzyl}$ and Ar-H$_{indole}$), 7.11 (d, *J* = 8.1 Hz, 2H, Ar-H$_{benzyl}$), 7.08 – 7.03 (m, 2H, Ar-H), 6.95 (t, *J* = 7.4 Hz, 1H, Ar-H), 5.47 (s, 2H, N7CH$_2$), 3.42 (s, 3H, N3CH$_3$), 3.21 (s, 3H, N1CH$_3$), 2.77 – 2.67 (m, 4H, 2x CH$_2$), 1.94 (p, *J* = 7.6 Hz, 2H, CH$_2$*CH*$_2$CH$_2$); **^{13}C NMR** (151 MHz, DMSO-*d*$_6$) δ 154.38, 154.30, 150.89, 147.71, 136.27, 135.67, 132.28, 128.67 (2C), 128.66 (2C), 127.03, 122.35, 120.80, 118.27, 118.08, 113.64, 111.28, 105.84, 46.42, 29.38, 27.84, 27.48, 25.78, 24.11; **LC-MS (m/z)**: 462.2 ([M+H]$^+$); **purity** by HPLC-UV (220 – 400 nm)-ESI-MS: 96.5%; **HRMS (ESI, m/z)** calcd for C$_{25}$H$_{24}$ClN$_5$O$_2$ [M + H]$^+$, 462.1691; found, 462.1694.

8-(2-(1*H*-indol-3-yl)ethyl)-1,3-dimethyl-3,7-dihydro-1*H*-purine-2,6-dione (FPE-181)

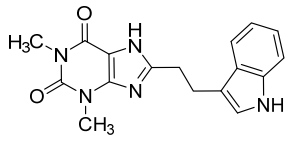

To a solution of 4-(1*H*-indol-3-yl)propanoic acid (61 mg, 0.32 mmol, 1.1 eq) in DMF was added COMU (137 mg, 0.32 mmol, 1 eq) and the mixture was stirred at RT for 10 minutes. Afterwards a solution of **FPE-116** (50 mg. 0.29 mmol, 1 eq) and DIPEA (0.03 mL, 0.32 mmol, 1.1 eq) in DMF was added dropwise. The mixture is further stirred at RT for 30 minutes. When no improvement was detected, the crude was partitioned between H$_2$O and EtOAc. Organic layers were combined, dried over MgSO$_4$ and concentrated in *vacuum*. This crude was then dissolved in 4N NaOH (2 mL) and stirred at 70°C for 10 minutes. When no improvement was detected, it was extracted with EtOAc. Organic layers were combined, dried over MgSO$_4$ and concentrated in *vacuum.* **Yield**: 34 mg, 0.11 mmol, 35% (over 2 steps); **M.p.**: 180°C; **LC-MS (m/z)**: 324.1 ([M+H]$^+$); **purity** by HPLC-UV (220 – 400 nm)-ESI-MS: 65.0%. The crude is used without further purification.

8-(2-(1*H*-indol-3-yl)ethyl)-7-(4-chlorobenzyl)-1,3-dimethyl-3,7-dihydro-1*H*-purine-2,6-dione (FPE-185)

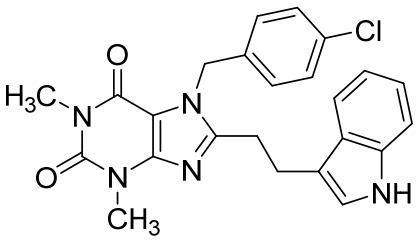

Synthesis according to **GP F**. **Yield**: 10 mg, 0.02 mmol, 20%; **M.p.:** 243°C**; ^{1}H NMR** (600 MHz, DMSO-*d*$_6$) δ 10.78 (s, 1H, NH$_{indole}$), 7.34 (dt, *J* = 8.1, 5.7 Hz, 4H, Ar-H), 7.13 – 7.08 (m, 3H, Ar-H), 7.08 – 7.01 (m, 1H, Ar-H), 6.94 (t, *J* = 7.4 Hz, 1H, Ar-H), 5.46 (s, 2H, N7CH$_2$), 3.48 (s, 3H, N3CH$_3$), 3.21 (s, 3H, N1CH$_3$), 3.03 (m, 4H, 2x CH$_2$); **^{13}C NMR** (151 MHz, DMSO-*d*$_6$) δ 154.48, 154.31, 151.10, 147.95, 136.31, 135.84, 132.40, 128.82 (2C), 128.66 (2C), 126.96, 122.83, 121.11, 118.41, 118.20, 113.01, 111.53, 106.07, 46.54, 29.64, 27.67, 27.57, 22.90; **LC-MS (m/z)**: 448.2 ([M+H]$^+$); **purity** by HPLC-UV (220 – 400 nm)-ESI-MS: 94.0%; **HRMS (ESI, m/z)** calcd for $C_{24}H_{22}ClN_5O_2$ [M + H]$^+$, 448.1535; found, 448.1534.

8-((2-(benzofuran-3-yl)ethyl)amino)-7-(4-chlorobenzyl)-1,3-dimethyl-3,7-dihydro-1*H*-purine-2,6-dione (FPE-203)

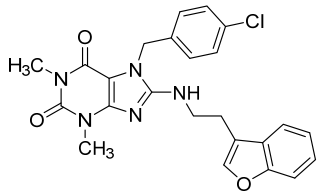

Synthesis according to **GP H** using 2-(benzofuran-3-yl)ethan-1-amine and **FPE-50** as the coupling partners. **Yield**: 70 mg, 0.16 mmol, 24%; **M.p**.: 198°C; **^{1}H NMR** (600 MHz, DMSO-*d*$_6$) δ 7.73 – 7.69 (m, 2H, Ar-H), 7.54 (d, *J* = 8.1 Hz, 1H, Ar-H), 7.40 (t, *J* = 5.7 Hz, 1H, *NH*CH$_2$), 7.34 – 7.32 (m, 2H, Ar-H$_{benzyl}$), 7.32 – 7.28 (m, 1H, Ar-H), 7.25 (t, *J* = 7.4 Hz, 1H, Ar-H), 7.19 (d, *J* = 8.3 Hz, 2H, Ar-H$_{benzyl}$), 5.26 (s, 2H, N7CH$_2$), 3.65 (q, *J* = 6.6 Hz, 2H, NH*CH$_2$*CH$_2$), 3.37 (s, 3H, N3CH$_3$), 3.16 (s, 3H, N3CH$_3$), 2.96 (t, *J* = 7.0 Hz, 2H, NHCH$_2$*CH$_2$*); **^{13}C NMR** (151 MHz, DMSO-*d*$_6$) δ 154.58, 153.53, 152.77, 150.93, 148.82, 142.41, 135.94, 131.99, 128.85 (2C), 128.39 (2C), 127.87, 124.20, 122.40, 119.73, 117.28, 111.24, 101.18, 44.65, 41.94, 29.25, 27.16, 23.38; ; **LC-MS (m/z)**: 464.2 ([M+H]$^+$); **purity** by HPLC-UV (220 – 400 nm)-ESI-MS: 97.7%; **HRMS (ESI, m/z)** calcd for $C_{24}H_{22}ClN_5O_3$ [M + H]$^+$, 464.1484; found, 464.1496.

3-(2-nitrovinyl)-3*H*-pyrrolo[2,3-b]pyridine (FPE-MP14)

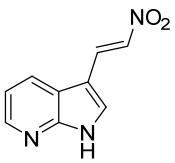

Starting material (0.6 g, 4.103 mmol, 1 eq) was dissolved in nitromethane (6 mL) and afterwards ammonium acetate (0.144 g, 2.052 mmol, 0.5 eq) was added to the solution. The reaction mixture was stirred at 110ºC under reflux for 2h and TLC monitoring was performed to see the consumption of the starting material. The reaction mixture was cooled down in an ice bath to achieve the precipitation of the product, which was filtered under reduced pressure and washed with methanol. **Yield**: 667 mg, 3.526 mmol, 86 %; **LC-MS** (m/z)**:** 189 ($[M+H]^+$); **purity** by HPLC-UV (220 – 400 nm)-ESI-MS: 99.6%; **^{1}H NMR** (500 MHz, DMSO-d_6) δ 12.68 (s, 1H), 8.46 (dd, *J* = 8.0, 1.6 Hz, 1H), 8.38 – 8.34 (m, 3H), 8.07 (d, *J* = 13.5 Hz, 1H), 7.25 (dd, *J* = 7.9, 4.7 Hz, 1H)**; ^{13}C NMR** (126 MHz, DMSO-d_6) δ 149.80, 144.44, 136.11, 134.03, 132.28, 129.03, 117.66, 116.98, 106.74.

3-(2-nitrovinyl)benzo[b]thiophene (FPE-MP17)

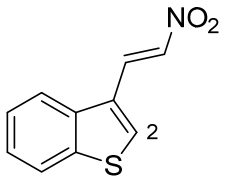

Benzothiophene-3-carbaldehyde (1 g, 6.165 mmol, 1 eq) was dissolved in nitromethane and afterwards ammonium acetate (0.24 g, 3.082 mmol, 0.5 eq) was added to the reaction mixture, stirred and heated at 110ºC under reflux for 2h. After TLC monitoring, the reaction mixture was cooled down in an ice bath to achieve the precipitation of the compound which was filtered under reduced pressure to obtain. **Yield**: 570 mg, 2.78 mmol, 45 %; **M.p.:** 96°C; **^{1}H NMR** (600 MHz, DMSO-d_6) δ 8.71 (s, 1H, C2-H), 8.42 (d, *J* = 13.6 Hz, 1H, CH_{vinyl}), 8.28 (d, *J* = 13.6 Hz, 1H, CH_{vinyl}), 8.24 (d, *J* = 7.9 Hz, 1H, Ar-H), 8.12 (d, *J* = 8.1 Hz, 1H, Ar-H), 7.54 (ddd, *J* = 8.1, 7.1, 1.2 Hz, 1H, Ar-H), 7.50 (td, *J* = 7.5, 1.2 Hz, 1H, Ar-H); **^{13}C NMR** (151 MHz, DMSO-d_6) δ 139.75, 137.46, 136.36, 134.95, 130.92, 126.81, 125.53, 125.45, 123.39, 122.48; **LC-MS (m/z)**: 206.1 ($[M+H]^+$); **purity** by HPLC-UV (220 – 400 nm)-ESI-MS: 98.1%.

2-(benzo[b]thiophen-3-yl)ethan-1-amine (FPE-MP18) (CAS: 14585-66-1)

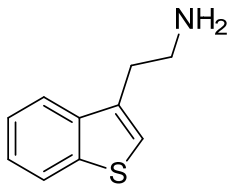

A solution of **FPE-MP17**, (0.562 g, 3.469 mmol, 1 eq) in THF (10mL) was stirred at 0ºC in a round-bottomed flask for 5 minutes. Afterwards, liquid $LiAlH_4$ (6 mL) was added dropwise. Reaction mixture was kept under stirring for 10 minutes and then refluxed overnight. After TLC monitoring, the mixture was carefully poured over ice-cold water and diluted with EtOAc and further mixed for 10 minutes

and filtered through celite. The filtrate underwent extraction and the organic phases were combined, dried over $MgSO_4$ and purified by flash column chromatography on silica gel (MeOH in DCM 0 to 5%). **Yield**: 93 mg, 0.525 mmol, 14 %; **M.p.:** 101°C; **^{1}H NMR** (500 MHz, DMSO-d_6) δ 7.96 (d, J = 7.7 Hz, 1H, Ar-H), 7.86 – 7.82 (m, 1H, Ar-H), 7.47 – 7.33 (m, 4H, Ar-H), 2.97 – 2.86 (m, 4H, CH_2CH_2); **^{13}C NMR** (151 MHz, DMSO-d_6) δ 139.63, 138.85, 134.68, 124.09, 123.95, 123.86, 122.78, 122.20, 121.69, 41.58, 32.34. **LC-MS (m/z)**: 178.1 ($[M+H]^+$); **purity** by HPLC-UV (220 – 400 nm)-ESI-MS: 90.87%.

8-((2-(benzo[b]thiophen-3-yl)ethyl)amino)-7-(4-chlorobenzyl)-1,3-dimethyl-3,7-dihydro-1*H*-purine-2,6-dione (FPE-MP19)

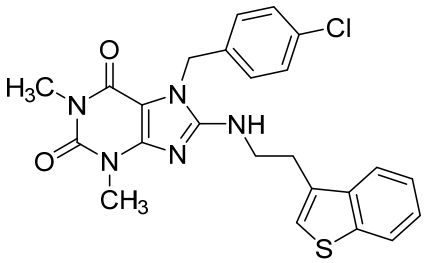

Synthesized according to **GP H** with FP-50 and FPE-MP18 as the coupling partners. Purification by flash column chromatography on silica gel (MeOH in DCM 0 to 7%); **Yield:** 20 mg, 0.04 mmol, 22%; **M.p.:** 179°C; **^{1}H NMR** (600 MHz, DMSO-d_6) δ 8.01 (d, J = 7.9 Hz, 1H, Ar-$H_{benzothiophene}$), 7.97 (d, J = 7.9 Hz, 1H, Ar-$H_{benzothiophene}$), 7.44 – 7.33 (m, 7H, Ar-H and $NHCH_2$), 7.20 (d, J = 8.1 Hz, 2H, Ar-H_{benzyl}), 5.26 (s, 2H, N7CH_2), 3.65 (q, J = 6.7 Hz, 2H, NHCH_2CH_2), 3.39 (s, 3H, N3CH_3), 3.16 (s, 3H, N1CH_3), 3.13 (t, J = 7.2 Hz, 2H, NHCH$_2CH_2$); **^{13}C NMR** (151 MHz, DMSO-d_6) δ 153.55, 152.78, 150.94, 148.85, 139.67, 138.78, 135.94, 133.46, 132.00, 128.90, 128.43, 124.21, 123.97, 123.07, 122.89, 121.77, 101.21, 44.67, 42.14, , 29.26, 28.29, 27.18; ; **LC-MS (m/z)**: 481.0 ($[M+H]^+$); **purity** by HPLC-UV (220 – 400 nm)-ESI-MS: 99.8%; **HRMS (ESI, m/z)** calcd for $C_{24}H_{22}ClN_5O_2S$ $[M + H]^+$, 480.1256; found, 480.1257.

5.3 Synthesis of antagonists for GPR183

5.3.1 General procedures (GPs)

General procedure 1 for the synthesis of benzoic acid amides

In a 50 mL round-bottomed flask, tryptamine (0.146 g, 1.00 eq.) and triethyl amine (1.20 eq.) were dissolved in DCM (5 mL). The appropriate benzyl carbonyl chloride (1.00 eq.) was slowly added for 5 min at 0°C. The reaction mixture was warmed up to RT and stirred at RT for 3 h. The reaction was controlled by TLC (MeOH: DCM / 5:95). When no further improvement was detected, the reaction mixture was diluted with DCM (10 mL) and washed with water. The organic layer was dried over $MgSO_4$ and concentrated under reduced pressure. If further purification is needed, the crude was purified by column chromatography.

General procedure 2 for the reaction 3-Indolepropionic acid with 1*N* substituted piperazine

In a 50 mL round-bottomed flask, 3-Indolepropionic acid (0.084 g, 1.00 eq.) and T_3P (1.00 eq.) were dissolved in DCM (2 mL) and stirred at 0°C. A solution of the appropriate 1*N*-substituted piperazine (1.00 eq.) and triethyl amine (1.00 eq.) in DCM (2 mL) was added at 0°C. The reaction mixture was stirred at RT overnight. The reaction was controlled by TLC (MeOH: DCM / 5:95). When no further improvement was detected, the reaction mixture was diluted with DCM (10 mL) and washed with water. The organic layer was washed with saturated $NaHCO_3$. concentrated under reduced pressure. When needed, the crude was purified by column chromatography.

General procedure 3 for the synthesis of cinnamic acid amides

In a 50 mL round-bottomed flask, the appropriate cinnamic acid derivative (0.100 g, 1.00 eq.) and T_3P (1.00 eq.) were dissolved in DCM (2 mL) at 0°C. Solution of the appropriate tryptamine (1.00 eq.) and triethyl amine (1.00 eq.) in DCM (2 mL) was added dropwise to a solution of the appropriate cinnamomic acid and T3P at 0°C. The reaction mixture was stirred at RT overnight. The reaction was controlled by TLC (MeOH: DCM / 5:95). When no further improvement was detected, the reaction mixture was diluted with DCM (10 mL) and washed with water. The organic

layer was washed with saturated $NaHCO_3$. concentrated under reduced pressure. When needed, the crude was purified by column chromatography.

General procedure 4 for the coupling of benzyl bromide derivative with piperazine

In a 50 mL round-bottomed flask, 3-(1*H*-indol-3-yl)-1-(piperazin-1-yl)propan-1-one (**FPE-ML35**) (0.077 g, 0.299 mmol, 1.00 eq.) and K_2CO_3 (0.136 g, 0.987 mmol, 3.30 eq.) were dissolved in acetone (4 mL) at rt. The appropriate bromo methyl benzene derivative (1.00 eq.) was added to the reaction mixture. The reaction mixture was stirred at 70°C for 2-3 h. When no further improvement was detected, the solvent was evaporated until the mixture became completely dry. The resulting precipitates were dissolved in EE and washed with water and brine. The organic layer was dried over $MgSO_4$ and concentrated under reduced pressure. If further purification is needed, the crude was purified by flash chromatography.

General procedure 5 for the coupling of benzoic acid derivative with piperazine (GP 5)

This reaction ran under an inert gas atmosphere. In a 100 mL round-bottomed two-neck flask, 3-(3-(piperazine-1-yl)propyl)-1*H*-indole (**FPE-ML50**) (0.100 g, 0.411 mmol, 1.00 eq.), 1-Hydroxybenzotriazol (1.35 eq.), 3-(((ethylimino)methylene)amino)-N,N-dimethylpropan-1-amine hydrochloride (1.50 eq.) and the appropriate benzoic acid derivative (2.00 eq.) were dissolved in acetone (10 mL) under inert gas atmosphere. The reaction mixture was stirred at RT for 2-4 h under inter gas atmosphere. When no further improvement was detected, the solvent was evaporated under reduced pressure and the crude was purified by column chromatography or flash chromatography.

5.3.2 Building blocks

***tert*-butyl 4-(3-(1*H*-indol-3-yl)propanoyl)piperazine-1-carboxylate (FPE-ML30)**

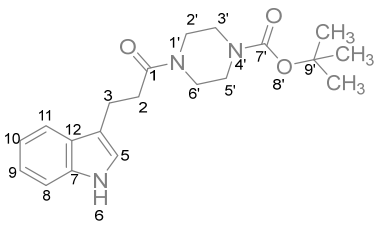

In a 50 mL round-bottomed flask, 3-(1*H*-indol-3-yl)propanoic acid (1.00 g, 5.29 mmol, 1.00 eq.) was dissolved in THF (50 mL) and after the addition of CDI (1.29 g, 7.93 mmol, 1.50 eq.), the mixture was stirred at RT for 0.5 h. BOC-Piperazine (1.18 g, 6.34 mmol, 1.20 eq.) was added to the resulting mixture and the reaction mixture was stirred at RT for 2 h. The reaction was controlled by TLC (MeOH: DCM / 5:95). When no further improvement was detected, the reaction mixture was concentrated under reduced pressure and the resulting solid was dissolved in EE (10 mL). The solution was washed with saturated aq. $NaHCO_3$ and brine and dried over $MgSO_4$. The resulting organic layer was concentrated under reduced pressure. **Yield**: quantitative; **M.p.**: 164°C; **LC-MS (*m/z*)**: 358.2 $[M+H]^+$; **purity** by HPLC-UV (220-600 nm): 97.1 %; **^{1}H-NMR** (600 MHz, DMSO-d_6) δ δ: 10.78 (s, 1 H, 6-H), 7.51 (d, J = 7.9 Hz, 1 H, 11-H), 7.32 (d, J = 8.1 Hz, 1 H, 8-H), 7.13 (d, J = 2.3 Hz, 1 H, 5-H), 7.05 (t, J = 7.4 Hz, 1 H, 9-H), 6.97 (t, J = 7.4 Hz, 1 H, 10-H), 3.45-3.40 (m, 2 H, $H_{piperazine}$), 3.37 (t, J = 5.2 Hz, 2 H, $H_{piperazine}$), 3.24 (t, J = 5.2 Hz, 2 H, $H_{piperazine}$), 3.19 (t, J = 5.2 Hz, 2 H, $H_{piperazine}$), 2.92 (dd, J = 8.9 Hz, 6.5 Hz, 2 H, 3-H), 2.67 (dd, J = 8.9 Hz, 6.6 Hz, 2 H, 2-H), 1.40 (s, 9 H, OC(CH_3)$_3$); **^{13}C NMR** (151 MHz, DMSO-d_6) δ: 170.6 (C-1), 153.8 (C-7'), 136.2 (C-7), 127.0 (C-12), 122.4 (C-5), 120.8 (C-9), 118.2 (C-10), 118.1 (C-11), 113.7 (C-4), 111.3 (C-8), 79.1 (C-9'), 44.6 (C-3', C-5'), 40.8 (C-2', C-6'), 33.2 (C-2), 28.0 (3C, OC(CH_3)$_3$), 20.5 (C-3).

3-(1*H*-indol-3-yl)-1-(piperazin-1-yl)propan-1-one (FPE-ML35), CAS: 563538-37-4

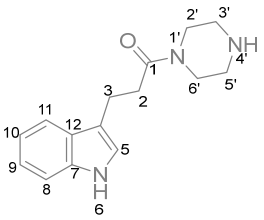

In a 50 mL round-bottomed flask, **FPE-ML30** (0.500 g, 1.40 mmol, 1.00 eq.) was dissolved in DCM (2 mL) at rt. TFA (1.61 mL, 21.0 mmol, 15.0 eq.) was added to this solution and the reaction mixture was stirred for 0.5 h at rt. When no further improvement was detected, TFA and solvent were evaporated under reduced pressure. The residue was dissolved in DCM and the solution was washed with saturated aq. Na_2CO_3 and brine. The organic layer was dried over $MgSO_4$ and concentrated under reduced pressure. **Yield**: 0.171 g, 0.664 mmol, 47.5 %; **M.p.:** 187°C; **LC-MS (*m/z*)**: 515.4 $[2M+H]^+$; used without further purification.

3-(1*H*-indol-3-yl)propan-1-ol (FPE-ML43), CAS: 3569-21-9

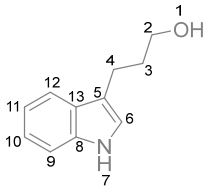

In a 250 mL round-bottomed flask, a solution of 3-(1*H*-indol-3-yl)propanoic acid (1.00 g, 5.29 mmol, 1.00 eq.) in dry THF (7 mL) was dropwise added to the suspension of $LiAlH_4$ (0.481 g, 12.7 mmol, 2.40 eq.) in dry THF (55 mL). The mixture was stirred at 35°C for 2 h. After this time, this reaction mixture was stirred at RT overnight. When no further improvement was detected, water was added to the reaction mixture very slowly, followed by the addition of H_2O: H_2SO_4 (3:1). NaOH was added to the resulting mixture until pH 7. The organic layer was dried over $MgSO_4$ and concentrated under reduced pressure. This compound is used without further purification. **Yield**: 0.773 g, 4.41 mmol, 83.5 %; **M.p.**:108°C; **LC-MS (*m/z*)**: 176.2 $[M+H]^+$; **purity by HPLC-UV (220-600 nm)**: 92.3 %; **^{1}H-NMR** (600 MHz, DMSO-*d*$_6$) δ δ: 10.7 (s, 1 H, 6-H), 7.52-7.47 (m, 1 H, 12-H), 7.32 (d, *J* = 8.1 Hz, 1 H, 9-H), 7.08 (d, *J* = 2.3 Hz, 1 H, 6-H), 7.05 (ddd, *J* = 8.1 Hz, 6.9 Hz, 1.2 Hz, 1 H, 10-H), 6.96 (td, *J* = 7.5 Hz, 1.0 Hz, 1 H, 11-H), 4.41 (t, *J* = 5.2 Hz, 1 H, 1-H), 3.47 (td, *J* = 6.5 Hz, 5.1 Hz, 2 H, 2-H), 2.71 (t, *J* = 7.6 Hz, 4-H), 1.83-1.74 (m, 2 H, 3-H); **^{13}C NMR** (151 MHz, DMSO-*d*$_6$) δ**:** 136.3 (C-8), 127.2 (C-13), 122.0 (C-6), 120.7 (C-10), 118.3 (C-11). 118.0 (C-12), 114.5 (C-9), 111.3 (C-5), 60.5 (C-2), 33.3 (C-3), 21.1 (C-4).

3-(1*H*-indol-3-yl)propyl 4-methylbenzenesulfonate (FPE-ML48)

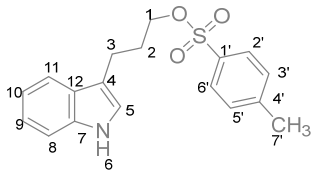

In a 100 mL round-bottomed and dried Schlenk flask, triethyl amine (0.580 mL, 4.17 mmol, 1.00 eq.), 4-(Dimethylamino)pyridine (0.007g, 0.062 mmol, 0.015 eq.) and tosyl chloride (0.794 g, 4.17 mmol, 1.00 eq.) was added to the solution of **FPE-ML43** (0.730 g, 4.17 mmol, 1.00 eq.) in dry DCM (15 mL) under argon atmosphere. The reaction mixture was stirred overnight at RT under an inert gas atmosphere. When no further improvement was detected, the solvent was evaporated under reduced pressure. The crude was purified by flash chromatography (CH: EE 15% to 35 % in 35 min, at 35 % for 5 min. **Yield:** 0.893 g, 2.71 mmol, 65.1%; **M.p.**: 158°C; **LC-MS (*m/z*)**: 330.2 $[M+H]^+$; **Purity** by HPLC-UV (220-600 nm): 95.5 %; **^{1}H-NMR** (600 MHz, DMSO-*d*$_6$) δ δ: 10.74 (s, 1 H, 6-H), 7.81-7.32 (m, 2 H, 2'-H, 6'-H), 7.45 (d, *J* = 8.0 Hz, 2 H, 3'-H, 5'-H), 7.41 (d, *J* = 7.9 Hz, 1 H, 11-H), 7.31 (d, *J* = 8.1 Hz, 1 H, 8-H), 7.05 (ddd, *J* = 8.1 Hz, 6.8 Hz, 1.2 Hz, 1 H, 5-H), 6.99 (d, *J* = 2.3 Hz, 1 H, 9-H), 6.94 (td, *J* = 7.3 Hz, 1.0 Hz, 1 H, 10-H), 4.06 (t, *J* = 6.3 Hz, 2 H, 1-H), 2.66 (t, *J* = 7.5 Hz, 2 H, 3-H), 2.41 (s 3 H, 7'-H), 1.93 (dt, *J* = 8.1 Hz, 6.4 Hz,

2 H, 2-H). **^{13}C NMR** (151 MHz, DMSO-*d*$_6$) δ: 144.8 (C-1'), 136.3 (C-4'), 132.5 (C-7), 130.1 (C-3', C-5'), 127.5 (C-2', C-6'), 126.9 (C-12), 122.3 (C-5), 120.9 (C-9), 118.2 (C-10), 118.1 (C-11), 112.7 (C-8), 111.3 (C-4). 70.6 (C-1), 28.9 (C-2), 21.1 (C-3), 20.4 (C-7').g

tert-butyl 4-(3-(1*H*-indol-3-yl)propyl)piperazine-1-carboxylate (FPE-ML49)

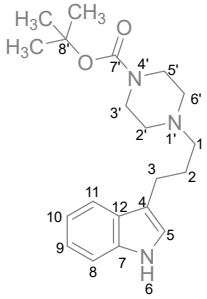

In a 250 mL round-bottomed flask, **FPE-ML48** (0.874 g, 2.65 mmol, 1.00 eq.) was dissolved in MeCN (80 mL). BOC-Piperazine (0.988 g, 5.31 mmol, 2.00 eq.) and K_2CO_3 (0.385 g, 2.79 mmol, 1.05 eq.) were added to the mixture. The reaction mixture was stirred under reflux for 6 h. When no further improvement was detected, water was slowly added to the mixture and the reaction mixture was extracted with EE. The combined organic layer was dried over $MgSO_4$ and concentrated under reduced pressure. The crude was purified by flash chromatography (MeOH in DCM 3 to 5%). **Yield**: 0.657 g, 1.91 mmol, 72.1 %; **M.p.**: 145°C; **LC-MS (*m/z*)**: 343.3 $[M+H]^+$.**Purity by HPLC-UV (220-600 nm)**: 100.0%; **^{1}H-NMR** (600 MHz, DMSO-*d*$_6$) δ δ: 10.71 (s, 1H, 6-H), 7.49 (dd, *J* = 7.8 Hz, 1.1 Hz, 1 H, 11-H), 7.32 (d, *J* = 8.1 Hz, 1 H, 8-H), 7.09 (d, *J* = 2.3 Hz, 1 H, 5-H), 7.04 (ddd, *J* = 8.0 Hz, 6.9 Hz, 1.2 Hz, 1 H, 9-H), 6.95 (ddd, *J* = 8.0 Hz, 6.9 Hz, 1.0 Hz, 1 H, 10-H), 3.30 (d, *J* = 4.5 Hz, 3 H, 3'-H, 5'-H), 2.68 (t, *J* = 7.5 Hz, 2 H, 3-H), 2.33 (t, *J* = 7.3 Hz, 2 H, 1-H), 1.79 (p, *J* = 7.4 Hz, 2 H, 2-H), 1.39 (s, 9 H, OC(C*H*$_3$)$_3$). **^{13}C NMR** (151 MHz, DMSO-*d*$_6$) δ: 153.8 (C-7'), 136.3 (C-7), 127.2 (C-12), 122.1 (C-5), 120.7 (C-9), 118.2 (C-10), 118.0 (C-11), 114.3 (C-8), 111.3 (C-4), 78.7 (C-8'), 57.6 (C-2', C-6'), 54.9 (C-1), 52.6 (C-3', C-5'), 28.0 (3C, OC(*C*H$_3$)$_3$), 27.0 (C-2), 22.4 (C-3).

3-(3-(piperazin-1-yl)propyl)-1*H*-indole (FPE-ML50), CAS: 610802-22-7

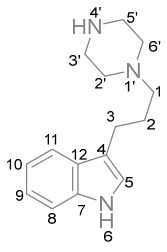

In a 50 mL round-bottomed flask, **FPE-ML49** (0.642 g, 1.87 mmol, 1.00 eq.) was dissolved in DCM (10 mL) at rt. TFA (2.15 mL, 28.0 mmol, 15.0 eq.) was added to this solution and the reaction mixture was stirred for 0.5 h at rt. When no further improvement was detected, it was concentrated under reduced pressure ad the residue washed with DCM. The water layer was dried by a lyophilizer for 2 days. **Yield**: 0.657 g, 1.91 mmol, 72.1 %; **M.p.:** 81°C; **LC-MS (*m/z*)**: 343.3 $[M+H]^+$.**Purity by HPLC-UV (220-600 nm)**: 100.0%; **^{1}H-NMR** (600 MHz, DMSO-*d*$_6$) δ δ: 10.71 (s, 1 H, 6-H), 7.49 (d, *J* = 7.8 Hz, 1 H, 11-H), 7.32 (d, *J* = 8.1 Hz, 1 H, 8-H), 7.09 (d, *J* = 2.3 Hz 1 H, 5-H), 7.04 (ddd, *J* =

8.0 Hz, 6.9 Hz, 1.2 Hz, 1 H, 9-H), 6.95 (ddd, *J* = 8.0 Hz, 6.9 Hz, 1.0 Hz, 1 H, 10-H), 3.30 (d, *J* = 4.5 Hz, 3 H, $H_{Piperazine}$), 2.68 (t, *J* = 7.5 Hz, 2 H, 3-H), 2.33 (t, *J* = 7.3 Hz, 2 H, 1-H), 2.29 (t, *J* = 5.1 Hz, 4 H, $H_{Piperazine}$), 1.79 (p, *J* = 7.4 Hz, 2 H, 2-H). **^{13}C NMR** (151 MHz, DMSO-*d*$_6$) δ: 136.8 (C-7), 127.5 (C-12), 123.1 (C-5), 122.0 (C-9), 119.3 (C-10), 119.0 (C-11), 113.4 (C-8), 112.2 (C-4), 56.8 (C-1), 48.7 ($C_{Piperazine}$), 41.0 ($C_{Piperazine}$), 24.7 (C-2), 22.2 (C-3).

5.3.3 Synthesis of *N*-(2-(1*H*-indol-3-yl)ethyl)benzamides

_N_-(2-(1_H_-indol-3-yl)ethyl)-4-chlorobenzamide (FPE-48B)

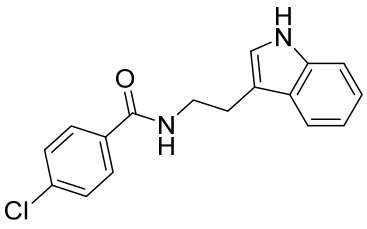

Synthesis according to **GP1**. Purification with flash column chromatography on silica gel (MeOH in DCM 0 to 3%). **Yield**: 200 mg, 0.67 mmol, 63%; **M.p.**: 155°C; **^{1}H NMR** (500 MHz, DMSO-*d*$_6$) δ 10.78 (s, 1H, NH_{indole}), 8.65 (d, *J* =5.5 Hz, 1H, CONH), 7.87 (dd, *J* =8.5, 2.2 Hz, 2H, Ar-H_{benzyl}), 7.57 (d, *J* =8.0 Hz, 1H, Ar-H), 7.53 (dd, *J* =8.6, 1.9 Hz, 2H, Ar-H_{benzyl}), 7.34 (d, *J* =8.2 Hz, 1H, Ar-H), 7.17 (s, 1H, Ar-H), 7.09 – 7.03 (m, 1H, Ar-H), 6.98 (dd, *J* =8.5, 6.2 Hz, 1H, Ar-H), 3.57 – 3.51 (m, 2H, NH*CH*$_2$CH$_2$), 2.95 (t, *J* =7.3 Hz, 2H, NHCH$_2$*CH*$_2$); **^{13}C NMR** (126 MHz, DMSO-d$_6$) δ 165.33, 136.54, 136.12, 133.73, 129.34, 128.59, 127.56, 122.88, 121.19, 118.53, 118.50, 112.13, 111.65, 40.58, 25.39; **LC-MS (m/z)**: 299.2 ([M+H]$^+$); **purity** by HPLC-UV (220 – 400 nm)-ESI-MS: 98.6%; **HRMS (ESI, m/z)** calcd for $C_{17}H_{15}ClN_2O$ [M + H]$^+$,299.095; found, 299.179.

_N_-(2-(1_H_-indol-5-methoxy-3-yl)ethyl)-4-chlorobenzamide (FPE150)

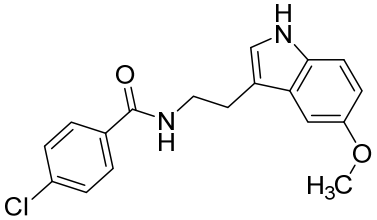

Synthesis according to **GP1**. Purification with column chromatography (MeOH in DCM 3%). **Yield:** 297 mg, 0,9 mmol, 58%; **M.p.**: 57°C; **^{1}H NMR** (500 MHz, DMSO-*d*$_6$) δ 10.62 (s, 1H, NH_{indole}), 8.65 (t, *J* =5.5 Hz, 1H, NHCO), 7.87 (dd, *J* =8.5, 1.8 Hz, 2H, Ar-H_{benzyl}), 7.54 – 7.51 (m, 2H, Ar-H_{benzyl}), 7.22 (d, *J* =8.7 Hz, 1H, Ar-H), 7.13 (d, *J* =2.4 Hz, 1H, Ar-H), 7.05 (d, *J* =2.4 Hz, 1H, Ar-H), 6.71 (dd, *J* =8.7, 2.3 Hz, 1H, Ar-H), 3.72 (s, 3H, OCH_3), 3.53 (q, *J* =6.6, 6.1 Hz, 2H, NH*CH*$_2$CH$_2$), 2.92 (t, *J* =7.3 Hz, 2H, NHCH$_2$*CH*$_2$); **^{13}C NMR** (126 MHz, DMSO-d$_6$) δ 164.98, 152.94, 135.79, 133.40, 131.35, 129.01,

128.25, 127.57, 123.24, 111.94, 111.63, 111.01, 100.17, 55.26, 40.23, 25.05; **LC-MS (m/z)**: 329.1 ([M+H]$^+$); **purity** by HPLC-UV (220 – 400 nm)-ESI-MS: 95.6%.

***N*-(2-(1*H*-indol-3-yl)ethyl)-benzamide (FPE151)**

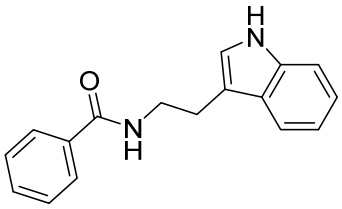

Synthesis according to **GP1**. Purification with column chromatography (MeOH in DCM 4%). **Yield:** 311 mg, 1,176 mmol, 75.4%; **M.p.**: 144°C; **^{1}H NMR** (500 MHz, DMSO-d_6) δ 10.78 (s, 1H, NH_{indole}), 8.57 (t, *J* =5.7 Hz, 1H, NHCO), 7.87 – 7.82 (m, 2H, Ar-H_{benzyl}), 7.59 (dd, *J* =8.1, 1.2 Hz, 1H, Ar-H), 7.54 – 7.49 (m, 1H, ar-H_{benzyl}), 7.48 – 7.43 (m, 2H, Ar-H_{benzyl}), 7.34 (dt, *J* =8.2, 1.0 Hz, 1H; Ar-H), 7.18 (d, *J* =2.3 Hz, 1H, Ar-H), 7.07 (ddd, *J* =8.2, 6.9, 1.2 Hz,1H, Ar-H), 6.98 (ddd, *J* =7.9, 6.9, 1.1 Hz, 1H, Ar-H), 3.56 (q, 2H, NH*CH*$_2$CH$_2$), 2.96 (t, *J* =7.6 Hz, 2H, NHCH$_2$*CH*$_2$); **^{13}C NMR** (126 MHz, DMSO-d$_6$) δ 166.06, 136.20, 134.69, 130.92, 128.15, 127.24, 127.05, 122.52, 120.84, 118.23, 118.15, 111.87, 111.30, 40.26, 25.14; **LC-MS (m/z)**: 265.1 ([M+H]$^+$); **purity** by HPLC-UV (220 – 400 nm)-ESI-MS: 99.9% .

***N*-(2-(1*H*-indol-5-methoxy -3-yl)ethyl)-benzamide (FPE154)**

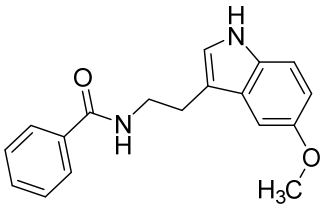

Synthesis according to **GP1**. Purification with column chromatography (MeOH in DCM 4%). **Yield:** 392 mg, 1.33 mmol, 85.4 %; **M.p.**: 44°C; **^{1}H NMR** (500 MHz, DMSO-d_6) δ 10.62 (s, 1H, NH_{indole}), 8.55 (t, *J* = 5.7 Hz, 1H, CONH), 7.86 – 7.83 (m, 2H, Ar-H_{benzyl}), 7.51 (tt, *J* = 7.2, 1.2 Hz, 1H, Ar-H_{benzyl}), 7.48 – 7.42 (m, 2H, Ar-H_{benzyl}), 7.22 (dd, *J* = 8.6, 0.6 Hz, 1H, Ar-H), 7.14 (d, *J* = 2.4 Hz, 1H, Ar-H), 7.06 (d, *J* = 2.4 Hz, 1H, Ar-H), 6.71 (dd, *J* = 8.7, 2.4 Hz, 1H, Ar-H), 3.72 (s, 3H, OCH_3), 3.57 – 3.51 (m, 2H, NH*CH*$_2$CH$_2$), 2.95 – 2.89 (t, *J* = 7.4 Hz, 2H).NHCH$_2$*CH*$_2$); **^{13}C NMR** (126 MHz, DMSO-d$_6$) δ 166.25, 153.14, 134.88, 131.55, 131.13, 128.35, 127.79, 127.26, 123.42, 112.12, 111.91, 111.20, 100.39, 55.45, 40.23, 25.31; **LC-MS (m/z)**: 295.2 ([M+H]$^+$); **purity** by HPLC-UV (220 – 400 nm)-ESI-MS: 98.6% .

***N*-(2-(1*H*-indol-3-yl)ethyl)-3,4-dichlorobenzamide (FPE156)**

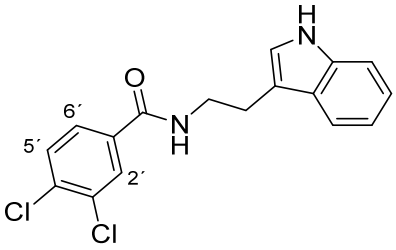

Synthesis according to **GP1**. Purification with column chromatography (MeOH in DCM 4%). **Yield:** 214 mg, 0.644 mmol, 41.3 %; **M.p.**: 135°C; **^{1}H NMR** (500 MHz, DMSO-d_6) δ 10.79 (s, 1H, NH_{indole}), 8.77 (t, *J* = 5.6 Hz, 1H, CONH), 8.07 (d, *J* = 2.0 Hz, 1H, C2′-H), 7.83 (dd, *J* = 8.4, 2.0 Hz, 1H, C6′-H), 7.75 (d, *J* = 8.4 Hz, 1H, C5′-H), 7.57 (dd, *J* = 7.9, 1.1 Hz, 1H, Ar-H), 7.34 (dd, *J* = 8.1, 0.9 Hz, 1H, Ar-H), 7.17 (d, *J* = 2.3 Hz, 1H, Ar-H), 7.07 (ddd, *J* = 8.1, 6.9, 1.2 Hz, 1H, Ar-H), 6.98 (ddd, *J* = 8.0, 7.0, 1.0 Hz, 1H, Ar-H), 3.55 (td, *J* = 7.5, 5.6 Hz, 2H, NH*CH*$_2$CH$_2$), 2.96 (t, *J* = 7.7 Hz, 2H, NH*CH*$_2$CH$_2$); **^{13}C NMR** (126 MHz, DMSO-d$_6$) δ 163.80, 136.21, 134.98, 133.78, 131.15, 130.61, 129.08, 127.43, 127.22, 122.61, 120.87, 118.18*, 111.71, 111.34, 40.36, 24.92; **LC-MS (m/z)**: 332.1 ([M+H]$^+$); **purity** by HPLC-UV (220 – 400 nm)-ESI-MS: 98.0%. *overlapping of 2 C from the indole ring (higher peak and comparison with >50 molecules with the same moiety inside).

***N*-(2-(1*H*-indol-5-methoxy-3-yl)ethyl)-3,4-dichlorobenzamide (FPE157)**

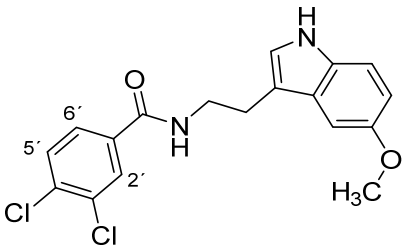

Synthesis according to **GP1.** Purifiecation with column chromatography (MeOH in DCM 4%). **Yield:** 470 mg, 1.29 mmol, 82.9 %; **M.p.:** 47°C; **^{1}H NMR** (500 MHz, DMSO-d_6) δ 10.61 (s, 1H, NH_{indole}), 8.75 (t, *J* =5.7 Hz, 1H, CONH), 8.05 (d, *J* =2.0 Hz, 1H, C2′-H), 7.82 (dd, *J* = 8.4, 2.1 Hz, 1H, C6′-H), 7.74 (d, *J* =8.4 Hz, 1H, C5′-H), 7.21 (d, *J* =8.7 Hz, 1H, Ar-H), 7.12 (d, *J* =2.4 Hz, 1H, Ar-H), 7.03 (d, *J* =2.4 Hz, 1H, Ar-H), 6.70 (dd, *J* =8.7, 2.4 Hz, 1H, Ar-H), 3.71 (s, 3H, OCH_3), 3.52 (td, *J* =7.5, 5.6 Hz, 2H, NH*CH*$_2$CH$_2$), 2.91 (t, *J* =7.4 Hz, 2H, NH*CH*$_2$CH$_2$); **^{13}C NMR** (126 MHz, DMSO-d$_6$) δ 163.78, 152.96, 134.99, 133.77, 131.35, 131.15, 130.60, 129.07, 127.57, 127.43, 123.30, 111.95, 111.54, 111.00, 100.15, 55.26, 40.36, 24.91; **LC-MS (m/z)**: 363.1 ([M+H]$^+$); **purity** by HPLC-UV (220 – 400 nm)-ESI-MS: 99.1%.

***N*-(2-(1*H*-indol-3-yl)ethyl)-3,4-dimethoxybenzamide (FPE158)**

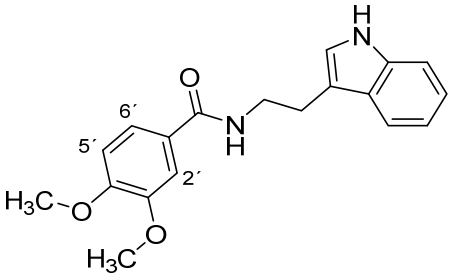

Synthesis according to **GP1.**. Purification with column chromatography (MeOH in DCM 4%). **Yield:** 342 mg, 1.054 mmol, 67.6 %; **M.p**.: 175°C; **^{1}H NMR** (600 MHz, DMSO-d_6) δ 8.45 (t, J = 5.7 Hz, 1H, NH_{indole}), 7.59 (d, J = 7.9 Hz, 1H, C5′-H), 7.48 (dd, J = 8.4, 2.0 Hz, 1H, C6′-H), 7.45 (d, J = 2.1 Hz, 1H, C2′-H), 7.34 (d, J = 8.0 Hz, 1H, Ar-H), 7.17 (d, J = 2.3 Hz, 1H, Ar-H), 7.07 (ddd, J = 8.1, 6.9, 1.2 Hz, 1H, Ar-H), 7.01 (d, J = 8.4 Hz, 1H, Ar-H), 6.98 (ddd, J = 7.8, 6.9, 1.0 Hz, 1H, Ar-H), 3.804 (s, 3H, OCH_3), 3.801 (s, 3H, OCH_3), 3.55 – 3.51 (m, 2H, NH$CH_2$$CH_2$), 2.95 (t, J = 7.6 Hz, 2H, NH$CH_2$$CH_2$); **^{13}C NMR** (126 MHz, DMSO-d_6) δ 165.61, 151.07, 148.17, 136.22, 127.28, 127.01, 122.55, 120.87, 120.25, 118.28, 118.18, 111.96, 111.33, 110.85, 110.64, 55.56, 55.51, 40.21, 25.29; **LC-MS (m/z)**: 324.2 ($[M+H]^+$); **purity** by HPLC-UV (220 – 400 nm)-ESI-MS: 99.6%.

***N*-(2-(1*H*-indol-3-yl)ethyl)-4-bromobenzamide (FPE-ML23)**

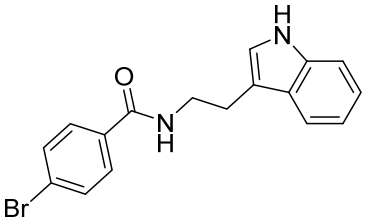

Synthesis according to **GP1**. Compound was used without further purification. **Yield**: 229 mg, 0.667 mmol, 73.2 %); **M.p.**: 154°C; **^{1}H-NMR** (600 MHz, DMSO-d_6) δ 10.79 (s, 1 H, NH_{indole}), 8.67 (t, J = 5.7 Hz, 1 H, CONH), 7.82-7.77 (m, 2 H, Ar-H_{benzyl}), 7.70-7-65 (m, 2 H, Ar-H_{benzyl}), 7.57 (dd, J = 7.9 Hz, 1.1 Hz, 1 H, Ar-H), 7.34 (dd, J = 8.1 Hz, 0.9 Hz, 1 H, Ar-H), 7.17 (d, J = 2.2 Hz, 1 H, Ar-H), 7.06 (ddd, J = 8.2 Hz, 6.9 Hz, 1.2 Hz, 1 H, Ar-H), 6.98 (ddd, J = 7.9 Hz, 6.9 Hz, 1.0 Hz, 1 H, Ar-H), 3.57-3.52 (m, 2 H, NH$CH_2$$CH_2$), 2.95 (t, J = 7.5 Hz, 2 H, NH$CH_2$$CH_2$); **^{13}C NMR** (151 MHz, DMSO-d_6) δ 165.13, 136.22, 133.77, 131.23 (2C), 129.25 (2C), 127.24, 124.71, 122.59, 120.89, 118.23, 118.19, 111.80, 111.34, 40.25, 25.05; **LC-MS (m/z)**: 345.0 ($[M+H]^+$); **purity** by HPLC-UV (220 – 400 nm)-ESI-MS: 98.7%.

5.3.4 Synthesis of cinnamic acid amides

***N*-(2-(1*H*-indol-3-yl)ethyl)-3-(4-bromo-2-fluorophenyl)acrylamide (FPE-ML25)**

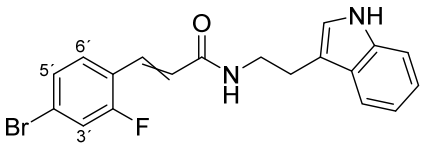

Synthesis according to **GP 3. Yield**: 0.067 g, 0.173 mmol, 42.4 %; **M.p.**: 140.0°C; **^{1}H-NMR** (600 MHz, DMSO-d_6) δ 10.80 (s, 1 H, NH_{indole}), 8.34 (t, *J* = 5.7 Hz, 1 H, NHCO), 7.66-7.58 (m, 2 H, C3´-H and C5´-H), 7.55 (dd, *J* = 7.8 Hz, 1.0 Hz, 1 H, Ar-H), 7.48 (dd, *J* = 8.3 Hz, 2.0 Hz, 1 H, C6´-H), 7.44 (d, *J* = 16 Hz, 1 H, *CH*=CHCO), 7.34 (dt, *J* = 8.1 Hz, 0.9 Hz, 1 H, Ar-H), 7.16 (d, *J* = 2.4 Hz, 1 H, Ar-H), 7.06 (ddd, *J* = 8.1 Hz, 7.0 Hz, 1.2 Hz, 1 H, Ar-H), 6.98 (ddd, *J* = 7.9 Hz, 6.9 Hz, 1.1 Hz, 1 H, Ar-H), 6.75 (d, *J* = 15.9 Hz, 1 H, CH=*CH*CO), 3.48 (td, *J* =7.5 Hz, 5.7 Hz, 2 H, NH*CH*$_2$CH$_2$), 2.89 (t, *J* = 7.4 Hz, 2 H, NHCH$_2$*CH*$_2$); **^{13}C NMR** (151 MHz, DMSO-d_6) δ 164.4, 161.0, 159.3, 136.2, 130.5, 128.2, 127.2, 125.9, 122.6, 122.5, 122.1, 120.9, 119.5, 119.4, 118.2, 111.7, 111.3, 40.1, 25.1; **LC-MS (m/z)**: 387.0 ($[M+H]^+$); **purity** by HPLC-UV (220 – 400 nm)-ESI-MS: 98.5% .

(E)-*N*-(2-(1*H*-indol-3-yl)ethyl)-3-(4-chlorophenyl)acrylamide (FPE-ML26)

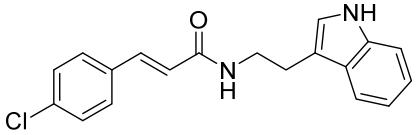

Synthesis according to **GP 3**. **Yield**: 0.081 g, 0.249 mmol, 45.5 %; **M.p.**: 174°C; **^{1}H-NMR** (600 MHz, DMSO-d_6) δ 10.80 (s, 1 H, NH_{indole}), 8.21 (t, *J* = 5.7 Hz, 1 H, NHCO), 7.61-7.57 (m, 2 H, Ar-H_{benzyl}), 7.55 (dd, *J* = 8.1 Hz, 1.0 Hz, 1 H, Ar-H), 7.50-7.44 (m 2 H, Ar-H_{benzyl}), 7.42 (d, *J* = 15.8 Hz, 1 H, *CH*=CHCO), 7.34 (dt, *J* = 8.2 Hz, 0.9 Hz, 1 H, Ar-H), 7.16 (d, *J* = 2.3 Hz, 1 H, Ar-H), 7.06 (ddd, *J* = 8.1 Hz, 6.9 Hz, 1.2 Hz, 1 H, Ar-H), 6.98 (ddd, *J* = 7.9 Hz, 6.9 Hz, 1.1 Hz, 1 H, Ar-H), 6.64 (d, *J* = 15.8 Hz, 1 H, CH=*CH*CO), 3.48 (td, *J* =7.5 Hz, 5.8 Hz, 2 H, Ar-H), 2.89 (t, *J* = 7.4 Hz, 2 H, Ar-H); **^{13}C NMR** (151 MHz, DMSO-d_6) δ 164.7, 137.1, 136.2, 133.9, 133.7, 129.1 (2C), 128.9 (2C), 127.2, 123.2, 122.6, 120.9, 118.3, 118.2, 111.7, 111.3, 40.5, 25.2; **LC-MS (m/z)**: 325.2 ($[M+H]^+$); **purity** by HPLC-UV (220 – 400 nm)-ESI-MS: 98.6% .

(E)-*N*-(2-(1*H*-indol-3-yl)ethyl)-3-(4-(trifluoromethyl)phenyl)acrylamide (**FPE-ML27**)

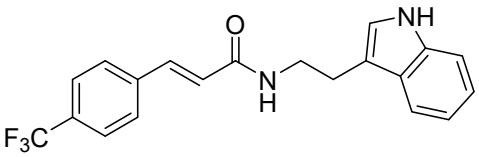

Synthesis according to **GP 3**. **Yield:** 0.080 g, 0.223 mmol, 48.3 %; **M.p.**: 162°C; **^{1}H-NMR** (600 MHz, DMSO-d_6) δ 10.81 (s, 1 H, NH_{indole}), 8.30 (t, *J* = 5.8 Hz, 1 H, NHCO), 7.58 (d, *J* = 8.5 Hz, 2H, Ar-H_{benzyl}), 7.56 (dd, *J* = 8.0, 1.1 Hz, 1H, Ar-H_{indole}), 7.47 (d, *J* = 8.5 Hz, 2H, Ar-H_{benzyl}), 7.42 (d, *J* = 15.8 Hz, 1H, *CH*=CHCO), 7.34 (d, *J* = 8.1 Hz, 1H, Ar-H), 7.17 (d, *J* = 2.1 Hz, 1 H, Ar-H), 7.06 (ddd, *J* = 8.1, 7.0, 1.1 Hz, 1H, Ar-H), 6.98 (ddd, *J* = 7.9, 7.0, 1.0 Hz, 1H, Ar-H), 6.64 (d, *J* = 15.8 Hz, 1H, CH=*CH*CO), 3.48 (td, *J* = 7.5, 5.7 Hz, 2H, NH*CH*$_2$CH$_2$), 2.89 (t, *J* = 7.4 Hz, 2H, NHCH$_2$*CH*$_2$); **^{13}C NMR** (151 MHz, DMSO-d_6) δ 164.4, 139.1, 136.8, 136.2, 129.2, 129.0 (C$\underline{\text{C}}$F$_3$), 128.1 (2C). 127.2, 125.8 (2C). 125.2, 125.0, 122.7, 120.9, 118.2, 111.7, 111.3, 40.1, 25.1; **LC-MS (m/z)**: 359.1 ([M+H]$^+$); **purity** by HPLC-UV (220 – 400 nm)-ESI-MS: 97.9%

.

(E)-*N*-(2-(1*H*-indol-3-yl)ethyl)-3-(3-chlorophenyl)acrylamide (**FPE-ML29**)

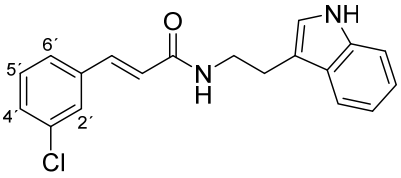

Synthesis according to **GP 3. Yield**: 0.097 g, 0.280 mmol, 51.2 %; **M.p.**: 60°C; **^{1}H-NMR** (600 MHz, DMSO-d_6) δ 10.80 (s, 1 H, NH_{indole}), 8.19 (t, *J* = 5.7 Hz, 1 H, Ar-H), 7.63 (d, *J* = 5.7 Hz, 1 H, C6′-H), 7.56 (d, *J* = 7.8 Hz, 1 H, Ar-H), 7.53 (dt, *J* = 5.7 Hz, 2.0 Hz, 1 H, C5′-H), 7.47-7.39 (m, 3 H, C2′-H, C4′-H and *CH*=CHCO), 7.34 (d, *J* = 8.1 Hz, 1 H, Ar-H), 7.17 (d, *J* = 2.3 Hz, 1 H, Ar-H), 7.07 (ddd, *J* = 8.2 Hz, 6.9 Hz, 1.2 Hz, 1 H, Ar-H), 6.98 (ddd, *J* = 8.0 Hz, 6.9 Hz, 1.0 Hz, 1 H, Ar-H), 6.70 (d, *J* = 15.8 Hz, 1 H, CH=*CH*CO), 3.49 (td, *J* = 7.5 Hz, 5.7 Hz, 2 H, NH*CH*$_2$CH$_2$), 2.89 (t, *J* = 7.3 Hz, 2 H, NHCH$_2$*CH*$_2$). **^{13}C NMR** (151 MHz, DMSO-d_6) δ 164.5, 137.3, 136.9, 136.2, 133.6, 130.7, 129.0, 127.2, 127.1, 126.0, 124.1, 122.7, 120.9, 118.2, 117.7, 111.7, 111.3, 40.1, 25.2; **LC-MS (m/z)**: 325.1 ([M+H]$^+$); **purity** by HPLC-UV (220 – 400 nm)-ESI-MS: 97.7%.

(E)-*N*-(2-(1*H*-indol-3-yl)ethyl)-3-(3,4-dichlorophenyl)acrylamide (**FPE-ML31**)

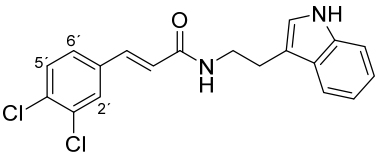

Synthesis according to **GP 3. Yield:** 0.033 g, 0.092 mmol, 19.9 %; **M.p.**: 85.0°C; **^{1}H-NMR** (600 MHz, DMSO-d_6) δ 10.80 (s, 1 H, NH_{indole}), 8.20 (t, *J* = 5.7 Hz, 1 H, Ar-H), 7.84 (d, *J* =2.0 Hz, 1 H, C6′-H), 7.67 (d, *J* = 8.3 Hz, 1 H, C5′-H), 7.56 (dd, *J* = 8.4 Hz, 1.9 Hz, 2 H, C2′-H and Ar-H_{indole}), 7.41 (d, *J* = 15.8 Hz, 1 H, *CH*=CHCO), 7.34 (d, *J* = 8.2 Hz, 1

H, Ar-H), 7.17 (d, *J* = 2.3 Hz, 1 H, Ar-H), 7.07 (ddd, *J* = 8.1 Hz, 6.9 Hz, 1.2 Hz, 1 H, Ar-H), 6.98 (ddd, *J* = 7.9 Hz, 6.9 Hz, 1.0 Hz, 1 H, Ar-H), 6.71 (d, *J* = 15.8 Hz, 1 H, CH=*CH*CO), 3.48 (td, *J* =7.4 Hz, 5.7 Hz, 2 H, NH*CH*$_2$CH$_2$), 2.89 (t, *J* = 7.3 Hz, 2 H, NHCH$_2$*CH*$_2$). **^{13}C NMR** (151 MHz, DMSO-*d*$_6$) δ164.4, 136.2, 135.9, 131.6, 131.5, 131.0, 129.3, 127.2, 124.7, 122.6, 120.1, 118.3, 118.2, 111.7, 111.3, 40.1, 25.1; **LC-MS (m/z)**: 359.1 ([M+H]$^+$); **purity** by HPLC-UV (220 – 400 nm)-ESI-MS: 98.7%.

***N*-(2-(1*H*-indol-3-yl)ethyl)cinnamamide (FPE-ML32)**

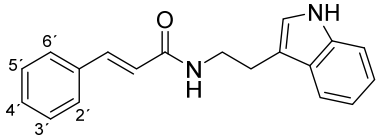

Synthesis according to **GP 3**. **Yield:** 0.044 g, 0.152 mmol, 22.5 %;. **M.p.**: 137°C; **^{1}H-NMR** (600 MHz, DMSO-*d*$_6$) δ 10.80 (s, 1 H, NH$_{indole}$), 8.20 (t, *J* = 5.8 Hz, 1 H, Ar-H), 7.58-7.53 (m, 3 H, 2-H, C6′-H and Ar-H$_{indole}$), 7.47-7.32 (m, 5 H, C3′-H, C4′-H, C5′-H. *CH*=CHCO and Ar-H$_{indole}$) 7.17 (d, *J* = 2.3 Hz, 1 H, Ar-H), 7.07 (ddd, *J* = 8.1 Hz, 6.9 Hz, 1.2 Hz, 1 H, Ar-H), 6.98 (ddd, *J* = 7.9 Hz, 6.9 Hz, 1.0 Hz, 1 H, Ar-H), 6.64 (d, *J* = 15.8 Hz, 1 H, CH=*CH*CO), 3.48 (td, *J* =7.5 Hz, 5.6 Hz, 2 H, NH*CH*$_2$CH$_2$), 2.89 (t, *J* = 7.4 Hz, 2 H, NHCH$_2$*CH*$_2$). **^{13}C NMR** (151 MHz, DMSO-*d*$_6$) δ164.9, 138.4, 136.2, 135.0, 129.3, 128.9 (2C), 127.4 (2C), 127.2, 122.6, 122.4, 120.9, 118.3, 118.2, 111.8, 111.3, 40.1, 25.2; **LC-MS (m/z)**: 289.2 ([M+H]$^+$); **purity** by HPLC-UV (220 – 400 nm)-ESI-MS: 99.4%.

(E)-*N*-(2-(1*H*-indol-3-yl)ethyl)-3-(4-bromophenyl)acrylamide (FPE-ML33)

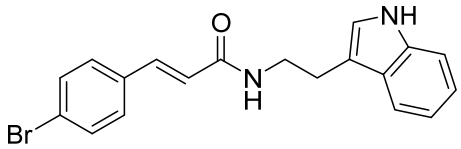

Synthesis according to **GP 3. Yield**: 0.051 g, 0.138 mmol, 31.4 %; **M.p.**: 172°C; **^{1}H-NMR** (600 MHz, DMSO-*d*$_6$) δ 10.80 (s, 1 H, NH$_{indole}$), 8.20 (t, *J* = 5.8 Hz, 1 H, Ar-H), 7.-7.48 (m, 2 H, Ar-H$_{benzyl}$), 7.56 (d, *J* = 8.2 Hz, 1 H, Ar-H), 7.54-7.48 (m, 2 H, Ar-H$_{benzyl}$), 7.40 (d, *J* = 15.8 Hz, 1 H, *CH*=CHCO), 7.36-7.32 (m, 1 H, Ar-H) 7.17 (d, *J* = 2.3 Hz, 1 H, Ar-H), 7.07 (ddd, *J* = 8.1 Hz, 6.9 Hz, 1.2 Hz, 1 H, Ar-H), 6.98 (ddd, *J* = 8.0 Hz, 7.0 Hz, 1.0 Hz, 1 H, Ar-H), 6.65 (d, *J* = 15.8 Hz, 1 H, CH=*CH*CO), 3.48 (td, *J* =7.5 Hz, 5.7 Hz, 2 H, NH*CH*$_2$CH$_2$), 2.89 (t, *J* = 7.4 Hz, 2 H, NHCH$_2$*CH*$_2$); **^{13}C NMR** (151 MHz, DMSO-*d*$_6$) δ 164.6, 137.1, 136.2, 134.3, 131.8 (2C), 129.4 (2C), 129.3, 127.2, 123.3, 122.6, 120.9, 118.3, 118.2, 111.7, 111.3, 40.1, 25.2; **LC-MS (m/z)**: 369.1 ([M+H]$^+$); **purity** by HPLC-UV (220 – 400 nm)-ESI-MS: 97.5%.

5.3.5 Synthesis of piperazine derivatives

5.3.5.1 Series A

3-(1*H*-indol-3-yl)-1-(4-(naphthalen-1-ylmethyl)piperazin-1-yl)propan-1-one (FPE-ML24)

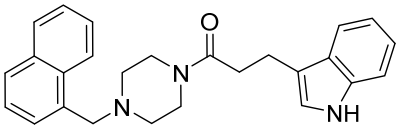

Synthesis according to **GP 2. Yield:** 0.229 g, 0.667 mmol, 73.2 %; **M.p.**: 109°C; **^{1}H-NMR** (600 MHz, DMSO-d_6) δ 10.75 (s, 1 H, NH_{indole}), 8.26 (d, J = 8.2 Hz, 1 H, Ar-$H_{naphtyl}$), 7.91 (dd, J = 7.8 Hz, 1.6 Hz, 1 H, Ar-$H_{naphtyl}$) 7.87-7.82 (m, 1 H, Ar-$H_{naphtyl}$), 7.54 (ddd, J = 8.5 Hz, 6.7 Hz, 1.7 Hz, 1 H, Ar-H), 7.57 – 7.48 (m, 3H, Ar-H), 7.47 – 7.40 (m, 2H, Ar-H), 7.33 (d, J = 8.1 Hz, 1 H, Ar-H), 7.13 (d, J = 2.3Hz, 1 H, Ar-H_{indole}), 7.08-7.03 (m, 1 H, Ar-H_{indole}), 6.96 (t, J = 7.4 Hz, 1 H, Ar-H_{indole}), 3.83 (s, 2 H, NCH_2), 3.43 (t, J = 5.2 Hz, 2 H, $H_{\text{-piperazine}}$), 3.38-3.32 (m, 2 H, $H_{\text{-piperazine}}$), 2.91 (dd, J = 8.8 Hz, 6.5 Hz, 2 H, $COCH_2CH_2$), 2.64 (dd, J =8.9 Hz, 6.6 Hz, 2 H, $COCH_2CH_2$), 2.34 (t, J = 5.2 Hz, 2 H, $H_{\text{-piperazine}}$), 2.27 (t, J = 5.0 Hz, 2 H, $H_{\text{-piperazine}}$); **^{13}C NMR** (151 MHz, DMSO-d_6) δ 170.29, 136.20, 133.54, 131.98, 128.19, 127.79, 127.43, 127.05, 125.64, 125.13, 124.68, 122.38, 120.81, 118.25, 118.14, 113.72, 111.26, 60.04, 52.91, 52.57, 44.98, 41.06, 33.18, 20.62; **LC-MS (m/z)**: 345.0 ($[M+H]^+$); **purity** by HPLC-UV (220 – 400 nm)-ESI-MS: 98.7% .

1-(4-(4-chlorobenzyl)piperazin-1-yl)-3-(1*H*-indol-3-yl)propan-1-one (FPE-ML39)

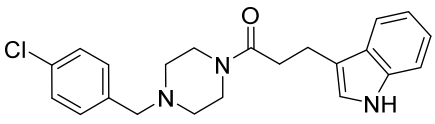

Synthesis according to **GP 4.** Purification with flash column chromatography on silica gel (MeOH in DCM 2 to 5%). **Yield:** 0.050 g, 0.131 mmol, 41.6 %; **M.p.**: 143°C; **^{1}H-NMR** (600 MHz, DMSO-d_6) δ 10.75 (s, 1 H, NH_{indole}), 7.49 (d, J = 7.8 Hz, 1 H, Ar-H), 7.40-7.35 (m, 2 H, Ar-H_{benzyl}), 7.35-7.28 (m, 3 H, 2 Ar-H_{benzyl} and 1 Ar-H_{indole}), 7.12 (d, J = 2.2 Hz, 1 H, Ar-H), 7.05 (ddd, J = 8.1 Hz, 6.8 Hz, 1.1 Hz, 1 H, Ar-H), 6.96 (ddd, J = 7.9 Hz, 6.9 Hz, 1.0 Hz, 1 H, Ar-H), 3.47-3.43 (m, 2 H, H-Piperazine), 3.42 (s, 2 H, NCH_2), 3.38 (t, J = 5.1 Hz, 2 H, H-Piperazine), 2.90 (dd, J = 8.9 Hz, 6.5 Hz, 2 H, $COCH_2CH_2$), 2.67-2.61 (m, 2 H, $COCH_2CH_2$), 2.25 (t, J = 5.1 Hz, 2H, H-Piperazine), 2.20 (t, J = 5.0 Hz, 2H, H-Piperazine). **^{13}C NMR (151 MHz, DMSO-d_6) δ** 170.33, 136.97, 136.20, 131.48, 130.58 (2C), 128.13 (2C), 127.04, 122.37, 120.81, 118.24, 118.13, 113.72, 111.25, 60.87, 52.59, 52.20, 44.90, 40.99, 33.18, 20.59; **LC-MS (m/z)**: 382.2 ($[M+H]^+$); **purity** by HPLC-UV (220 – 400 nm)-ESI-MS: 99.6% .

1-(4-benzylpiperazin-1-yl)-3-(1*H*-indol-3-yl)propan-1-one (FPE-ML40)

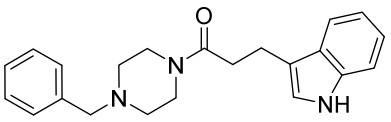

Synthesis according to **GP 4.** Purification with flash column chromatography on silica gel (MeOH in DCM 2 to 4%). **Yield**: 0.037 g, 0.106 mmol, 35.6 %; **M.p.**: 138°C; **^{1}H-NMR** (600 MHz, DMSO-d_6) δ 10.75 (s, 1 H, NH_{indole}), 7.49 (d, J = 7.8 Hz, 1 H, Ar-H_{indole}), 7.32 (t, J = 7.7 Hz, 3 H, Ar-H), 7.29-7.22 (m, 3 H, Ar-H), 7.12 (d, J = 2.2 Hz, 1 H, Ar-H_{indole}), 7.09-7.02 (m, 1 H, Ar-H_{indole}), 6.96 (t, J = 7.4 Hz, 1 H, Ar-H_{indole}), 3.45 (t, J = 5.0 Hz, 2 H, H-Piperazine), 3.43 (s, 2 H, NCH_2), 3.38 (t, J = 4.9 Hz, 2 H, H-Piperazine), 2.90 (dd, J = 8.9 Hz, 6.5 Hz, 2 H, $COCH_2CH_2$), 2.64 (dd, J = 8.9 Hz, 6.6 Hz, 2 H, $COCH_2CH_2$), 2.26 (t, J = 5.1 Hz, 2H, H-Piperazine), 2.20 (t, J = 5.0 Hz, 2H, H-Piperazine); **^{13}C NMR** (151 MHz, DMSO-d_6) δ 170.30, 137.85, 136.19, 128.82 (2C), 128.15 (2C), 127.04, 126.95, 122.36, 120.80, 118.24, 118.13, 113.72, 111.25, 61.84, 52.67, 52.29, 44.91, 41.00, 33.18, 20.59; **LC-MS (m/z)**: 348.2 ($[M+H]^+$); **purity** by HPLC-UV (220 – 400 nm)-ESI-MS: 98.7% .

1-(4-(4-bromobenzyl)piperazin-1-yl)-3-(1*H*-indol-3-yl)propan-1-one (FPE-ML47)

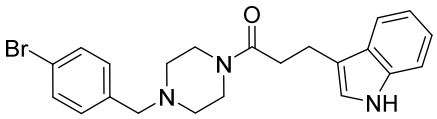

Synthesis according to **GP 4**. Purification with flash column chromatography on silica gel (MeOH in DCM 2 to 5 %). **Yield:** 0.025 g, 0.059 mmol, 18.9 %; **M.p.**: 138°C; **^{1}H-NMR** (600 MHz, DMSO-d_6) δ 10.75 (s, 1 H, NH_{indole}), 7.51 (d, J = 2.0 Hz, 1 H, Ar-H), 7.49 (d, J = 7.9 Hz, 2 H, Ar-H_{benzyl}), 7.32 (d, J = 8.1 Hz, 1 H, Ar-H), 7.27-7.23 (m, 2 H, Ar-H_{benzyl}), 7.12 (d, J = 2.2 Hz, 1 H, Ar-H), 7.09-7.02 (m, 1 H, Ar-H), 6.96 (t, J = 7.3 Hz, 1 H, Ar-H), 3.44 (t, J = 5.0 Hz, 2 H, NCH_2), 3.39 (t, J = 15.1 Hz, 4 H, H-Piperazine), 2.90 (dd, J = 8.9 Hz, 6.5 Hz, 2 H, $COCH_2CH_2$), 2.64 (dd, J = 8.9 Hz, 6.6 Hz, 2 H, $COCH_2CH_2$), 2.25 (t, J = 5.0 Hz, 2H, H-Piperazine), 2.20 (t, J = 4.9 Hz, 2H, H-Piperazine); **^{13}C NMR** (151 MHz, DMSO-d_6) δ 170.32, 137.40, 136.19, 131.05 (2C), 130.96 (2C), 127.04, 122.37, 120.81, 119.98, 118.24, 118.13, 113.72, 111.25, 60.91, 52.60, 52.20, 44.90, 40.98, 33.18, 20.59; **LC-MS (m/z)**: 428.2 ($[M+H]^+$); **purity** by HPLC-UV (220 – 400 nm)-ESI-MS: 98.8% .

(4-(3-(1*H*-indol-3-yl)propyl)piperazin-1-yl)(4-chlorophenyl)methanone (FPE-ML53)

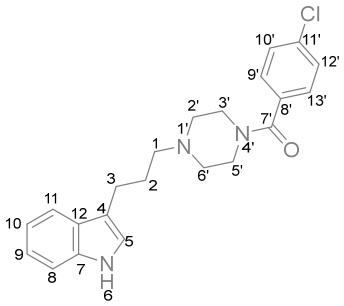

In a 50 mL round-bottomed flask, **FPE-ML50** (0.100 g, 0.411 mmol, 1.00 eq.) was dissolved in dry DCM (5 mL) and this solution was cooled down to 0°C. triethylamine (1.71 mL, 1.23 mmol, 3.00 eq.) was added to the cold mixture and stirred at this temperature for 10 min. benzoyl chloride (0.46 mL, 0.411 mmol, 1.00 eq.) was added to the mixture and stirred at RT for 5 h. When no further improvement was detected, the solvent was removed under reduced pressure. The residue was extracted with EE. The organic layer was dried over $MgSO_4$ and concentrated under reduced pressure. The crude was purified by flash chromatography (MeOH in DCM 2% to 5 %). **Yield**: 0.045 g, 0.118 mmol, 28.7 %; **LC-MS (*m/z*)**: 382.2 $[M+H]^+$; **Purity** by HPLC-UV (220-600 nm): 97.2 %; **M.p.**: 163°C; **^{1}H-NMR** (600 MHz, DMSO-d_6) δ **δ**: 10.72 (s, 1 H, 6-H), 7.52-7.47 (m, 3 H, 11-H, 9'-H, 13'-H), 7.43-7.38 (m, 2 H, 10'-H, 12'-H), 7.32 (d, *J* = 8.1 Hz, 1 H, 8-H), 7.09 (d, *J* = 2.2 Hz, 1 H, 5-H), 7.04 (ddd, *J* = 8.1 Hz, 6.8 Hz, 1.2 Hz, 1 H, 9-H), 6.95 (t, *J* = 7.5 Hz, 1 H, 10-H), 3.61 (brs, 2H, $H_{\text{-piperazine}}$), 2.69 (t, *J* = 7.5 Hz, 2 H, 3-H), 2.41 (brs, 2 H, $H_{\text{-piperazine}}$), 2.36 (t, *J* = 6.1 Hz, 2 H, 1-H), 2.32 (brs, 1 H, $H_{\text{-piperazine}}$), 1.80 (p, *J* = 7.4 Hz, 2 H, 2-H). **^{13}C NMR (151 MHz, DMSO-d_6) δ** 167.8 (C-7'), 136.3 (C-7), 134.7 (C-11'), 134.1 (C-8'), 128.9 (C-9', C-13'), 128.5 (C-10', C-12'), 127.2 (C-12), 122.1 (C-5), 120.7 (C-9), 118.2 (C-10), 118.0 (C-11), 114.3 (C-8), 111.3 (C-4), 57.4 (C-1), 52.9 ($C_{\text{-Piperazine}}$), 52.5 ($C_{\text{-Piperazine}}$), 47.2 ($C_{\text{-Piperazine}}$), 41.6 ($C_{\text{-Piperazine}}$), 27.0 (C-2), 22.4 (C-3).

(4-(3-(1*H*-indol-3-yl)propyl)piperazin-1-yl)(3,4-dichlorophenyl)methanone (FPE-ML54)

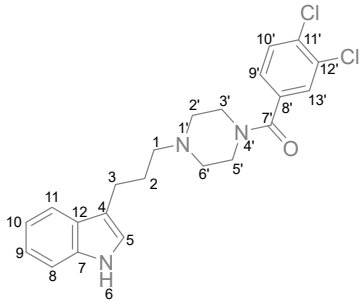

FPE-ML54 was synthesized according to **GP5**. Flash chromatography was used for further purification (MeOH in DCM 3 % to 7 %). **Yield**: 0.033 g, 0.079 mmol, 19.3 %; **LC-MS (*m/z*)**: 416.2 $[M+H]^+$; **purity** by HPLC-UV (220-600 nm): 97.9 %; **M.p.**: 180°C; **^{1}H-NMR** (600 MHz, DMSO-d_6) δ δ: 10.72 (s, 1 H, 6-H), 7.70 (d, *J* = 8.2 Hz, 1 H, 13'-H), 7.66 (d, *J* = 1.9 Hz, 1 H, 9'-H), 7.49 (d, *J* = 7.8 Hz, 1 H, 10'-H), 7.38 (dd, *J* = 8.2 Hz, 1.9 Hz, 1 H, 11-H), 7.32 (d, *J* = 8.0 Hz, 1 H, 8-H), 7.09 (d, *J* = 2.2 Hz, 1 H, 5-H), 7.07-7.02 (m, 1 H, 9-H), 6.95 (t, *J* =

7.4 Hz, 1 H, 10-H), 3.61 (brs, 2 H, $H_{\text{-piperazine}}$), 3.31-3.28 (m, 2 H, $H_{\text{-piperazine}}$), 2.69 (t, *J* = 7.5 Hz, 2 H, 3-H), 2.42 (brs, 2 H, H-piperazine), 2.36 (t, *J* = 7.3 Hz, 2 H, 1-H), 2.33 (brs, 2 H, H-piperazine), 1.80 (p, *J* = 7.5 Hz, 2 H, 2-H). **^{13}C NMR** (151 MHz, DMSO-*d*$_6$) δ: 166.4 (C-7'), 136.5 (C-8'), 136.3 (C-7), 132.1 (C-11'), 131.3 (C-12'), 130.8 (C-10'), 129.0 (C-13'), 127.2 (C-12), 122.1 (C-9'), 122.0 (C-5), 120.7 (C-9), 118.2 (C-10), 118.0 (C-11), 114.3 (C-8), 111.3 (C-4), 57.4 (C-1), 52.8 ($C_{\text{-Piperazine}}$), 52.3 ($C_{\text{-Piperazine}}$), 47.2 ($C_{\text{-Piperazine}}$), 41.7 ($C_{\text{-Piperazine}}$), 27.0 (C-2), 22.4 (C-3).

(4-(3-(1*H*-indol-3-yl)propyl)piperazin-1-yl)(4-nitrophenyl)methanone (FPE-ML55)

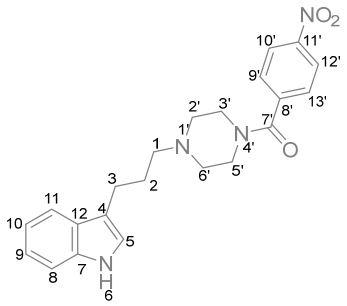

FPE-ML55 was synthesized according to **GP5**. Flash chromatography was used for further purification (MeOH in DCM 2 to 5%)**; Yield**: 0.043 g, 0.110 mmol, 26.7 %; **LC-MS (*m/z*)**: 382.2 $[M+H]^+$; **purity** by HPLC-UV (220-600 nm): 95.4%; **M.p.**: 185°C; **^{1}H-NMR** (600 MHz, DMSO-*d*$_6$) δ : 10.84 (s, 1 H, 6-H), 8.33-8.28 (m, 2 H, 10'-H, 12'-H), 7.74-7.69 (m, 2 H, 9'-H, 13'-H), 7.53 (d, *J* = 7.9 Hz, 1 H, 11-H), 7.35 (d, *J* = 8.0 Hz, 1 H, 8-H), 7.16 (d, *J* = 2.3 Hz, 1 H, 5-H), 7.09 (t, *J* = 7.5 Hz, 1 H, 9-H), 6.98 (t, *J* = 7.4 Hz, 1 H, 10-H), 3.49 (brs, 3 H, H-piperazine), 3.07 (brs, 4 H, $H_{\text{-piperazine}}$), 2.75 (t, *J* = 7.4 Hz, 2 H, 3-H), 2.01 (p, *J* = 6.0 Hz, 2 H, 2-H). **^{13}C NMR** (151 MHz, DMSO-*d*$_6$) δ:167.2 (C-7'), 148.1 (C-11'), 141.2 (C-8'), 136.4 (C-7), 128.5 (C-9', C-13'), 126.9 (C-12), 123.8 (C-10', C-12'), 122.5 (C-5), 121.1 (C-9). 118.2 (C-11), 118.2 (C-8), 111.4 (C-4), 56.0 (C-1), 50.8 ($C_{\text{-Piperazine}}$), 44.3 ($C_{\text{-Piperazine}}$), 24.4 (C-2), 21.8 (C-3).

(4-(3-(1*H*-indol-3-yl)propyl)piperazin-1-yl)(4-bromophenyl)methanone (FPE-ML57)

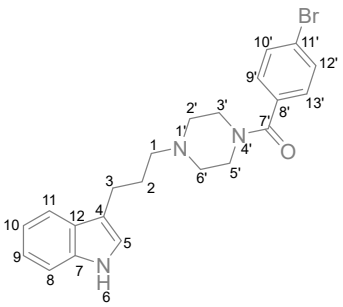

FPE-ML57 was synthesized according to **GP5**. Column chromatography was used for further purification (MeOH: DCM / 5:95). **Yield**: 0.016 g, 0.038 mmol, 9.13 %; **LC-MS (*m/z*)**: 426.2 $[M+H]^+$; **purity** by HPLC-UV (220-600 nm): 98.6%; **M.p.**: 160°C; **^{1}H-NMR** (600 MHz, DMSO-*d*$_6$) δ 10.72 (s, 1 H, 6-H), 7.66-7.61 (m, 2 H, 9'-H, 13'-H), 7.49 (d, *J* = 7.8 Hz, 1 H, 11-H), 7.37-7.33 (m, 1 H, 10'-H, 12'-H), 7.32 (d, *J* = 8.1 Hz, 1 H, 8-H), 7.09 (d, *J* = 2.3 Hz, 1 H, 5-H), 7.04 (ddd, *J* = 8.0 Hz, 6.8 Hz, 1.2 Hz, 1 H, 9-H), 6.95 (td, *J* = 7.4 Hz, 1.1 Hz, 1 H, 10-H), 3.61 (brs, 2 H, $H_{\text{-piperazine}}$),

2.69 (t, *J* = 7.5 Hz, 2 H, 3-H), 2.41 (brs, 4 H, $H_{\text{-piperazine}}$), 2.36 (t, *J* = 7.3 Hz, 2 H, 1-H), 2.32 (brs, 2 H, $H_{\text{-piperazine}}$), 1.80 (p, *J* = 7.4 Hz, 2 H, 2-H). **^{13}C NMR** (151 MHz, DMSO-*d*$_6$) δ: 167.8 (C-7'), 136.2 (C-7), 135.1 (C-8'), 131.4 (C-10', C-12'), 129.1 (C-9', C-13'), 127.8 (C-12), 127.2 (C-11'), 122.1 (C-5), 120.8 (C-9), 118.2 (C-10), 118.0 (C-11), 114.3 (C-8), 111.3 (C-4), 57.4 (C-1), 52.9 ($C_{\text{-Piperazine}}$), 52.5 ($C_{\text{-Piperazine}}$), 47.1 ($C_{\text{-Piperazine}}$), 41.7 ($C_{\text{-Piperazine}}$), 27.0 (C-2), 22.4 (C-3).

(4-(3-(1*H*-indol-3-yl)propyl)piperazin-1-yl)(4-aminophenyl)methanone (FPE-ML60)

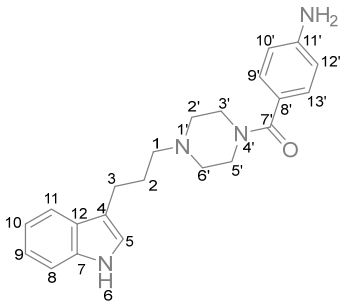

In a 100 mL round-bottomed flask, **FPE-55** (0.024 g, 0.062 mmol, 1.00 eq.) was dissolved in EtOH (5 mL) and $SnCl_2 \cdot 2H_2O$ (0.069 g, 0.306 mmol, 5.00 eq.) was added in portions. The reaction mixture was stirred at 90°C for 2 h. After the solvent was evaporated under reduced pressure, ice-cold water was added to the reaction mixture and the mixture was basified with $NaHCO_3$. It was extracted with EE (5*30 mL). The organic layer was dried over $MgSO_4$ and concentrated under reduced pressure. **Yield**: 0.003 g, 0.009 mmol, 14.9 %; **LC-MS (*m/z*)**: 363.3 $[M+H]^+$; **purity** by HPLC-UV (220-600 nm): 99.5%; **M.p.**: 182°C; **^{1}H-NMR** (600 MHz, DMSO-*d*$_6$) δ : 10.71 (s, 1 H, 6-H), 7.50 (d, *J* = 7.8 Hz, 1 H, 11-H), 7.32 (d, *J* = 8.0 Hz, 1 H, 8-H), 7.12-7.07 (m, 3 H, 9-H, 9'-H, 13'-H), 7.07-7.02 (m, 1 H, H-5), 6.98-6.93 (m, 1 H, 10-H), 6.56-6.51 (m, 2 H, 10'-H, 12'-H), 5.46 (s, 2 H, -N$\underline{H}_2$), 3.48 (t, *J* = 4.8 Hz, 4 H, 3'-H, 5'-H), 2.69 (t, *J* = 7.5 Hz, 2 H, 3-H), 2.36 (dt, *J* = 7.8 Hz, 4.6 Hz, 6 H, 1-H, 2'-H, 6-H), 1.80 (p, *J* =7.5 Hz, 2 H, 2-H). **^{13}C NMR** (151 MHz, DMSO-*d*$_6$) δ: 169.7 (C-7'), 150.4 (C-11'), 136.3 (C-7), 129.1 (C-9', C-13'), 127.2 (C-12), 122.1 (C-8'), 122.0 (C-5), 120.7 (C-9), 118.3 (C-10), 118.0 (C-11), 114.3 (C-8), 112.6 (C-10', C-12'), 111.3 (C-4), 57.5 (C-2', C-6'), 54.6 (C-1), 52.9 (C-3', C-5'), 27.0 (C-2), 22.4 (C-3).

1-(4-(4-bromobenzoyl)piperazin-1-yl)-3-(1*H*-indol-3-yl)propan-1-one (FPE-ML61)

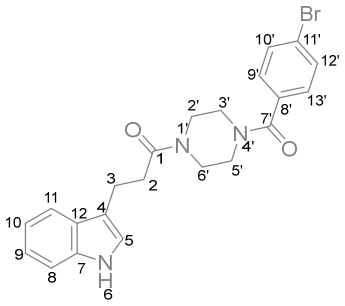

The reaction runs under an inert gas atmosphere. In a 100 mL two-neck round-bottomed flask, **FPE-ML35** (0.384 g, 1.49 mmol, 2.00 eq.), 1-Hydroxybenzotriazol (0.136 g, 1.01 mmol, 1.35 eq.), 3-(((ethylimino)methylene)amino)-N,N-dimethylpropan-1-amine hydrochloride (0.215 g, 1.12 mmol, 1.50 eq.) and 4-bromobenzoic acid (0.150 g, 0.746 mmol, 1.00 eq.) were dissolved in acetone (10 mL). After the reaction mixture was stirred for 1 h, triethylamine was added to the mixture at RT and it was stirred for 2 h. When no further improvement was detected, the solvent was evaporated under reduced pressure. The crude was purified by column chromatography. (MeOH in DCM 5 to 7%). **Yield**: 0.08 g, 0.18 mmol, 38 %; **LC-MS (*m/z*)**: 442.1 $[M+H]^+$; **purity** by HPLC-UV (220-600 nm): 99.2 %; **M.p.**:186°C; **^{1}H-NMR** (600 MHz, DMSO-d_6) δ 10.76 (s, 1 H, 6-H), 7.68-7.62 (m, 2 H, 9'-H, 13'-H), 7.51 (d, J = 7.9 Hz, 1 H, H-11), 7.36 (d, J = 8.5 Hz, 2 H, 10'-H, 12'-H), 7.33 (d, J = 8.0 Hz, 1 H, 8-H), 7.14 (s, 1 H, 5-H), 7.06 (t, J = 7.4 Hz, 1 H, 9-H), 6.97 (t, J = 7.4 Hz, 1 H, 10-H), 3.65-3.35 (m, 6 H, H-Piperazine), 3.28-3.11 (m, 2 H, H-Piperazine), 2.93 (dd, J = 9.0 Hz, 6.4 Hz, 2 H, 3-H), 2.69 (s, 2 H, 2-H). **^{13}C NMR** (151 MHz, DMSO-d_6) δ 170.7 (C-1), 168.1 (C-7'), 136.2 (C-7), 134.8 (C-8'), 131.4 (C-10', C-12'), 129.1 (C-9', C-13'), 127.0 (C-12), 122.9 (C-11'), 122.5 (C-5), 120.8 (C-9), 118.2 (C-10), 118.1 (C-11), 113.6 (C-4), 111.12 (C-8), 33.21 (C-2), 20.5 (C-3).

References

(1) Sriram, K.; Insel, P. A. G Protein-Coupled Receptors as Targets for Approved Drugs: How Many Targets and How Many Drugs? *Mol. Pharmacol.* **2018**, *93*, 251–258. https://doi.org/10.1124/mol.117.111062.

(2) Schiöth, H. B.; Lagerström, M. C. Structural Diversity of g Proteincoupled Receptors and Significance for Drug Discovery. *Nat. Rev. Drug Discov.* **2008**, *7* (4), 339-57 https://doi.org/10.1038/nrd2518.

(3) Wu, C.; Xu, M.; Dong, J.; Cui, W.; Yuan, S. The Structure and Function of Olfactory Receptors. *Trends Pharmacol. Sci.* **2024**, *45* (3), 268–280. https://doi.org/10.1016/j.tips.2024.01.004.

(4) Orecchioni, M.; Kobiyama, K.; Winkels, H.; Ghosheh, Y.; McArdle, S.; Mikulski, Z.; Kiosses, W. B.; Fan, Z.; Wen, L.; Jung, Y.; Roy, P.; Ali, A. J.; Miyamoto, Y.; Mangan, M.; Makings, J.; Wang, Z.; Denn, A.; Vallejo, J.; Owens, M.; Durant, C. P.; Braumann, S.; Mader, N.; Li, L.; Matsunami, H.; Eckmann, L.; Latz, E.; Wang, Z.; Hazen, S. L.; Ley, K. Olfactory Receptor 2 in Vascular Macrophages Drives Atherosclerosis by NLRP3-Dependent IL-1 Production. *Science* **2022**, *375* (6577), 214-221 https://doi.org/10.1126/science.abg3067.

(5) Casadó, V.; Casadó-Anguera, V. What Are the Current Trends in G Protein-Coupled Receptor Targeted Drug Discovery? *Expert Opin. Drug Discov.* **2023**, *18* (8), 815–820. https://doi.org/10.1080/17460441.2023.2216014.

(6) Hauser, A. S.; Attwood, M. M.; Rask-Andersen, M.; Schiöth, H. B.; Gloriam, D. E. Trends in GPCR Drug Discovery: New Agents, Targets and Indications. *Nat. Rev. Drug Discov.* **2017**, *16*, 829–842. https://doi.org/10.1038/nrd.2017.178.

(7) Zhang, M.; Chen, T.; Lu, X.; Lan, X.; Chen, Z.; Lu, S. G Protein-Coupled Receptors (GPCRs): Advances in Structures, Mechanisms, and Drug Discovery. *Signal Transduct. Target. Ther.* **2024**, *9* (1), 1–43. https://doi.org/10.1038/s41392-024-01803-6.

(8) Yang, D.; Zhou, Q.; Labroska, V.; Qin, S.; Darbalaei, S.; Wu, Y.; Yuliantie, E.; Xie, L.; Tao, H.; Cheng, J.; Liu, Q.; Zhao, S.; Shui, W.; Jiang, Y.; Wang, M. W. G Protein-Coupled

Receptors: Structure- and Function-Based Drug Discovery. *Signal Transduct. Target. Ther.* **2021**, *6* (1). https://doi.org/10.1038/s41392-020-00435-w.

(9) García-Nafría, J.; Tate, C. G. Structure Determination of GPCRs: Cryo-EM Compared with X-Ray Crystallography. *Biochem. Soc. Trans.* **2021**, *49* (5), 2345-2355. https://doi.org/10.1042/BST20210431.

(10) Jumper, J.; Evans, R.; Pritzel, A.; Green, T.; Figurnov, M.; Ronneberger, O.; Tunyasuvunakool, K.; Bates, R.; Žídek, A.; Potapenko, A.; Bridgland, A.; Meyer, C.; Kohl, S. A. A.; Ballard, A. J.; Cowie, A.; Romera-Paredes, B.; Nikolov, S.; Jain, R.; Adler, J.; Back, T.; Petersen, S.; Reiman, D.; Clancy, E.; Zielinski, M.; Steinegger, M.; Pacholska, M.; Berghammer, T.; Bodenstein, S.; Silver, D.; Vinyals, O.; Senior, A. W.; Kavukcuoglu, K.; Kohli, P.; Hassabis, D. Highly Accurate Protein Structure Prediction with AlphaFold. *Nature* **2021**, *596* (7873), 583–589. https://doi.org/10.1038/s41586-021-03819-2.

(11) Nichols, C. D.; Roth, B. Engineered G-Protein Coupled Receptors Are Powerful Tools to Investigate Biological Processes and Behaviors. *Front. Mol. Neurosci.* **2009**, *2* (16). https://doi.org/10.3389/neuro.02.016.2009.

(12) Attwood, T. K.; Findlay, J. B. C. Fingerprinting G-Protein-Coupled Receptors. *Protein Eng.* **1994**, *7*(2), 195-203. https://doi.org/10.1093/protein/7.2.195.

(13) Fredriksson, R.; Lagerström, M. C.; Lundin, L. G.; Schiöth, H. B. The G-Protein-Coupled Receptors in the Human Genome Form Five Main Families. Phylogenetic Analysis, Paralogon Groups, and Fingerprints. *Mol. Pharmacol.* **2003**, *63* (6), 1256–1272. https://doi.org/10.1124/mol.63.6.1256.

(14) Gamgee, A. Kühne's Researches on Photo-Chemical Processes in the Retina. *Nature* **1877**, *15*, 296. https://doi.org/10.1038/015296a0.

(15) Fredriksson, R.; Höglund, P. J.; Gloriam, D. E. I.; Lagerström, M. C.; Schiöth, H. B. Seven Evolutionarily Conserved Human Rhodopsin G Protein-Coupled Receptors Lacking Close Relatives. *FEBS Lett.* **2003**, *554*(3), 381-388. https://doi.org/10.1016/S0014-5793(03)01196-7.

(16) Baldwin, J. M. Structure and Function of Receptors Coupled to G Proteins. *Curr. Opin. Cell Biol.* **1994**, *6*(2), 180-90. https://doi.org/10.1016/0955-0674(94)90134-1.

(17) Rinne, M.; Tanoli, Z. U. R.; Khan, A.; Xhaard, H. Cartography of Rhodopsin-like G Protein-Coupled Receptors across Vertebrate Genomes. *Sci. Rep.* **2019**, *9* (1), 1–16. https://doi.org/10.1038/s41598-018-33120-8.

(18) Nordström, K. J. V.; Sällman Almén, M.; Edstam, M. M.; Fredriksson, R.; Schiöth, H. B. Independent HHsearch, Needleman-Wunsch-Based, and Motif Analyses Reveal the Overall Hierarchy for Most of the g Protein-Coupled Receptor Families. *Mol. Biol. Evol.* **2011**, *28* (9), 2471–2480. https://doi.org/10.1093/molbev/msr061.

(19) Kobilka, B. K.; Deupi, X. Conformational Complexity of G-Protein-Coupled Receptors. *Trends Pharmacol. Sci.* **2007**, *28*(8), 397-406. https://doi.org/10.1016/j.tips.2007.06.003.

(20) Jelinek, V.; Mösslein, N.; Bünemann, M. Structures in G Proteins Important for Subtype Selective Receptor Binding and Subsequent Activation. *Commun. Biol.* **2021**, *4* (1), 1–11. https://doi.org/10.1038/s42003-021-02143-9.

(21) Smrcka, A. V. Review G Protein Bg Subunits: Central Mediators of G Protein-Coupled Receptor Signaling. *Cell Mol. Life Sci.* **2008**, *65*(14), 2191-214. https://doi.org/10.1007/s00018-008-8006-5.

(22) Wettschureck, N.; Offermanns, S. Mammalian G Proteins and Their Cell Type Specific Functions. *Physiol Rev.* **2005**, *85*(4), 1159-204. https://doi.org/10.1152/physrev.00003.2005.-Heterotrimeric.

(23) Dores, M. R.; Trejo, J. A. Atypical Regulation of G Protein-Coupled Receptor Intracellular Trafficking by Ubiquitination. *Curr. Opin. Cell Biol.* **2014**, *27* (1), 44–50. https://doi.org/10.1016/J.CEB.2013.11.004.

(24) Luttrell, L. M.; Lefkowitz, R. J. The Role of β-Arrestins in the Termination and Transduction of G-Protein-Coupled Receptor Signals. *J. Cell Sci.* **2002**, *115* (3), 455–465.

(25) Sun, Y.; McGarrigle, D.; Huang, X. Y. When a G Protein-Coupled Receptor Does Not Couple to a G Protein. *Mol. Biosyst.* **2007**, *3*, 849-854. https://doi.org/10.1039/b706343a.

(26) Johnson, D. E. Src Family Kinases and the MEK/ERK Pathway in the Regulation of Myeloid Differentiation and Myeloid Leukemogenesis. *Adv Enzyme Regul.* **2008**, *48*, 98-112https://doi.org/10.1016/j.advenzreg.2007.11.002.

(27) McGarrigle, D.; Huang, X. Y. GPCRs Signaling Directly Through Src-Family Kinases. *Sci. STKE* **2007**, *2007* (392). https://doi.org/10.1126/STKE.3922007PE35.

(28) Sun, Y.; McGarrigle, D.; Huang, X. Y. When a G Protein-Coupled Receptor Does Not Couple to a G Protein. *Mol. Biosyst.* **2007**, *3* (12), 849–854. https://doi.org/10.1039/B706343A.

(29) Van Gastel, J.; Hendrickx, J. O.; Leysen, H.; Santos-Otte, P.; Luttrell, L. M.; Martin, B.; Maudsley, S. β-Arrestin Based Receptor Signaling Paradigms: Potential Therapeutic Targets for Complex Age-Related Disorders. *Front. Pharmacol.* **2018**, *9*, 1369. https://doi.org/10.3389/FPHAR.2018.01369/BIBTEX.

(30) Shukla, A. K.; Xiao, K.; Lefkowitz, R. J. Emerging Paradigms of β-Arrestin-Dependent Seven Transmembrane Receptor Signaling. *Trends Biochem. Sci*. **2011.** *36* (9), 457-69. https://doi.org/10.1016/j.tibs.2011.06.003.

(31) Smith, J. S.; Pack, T. F. Noncanonical Interactions of G Proteins and β-Arrestins: From Competitors to Companions. *FEBS J.* **2021**, *288* (8), 2550-2561. https://doi.org/10.1111/febs.15749.

(32) Maudsley, S.; Martin, B.; Luttrell, L. M. The Origins of Diversity and Specificity in G Protein-Coupled Receptor Signaling. *J. Pharmacol. Exp. Ther.* **2005**, *314*(2), 485-94. https://doi.org/10.1124/jpet.105.083121.

(33) Violin, J. D.; Lefkowitz, R. J. β-Arrestin-Biased Ligands at Seven-Transmembrane Receptors. *Trends Pharmacol. Sci.* **2007***,* *28*(8), 416-22. https://doi.org/10.1016/j.tips.2007.06.006.

(34) Steen, A.; Larsen, O.; Thiele, S.; Rosenkilde, M. M. Biased and G Protein-Independent Signaling of Chemokine Receptors. *Front. Immunol*. **2014**, *5*, 277. https://doi.org/10.3389/fimmu.2014.00277.

(35) Weis, W. I.; Kobilka, B. K. The Molecular Basis of G Protein-Coupled Receptor Activation. Annu. Rev. Biochem. **2018,** *20*(87), 897-919. https://doi.org/10.1146/annurev-biochem-060614-033910.

(36) Che, T.; Agnihotri, H. D.; Shukla, A. K.; Roth, B. L. Biased Ligands at Opioid Receptors:

Current Status and Future Directions. *Sci. Signal.* **2021**, *14* (677). https://doi.org/10.1126/SCISIGNAL.AAV0320.

(37) Samuelson, L. C.; Swanberg, L. J.; Gantz, I. Mapping of the Novel G Protein-Coupled Receptor Gpr18 to Distal Mouse Chromosome 14. *Mamm. Genome* **1996**, *7*(12), 920-1. https://doi.org/10.1007/s003359900272.

(38) Reyes-Resina, I.; Navarro, G.; Aguinaga, D.; Canela, E. I.; Schoeder, C. T.; Załuski, M.; Kieć-Kononowicz, K.; Saura, C. A.; Müller, C. E.; Franco, R. Molecular and Functional Interaction between GPR18 and Cannabinoid CB2 G-Protein-Coupled Receptors. Relevance in Neurodegenerative Diseases. *Biochem. Pharmacol.* **2018**, *157*, 169–179. https://doi.org/10.1016/j.bcp.2018.06.001.

(39) Funke, M.; Thimm, D.; Schiedel, A. C.; Müller, C. E. 8-Benzamidochromen-4-One-2-Carboxylic Acids: Potent and Selective Agonists for the Orphan G Protein-Coupled Receptor GPR35. *J. Med. Chem.* **2013**, *56* (12), 5182–5197. https://doi.org/10.1021/jm400587g.

(40) Schoeder, C. T.; Kaleta, M.; Mahardhika, A. B.; Olejarz-Maciej, A.; Łażewska, D.; Kieć-Kononowicz, K.; Müller, C. E. Structure-Activity Relationships of Imidazothiazinones and Analogs as Antagonists of the Cannabinoid-Activated Orphan G Protein-Coupled Receptor GPR18. *Eur. J. Med. Chem.* **2018**, *155*, 381–397. https://doi.org/10.1016/j.ejmech.2018.05.050.

(41) Tang, X. L.; Wang, Y.; Li, D. L.; Luo, J.; Liu, M. Y. Orphan G Protein-Coupled Receptors (GPCRs): Biological Functions and Potential Drug Targets. *Acta Pharmacol. Sin.* **2012**, *33*, 363–371. https://doi.org/10.1038/aps.2011.210.

(42) Chung, S.; Funakoshi, T.; Civelli, O. Orphan GPCR Research. In *Br. J. Pharmacol*. **2008**, *153* (S1), S339-S346. https://doi.org/10.1038/sj.bjp.0707606.

(43) Stoddart, L. A.; Kilpatrick, L. E.; Hill, S. J. NanoBRET Approaches to Study Ligand Binding to GPCRs and RTKs. *Trends Pharmacol. Sci.* **2018**, *39* (2), 136–147. https://doi.org/10.1016/j.tips.2017.10.006.

(44) Walker, J. R.; Hall, M. P.; Zimprich, C. A.; Robers, M. B.; Duellman, S. J.; Machleidt, T.; Rodriguez, J.; Zhou, W. Highly Potent Cell-Permeable and Impermeable NanoLuc

Luciferase Inhibitors. *ACS Chem. Biol.* **2017,** *12*(4), 1028-1037. https://doi.org/10.1021/acschembio.6b01129.

(45) Dale, N. C.; Johnstone, E. K. M.; White, C. W.; Pfleger, K. D. G. NanoBRET: The Bright Future of Proximity-Based Assays. *Front. Bioeng. Biotechnol.* **2019**, *7*, 1–13. https://doi.org/10.3389/fbioe.2019.00056.

(46) Loudet, A.; Burgess, K. BODIPY Dyes and Their Derivatives: Syntheses and Spectroscopic Properties. *Chem. Rev.* **2007**, *107* (11), 4891–4932. https://doi.org/10.1021/cr078381n.

(47) Dong, Y.; Ma, T.; Xu, T.; Feng, Z.; Li, Y.; Song, L.; Yao, X.; Ashby, C. R.; Hao, G. F. Characteristic Roadmap of Linker Governs the Rational Design of PROTACs. *Acta Pharm. Sin. B.* **2024,** *14*(10), 4266–4295. https://doi.org/10.1016/j.apsb.2024.04.007.

(48) Gao, Y.; Joshi, M.; Zhao, Z.; Mitragotri, S. PEGylated Therapeutics in the Clinic. *Bioeng. Transl. Med.* **2024**, *9* (1), 1–28. https://doi.org/10.1002/btm2.10600.

(49) Gantz, I.; Muraoka, A.; Yang, Y. K.; Samuelson, L. C.; Zimmerman, E. M.; Cook, H.; Yamada, T. Cloning and Chromosomal Localization of a Gene (GPR18) Encoding a Novel Seven Transmembrane Receptor Highly Expressed in Spleen and Testis. *Genomics* **1997**, *42* (3), 462–466. https://doi.org/10.1006/geno.1997.4752.

(50) Norregaard, K.; Benned-Jensen, T.; Marie Rosenkilde, M. EBI2, GPR18, and GPR17 – Three Structurally Related but Biologically Distinct 7TM Receptors. *Curr. Top. Med. Chem.* **2011**, *11*(6), 618-628. https://doi.org/10.2174/1568026611109060618.

(51) Kohno, M.; Hasegawa, H.; Inoue, A.; Muraoka, M.; Miyazaki, T.; Oka, K.; Yasukawa, M. Identification of N-Arachidonylglycine as the Endogenous Ligand for Orphan G-Protein-Coupled Receptor GPR18. *Biochem. Biophys. Res. Commun.* **2006**, *347* (3), 827–832. https://doi.org/10.1016/j.bbrc.2006.06.175.

(52) Becker, A. M.; Callahan, D. J.; Richner, J. M.; Choi, J.; DiPersio, J. F.; Diamond, M. S.; Bhattacharya, D. GPR18 Controls Reconstitution of Mouse Small Intestine Intraepithelial Lymphocytes Following Bone Marrow Transplantation. *PLoS One* **2015**, *10* (7), 1–20. https://doi.org/10.1371/journal.pone.0133854.

(53) Burstein, S. H.; McQuain, C. A.; Ross, A. H.; Salmonsen, R. A.; Zurier, R. E. Resolution of

Inflammation by N-Arachidonoylglycine. *J. Cell. Biochem.* **2011**, *112*(11), 3227–3233. https://doi.org/10.1002/jcb.23245.

(54) Guerrero-Alba, R.; Barragán-Iglesias, P.; González-Hernández, A.; Valdez-Moráles, E. E.; Granados-Soto, V.; Condés-Lara, M.; Rodríguez, M. G.; Marichal-Cancino, B. A. Some Prospective Alternatives for Treating Pain: The Endocannabinoid System and Its Putative Receptors GPR18 and GPR55. *Front. Pharmacol*. **2019,** *9*, 1496. https://doi.org/10.3389/fphar.2018.01496.

(55) Chiang, N.; Dalli, J.; Colas, R. A.; Serhan, C. N. Identification of Resolvin D2 Receptor Mediating Resolution of Infections and Organ Protection. *J. Exp. Med.* **2015**, *212* (8), 1203–1217. https://doi.org/10.1084/jem.20150225.

(56) Zhao, M.; Zheng, Z.; Yin, Z.; Zhang, J.; Qin, J.; Wan, J.; Wang, M. Resolvin D2 and Its Receptor GPR18 in Cardiovascular and Metabolic Diseases: A Promising Biomarker and Therapeutic Target. *Pharmacol. Res.* **2023**, *195* (June), 106832. https://doi.org/10.1016/j.phrs.2023.106832.

(57) Járai, Z.; Wagner, J. A.; Varga, K.; Lake, K. D.; Compton, D. R.; Martin, B. R.; Zimmer, A. M.; Bonner, T. I.; Buckley, N. E.; Mezey, E.; Razdan, R. K.; Zimmer, A.; Kunos, G. Cannabinoid-Induced Mesenteric Vasodilation through an Endothelial Site Distinct from CB1 or CB2 Receptors. *Proc. Natl. Acad. Sci. U. S. A.* **1999**, *96* (24), 14136–14141. https://doi.org/10.1073/pnas.96.24.14136.

(58) Penumarti, A.; Abdel-Rahman, A. A. The Novel Endocannabinoid Receptor GPR18 Is Expressed in the Rostral Ventrolateral Medulla and Exerts Tonic Restraining Influence on Blood Pressure. *J. Pharmacol. Exp. Ther.* **2014**, *349* (4), 29–38. https://doi.org/10.1124/jpet.113.209213.

(59) Miller, S.; Leishman, E.; Oehler, O.; Daily, L.; Murataeva, N.; Wager-Miller, J.; Bradshaw, H.; Straiker, A. Evidence for a GPR18 Role in Diurnal Regulation of Intraocular Pressure. *Investig. Ophthalmol. Vis. Sci.* **2016**. , *57*(14), 6419-6426. https://doi.org/10.1167/iovs.16-19437.

(60) Caldwell, M. D.; Hu, S. S. J.; Viswanathan, S.; Bradshaw, H.; Kelly, M. E. M.; Straiker, A. A GPR18-Based Signalling System Regulates IOP in Murine Eye. *Br. J. Pharmacol.* **2013**,

169(4), 834-43. https://doi.org/10.1111/bph.12136.

(61) Finlay, D. B.; Joseph, W. R.; Grimsey, N. L.; Glass, M. GPR18 Undergoes a High Degree of Constitutive Trafficking but Is Unresponsive to N-Arachidonoyl Glycine. *PeerJ* **2016**, *2016* (3), 1–29. https://doi.org/10.7717/peerj.1835.

(62) Qin, Y.; Verdegaal, E. M. E.; Siderius, M.; Bebelman, J. P.; Smit, M. J.; Leurs, R.; Willemze, R.; Tensen, C. P.; Osanto, S. Quantitative Expression Profiling of G-Protein-Coupled Receptors (GPCRs) in Metastatic Melanoma: The Constitutively Active Orphan GPCR GPR18 as Novel Drug Target. *Pigment Cell Melanoma Res.* **2011**, *24* (1), 207–218. https://doi.org/10.1111/j.1755-148X.2010.00781.x.

(63) Pascoal, L. B.; Bombassaro, B.; Ramalho, A. F.; Coope, A.; Moura, R. F.; Correa-da-Silva, F.; Ignacio-Souza, L.; Razolli, D.; de Oliveira, D.; Catharino, R.; Velloso, L. A. Resolvin RvD2 Reduces Hypothalamic Inflammation and Rescues Mice from Diet-Induced Obesity. *J. Neuroinflammation* **2017**, *14* (1), 1–12. https://doi.org/10.1186/s12974-016-0777-2.

(64) Rajaraman, G.; Simcocks, A.; Hryciw, D. H.; Hutchinson, D. S.; McAinch, A. J. G Protein Coupled Receptor 18: A Potential Role for Endocannabinoid Signaling in Metabolic Dysfunction. *Mol. Nutr. Food Res.* **2016**, *60* (1), 92–102. https://doi.org/10.1002/mnfr.201500449.

(65) Ramírez-Orozco, R. E.; García-Ruiz, R.; Morales, P.; Villalón, C. M.; Villafán-Bernal, J. R.; Marichal-Cancino, B. A. Potential Metabolic and Behavioural Roles of the Putative Endocannabinoid Receptors GPR18, GPR55 and GPR119 in Feeding. *Curr. Neuropharmacol.* **2019**, *17*(10), 947-960. https://doi.org/10.2174/1570159x17666190118143014.

(66) Walter, L.; Franklin, A.; Witting, A.; Wade, C.; Xie, Y.; Kunos, G.; Mackie, K.; Stella, N. Nonpsychotropic Cannabinoid Receptors Regulate Microglial Cell Migration. *J. Neurosci.* **2003**, *23*(4), 1398-405. https://doi.org/10.1523/jneurosci.23-04-01398.2003.

(67) Franklin, A.; Stella, N. Arachidonylcyclopropylamide Increases Microglial Cell Migration through Cannabinoid CB2 and Abnormal-Cannabidiol-Sensitive Receptors. *Eur. J. Pharmacol.* **2003**, *474* (2–3), 195–198. https://doi.org/10.1016/S0014-2999(03)02074-0.

(68) Reyes-Resina, I.; Navarro, G.; Aguinaga, D.; Canela, E. I.; Schoeder, C. T.; Załuski, M.;

Kieć-Kononowicz, K.; Saura, C. A.; Müller, C. E.; Franco, R. Molecular and Functional Interaction between GPR18 and Cannabinoid CB2 G-Protein-Coupled Receptors. Relevance in Neurodegenerative Diseases. *Biochem. Pharmacol.* **2018**. *157*, 169-169. https://doi.org/10.1016/j.bcp.2018.06.001.

(69) Mirchandani-Duque, M.; Choucri, M.; Hernández-Mondragón, J. C.; Crespo-Ramírez, M.; Pérez-Olives, C.; Ferraro, L.; Franco, R.; Pérez de la Mora, M.; Fuxe, K.; Borroto-Escuela, D. O. Membrane Heteroreceptor Complexes as Second-Order Protein Modulators: A Novel Integrative Mechanism through Allosteric Receptor–Receptor Interactions. *Membranes.* **2024**, *14* (5), 1–24. https://doi.org/10.3390/membranes14050096.

(70) Járai, Z.; Wagner, J. A.; Varga, K.; Lake, K. D.; Compton, D. R.; Martin, B. R.; Zimmer, A. M.; Bonner, T. I.; Buckley, N. E.; Mezey, E.; Razdan, R. K.; Zimmer, A.; Kunos, G. Cannabinoid-Induced Mesenteric Vasodilation through an Endothelial Site Distinct from CB1 or CB2 Receptors. *Proc. Natl. Acad. Sci. U. S. A.* **1999**, *96*(24), 14136-41. https://doi.org/10.1073/pnas.96.24.14136.

(71) Offertáler, L.; Mo, F. M.; Bátkai, S.; Liu, J.; Begg, M.; Razdan, R. K.; Martin, B. R.; Bukoski, R. D.; Kunos, G. Selective Ligands and Cellular Effectors of a G Protein-Coupled Endothelial Cannabinoid Receptor. *Mol. Pharmacol.* **2003**, *63*(3), 699-705. https://doi.org/10.1124/mol.63.3.699.

(72) Begg, M.; Mo, F. M.; Offertáler, L.; Bátkai, S.; Pacher, P.; Razdan, R. K.; Lovinger, D. M.; Kunos, G. G Protein-Coupled Endothelial Receptor for Atypical Cannabinoid Ligands Modulates a Ca2+-Dependent K+ Current. *J. Biol. Chem.* **2003**, *278* (46), 46188–46194. https://doi.org/10.1074/jbc.M307258200.

(73) McHugh, D.; Page, J.; Dunn, E.; Bradshaw, H. B. Δ 9-Tetrahydrocannabinol and N-Arachidonyl Glycine Are Full Agonists at GPR18 Receptors and Induce Migration in Human Endometrial HEC-1B Cells. *Br. J. Pharmacol*. **2012**, *165*(8), 2414–2424. https://doi.org/10.1111/j.1476-5381.2011.01497.x.

(74) C. Ashton, J. The Atypical Cannabinoid O-1602: Targets, Actions, and the Central Nervous System. *Cent. Nerv. Syst. Agents Med. Chem.* **2012**, *12*(3), 233-9. https://doi.org/10.2174/187152412802430156.

(75) Console-Bram, L.; Brailoiu, E.; Brailoiu, G. C.; Sharir, H.; Abood, M. E. Activation of GPR18 by Cannabinoid Compounds: A Tale of Biased Agonism. *Br. J. Pharmacol.* **2014**, *171* (16), 3908–3917. https://doi.org/10.1111/bph.12746.

(76) McHugh, D.; Hu, S. S. J.; Rimmerman, N.; Juknat, A.; Vogel, Z.; Walker, J. M.; Bradshaw, H. B. N-Arachidonoyl Glycine, an Abundant Endogenous Lipid, Potently Drives Directed Cellular Migration through GPR18, the Putative Abnormal Cannabidiol Receptor. *BMC Neurosci.* **2010**, *11*. https://doi.org/10.1186/1471-2202-11-44.

(77) Takenouchi, R.; Inoue, K.; Kambe, Y.; Miyata, A. N-Arachidonoyl Glycine Induces Macrophage Apoptosis via GPR18. *Biochem. Biophys. Res. Commun.* **2012**, *418*(2), 366-71. https://doi.org/10.1016/j.bbrc.2012.01.027.

(78) Yin, H.; Chu, A.; Li, W.; Wang, B.; Shelton, F.; Otero, F.; Nguyen, D. G.; Caldwell, J. S.; Chen, Y. A. Lipid G Protein-Coupled Receptor Ligand Identification Using β-Arrestin PathHunter™ Assay. *J. Biol. Chem.* **2009**, *284* (18), 12328–12338. https://doi.org/10.1074/jbc.M806516200.

(79) Lu, V. B.; Puhl, H. L.; Ikeda, S. R. N-Arachidonyl Glycine Does Not Activate G Protein-Coupled Receptor 18 Signaling via Canonical Pathways. *Mol. Pharmacol.* **2013**, *83* (1), 267–282. https://doi.org/10.1124/mol.112.081182.

(80) Morales, P.; Lago-Fernandez, A.; Hurst, D. P.; Sotudeh, N.; Brailoiu, E.; Reggio, P. H.; Abood, M. E.; Jagerovic, N. Therapeutic Exploitation of GPR18: Beyond the Cannabinoids? *J. Med. Chem.* **2020**, *63*(23), 14216-14227. https://doi.org/10.1021/acs.jmedchem.0c00926.

(81) Jagerovic N., Lago Fernández A., Morales Lazaro P., Abood M.E., Brailoiu E., Magalhaes Leo L., Zhao P., Reggio P. H., Hurst D.P., Chafi N.S. Lazaro, M.; Ellen, M.; Leo, M. **(2021)** Pyrazolylbenzene-1,3-Diols For Diseases Associated With G Protein-Coupled Receptor 18 And In Combination With Transient Receptor Potential Vanilloid 1. (European Patent No. EP003901142A1). European Patent Office. https://data.epo.org/publication-server/rest/v1.2/patents/EP3901142NWA1/document.pdf

(82) Harms, H.; Rempel, V.; Kehraus, S.; Kaiser, M.; Hufendiek, P.; Müller, C. E.; König, G. M. Indoloditerpenes from a Marine-Derived Fungal Strain of Dichotomomyces Cejpii with Antagonistic Activity at GPR18 and Cannabinoid Receptors. *J. Nat. Prod.* **2014**, *77* (3),

673–677. https://doi.org/10.1021/np400850g.

(83) Nazir, M.; Harms, H.; Loef, I.; Kehraus, S.; El Maddah, F.; Arslan, I.; Rempel, V.; Müller, C. E.; König, G. M. GPR18 Inhibiting Amauromine and the Novel Triterpene Glycoside Auxarthonoside from the Sponge-Derived Fungus Auxarthron Reticulatum. *Planta Med.* **2015**, *81* (12–13), 1141–1145. https://doi.org/10.1055/s-0035-1545979.

(84) Rempel, V.; Atzler, K.; Behrenswerth, A.; Karcz, T.; Schoeder, C.; Hinz, S.; Kaleta, M.; Thimm, D.; Kiec-Kononowicz, K.; Müller, C. E. Bicyclic Imidazole-4-One Derivatives: A New Class of Antagonists for the Orphan G Protein-Coupled Receptors GPR18 and GPR55. *Medchemcomm* **2014**, *5* (5), 632–649. https://doi.org/10.1039/c3md00394a.

(85) Neumann, A.; Engel, V.; Mahardhika, A. B.; Schoeder, C. T.; Namasivayam, V.; Kieć-Kononowicz, K.; Müller, C. E. Computational Investigations on the Binding Mode of Ligands for the Cannabinoid-Activated G Protein-Coupled Receptor GPR18. *Biomolecules* **2020**, *10*(5), 686. https://doi.org/10.3390/biom10050686.

(86) Schoeder, C. T.; Schoeder, C. T.; Mahardhika, A. B.; Mahardhika, A. B.; Drabczyńska, A.; Kieć-Kononowicz, K.; Müller, C. E. Discovery of Tricyclic Xanthines as Agonists of the Cannabinoid-Activated Orphan G-Protein-Coupled Receptor GPR18. *ACS Med. Chem. Lett.* **2020**, *11*(10), 2024-2031. https://doi.org/10.1021/acsmedchemlett.0c00208.

(87) Schoeder, C. T. Identification, Optimization and Characterization of Pharmacological Tools for the Cannabinoid-Activated Orphan G Protein-Coupled Receptor GPR18 and Related Receptors, Rheinischen Friedrich-Wilhelms-Universität Bonn, 2017.

(88) Mahardhika, A. B.; Załuski, M.; Schoeder, C. T.; Boshta, N. M.; Schabikowski, J.; Perri, F.; Łażewska, D.; Neumann, A.; Kremers, S.; Oneto, A.; Ressemann, A.; Latacz, G.; Namasivayam, V.; Kieć-Kononowicz, K.; Müller, C. E. Potent, Selective Agonists for the Cannabinoid-like Orphan G Protein-Coupled Receptor GPR18: A Promising Drug Target for Cancer and Immunity. *J. Med. Chem.* **2024**, *67* (12), 9896–9926. https://doi.org/10.1021/acs.jmedchem.3c02423.

(89) Frankowska, M.; Wydra, K.; Suder, A.; Zaniewska, M.; Gawliński, D.; Miszkiel, J.; Furgała-Wojas, A.; Sałat, K.; Filip, M.; Müller, C. E.; Kieć-Kononowicz, K.; Kotańska, M. Novel GPR18 Ligands in Rodent Pharmacological Tests: Effects on Mood, Pain, and Eating

Disorders. *Int. J. Mol. Sci.* **2023**, *24* (10). https://doi.org/10.3390/ijms24109046.

(90) Kozłowska, H.; Malinowska, B.; Baranowska-kuczko, M.; Kusaczuk, M.; Nesterowicz, M.; Kozłowski, M.; Müller, C. E.; Kieć-kononowicz, K.; Schlicker, E. GPR18-Mediated Relaxation of Human Isolated Pulmonary Arteries. *Int. J. Mol. Sci.* **2022**, *23* (3). https://doi.org/10.3390/ijms23031427.

(91) Fabisiak, A.; Fabisiak, N.; Mokrowiecka, A.; Malecka-Panas, E.; Jacenik, D.; Kordek, R.; Zielińska, M.; Kieć-Kononowicz, K.; Fichna, J. Novel Selective Agonist of GPR18, PSB-KK-1415 Exerts Potent Anti-Inflammatory and Anti-Nociceptive Activities in Animal Models of Intestinal Inflammation and Inflammatory Pain. *Neurogastroenterol. Motil.* **2021**, *33* (3), 1–10. https://doi.org/10.1111/nmo.14003.

(92) Rempel, V.; Volz, N.; Gläser, F.; Nieger, M.; Bräse, S.; Müller, C. E. Antagonists for the Orphan G-Protein-Coupled Receptor GPR55 Based on a Coumarin Scaffold. *J. Med. Chem.* **2013**, *56* (11), 4798–4810. https://doi.org/10.1021/jm4005175.

(93) McHugh, D.; Sherry S. J. Hu; Rimmerman, N.; Juknat, A.; Vogel, Z.; Walker, J. M.; Bradshaw, H. B. N-Arachidonoyl Glycine, an Abundant Endogenous Lipid, Potently Drives Directed Cellular Migration through GPR18, the Putative Abnormal Cannabidiol Receptor. *BMC Neurosci.* **2010**, *26*(11),44. https://doi: 10.1186/1471-2202-11-44.

(94) McHugh, D.; Roskowski, D.; Xie, S.; Bradshaw, H. B. Δ9-THC and N-Arachidonoyl Glycine Regulate BV-2 Microglial Morphology and Cytokine Release Plasticity: Implications for Signaling at GPR18. *Front. Pharmacol.* **2014**, *4*(162). https://doi.org/10.3389/fphar.2013.00162.

(95) Birkenbach, M.; Josefsen, K.; Yalamanchili, R.; Lenoir, G.; Kieffl, E. Epstein-Barr Virus-Induced Genes: First Lymphocyte-Specific G Protein-Coupled Peptide Receptors. *J. Virol.* **1993**, *67* (4), 2209–2220. https://doi.org/10.1128/JVI.67.4.2209-2220.1993.

(96) Reboldi, A.; Cyster, J. G. Peyer's Patches: Organizing B-Cell Responses at the Intestinal Frontier. *Immunol. Rev.* **2016**, *271* (1). https://doi.org/10.1111/imr.12400.

(97) Gatto, D.; Wood, K.; Caminschi, I.; Murphy-Durland, D.; Schofield, P.; Christ, D.; Karupiah, G.; Brink, R. The Chemotactic Receptor EBI2 Regulates the Homeostasis, Localization and Immunological Function of Splenic Dendritic Cells. *Nat. Immunol.* **2013**,

14 (5). https://doi.org/10.1038/ni.2555.

(98) Gatto, D.; Brink, R. B Cell Localization: Regulation by EBI2 and Its Oxysterol Ligand. *Trends Immunol*. **2013,** *34*(7), 336-41. https://doi.org/10.1016/j.it.2013.01.007.

(99) Hannedouche, S.; Zhang, J.; Yi, T.; Shen, W.; Nguyen, D.; Pereira, J. P.; Guerini, D.; Baumgarten, B. U.; Roggo, S.; Wen, B.; Knochenmuss, R.; Noël, S.; Gessier, F.; Kelly, L. M.; Vanek, M.; Laurent, S.; Preuss, I.; Miault, C.; Christen, I.; Karuna, R.; Li, W.; Koo, D.-I.; Suply, T.; Schmedt, C.; Peters, E. C.; Falchetto, R.; Katopodis, A.; Spanka, C.; Roy, M.-O.; Detheux, M.; Chen, Y. A.; Schultz, P. G.; Cho, C. Y.; Seuwen, K.; Cyster, J. G.; Sailer, A. W. Oxysterols Direct Immune Cell Migration via EBI2. *Nature* **2011**, *287*(42), 35470-35483. https://doi.org/10.1038/nature10280.

(100) Pereira, J. P.; Kelly, L. M.; Xu, Y.; Cyster, J. G. EBI2 Mediates B Cell Segregation between the Outer and Centre Follicle. *Nature* **2009**, *460* (7259). https://doi.org/10.1038/nature08226.

(101) Cahir-McFarland, E. D.; Carter, K.; Rosenwald, A.; Giltnane, J. M.; Henrickson, S. E.; Staudt, L. M.; Kieff, E. Role of NF-KB in Cell Survival and Transcription of Latent Membrane Protein 1-Expressing or Epstein-Barr Virus Latency III-Infected Cells. *J. Virol.* **2004**, *78* (8), 4108–4119. https://doi.org/10.1128/JVI.78.8.4108-4119.2004/FORMAT/EPUB.

(102) Nair, S.; Sun, S.; Liu, C. 7α, 25-Dihydroxycholesterol-Mediated Activation of EBI2 in Immune Regulation and Diseases. *Front. Pharmacol***. 2015,** *24*(6), 60. https://doi.org/10.3389/fphar.2015.00060.

(103) Clottu, A. S.; Mathias, A.; Sailer, A. W.; Schluep, M.; Seebach, J. D.; Du Pasquier, R.; Pot, C. EBI2 Expression and Function: Robust in Memory Lymphocytes and Increased by Natalizumab in Multiple Sclerosis. *Cell Rep.* **2017**, *18* (1). https://doi.org/10.1016/j.celrep.2016.12.006.

(104) Bartlett, S.; Tandhyka Gemiarto, A.; Dao Ngo, M.; Sajiir, H.; Hailu, S.; Sinha, R.; Xiang Foo, C.; anie Kleynhans, L.; Tshivhula, H.; Webber, T.; Bielefeldt-Ohmann, H.; West, N. P.; Hiemstra, A. M.; MacDonald, C. E.; von Voss Christensen, L.; Schlesinger, L. S.; Walzl, G.; Marie Rosenkilde, M.; Mandrup-Poulsen, T.; Ronacher, K.; Penn-Nicholson, A.;

Verreck, F.; Kupz, A. GPR183 Regulates Interferons, Autophagy, and Bacterial Growth During Mycobacterium Tuberculosis Infection and Is Associated With TB Disease Severity. **2020**, *11*, 1. https://doi.org/10.3389/fimmu.2020.601534.

(105) Rutkowska, A.; Preuss, I.; Gessier, F.; Sailer, A. W.; Dev, K. K. EBI2 Regulates Intracellular Signaling and Migration in Human Astrocyte. *Glia* **2015**, *63*, 341–351. https://doi.org/10.1002/glia.22757.

(106) Copperi, F.; Schleis, I.; Roumain, M.; Muccioli, G. G.; Casola, S.; Klingenspor, M.; Pfeifer, A.; Gnad, T. EBI2 Is a Negative Modulator of Brown Adipose Tissue Energy Expenditure in Mice and Human Brown Adipocytes. **2022**, *5*(1), 280. https://doi.org/10.1038/s42003-022-03201-6.

(107) Zhang, L. GPR183 Expression on Pulmonary Conventional Dendritic Cell Type 2 Dictates Subtissular Localisation and Instructs Their Survival via the Thymic Stromal Lymphopoietin (TSLP) – TSLP Receptor (TSLPR) Axis. Rheinischen Friedrich-Wilhelms-Universität Bonn, **2021**.

(108) Shen, Z. J.; Hu, J.; Kashi, V. P.; Kelly, E. A.; Denlinger, L. C.; Lutchman, K.; McDonald, J. G.; Jarjour, N. N.; Malter, J. S. Epstein-Barr Virus-Induced Gene 2 Mediates Allergen-Induced Leukocyte Migration into Airways. *Am. J. Respir. Crit. Care Med.* **2017**, *195* (12), 1576–1585. https://doi.org/10.1164/rccm.201608-1580OC.

(109) Foo, C. X.; Bartlett, S.; Chew, K. Y.; Dao Ngo, M.; Bielefeldt-Ohmann, H.; Arachchige, B. J.; Matthews, B.; Reed, S.; Wang, R.; Smith, C.; Sweet, M. J.; Burr, L.; Bisht, K.; Shatunova, S.; Sinclair, J. E.; Parry, R.; Yang, Y.; Lévesque, J.-P.; Khromykh, A.; Rosenkilde, M. M.; Short, K. R.; Ronacher, K. GPR183 Antagonism Reduces Macrophage Infiltration in Influenza and SARS-CoV-2 Infection. *Eur Respir J* **2023**, *61*, 2201306. https://doi.org/10.1183/13993003.01306-2022.

(110) Lu, E.; Dang, E. V.; McDonald, J. G.; Cyster, J. G. Distinct Oxysterol Requirements for Positioning Naïve and Activated Dendritic Cells in the Spleen. *Sci. Immunol.* **2017**, *2* (10). https://doi.org/10.1126/sciimmunol.aal5237.

(111) Arfelt, K. N.; Fares, S.; Rosenkilde, M. M. EBV, the Human Host, and the 7TM Receptors: Defense or Offense? *Prog. Mol. Biol. Transl. Sci.* **2015**, *129*, 395–427.

https://doi.org/10.1016/BS.PMBTS.2014.10.011.

(112) Benned-Jensen, T.; Smethurst, C.; Holst, P. J.; Page, K. R.; Sauls, H.; Sivertsen, B.; Schwartz, T. W.; Blanchard, A.; Jepras, R.; Rosenkilde, M. M. Ligand Modulation of the Epstein-Barr Virus-Induced Seven-Transmembrane Receptor EBI2: Identification of a Potent and Efficacious Inverse Agonist. *J. Biol. Chem.* **2011**, *286* (33), 29292–29302. https://doi.org/10.1074/jbc.M110.196345.

(113) Benned-Jensen, T.; Madsen, C. M.; Arfelt, K. N.; Smethurts, C.; Blanchard, A.; Jepras, R.; Rosenkilde, M. M. Small Molecule Antagonism of Oxysterol-Induced Epstein-Barr Virus Induced Gene 2 (EBI2) Activation. *FEBS Open Bio* **2013**, *3*, 156–160. https://doi.org/10.1016/j.fob.2013.02.003.

(114) Benned-Jensen, T.; Norn, C.; Laurent, S.; Madsen, C. M.; Larsen, H. M.; Arfelt, K. N.; Wolf, R. M.; Frimurer, T.; Sailer, A. W.; Rosenkilde, M. M. Molecular Characterization of Oxysterol Binding to the Epstein-Barr Virus-Induced Gene 2 (GPR183). *J. Biol. Chem.* **2012**, *287* (42), 35470–35483. https://doi.org/10.1074/jbc.M112.387894.

(115) Ardecky, R.; Sergienko, E.; Zou, J.; Ganji, S.; Brown, B.; Sun, Q.; Ma, C.-T.; Hood, B.; Nguyen, K.; Vasile, S.; Suyama, E.; Mangravita-Novo, A.; Salaniwal, S.; Kung, P.; Smith, L. H.; Chung, T. D. Y.; Jackson, M. R.; Pinkerton, A. B.; Rickert, R. *Functional Antagonists of EBI-2*. In: Probe Reports from the NIH Molecular Libraries Program [Internet]. Bethesda (MD): National Center for Biotechnology Information (US); **2010**.

(116) Gessier, F.; Preuss, I.; Yin, H.; Rosenkilde, M. M.; Laurent, S.; Endres, R.; Chen, Y. A.; Marsilje, T. H.; Seuwen, K.; Nguyen, D. G.; Sailer, A. W. Identification and Characterization of Small Molecule Modulators of the Epstein-Barr Virus-Induced Gene 2 (EBI2) Receptor. *J. Med. Chem.* **2014**, *57* (8), 3358–3368. https://doi.org/10.1021/jm4019355.

(117) Latzo, N. G.; Braden, K.; Giancotti, L.; Chen, Z.; DeLeon, C.; Boehm, T.; D'Cunha, N.; Luongo, L.; Doyle, T.; Kolar, G.; Walker, J.; Arnatt, C.; Salvemini, D. Development of GPR183 Antagonists to Treat Neuropathic Pain. *FASEB J.* **2020**, *34* (S1), 1. https://doi.org/https://doi.org/10.1096/fasebj.2020.34.s1.09724.

(118) Braden, K.; Giancotti, L. A.; Chen, Z.; DeLeon, C.; Latzo, N.; Boehm, T.; D'Cunha, N.;

Thompson, B. M.; Doyle, T. M.; McDonald, J. G.; Walker, J. K.; Kolar, G. R.; Arnatt, C. K.; Salvemini, D. GPR183-Oxysterol Axis in Spinal Cord Contributes to Neuropathic Pain. *J. Pharmacol. Exp. Ther.* **2020**, *375* (2), 367–375. https://doi.org/10.1124/JPET.120.000105.

(119) Braden, K.; Campolo, M.; Chen, Z.; Giancotti, L.; Doyle, T. M.; Esposito, E.; Zhang, J.; Cuzzocrea, S.; Arnatt, C. K.; Salvemini, D. Investigating the Molecular Mechanisms Driving 7α,25-Dihydroxycholesterol-GPR183-Induced Hypersensitivity. *FASEB J.* **2022**, *36* (S1). https://doi.org/https://doi.org/10.1096/fasebj.2022.36.S1.R2071.

(120) Latzo, N. G.; Braden, K.; Giancotti, L.; Chen, Z.; DeLeon, C.; Boehm, T.; D'Cunha, N.; Luongo, L.; Doyle, T.; Kolar, G.; Walker, J.; Arnatt, C.; Salvemini, D. Development of GPR183 Antagonists to Treat Neuropathic Pain. *FASEB J.* **2020**, *34* (S1), 1. https://doi.org/https://doi.org/10.1096/fasebj.2020.34.s1.09724.

(121) Kjær, V. M. S.; Ieremias, L.; Daugvilaite, V.; Lückmann, M.; Frimurer, T. M.; Ulven, T.; Rosenkilde, M. M.; Våbenø, J. Discovery of GPR183 Agonists Based on an Antagonist Scaffold. *ChemMedChem* **2021**, *16* (17), 2623–2627. https://doi.org/10.1002/cmdc.202100301.

(122) Rosenkilde, M. M.; Benned-Jensen, T.; Andersen, H.; Holst, P. J.; Kledal, T. N.; Lüttichau, H. R.; Larsen, J. K.; Christensen, J. P.; Schwartz, T. W. Molecular Pharmacological Phenotyping of EBI2: An Orphan Seven-Transmembrane Receptor with Constitutive Activity. *J. Biol. Chem.* **2006**, *281* (19), 13199–13208. https://doi.org/10.1074/jbc.M602245200.

(123) Daugvilaite, V.; Madsen, C. M.; Lückmann, M.; Echeverria, C. C.; Sailer, A. W.; Frimurer, T. M.; Rosenkilde, M. M.; Benned-Jensen, T. Biased Agonism and Allosteric Modulation of G Protein-Coupled Receptor 183 – a 7TM Receptor Also Known as Epstein–Barr Virus-Induced Gene 2. *Br. J. Pharmacol.* **2017**, *174* (13), 2031–2042. https://doi.org/10.1111/bph.13801.

(124) Chen, H.; Huang, W.; Li, X. Structures of Oxysterol Sensor EBI2/GPR183, a Key Regulator of the Immune Response. *Structure* **2022**, *30* (7), 1016-1024.e5. https://doi.org/10.1016/J.STR.2022.04.006.

(125) Kjær, V. M. S.; Daugvilaite, V.; Stepniewski, T. M.; Madsen, C. M.; Jørgensen, A. S.; Bhuskute, K. R.; Inoue, A.; Ulven, T.; Benned-Jensen, T.; Hjorth, S. A.; Hjortø, G. M.; Moo, E. Von; Selent, J.; Rosenkilde, M. M. Migration Mediated by the Oxysterol Receptor GPR183 Depends on Arrestin Coupling but Not Receptor Internalization. *Sci. Signal.* **2023**, *16* (779), eabl4283. https://doi.org/10.1126/scisignal.abl4283.

(126) Sievers, F.; Wilm, A.; Dineen, D.; Gibson, T. J.; Karplus, K.; Li, W.; Lopez, R.; McWilliam, H.; Remmert, M.; Söding, J.; Thompson, J. D.; Higgins, D. G. Fast, Scalable Generation of High-Quality Protein Multiple Sequence Alignments Using Clustal Omega. *Mol. Syst. Biol.* **2011**, *7* (539). https://doi.org/10.1038/msb.2011.75.

(127) Li, K.; Lai, C.; Hei, S.; Liu, C.; Li, Z.; Xu, K. Identification of a Potential Structure-Based GPCR Drug for Interstitial Cystitis/Bladder Pain Syndrome: In Silico Protein Structure Analysis and Molecular Docking. *Int. Urogynecol. J.* **2022**, *34* (7), 1559–1565. https://doi.org/10.1007/s00192-022-05424-x.

(128) Stoddart, L. A.; White, C. W.; Nguyen, K.; Hill, S. J.; Pfleger, K. D. G. Fluorescence- and Bioluminescence-Based Approaches to Study GPCR Ligand Binding. *Br. J. Pharmacol.* **2016**, *173* (20), 3028–3037. https://doi.org/10.1111/bph.13316.

(129) Muller, C. E. General Synthesis and Properties of 1-Monosubstituted Xanthines. *Synthesis* **1993**, *1*, 125-128. https://doi.org/10.1055/s-1993-25814.

(130) Shelke, R. U.; Degani, M. S.; Raju, A.; Ray, M. K.; Rajan, M. G. R. Fragment Discovery for the Design of Nitrogen Heterocycles as Mycobacterium Tuberculosis Dihydrofolate Reductase Inhibitors. *Arch. Pharm.* **2016**, *349*(8), 602–613. https://doi.org/10.1002/ardp.201600066.

(131) Szardenings, Anna Katrin; Zhang, Wei; Kolb, Hartmuth C.; Cashion, Daniel Kurt; Chen, Gang; Kasi, Dhanalakshmi; Liu, Changhui; Sinha, Anjana; Wang, Eric; Yu, Chul; Gangadharmath, Umesh B.; Walsh, J. C. Imaging Agents for Detecting Neurological Disorders. US 20110182812 A1, **2011**.

(132) Patani, G. A.; LaVoie, E. J. Bioisosterism: A Rational Approach in Drug Design. *Chem. Rev.* **1996**, *96* (8), 3147–3176. https://doi.org/10.1021/cr950066q.

(133) Nobusuke Kashiki, N.; Toshiki Mori, I. K.; Ujita, N. Production Method Of 6-Halogeno-3-

Arylpyridine Derivative. US 8,742,127 B2, **2014**.

(134) Subbaiah, M. A. M.; Meanwell, N. A. Bioisosteres of the Phenyl Ring: Recent Strategic Applications in Lead Optimization and Drug Design. *J. Med. Chem.* **2021**, *64* (19), 14046–14128. https://doi.org/10.1021/acs.jmedchem.1c01215.

(135) Bénard, S.; Neuville, L.; Zhu, J. Copper-Promoted N-Cyclopropylation of Anilines and Amines by Cyclopropylboronic Acid. *Chem. Commun.* **2010**, *46* (19), 3393–3395. https://doi.org/10.1039/b925499d.

(136) Wu, J. W.; Wu, Y. D.; Dai, J. J.; Xu, H. J. Benzoic Acid-Catalyzed Transamidation Reactions of Carboxamides, Phthalimide, Ureas and Thioamide with Amines. *Adv. Synth. Catal.* **2014**, *356* (11–12), 2429–2436. https://doi.org/10.1002/adsc.201400068.

(137) Guha, S.; Kazi, I.; Mukherjee, P.; Sekar, G. Halogen-Bonded Iodonium Ion Catalysis: A Route to α-Hydroxy Ketones: Via Domino Oxidations of Secondary Alcohols and Aliphatic C-H Bonds with High Selectivity and Control. *Chem. Commun.* **2017**, *53* (79), 10942–10945. https://doi.org/10.1039/c7cc05697d.

(138) Soltani Rad, M. N.; Behrouz, S.; Najafi, H. N 7-Tosyltheophylline (TsTh): A Highly Efficient Reagent for the One-Pot Synthesis of n 7-Alkyltheophyllines from Alcohols. *Synth.* **2014**, *46*(10), 1380-1388. https://doi.org/10.1055/s-0033-1341026.

(139) Wu, P.; Givskov, M.; Nielsen, T. E. Reactivity and Synthetic Applications of Multicomponent Petasis Reactions. *Chem. Rev.* **2019**, *119* (20), 11245–11290. https://doi.org/10.1021/acs.chemrev.9b00214.

(140) Follmann, M.; Graul, F.; Schäfer, T.; Kopec, S.; Hamley, P. Petasis Boronic Mannich Reactions of Electron-Poor Aromatic Amines under Microwave Conditions. *Synlett* **2005**, *6*, 1009–1011. https://doi.org/10.1055/s-2005-864817.

(141) Morin, M. S. T.; Lu, Y.; Black, D. A.; Arndtsen, B. A. Copper-Catalyzed Petasis-Type Reaction: A General Route to α-Substituted Amides from Imines, Acid Chlorides, and Organoboron Reagents. *J. Org. Chem.* **2012**, *77* (4), 2013–2017. https://doi.org/10.1021/jo202339v.

(142) Greenberg, J. A.; Sammakia, T. The Conversion of Tert-Butyl Esters to Acid Chlorides

Using Thionyl Chloride. *J. Org. Chem.* **2017**, *82* (6), 3245–3251. https://doi.org/10.1021/acs.joc.6b02931.

(143) Zhang, Z.; Chen, Z.-B.; Du, Q.-S.; Feng, Y.-L. Synthesis of N-Aryl Substituted Heterocyclic Compounds by Copper-(0) Catalyst. *Chinese J. Org. Chem.* **1989**, *9* (6), 555–557.

(144) Smith, A. J.; Dimitrova, D.; Arokianathar, J. N.; Kolodziejczak, K.; Young, A.; Allison, M.; Poole, D. L.; Leach, S. G.; Parkinson, J. A.; Tuttle, T.; Murphy, J. A. New Reductive Rearrangement of: N-Arylindoles Triggered by the Grubbs-Stoltz Reagent Et3sih/Kotbu. *Chem. Sci.* **2020**, *11* (14), 3719–3726. https://doi.org/10.1039/d0sc00361a.

(145) Heisig, F.; Gollos, S.; Freudenthal, S. J.; El-Tayeb, A.; Iqbal, J.; Müller, C. E. Synthesis of BODIPY Derivatives Substituted with Various Bioconjugatable Linker Groups: A Construction Kit for Fluorescent Labeling of Receptor Ligands. *J. Fluoresc.* **2014**, *24*(1), 213-30. https://doi.org/10.1007/s10895-013-1289-4.

(146) Kraljevic, T. G.; Petrovic, M.; Krištafor, S.; Makuc, D.; Plavec, J.; Ross, T. L.; Ametamey, S. M.; Raic-Malic, S. Methoxymethyl (MOM) Group Nitrogen Protection of Pyrimidines Bearing C-6 Acyclic Side-Chains. *Molecules* **2011**, *16* (6), 5113–5129. https://doi.org/10.3390/molecules16065113.

(147) Himo, F.; Lovell, T.; Hilgraf, R.; Rostovtsev, V. V.; Noodleman, L.; Sharpless, K. B.; Fokin, V. V. Copper(I)-Catalyzed Synthesis of Azoles. DFT Study Predicts Unprecedented Reactivity and Intermediates. *J. Am. Chem. Soc.* **2005**, *127* (1), 210–216. https://doi.org/10.1021/ja0471525.

(148) Larin, E. M.; Lautens, M. Intramolecular Copper(I)-Catalyzed Interrupted Click–Acylation Domino Reaction. *Angew. Chemie* **2019**, *131* (38), 13572–13576. https://doi.org/10.1002/ange.201907448.

(149) Vilé, G.; Di Liberto, G.; Tosoni, S.; Sivo, A.; Ruta, V.; Nachtegaal, M.; Clark, A. H.; Agnoli, S.; Zou, Y.; Savateev, A.; Antonietti, M.; Pacchioni, G. Azide-Alkyne Click Chemistry over a Heterogeneous Copper-Based Single-Atom Catalyst. *ACS Catal.* **2022**, *12* (5), 2947–2958. https://doi.org/10.1021/acscatal.1c05610.

(150) Appukkuttan, P.; Dehaen, W.; Fokin, V. V; Eycken, E. Van Der. A Microwave-Assisted Click Chemistry Synthesis of 1 , 4-Disubstituted Three-Component Reaction. *Org. Lett.*

2004, *6* (23), 4223–4225.

(151) Müller, C. E.; Jacobson, K. A. Xanthines as Adenosine Receptor Antagonists. *Handb. Exp. Pharmacol.* **2011**, *200*, 151–199. https://doi.org/10.1007/978-3-642-13443-2_6.

(152) Stefanachi, A.; Brea, J. M.; Cadavid, M. I.; Centeno, N. B.; Esteve, C.; Loza, M. I.; Martinez, A.; Nieto, R.; Raviña, E.; Sanz, F.; Segarra, V.; Sotelo, E.; Vidal, B.; Carotti, A. 1-, 3- and 8-Substituted-9-Deazaxanthines as Potent and Selective Antagonists at the Human A2B Adenosine Receptor. *Bioorganic Med. Chem.* **2008**, *16* (6), 2852–2869. https://doi.org/10.1016/j.bmc.2008.01.002.

(153) Kim, D.; Jun, H.; Lee, H.; Hong, S. S.; Hong, S. Development of New Fluorescent Xanthines as Kinase Inhibitors. *Org. Lett.* **2010**, *12* (6), 1212–1215. https://doi.org/10.1021/ol100011n.

(154) Grahner, B.; Winiwarter, S.; Lanzner, W.; Müller, C. E. Synthesis and Structure-Activity Relationships of Deazaxanthines: Analogs of Potent A1- and A2-Adenosine Receptor Antagonists. *J. Med. Chem.* **1994**, *37* (10), 1526–1534. https://doi.org/10.1021/jm00036a019.

(155) Bartoccini, F.; Piersanti, G.; Mor, M.; Tarzia, G.; Minetti, P.; Cabri, W. Divergent Synthesis of Novel 9-Deazaxanthine Derivatives via Late-Stage Cross-Coupling Reactions. *Org. Biomol. Chem.* **2012**, *10* (44), 8860–8867. https://doi.org/10.1039/c2ob26516h.

(156) Platts, J. A.; Howard, S. T.; Bracke, B. R. F. Directionality of Hydrogen Bonds to Sulfur and Oxygen. *J. Am. Chem. Soc.* **1996**. *118*(11), 2726–2733. https://doi.org/10.1021/ja952871s.

(157) Wierzejewska, M.; Sałdyka, M. Are Hydrogen Bonds to Sulfur and Oxygen Different? Theoretical Study of Dimethylsulfide and Dimethylether Complexes with Nitric Acid. *Chem. Phys. Lett.* **2004**, *391* (1-3), 143-147. https://doi.org/10.1016/j.cplett.2004.04.101.

(158) Burgison, R. M.; Dietz, A. J. The Synthesis and Pharmacologic Evaluation of a Series of 8-Alkylthio-Thiated Theophyllines. *J. Med. Chem.* **1966**, *1* (6), 500–506.

(159) Rico-Gómez, R.; Nájera, F.; López-Romero, J. M.; Ca, P. Solvent-Free Synthesis of Thio-Alkylxanthines from Alkylxanthines Using Microwave Irradiation. *Heterocycles* **2000**, *53*(10), 2275-2278. https://doi.org/10.3987/COM-00-9003.

(160) Aragoni, M. C.; Arca, M.; Demartin, F.; Devillanova, F. A.; Graiff, C.; Isaia, F.; Lippolis, V.; Tiripicchio, A.; Verani, G. Ring-Opening of Lawesson's Reagent: New Syntheses of Phosphono- and Amidophosphono-Dithioato Complexes − Structural and CP-MAS31P-NMR Characterization of [p-CH3OPh(X)PS2]2M (X = MeO,IPrNH; M = NiII, PdII, and PtII). *Eur. J. Inorg. Chem.* **2000**, *10*, 2239-2244. https://doi.org/10.1002/1099-0682(200010)2000:10<2239::aid-ejic2239>3.0.co;2-0.

(161) Wooldridge, K. R. H.; Slack, R. The Synthesis of Some 6-Thioxanthines. *J. Chem. Soc.* **1962**, 1863–1868.

(162) El-Kalyoubi, S.; Agili, F.; Youssif, S. Novel 2-Thioxanthine and Dipyrimidopyridine Derivatives: Synthesis and Antimicrobial Activity. *Molecules* **2015**, *20* (10), 19263–19276. https://doi.org/10.3390/molecules201019263.

(163) Brennman, J. B.; Ginn, J. D.; Sarko, C. R.; Westbrook, J.; Zhang, Z.; Yu, M.; Hopkins, T. D.; Lowe, M. D. Heterocyclic Carboxylic Acids as Activators of Soluble Guanylate Cyclase (International Publication Number WO2016/014463A1) International Application Published Under the Patent Cooperation Treaty (PCT). **2016**.

(164) Marx, D.; Wingen, L. M.; Schnakenburg, G.; Müller, C. E.; Scholz, M. S. Fast, Efficient, and Versatile Synthesis of 6-Amino-5-Carboxamidouracils as Precursors for 8-Substituted Xanthines. *Front. Chem.* **2019**, *7*, 1–15. https://doi.org/10.3389/fchem.2019.00056.

(165) Kraupner, N.; Dinh, C. P.; Wen, X.; Landry, V.; Herledan, A.; Leroux, F.; Bosc, D.; Charton, J.; Maillard, C.; Warenghem, S.; Duplan, I.; Piveteau, C.; Hennuyer, N.; Staels, B.; Deprez, B.; Deprez-Poulain, R. Identification of Indole-Based Activators of Insulin Degrading Enzyme. *Eur. J. Med. Chem.* **2022**, *228*. https://doi.org/10.1016/j.ejmech.2021.113982.

(166) Cerda-Cavieres, C.; Quiroz, G.; Iturriaga-Vásquez, P.; Rodríguez-Lavado, J.; Alarcón-Espósito, J.; Saitz, C.; Pessoa-Mahana, C. D.; Chung, H.; Araya-Maturana, R.; Mella-Raipán, J.; Cabezas, D.; Ojeda-Gómez, C.; Reyes-Parada, M.; Pessoa-Mahana, H. Synthesis, Docking, 3-D-Qsar, and Biological Assays of Novel Indole Derivatives Targeting Serotonin Transporter, Dopamine D2 Receptor, and Mao-a Enzyme: In the Pursuit for Potential Multitarget Directed Ligands. *Molecules* **2020**, *25* (20). https://doi.org/10.3390/molecules25204614.

(167) Pessoa-Mahana, H.; González-Lira, C.; Fierro, A.; Zapata-Torres, G.; Pessoa-Mahana, C. D.; Ortiz-Severin, J.; Iturriaga-Vásquez, P.; Reyes-Parada, M.; Silva-Matus, P.; Saitz-Barría, C.; Araya-Maturana, R. Synthesis, Docking and Pharmacological Evaluation of Novel Homo- and Hetero-Bis 3-Piperazinylpropylindole Derivatives at SERT and 5-HT1A Receptor. *Bioorg. Med. Chem.* **2013**, *21* (24), 7604–7611. https://doi.org/10.1016/j.bmc.2013.10.036.

(168) Nandikolla, A.; Mahadu Khetmalis, Y.; Mahalakshmi Naidu, K.; Karan Kumar, B.; Murugesan, S.; Chandra Sekhar, K. V. G. Discovery of Potent Antitubercular Agents: Design, Synthesis and Biological Evaluation of 4-(3-(4-Substitutedpiperazin-1-Yl)-Quinoxalin-2-Yl)-Naphthalen-1-Ol Analogues. *Toxicol. Vitr.* **2022**, *82* (March), 105370. https://doi.org/10.1016/j.tiv.2022.105370.

(169) Fernandes, J. L. N.; De Souza, M. C.; Brenelli, E. C. S.; Brenelli, J. A. Reduction of Acetophenones Using Borohydride Exchange Resins (BER) and a BER-Lithium Salt System. *Synthesis* **2009** https://doi.org/10.1055/s-0029-1217040.

ACKNOWLEDGMENTS

This work was supported by the German Research Foundation (DFG, Research Training group GRK 1873).

I would like to express my gratitude to Prof. Dr. Christa Müller for her supervision throughout my doctoral studies.

I also thank the entire working group for their support over the years.

To Mom and Dad, my home, wherever I am and will be.